

LIBRARY
Michigan State
University

This is to certify that the
dissertation entitled

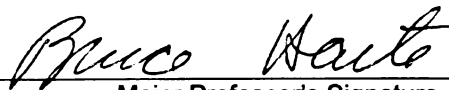
EVALUATION OF LIGHT-OXIDIZED OFF-FLAVORS IN
REDUCED FAT MILK AND CHEDDAR CHEESE USING
SENSORY EVALUATION AND THE ELECTRONIC NOSE

presented by

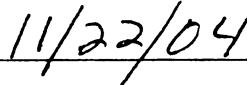
HSIN-YEN CHUNG

has been accepted towards fulfillment
of the requirements for the

Doctoral degree in Packaging



Major Professor's Signature



Date

PLACE IN RETURN BOX to remove this checkout from your record.
TO AVOID FINES return on or before date due.
MAY BE RECALLED with earlier due date if requested.

DATE DUE	DATE DUE	DATE DUE
JAN 10 2007	JUL 05 2008	
JUN 11 2007		
08 25 10		
MAY 24 2010		

**EVALUATION OF LIGHT-OXIDIZED OFF-FLAVORS IN REDUCED FAT MILK
AND CHEDDAR CHEESE USING SENSORY EVALUATION AND THE
ELECTRONIC NOSE**

By

Hsin-Yen Chung

A DISSERTATION

**Submitted to
Michigan State University
in partial fulfillment of the requirements
for the degree of**

DOCTOR OF PHILOSOPHY

School of Packaging

2004

ABSTRACT

EVALUATION OF LIGHT-OXIDIZED OFF-FLAVORS IN REDUCED FAT MILK AND CHEDDAR CHEESE USING SENSORY EVALUATION AND THE ELECTRONIC NOSE

By

Hsin-Yen Chung

Exposure to light can result in changes of sensory and nutritional qualities of foods, including milk and other dairy products. This study was to evaluate the light-oxidized and/or packaging off-flavors in milk and Cheddar cheese using sensory evaluation, solid-phase microextraction coupled with gas chromatography (SPME-GC), and an electronic nose (FOX 3000, AlphaMOS) equipped with 12 metal oxide semiconductor (MOS) sensors.

Reduced fat (2%) milk in glass bottles exposed to fluorescent light (1000 lx) at 5°C developed a significant light-oxidized off-flavor in 8 hours, which was detected by both consumer and trained panelists. Headspace pentanal and hexanal increased as the light exposure time increased. Using a 95°C headspace temperature for the electronic nose analysis provided better model discrimination than 45°C or 70°C. By defining the harmful light exposure time as a milk deterioration threshold, the 95°C linear discriminant analysis (LDA) model correctly recognized 97% of the milk samples exposed to light for 8 hours or longer. Quantitatively, the 95°C partial least squares (PLS) model provided better prediction of the sensory scores than the 95°C multilayer perceptrons (MLP) model.

The different packaging materials (237 ml glass, HDPE, HDPE-TiO₂, PET bottles, and PE-coated paper cartons) were clearly discriminated and identified using the electronic nose. However, packaging off-flavors in water and 2% milk were not clearly defined by both sensory evaluation and electronic nose analysis. The effect of packaging materials on light-induced oxidation in milk was closely related to their light barrier properties. PE-coated paper cartons reduced light-oxidation of 2% milk significantly (12 hours of light exposure, 1000 lx), while HDPE-TiO₂ gave only partial light protection.

Light-induced quality changes (color and flavor) were limited to the top surface of the vacuum-packaged Cheddar cheese, which was the portion that was exposed to light (2000 lx). Discoloration and off-flavors were detected by the trained panel after exposure to light for 2 weeks. Color measurement showed a continuous decrease in yellowness contributed the most to the discoloration, along with a relatively small decrease in redness and increase in lightness. The discriminant models of sensor responses using 90°C headspace samples had higher correct identification rates and better discrimination than at 60°C. The 90°C PLS model provided better prediction of the sensory scores than the 90°C MLP model.

The established discriminant and correlation models have shown the potential of the electronic nose to be used as a complementary approach to sensory evaluation to determine light-oxidized off-flavors in packaged milk and Cheddar cheese.

**Copyright by
HSIN-YEN CHUNG
2004**

ACKNOWLEDGMENTS

I would like to express my sincere gratitude to Dr. Bruce Harte, the most wonderful teacher, advisor, and mentor a graduate student can have, for all of his guidance on this dissertation study and his help, support and trust since the very first day of my student life in Michigan State University.

I would like to thank Dr. John Partridge, for showing me the ropes in judging sensory qualities of milk and dairy products, and having the MSU dairy judging team involved as the trained panel in this study. I would also like to thank Dr. Theron Downes, Dr. Susan Selke and Dr. Zeynep Ustunol, for their invaluable advices and suggestions in the graduate committee.

I am very grateful for the help and friendship from all the graduate students in the School of Packaging, including their kindness of participating as consumer panelists. Many thanks to many of them who provided direct assistance to me: Krittika Tanprasert, Antonis Kanavouras, Ubonratana Siripatrawan, Pattra Maneesin, Young Suk Lee, Rafael Auras, Li Xiong and Isinay Yuzay. I also wish to extend my thanks to Robert Hurwitz and Mr. Nate for their great help in setting up and troubleshooting the hardware for the experiments.

I would like to thank the Center for Food and Pharmaceutical Packaging Research (CFPPR) for the financial support. I would also like to thank Melody Farms in Lansing, Michigan for providing paper carton samples with no charge.

TABLE OF CONTENTS

LIST OF TABLES.....	x
LIST OF FIGURES	xii
CHAPTER 1 INTRODUCTION	1
CHAPTER 2 REVIEW OF LITERATURE	4
2.1. Light-induced oxidation of milk.....	4
2.1.1. Photosensitized oxidation.....	5
2.1.1.1. Degradation of milk proteins	7
2.1.1.2. Oxidation of milk lipids	9
2.1.1.3. Vitamin destruction	10
2.1.2. Wavelength dependent impact of light	12
2.1.2.1. Light absorption	12
2.1.2.2. Quantum yield.....	15
2.1.2.3. Light sources	16
2.1.3 Occurrences of light-oxidized off-flavors in milk	19
2.2. Effects of milk packaging.....	23
2.2.1. Off-flavors from milk packaging materials.....	23
2.2.1.1. Polyethylene (PE)	24
2.2.1.2. Polyethylene terephthalate (PET)	26
2.2.1.3. Paper cartons	27
2.2.2. Light barrier properties of packaging materials.....	29
2.2.3. Other packaging factors affecting milk quality	32
2.2.3.1. Size and shape	32
2.2.3.2. Oxygen permeability	33
2.3. Light oxidation of cheese.....	34
2.3.1. Discoloration of cheese	34
2.3.2. Light-induced flavor changes of cheese	37
2.4. Electronic nose	41
2.4.1. Sensor arrays	45
2.4.1.1. Metal oxide semiconductors (MOS).....	49
2.4.1.2. Conductive organic polymer (CP)	50
2.4.1.3. Quartz crystal microbalance (QCM) and surface acoustic wave (SAW)	52
2.4.1.4. Metal-oxide semiconductors field-effect transistors (MOSFET)	53
2.4.2. Signal processing	54

2.4.3. Data processing	58
2.4.4. Applications of the electronic nose	60
2.4.4.1. Electronic nose in milk applications	60
2.4.4.2. Electronic nose in cheese applications	63
2.4.4.3. Electronic nose in packaging applications	66
2.5 Solid-phase microextraction (SPME)	68
2.6. Multivariate statistical techniques.....	75
2.6.1. Unsupervised learning techniques	75
2.6.1.1 Hierarchical clustering analysis (HCA).....	75
2.6.1.2 Principle component analysis (PCA).....	77
2.6.2. Supervised learning techniques	81
2.6.2.1 Linear/quadratic discriminant function analysis (LDA/QDA).....	81
2.6.2.2. k-nearest neighbor (k-NN)	87
2.6.3. Quantitative analyses	89
2.6.3.1 Partial least square (PLS) regression	89
CHAPTER 3 MATERIALS AND METHODS	94
3.1. Sample preparation	94
3.1.1. Light-oxidized off-flavors in 2% milk	94
3.1.2. Packaging off-flavors in 2% milk.....	96
3.1.3. Light-oxidized and packaging off-flavors in 2% milk	99
3.1.4. Cheddar cheese samples.....	100
3.2. Sensory evaluation	104
3.2.1. Triangle tests performed by a consumer panel	104
3.2.2. Rating based on ADSA guidelines performed with a trained panel	105
3.2.3. Difference-from-control tests using a trained panel.....	108
3.3. Electronic nose analysis	108
3.4. Solid-Phase Microextraction-Gas Chromatography (SPME-GC)	110
3.4.1. SPME-GC for milk samples.....	111
3.4.2. SPME-GC for Cheddar cheese samples	112
3.5. Light transmission of milk packaging materials	112
3.6 Color measurement of cheese.....	113
3.7. Multivariate statistical techniques.....	115
3.7.1. Data preprocessing	115
3.7.2. Unsupervised learning techniques	115
3.7.3. Supervised learning techniques	116
3.7.4. Quantitative analyses	117

CHAPTER 4 RESULTS AND DISCUSSION	120
4.1. Light-oxidized off-flavors in 2% milk.....	120
4.1.1. Sensory evaluation	120
4.1.2. Headspace analysis using SPME-GC	124
4.1.2.1. Optimizing the headspace sampling parameters	124
4.1.2.2. Quantifying the headspace volatiles of light-oxidized milk	128
4.1.3. Headspace analysis using the electronic nose.....	131
4.1.4. Correlation of results from sensory and instrumental analyses	147
4.2. Packaging and light-oxidized off-flavors	157
4.2.1. Off-flavors from packaging materials	157
4.2.2. Packaging off-flavors in water and 2% milk	167
4.2.2.1. Sensory evaluation	167
4.2.2.2. Headspace analysis using the electronic nose	171
4.2.3. Packaging and light oxidized off-flavors in 2% milk	178
4.2.3.1. Sensory evaluation	180
4.2.3.2. Headspace analysis using the electronic nose	182
4.3. Light oxidation of Cheddar cheese	186
4.3.1. Discoloration of Cheddar cheese	186
4.3.2. Body and texture of Cheddar cheese	191
4.3.3. Light-induced flavor changes of cheese	194
4.3.3.1. Sensory evaluation	194
4.3.3.2. Headspace analysis using SPME-GC.....	194
4.3.3.3. Headspace analysis using the electronic nose	205
CHAPTER 5 CONCLUSIONS	219
APPENDICES.....	222
A.1. SAS and Matlab programs.....	222
A.1.1. Data import in SAS	222
A.1.2. HCA and PCA using SAS	223
A.1.3. LDA/QDA and k-NN using SAS	225
A.1.4. PLS using SAS and MLP using Matlab	229
A.2 Designs and Forms of Sensory Tests	233
A.2.1. Triangle tests	233
A.2.2. Milk scoring card based on ADSA guidelines.....	238
A.3 Boxplot Interpretation	242
A.4. Preliminary results	243
A.4.1. Light-oxidized off-flavors in 2% milk.....	243
A.4.2. Light oxidation of Cheddar cheese.....	246

BIBLIOGRAPHY247

LIST OF TABLES

Table 1 Internal and external factors affecting the photosensitivity of milk and dairy products to visible light.....	19
Table 2 Commercially available electronic nose instruments.	44
Table 3 Classification of chemical sensors that have been used.	46
Table 4 Comparative properties and performance of the most frequently used gas sensors in electronic nose instruments.	48
Table 5 Recent electronic nose applications in natural products.....	61
Table 6 Types of SPME fibers and their recommended use.	71
Table 7 Oxygen and water vapor transmission rates of the Cryovac® B-series bags, given the temperature (°C) and relative humidity (%RH).	100
Table 8 Product attributes and scores of the ADSA guideline for scoring off-flavors in milk.	106
Table 9 Product attributes and scores of the ADSA guideline for scoring flavor and body/texture defects of Cheddar cheese.	107
Table 10 Triangle test results on light-oxidized 2% milk in glass bottles against control.....	121
Table 11 Sensory scores of light-oxidized 2% milk based on ADSA guidelines.	123
Table 12 Coefficient of variation (%CV) for the CAR/PDMS fiber used to quantify volatiles in the standard aqueous solution.	126
Table 13 Coefficient of variation (%CV) for the DVB/PDMS fiber used to quantify volatiles in the standard aqueous solution.	126
Table 14 Triangle test results on HPLC grade water in glass, HDPE, PET bottles and PE-coated paper cartons at 5°C for 3 days.....	168
Table 15 Triangle test results on 2% milk in glass, HDPE, PET bottles and PE-coated paper cartons, at 5°C for 3 days.....	168
Table 16 Sensory scores of 2% milk in glass, HDPE, HDPE-TiO ₂ , PET bottles and PE-coated paper cartons at 5°C for 3 days.....	170

Table 17 Thickness of the tested packaging materials.	179
Table 18 A series of triangle tests on 2% milk stored in HDPE, HDPE-TiO ₂ , PET bottles and PE-coated paper cartons, and exposed to 12 hours of fluorescent light at 5°C.	180
Table 19 Sensory scores of 2% milk stored in glass, HDPE, HDPE-TiO ₂ , PET bottles, and PE-coated paper cartons, and exposed to 12 hours of fluorescent light at 5°C.	181
Table 20 Difference-from-control sensory scores in color ¹ of Cheddar cheese samples.	187
Table 21 Color measurements (CIE L* a* b*) of the Cheddar cheese samples exposed to 0, 2, 4 or 6 weeks of the fluorescent light (2000 lx).	189
Table 22 Hue angle, $\tan^{-1}(b/a)$, of the Cheddar cheese samples exposed to 0, 2, 4 or 6 weeks of the fluorescent light (2000 lx).	190
Table 23 Difference-from-control sensory scores of body and texture ¹ of Cheddar cheese samples.	192
Table 24 Sensory scores of body and texture of Cheddar cheese samples, based on ADSA guidelines.	193
Table 25 Difference-from-control sensory scores in flavor ¹ of Cheddar cheese samples.	195
Table 26 Flavor sensory scores of Cheddar cheese samples based on ADSA guidelines.	196
Table 27 Volatiles identified ¹ in the headspace (60°C, 15 minutes) of Cheddar cheese.	197
Table 28 Sensory scores of light-oxidized 2% milk based on ADSA guidelines. Scores were given by an 8-member trained panel.	243
Table 29 CIE L* a* b* values of Cheddar cheese samples exposed to fluorescent light (2000 lx) for 0 and 2 weeks.	246

LIST OF FIGURES

Figure 1	Mechanisms of photosensitized oxidation catalyzed by riboflavin.....	6
Figure 2	Mechanism of methionine reacting with singlet oxygen ($^1\text{O}_2$).	8
Figure 3	Lipid oxidation initiated by free radicals or singlet oxygen ($^1\text{O}_2$), which is generated in the presence of riboflavin.	9
Figure 4	Absorption spectrum of riboflavin at different wavelength.....	13
Figure 5	Absorption spectra of (a) vitamin A and (b) vitamin C.....	14
Figure 6	Emission spectra of (a) sunlight, (b) Philips 83/36 W white, (c) Philips 16/40 W yellow, (d) Philips 33/40 W white.....	17
Figure 7	Energy output for a typical supermarket white lamp.	18
Figure 8	Light transmission through various packaging materials.....	30
Figure 9	Absorption spectra of the major naturally occurring colorants of cheeses at concentrations found in milk.	39
Figure 10	Basic diagram showing the analogy between biological and artificial noses.....	42
Figure 11	Schematic diagrams of five different kinds of sensors.	47
Figure 12	Sensor responses of (a) an ideal first order odor sensor responding to a step odor input (b) MOS sensors in this study (R: resistance).....	55
Figure 13	Example of PCA (a) without mean centering and (b) after mean centering.....	57
Figure 14	Classification scheme of the multivariate pattern analysis techniques applied to the electronic nose data.	59
Figure 15	Solid phase microextraction (SPME) to concentrate headspace volatiles: (a) extraction; (b) desorption.....	69
Figure 16	Effect of time on amount of analyte absorbed.....	70
Figure 17	An example of hierarchical clustering analysis (HCA).....	76
Figure 18	An example of principle component analysis (PCA).	80

Figure 19	Decision boundaries defined based on the discriminant functions....	83
Figure 20	Examples of canonical discriminant analysis.	86
Figure 21	Examples of k-nearest neighbor (k-NN).	88
Figure 22	The indirect modeling concept of partial least squares (PLS) approach.	90
Figure 23	Multiplayer perceptron (MLP) structure. (a) A neuron, the basic neural unit; (b) a multilayer perceptron.	93
Figure 24	Experimental flowchart to investigate the light-oxidized off-flavors in 2% milk, using sensory evaluation and instrumental analyses.	95
Figure 25	Packaging materials used for milk and/or water.....	96
Figure 26	Experimental flowchart to investigate packaging off-flavors in 2% milk, using sensory evaluation (triangle tests and flavor rating based on ADSA guidelines) and instrumental analysis (electronic nose).....	97
Figure 27	Experimental flowchart to investigate the light-oxidized and packaging off-flavors in 2% milk, using sensory evaluation and instrumental analysis (electronic nose).	99
Figure 28	The arrangement of the Cheddar cheese samples exposed to fluorescent light (2000 lx) at 5°C for 0, 2, 4, or 6 weeks.....	102
Figure 29	Experimental flowchart to investigate the light-induced deterioration of Cheddar cheese in color, body/texture, and flavor, using sensory evaluation and instrumental analyses.	103
Figure 30	The electronic nose system (Fox 3000, Alpha-MOS).....	109
Figure 31	Schematic diagram of (a) 45°/0° geometry of the spectrophotometer (b) the CIE L* a* b* color space.	114
Figure 32	The feed-forward backpropagation network with 12 input nodes, which correspond to the mean-centered 12 sensor responses), and one output node.....	118
Figure 33	Training parameters of the feed-forward backpropagation network.	118
Figure 34	Flavor sensory scores based on ADSA guidelines of 2% milk in glass bottles exposed to 0, 2, 4, 8, 12, 24 or 48 hours of fluorescent light (1000 lx, 5°C).....	123

Figure 35 Area responses for (a) pentanal, (b) hexanal and (c) dimethyl disulfide sampling using CAR/PDMS, or DVB/PDMS fiber (d, e, f, respectively), at different sampling temperatures.	125
Figure 36 The amount of (a) pentanal (b) hexanal, and (c) dimethyl disulfide in 2% milk with and without light exposure for 0 to 48 hours.	130
Figure 37 Sensor responses of the electronic nose to 95°C headspace of 2% milk (a) without (b) with 48 hours of light exposure at 5°C.	132
Figure 38 (a) HCA and (b) PCA of the sensor responses for 45°C headspace of 2% milk exposed to 0, 2, 4, 8, 12, 24, 36, or 48 hours of light at 5°C.	133
Figure 39 (a) HCA and (b) PCA of the sensor responses for 70°C headspace of 2% milk exposed to 0, 2, 4, 8, 12, 24, 36, or 48 hours of light at 5°C.	134
Figure 40 (a) HCA and (b) PCA of the sensor responses for 95°C headspace of 2% milk exposed to 0, 2, 4, 8, 12, 24, 36, or 48 hours of light at 5°C.	135
Figure 41 Classification rates for discrimination methods applied to the sensor responses using a headspace temperature of 45°C for 2% milk exposed to 0, 2, 4, 8, 12, 24, 36, or 48 hours of light, using LDA, QDA, and k-NN for k = 1, 2, 3, and 4.	137
Figure 42 Classification rates for discrimination methods applied to the sensor responses using a headspace temperature of 70°C for 2% milk exposed to 0, 2, 4, 8, 12, 24, 36, or 48 hours of light, using LDA, QDA, and k-NN for k = 1, 2, 3, and 4.	138
Figure 43 Classification rates for discrimination methods applied to the sensor responses using a headspace temperature of 95°C for 2% milk exposed to 0, 2, 4, 8, 12, 24, 36, or 48 hours of light, using LDA, QDA, and k-NN for k = 1, 2, and 3.	138
Figure 44 Canonical discriminant scatter plots of the (a) training (b) test data sets. Headspace of 2% milk samples exposed to 0, 2, 4, 8, 12, 24, 36, or 48 hours of light was generated at 45°C.	140
Figure 45 Canonical discriminant scatter plots of the (a) training (b) test data sets. Headspace of 2% milk samples exposed to 0, 2, 4, 8, 12, 24, 36, or 48 hours of light was generated at 70°C.	141
Figure 46 Canonical discriminant scatter plots of the (a) training (b) test data sets. Headspace of 2% milk samples exposed to 0, 2, 4, 8, 12, 24, 36, or 48 hours of light was generated at 95°C.	142
Figure 47 Classification rates of the defined threshold of harmful light exposure for discrimination methods applied to the sensor responses using a	

headspace temperature of 45°C using LDA, QDA, and k-NN for k = 1, 2, 3, and 4.....	144
Figure 48 Classification rates of the defined threshold of harmful light exposure for discrimination methods applied to the sensor responses using a headspace temperature of 70°C using LDA, QDA, and k-NN for k = 1, 2, 3, and 4.....	145
Figure 49 Classification rates of the defined threshold of harmful light exposure for discrimination methods applied to the sensor responses using a headspace temperature of 95°C using LDA, QDA, and k-NN for k = 1, 2, 3.	146
Figure 50 PLS predicted versus actual flavor scores of 2% milk exposed to 0, 2, 4, 8, 12, 24, 36, or 48 hours of light, based on levels of pentanal, hexanal and dimethyl disulfide quantified using SPME-GC. Models were applied to (a) training data and (b) test data.	148
Figure 51 MLP predicted versus actual flavor scores of 2% milk exposed to 0, 2, 4, 8, 12, 24, 36, or 48 hours of light, based on levels of pentanal, hexanal and dimethyl disulfide quantified using SPME-GC.....	149
Figure 52 PLS predicted versus actual flavor scores of 2% milk exposed to 0, 2, 4, 8, 12, 24, 36, or 48 hours of light, based on the sensor responses using a headspace temperature of 45°C.	151
Figure 53 PLS predicted versus actual flavor scores of 2% milk exposed to 0, 2, 4, 8, 12, 24, 36, or 48 hours of light, based on the sensor responses using a headspace temperature of 70°C.	152
Figure 54 PLS predicted versus actual flavor scores of 2% milk exposed to 0, 2, 4, 8, 12, 24, 36, or 48 hours of light, based on the sensor responses using a headspace temperature of 95°C.	153
Figure 55 MLP predicted versus actual flavor scores of 2% milk exposed to 0, 2, 4, 8, 12, 24, 36, or 48 hours of light, based on the sensor responses using a headspace temperature of 45°C.	154
Figure 56 MLP predicted versus actual flavor scores of 2% milk exposed to 0, 2, 4, 8, 12, 24, 36, or 48 hours of light, based on the sensor responses using a headspace temperature of 70°C.	155
Figure 57 MLP predicted versus actual flavor scores of 2% milk exposed to 0, 2, 4, 8, 12, 24, 36, or 48 hours of light, based on the sensor responses using a headspace temperature of 95°C.	156

CHAPTER 1

INTRODUCTION

Exposure to light can result in changes in sensory and nutritional qualities of foods. Photosensitized oxidation in the presence of riboflavin is believed to be mainly responsible for the quality deterioration of milk and other dairy products due to fluorescent light exposure on dairy shelves in retail stores [1-5].

Depending on the lighting conditions, e.g. exposure duration, intensity and wavelength, and barrier properties of packaging materials, the occurrence of light-oxidized off-flavors in milk can take place in as soon as 15 minutes [6] to 12 hours [7, 8]. Turnover times of fluid milk average somewhere between 8 hours [6, 9] and 2-3 days [10]. Light-induced discoloration and oxidized off-flavors may occur at the surface of cheeses, since cheeses are often wrapped in transparent packaging and displayed in small pieces with large surface areas exposed to light.

Potential migrants in milk packaging materials, such as oxidative hydrocarbons from processed HDPE, PET or PE-coated paperboard [11-13], may cause a defect referred to “packaging off-flavors” in milk. On the other hand, packaging light and oxygen barriers reduce light oxidation by minimizing the impact of fluorescent light in retail display and headspace oxygen content inside the package, respectively.

An electronic nose is an instrument which comprises an array of electronic chemical sensors with partial specificity and an appropriate pattern recognition

system, capable of recognizing simple or complex odors [14]. An electronic nose analyzes all substances in gaseous samples as a whole, as an analogy to the human olfactory system. It is more of a complementary approach than a substitute for reference methods that use sensory panels [15]. An electronic nose can be used as an automated discriminatory analysis tool for odors and flavors in foods, and has the potential for applications such as quality control, process control, and off-flavor detection [16].

This study was done to evaluate the light-oxidized and/or packaging off-flavors in milk and Cheddar cheese using sensory evaluation, solid-phase microextraction coupled with gas chromatography (SPME-GC), and an electronic nose (FOX 3000, AlphaMOS) equipped with 12 metal oxide semiconductor (MOS) sensors. In addition to the flavor changes, the light-induced discoloration of Cheddar cheese was quantified using sensory evaluation and instrumental color measurement.

Significance

Electronic noses, which can be automated and require less extensive operating and preparatory measures, have the potential to be a complementary approach for sensory evaluation. This study used a commercial electronic nose system as the discriminatory analysis tool for light oxidized off-flavors in milk and Cheddar cheese, and to determine a correlation between the sensory quality and the electronic nose responses. The effect of current packaging materials as both light barriers and sources of potential migrants was also investigated.

Hypothesis

The electronic nose equipped with 12 MOS sensors can perform effectively in discriminating and predicting the sensory quality of the light-oxidized and packaging off-flavors in milk, and light-oxidized off-flavors in Cheddar cheese.

Objectives

1. To discriminate light-oxidized off-flavors in milk using sensory evaluation and instrumental headspace analyses, including the electronic nose and SPME-GC.
2. To evaluate the quality of milk packaged in different packaging materials of differing light barrier properties and having different potential packaging off-flavor problems.
3. To discriminate light-induced discoloration and off-flavors in Cheddar cheese using sensory evaluation and instrumental analyses, including color measurements, electronic nose and SPME-GC.
4. To correlate the results of sensory evaluation and instrumental analyses using multivariate statistical techniques.

CHAPTER 2

REVIEW OF LITERATURE

2.1. Light-induced oxidation of milk

Light exposure can have a deteriorative effect on both sensory and nutritional qualities of foods, including milk and other dairy products. Two types of light-induced off-flavors in milk have been identified: a “burnt-feather” off-flavor from protein oxidation usually appears early during light exposure but dissipates in a few days, and a “cardboardy” off-flavor from lipid oxidation develops with more prolonged light exposure and does not dissipate. Other nutrients, such as vitamins, may also decompose in oxidative reactions.

Light absorption can directly initiate the oxidation; however, milk proteins and lipids absorb very limited amounts of ultraviolet (UV) light and do not absorb visible light [3]. Lipids such as unsaturated fatty acids are susceptible to photolytic free radical autooxidation, which involves direct formation of free radicals when exposed to high energy light such as UV. Most retail stores use fluorescent light which is designed to generate only a very limited photon flux of such detrimental wavelengths [5]. Similarly, aromatic amino acids, i.e. tryptophan, tyrosine and phenylalanine, can absorb UV light below 310 nm, which can result in direct photochemical changes, but it is not the main contributor responsible for oxidative byproducts.

A photosensitizer, such as riboflavin, will absorb light energy and cause photosensitized oxidation and result in the generation of oxidative active

compounds, which can cause further oxidative decomposition of milk proteins, lipids and vitamins.

2.1.1. Photosensitized oxidation

Photosensitized oxidation is a light-induced oxidation which occurs in the presence of photosensitizers such as chlorophyll and riboflavin, and generates free radicals or singlet oxygen via Type I or Type II mechanisms, respectively (Figure 1). The conjugated double bond structure of riboflavin readily absorbs visible light energy ($h\nu$) [17] and forms an excited singlet state, $^1\text{Rib}^*$, which by intersystem crossing forms a triplet state, $^3\text{Rib}^*$. Triplet riboflavin subsequently generates substrate radicals and/or superoxide anions (Type I), or yields singlet oxygen (Type II). Competition between substrate (Sub), i.e. proteins or lipids, and oxygen ($^3\text{O}_2$) for triplet riboflavin ($^3\text{Rib}^*$) determines the predominant reaction path. The type I reaction is predominant under conditions of high reactivity and/or concentration of substrates, low oxygen concentration in the system, or short singlet oxygen lifetime. Milk has low oxygen solubility and, therefore, the type I path may be predominant, compared to a lipid-based system such as olive oil containing chlorophyll as the photosensitizer. However, studies using Electron Spin Resonance Spectroscopy (ESR) have found evidence of singlet oxygen formation in light-oxidized skim milk [18].

The activation energy of photochemical reactions is often much lower than that of non-photochemical reactions. The activation energy of oxygen in the singlet state ($^1\text{O}_2$) and the triplet state ($^3\text{O}_2$) is only 92 and 104 kJ/mol higher than

the ground state, respectively. The energy associated with any region in the visible spectrum is sufficient (e.g. the energy of a photon at 800 nm is 149 kJ/mol) to produce singlet oxygen in the presence of a photosensitizer such as riboflavin [4]. The temperature dependency of photosensitized oxidation is usually negligible in the temperature range of food storage due to its low activation energy, although temperature does affect the decomposition processes initiated by singlet oxygen [5].

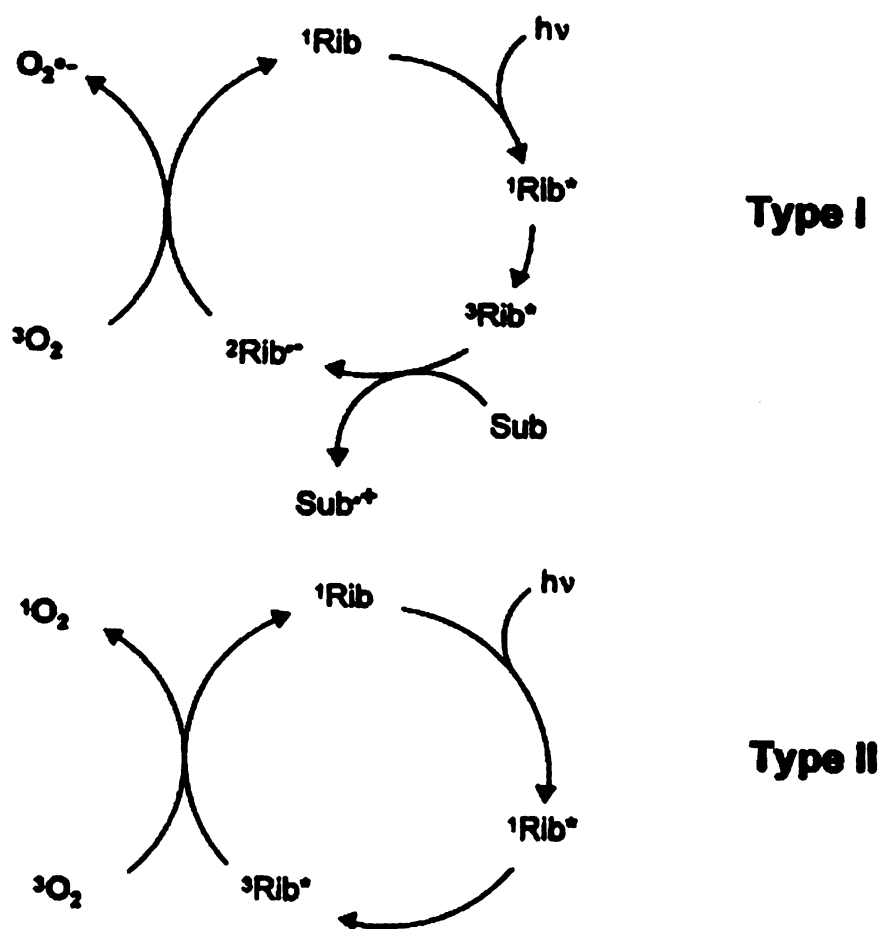


Figure 1 Mechanisms of photosensitized oxidation catalyzed by riboflavin, the photosensitizer. Riboflavin (Rib) absorbs a photon ($h\nu$) and forms an excited singlet state, $^1\text{Rib}^*$, which by intersystem crossing forms a triplet state, $^3\text{Rib}^*$. Triplet riboflavin subsequently generates substrate radicals and/or superoxide anions (Type I), or yields singlet oxygen (Type II) (modified from [3], Figure 3).

2.1.1.1. Degradation of milk proteins

Reaction of singlet oxygen with sulfur-containing amino acids, e.g. methionine, results in the “sunlight flavor” or “activated flavor”, which is described as “burnt feather”. The oxidative degradation of methionine results in the formation of low molecular weight sulfur-containing volatiles such as methional or dimethyldisulfide [19, 20] (Figure 2). Methional is relatively unstable and breaks down into more stable components, including mercaptans, sulfides, and disulfides [1, 21]. In skim milk an increased level of dimethyldisulfide was found with an increased level of sensory off-flavor scores [20]. The formation of dimethyldisulfide requires only cleavage of the methionine side chain and thus it is more likely to occur than methional formation, which depends on cleavage of the protein backbone [3, 5].

Several studies have shown the effects of light exposure on amino acids and milk proteins, such as photoaggregation of whey proteins [22] and loss of amino acids, e.g. methionine, cysteine and tryptophan [23-25]. However, other studies designed to evaluate the level of amino acid destruction in commercially packaged milk under fluorescent light exposure have found insignificant changes in the amino acid content. Dimick (1973) [7] exposed homogenized milk in half-gallon containers (fiberboard, blow-molded plastic, and glass) to 100 ft-c (1076 lx) of fluorescent light for 144 hours, which resulted in no significant difference in the amino acid concentration when compared to the unexposed control. Hedrick and Glass (1975) [26] drew a similar conclusion by comparing the amino acid content

of 17 amino acid in milk packaged in paperboard and plastic gallon containers subjected to 150 ft-c (1614 lx) of fluorescent light.

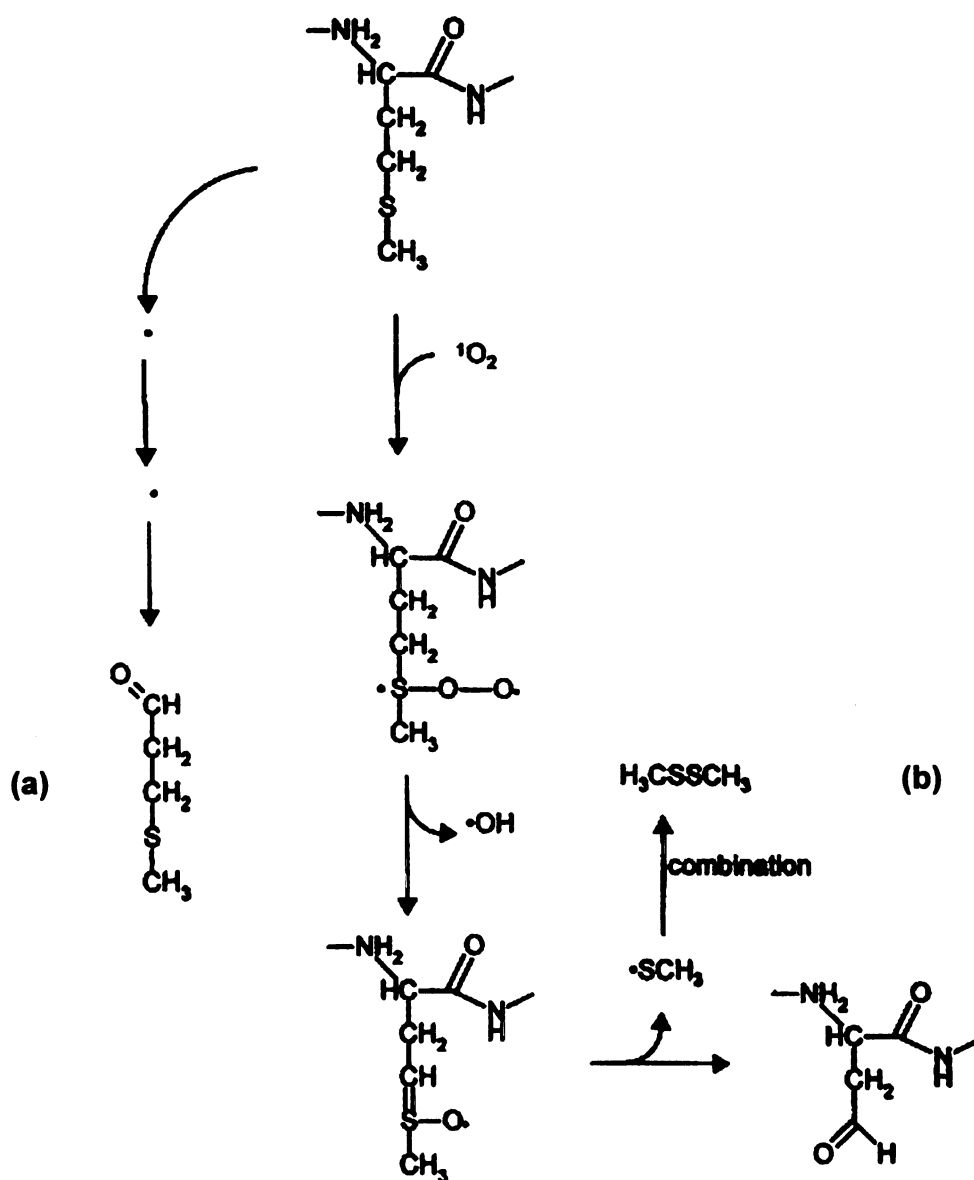


Figure 2 Mechanism of methionine reacting with singlet oxygen ($^1\text{O}_2$): (a) The formation of methional depends on cleavage of the protein backbone; (b) dimethyldisulfide is formed by cleavage of the methionine side chain (modified from [3], Figure 1).

2.1.1.2. Oxidation of milk lipids

The “cardboardy” or “metallic” off-flavor is caused by oxidation of unsaturated fatty acids in milk lipids, particularly phospholipids [27], and is initiated by free radicals or singlet oxygen (Figure 3).

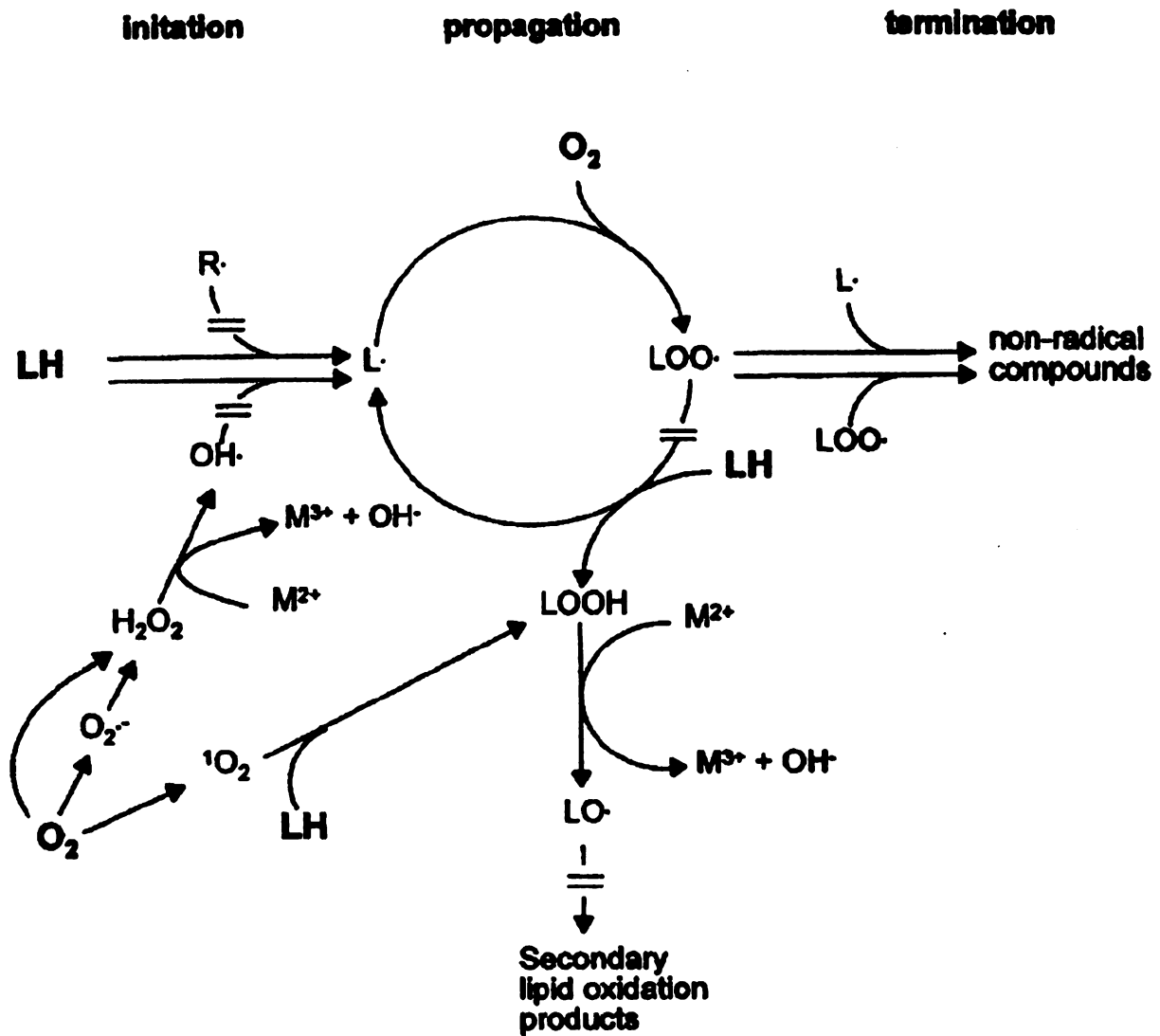


Figure 3 Lipid oxidation initiated by free radicals ($O_2^{\cdot-}$ or $R\cdot$) or singlet oxygen (1O_2), which is generated in the presence of riboflavin. Autooxidation involving cleavages of lipid hydroperoxides ($LOOH$) depends on the presence of catalytic metal ions (M^{2+}) or enzymes such as peroxidases. The sign “=” indicates reactions affected by primary antioxidants (from [3], Figure 2).

Secondary lipid oxidation products are formed when lipid hydroperoxides decompose to alkanes, alkenes, aldehydes, alcohols, ketones, esters, and acids. Due to their low sensory thresholds, the unsaturated aldehydes and ketones are usually considered the primary sources of oxidized off-flavors. Odor-active compounds such as hexanal and pentanal have been found to increase in milk on exposure to fluorescent light, where hexanal is the predominant lipid oxidation byproduct in light-oxidized milk [28].

2.1.1.3. Vitamin destruction

Riboflavin (0.41 mg riboflavin in 8 oz. of milk, [29]) is consumed rapidly when exposed to light, and the two main photosensitized oxidative pathways are cyclic (Figure 1). The degradation is probably due to attack by some of the activated oxygen species generated by deactivation of the excited states of riboflavin, including singlet oxygen, superoxide, peroxides, and the hydroxyl radical [3]. Photolysis of riboflavin in aqueous solutions is proportional to time of light exposure and light intensity [30]. The decrease in riboflavin content has been used to indicate the extent of riboflavin-sensitized light oxidation in milk [31-33] and other dairy products [34-36], and the effectiveness of the package used to protect the milk [37, 38] or other dairy products [39, 40] from light oxidation.

Besides riboflavin (vitamin B₂), other nutrients such as vitamin A and its precursor carotenoids, other B vitamins, vitamin C (ascorbic acid), and vitamin D are also light sensitive. The oxidative reactions affecting these nutrients can be affected by the presence of riboflavin [1, 3], especially by the singlet oxygen generated in photosensitized reactions (Figure 1).

Naturally occurring vitamin A and its precursors (retinol and retinyl esters) in milk (about 10-60 µg/100mL) were found to be relatively more stable to light exposure than riboflavin [1]. However, a significant reduction in vitamin A (retinyl palmitate) was caused by light exposure in supplemented low fat and nonfat milks containing vitamin A fortification levels between 2000 and 3000 IU per quart (Federal Regulations 21 CFR 131.135 and 21 CFR 131.143 for low fat and nonfat milk, respectively) [41]. It was reported that 50% loss of total vitamin A occurred in milk packed in HDPE containers exposed to 200 ft-c (2152 lx) fluorescent light for 3 hours [42]. A more recent study showed that even a brief, moderate light exposure (2000 lx for 2 hours) can significantly reduce the vitamin A content in reduced fat (2%) and skim milk in HDPE gallon containers [41]. The photostability of fortified vitamin A is affected by the carrier used and the chemical form of the vitamin [43, 44].

The vitamin C (ascorbic acid) content is about 2 to 5 mg/100g in fresh milk [45]. Its degradation was found to be proportional to the amount of light transmitted into the container in the presence of riboflavin. The stability of ascorbic acid is maintained in the absence of riboflavin [46, 47]. Ascorbic acid, acting as a singlet oxygen quencher, has been reported to effectively reduce the level of dimethyl disulfide and other oxidative volatiles generated in photosensitized oxidation in the presence of riboflavin [20, 48-50].

Light exposure is essential to change provitamin D into vitamin D and its related compounds [51]. However, vitamin D can be also be destroyed by riboflavin-photosensitized oxidation. Light accelerates the loss of vitamin D in

skim milk containing riboflavin, but that decomposition rate was not affected by light in a model system in the absence of riboflavin [52]. Similar results were observed in two other studies [51, 53], though oxidation of vitamin D was not observed in the systems without riboflavin under light exposure, nor in those with riboflavin but stored in the dark.

2.1.2. Wavelength dependent impact of light

Light absorption and light stability (i.e. quantum yield) of photosensitizers and other light sensitive components are wavelength dependent. Light sources with distinct spectral distributions can have very different impacts. Yellow colored lighting, which filters out the light below 500 nm, is suggested for dairy retail displays [54, 55] to reduce the photosensitized oxidation in the presence of riboflavin.

2.1.2.1. Light absorption

Only absorbed light can initiate chemical reactions [3]. Riboflavin as the photosensitizer in milk and dairy products has three absorption bands as shown in Figure 4. The third band in the visible region (blue to green, broad maximum at 430–460 nm) is the main band responsible for the photosensitized oxidation in milk and dairy products [4].

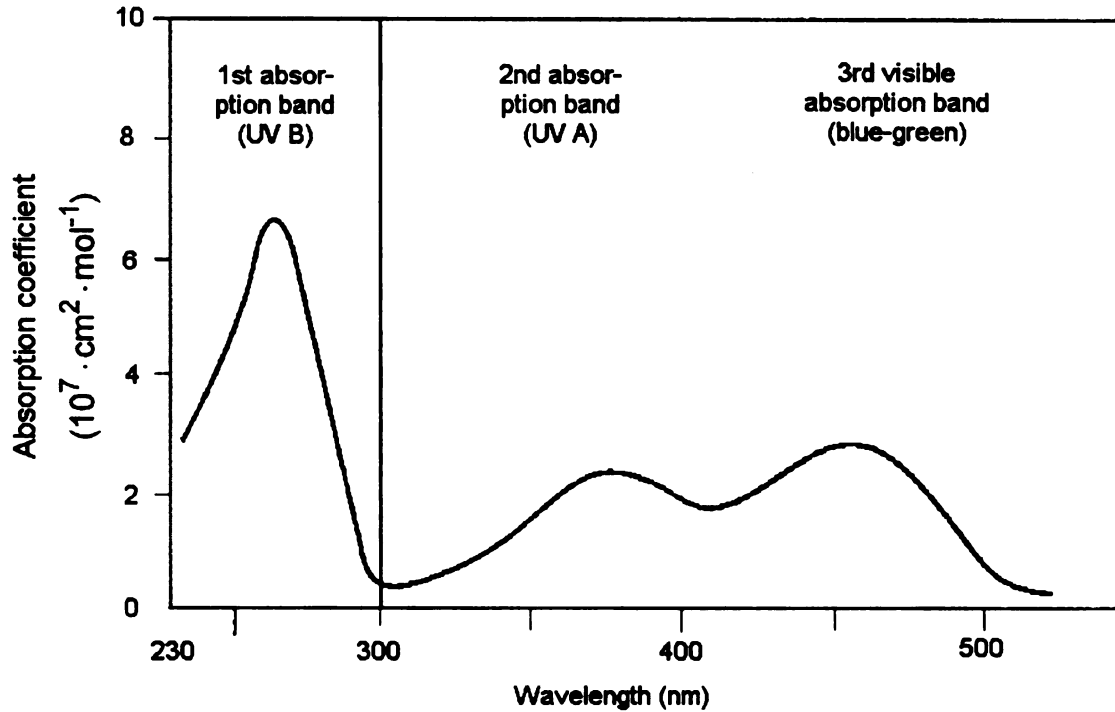


Figure 4 Absorption spectrum of riboflavin at different wavelength (from [4], Figure 3).

Other photo-sensitive components in milk such as vitamin A (retinyl palmitate) and vitamin C (ascorbic acid) have strong absorption bands at maximums of 325 and 270 nm, respectively (Figure 5). Protection from light at these wavelengths (UV range < 380 nm) may protect vitamin A and C from primary photooxidation; however, photosensitized oxidation in the presence of riboflavin can still cause losses of vitamin A and C in most of the visible light region [4], especially the light below 500 nm [54, 55].

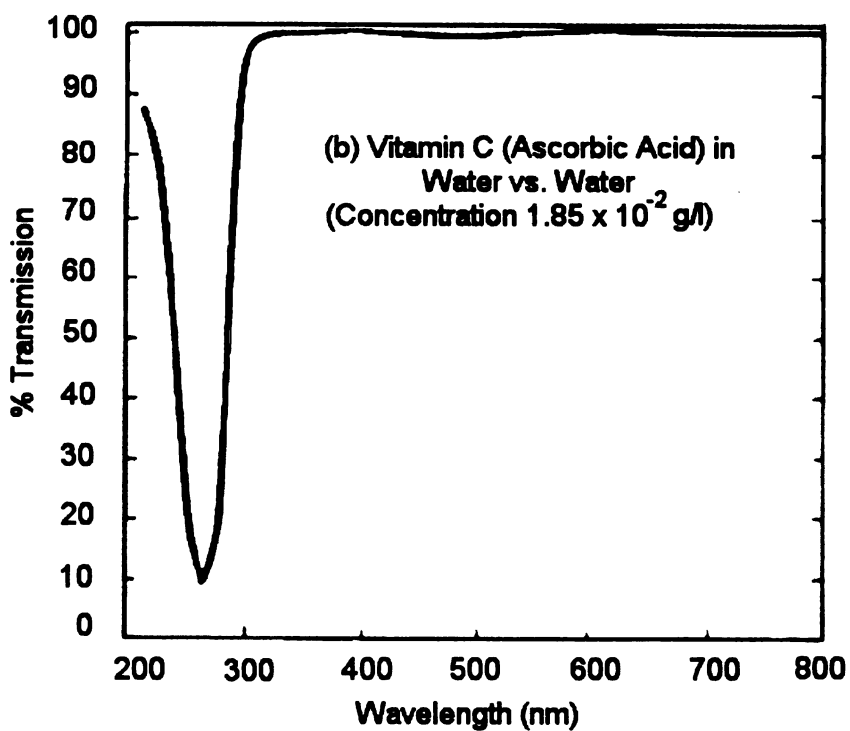
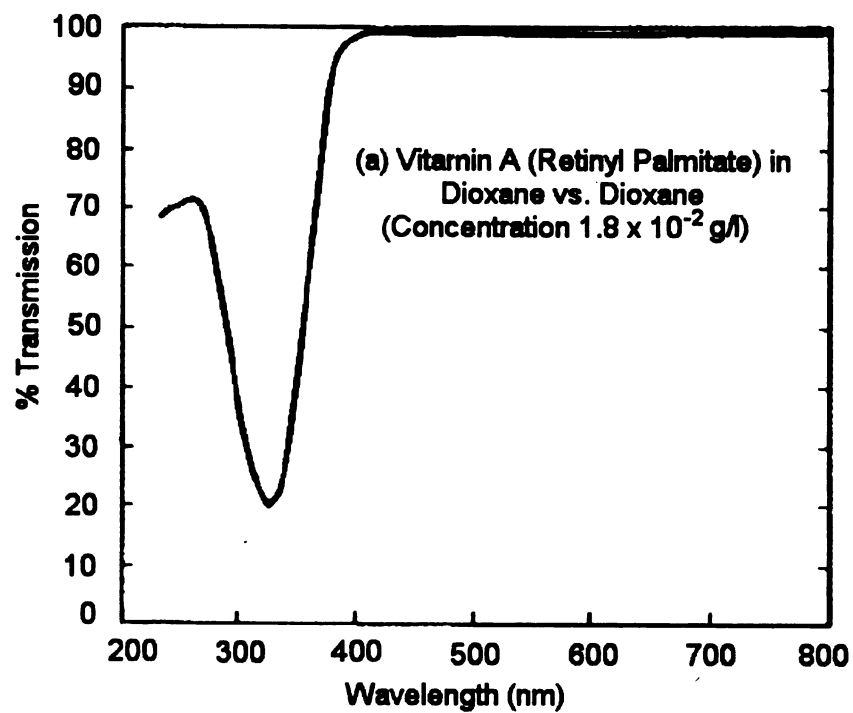


Figure 5 Absorption spectra of (a) vitamin A and (b) vitamin C (modified from [37], Figure 3).

2.1.2.2. Quantum yield

The quantum yield can be explained as the light stability (or sensitivity) of molecules at varying wavelengths. This parameter has been suggested as a replacement of rate constants for light-induced changes in foods [3]. It is defined as the number of molecules converted by one photon, as shown below:

$$\Phi = \frac{\text{molecules reacted}}{\text{photons absorbed by reacting compound}} = \frac{\Delta C_i}{Q_i}$$

where ΔC_i is the change in concentration of the specific compound during a period of time resulting from the number of photons absorbed by the compound, Q_i , during the sample period. Quantum yield ranges between zero and one, with the exception of chain reactions where Φ may be larger than one. Combining the absorption spectra with light intensities at different wavelengths allows the calculation of the number of photons absorbed [3].

The apparent quantum yield is based on total light absorption and may be used for comparison with photo-induced processes in comparable systems, as shown below:

$$\Phi_{app} = \frac{\text{moles reacted}}{\text{photons absorbed by food matrices}} = \frac{\Delta C_i N_A m}{Q_{total}}$$

where ΔC_i is the change in concentration of the reacting compound determined by a specific chemical analysis such as gas chromatography, N_A is Avogadro's number, m is the mass of the illuminated sample of food matrix, and Q_{total} is the total number of photons absorbed by the system. Assuming no light transmission and minimum reflection from the food matrix, the apparent quantum yields were

calculated for the secondary oxidation volatiles generated in light-induced oxidation of Havarti cheese [36].

2.1.2.3. Light sources

Different light sources, e.g. sunlight or fluorescent light, can have very different emitting spectra (Figure 6), and therefore can have very different impacts on light sensitive food ingredients. The light sources with high light emission at the critical wavelength ranges (considering both the light absorption and quantum yields) are expected to cause more product damage. Since light oxidized off-flavors in milk and dairy products are mainly generated by riboflavin photosensitized oxidation, light sources with lower emission below 500 nm are believed to be less harmful, since the absorption band of riboflavin at 430–460 nm is believed to be the main band responsible for photosensitized oxidation [4]. For instance, warm white fluorescent lights generally have less impact than cool white lights.

Alternatively, filtering out the light in the critical wavelength ranges can reduce the impact of light. Use of pigmented packaging materials or putting a colored filter directly on the light source can reduce the light transmission in specified wavelength ranges. To protect milk and other dairy products from photosensitized oxidation, it is critical to filter out the visible light below 500 nm, particularly at the harmful blue-violet visible range of 400–500 nm, by colored or opaque light barriers (Figure 7, [56]). IDF (International Dairy Federation)

recommends that the maximum permissible light transmission through packaging material should be 8% at 500 nm and 2% at 400 nm [57, 58].

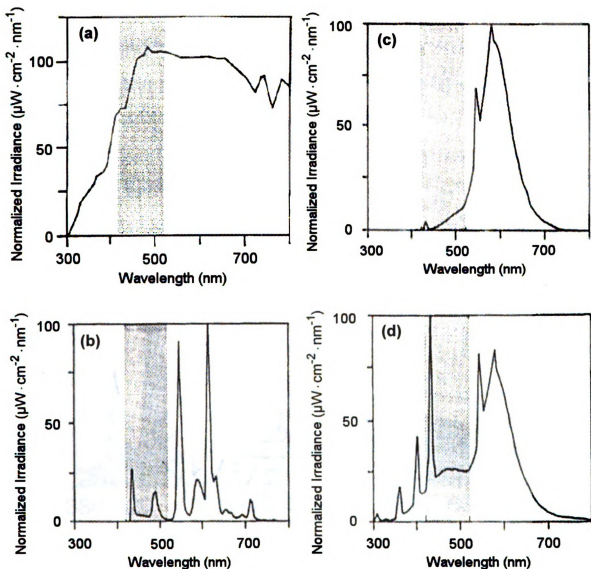


Figure 6 Emission spectra of (a) sunlight, (b) Philips 83/36 W white, (c) Philips 16/40 W yellow, (d) Philips 33/40 W white (modified from [2], Figure 3).

A light source or packaging material with reduced light transmission below 500 nm has a yellow appearance, since relatively more yellow-orange-red light (i.e. above 500 nm) is perceived by human eyes (Figure 7). Hansen *et al.* (1975) [55] studied the effects of colored lamps and lamp filters on milk packaged in HDPE containers, and found that yellow lamps or yellow/green filters protected milk from light-induced oxidation, where the off-flavor development was delayed from 5-7 hours (cool-white lamp) to 30-40 hours (yellow lamp).

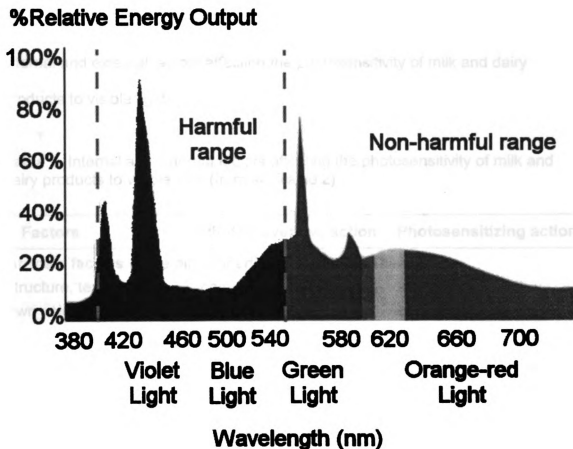


Figure 7 Energy output for a typical supermarket white lamp (modified from [56], Figure 1).

2.1.3 Occurrences of light-oxidized off-flavors in milk

Light-oxidized off-flavors in milk have been widely studied [2-4, 27, 59]. Since the 1960's, many studies have been conducted using various light exposure conditions, e.g. light sources with different spectral emissions, light intensities (distance-dependent), exposure times, and storage temperatures. Milk composition (e.g. fat or prooxidant/antioxidant contents) and packaging size/material also significantly affect the development of light-induced off-flavors. In addition, sensory scores and measurement of headspace volatiles are often used to define the occurrence of light-oxidized off-flavors. Table 1 lists the internal and external factors affecting the photosensitivity of milk and dairy products to visible light.

Table 1 Internal and external factors affecting the photosensitivity of milk and dairy products to visible light (from [4], Table 2).

Factors	Photopreventive action	Photosensitizing action
Intrinsic factors (generally properties of the product itself)		
Structure, texture	compact, scattering	translucent
Own coloration	dark	colorless, bright
Content of	reducing substances/ antioxidants	(pro)oxidants
- vitamins	C (ascorbic acid)	B ₂ (riboflavin)
- unsaturated fatty acids	--	peroxide formation
- fat	photodiffusion	degree of unsaturation
- heavy metals	--	catalysis (e.g. Cu ⁺⁺)
- dissolved O ₂	reducing microflora	synergy with light
- free amino acids (proteolysis)	--	formation of methional

Table 1 (continued)

Factors	Photopreventive action	Photosensitizing action
Heat treatments:	harsh	gentle
pasteurization, UHT treatment, etc.	formation of –SH (= reducing)	formation of –S-S- (= oxidants)
Mechanical treatment:		
homogenization	?	?
Extrinsic factors (to be considered)		
Source of light		
spectrum UV ($\lambda < 350$ nm)	“cut-off” (material)	–
source: day light	–	high energy available
source: artificial light	“white warm”	“white cold”
light (= intensity)	weak	strong
duration of the exposure	short	long
Geometry		
distance from the source	great	short
presentation, disposition of products	closely packed	dispersed
possible auxiliary means	framed crate, baskets	–
Packaging		
light transmission of packaging	weak/zero	high
- with coloring	brown-red	blue-green
- with pigmentation	turbid/light scattering	translucent
material thickness	thick	(ultra)thin
oxygen permeability	weak/zero	high
Storage		
effect of temperature on:		
- O ₂ solubility	room temperature	low
- activation energy	low	room temperature
shelf life	short	long

According to the Plastic Bottle Institute, approximately one half of the fluid milk products in plastic containers remain in the dairy case (and therefore maybe exposed to light) for at least 8 hours [6, 9]. A New Zealand study revealed that the fluid milk turnover time may be as much as 2-3 days, resulting in severe light exposure [10]. Light intensity depends on the light source as well as distance from the light source, with ranges reported from 80 to 12000 lx in dairy retail display cabinets [5]. Measurements took place in dairy cases bearing products in 5 supermarkets and 3 convenience stores in the area around Ithaca, New York, with light intensities ranging from 750 to 6460 lx [6]. Different packaging materials have different light barrier properties, and different container sizes have different surface-to-volume ratios, which results in various light exposure conditions for the fluid milk.

Dunkley *et al.* (1963) [54] reported that the minimum light exposure conditions to develop a detectable “light flavor” for milk in clear quart bottles (946 ml), were one half inch from a cool white lamp, for 20 minutes. Satter and deMan (1973) [60] exposed homogenized whole milk in returnable plastic 3 quart jugs (2.84 L) to 100 ft-c (1076 lx) and 200 ft-c (2152 lx) of 40W cool-white fluorescent light, which resulted in significant off-flavors in 12 and 3 hours, respectively, as determined by 12-18 trained panelists using a duo-trio test. Dimick (1973) [7] and Coleman *et al.* (1976) [8] tested homogenized milk in half-gallon (1.89 L) plastic containers and reported that the milk had a sharply decreased flavor score after 12 hours of light exposure (100 ft-c, i.e. 1076 lx) at a refrigerated temperature. Hansen *et al.* (1975) [55] reported light oxidized off-

flavors in milk stored in HDPE containers and exposed to 200 ft-c (2152 lx) of cool-white fluorescent light at 3.3°C. The light oxidized off-flavor was first perceived by a trained panel at 2-4 hours, and a more intense off-flavor was developed at 5-7 hours, which was expected to be detectable by average consumers.

Chapman *et al.* (2002) [6] exposed 2% milk in HDPE gallon (3.785 L) containers to 2000 lx of fluorescent light at 6°C, which resulted in a significantly detectable quality change for a 10-member trained panel in 30 minutes, and for a 94-member consumer panel in 2 hours. The minimum light exposure times in order for the quality change to be noticed by 50% of the panelists, determined by interpolation, were 15 minutes and 54 minutes for trained and consumer panels, respectively. The tests were performed using a semi-ascending paired difference method [61] with an 11-point intensity line scale of difference from control. In another study [62], it was shown that half of the teen and adult consumers could detect an off-flavor in less than 2 hours of light exposure. The light-oxidized milk was objectionable to teen consumers.

2.2. Effects of milk packaging

Storage of milk in different packaging materials may affect milk quality by impacting the development of packaging and light-oxidized off-flavors. Packaging off-flavors from high density polyethylene (HDPE), polyethylene terephthalate (PET), and PE-coated paper cartons has been reported as “plastic”, “bitter”, “oxidative”, or “lacks freshness”. On the other hand, packaging materials with good light barrier properties minimize the impact of fluorescent lighting in retail display, and reduce light-oxidized off-flavors.

2.2.1. Off-flavors from milk packaging materials

Potential migrants in milk packaging materials may cause a defect referred to as “packaging off-flavors” in beverages such as milk. Migrants may include oxidative hydrocarbons from processed HDPE, PET and plastic coated paper cartons, or solvents used during lamination, coating or printing processes. Shelf-life needed and storage temperatures of various milk products are also critical factors. For instance, fresh milk is expected to be stored at refrigerated temperature for less than two weeks, while UHT aseptic milk may have a shelf-life greater than six months at room temperature.

Studies using gas chromatography (GC) have been widely conducted to identify the problematic compounds. An “indicator” compound, e.g. hexanal, is used to “measure” the extent of oxidative degradation and is often correlated to the off-flavor intensity. In order to precisely reveal the actual consumer impact of the packaging off-flavor, sensory evaluation is essential. It has been suggested

that sensory evaluation is the most reliable way to determine off-flavors originating from packaging [63].

2.2.1.1. Polyethylene (PE)

Polyethylene, especially high-density polyethylene (HDPE), dominates the milk packaging business because it is low-cost, durable and lightweight [64]. Off-flavors in milk packaged in polyethylene containers have been described as “plastic”, “off-flavor”, “bitter”, and “oxidative”. It was found that the off-flavor compounds were already present in the granular PE [11, 65, 66], and the converting and extrusion processes may further increase the amount of off-flavor volatiles [67]. Oxidative hydrocarbons generated at high temperature and/or substantial shear stress during processing, may be present at the surface of polyethylene pouches or bottles [11, 65]. Those low molecular weight byproducts from oxidation or thermal degradation may migrate to food systems, such as water or milk, and result in off-flavors. Addition of antioxidants, e.g. Irganox 1010, butylated hydroxytoluene (BHT) and α -tocopherol, are often used to reduce the oxidation and thermal degradation of polyethylene [68-70]. Other potential migrants (but which may not be significant) [67] from PE containers include antioxidants, plasticizers, solvents, and other additives used in making or converting polyethylene.

Although alkanes and alkenes make up a significant portion of the thermal degradation fragments of polyethylene [71], aldehydes and ketones are of particular concern, due to their low odor thresholds and high polarity, which make

them more likely to desorb from a non-polar polymer like polyethylene [71, 72]. Using a gas chromatography/olfactometry technique (GCO), Bravo (1992) [11] found that 14 odor-active compounds were present, but only eight of them were identified, i.e. hexanal, 1-hepten-3-one, 1-octen-3-one, octanal, 1-nonen-3-one, nonanal, trans-2-nonenal, and diacetyl. A “wax-like” descriptor was assigned to the overall odor, while the individual components were fruity, herbaceous, rancid, metallic, waxy, pungent, or orangy. The study confirmed that α -unsaturated aldehydes and ketones are responsible for much of the off-odor associated with thermally oxidized polyethylene.

Polyethylene used for milk packaging is formed as mainly blow-molded high-density polyethylene (HDPE) jugs, low-density polyethylene (LDPE) pouches, and the inner LDPE seal layer of paper cartons. Ho *et al.* (1995) [71] evaluated the packaging off-flavors in drinking water contained in blow molded HDPE bottles containing various antioxidants (vitamin E, Irganox 1010, and BHT), using sensory evaluation and purge-and-trap GC-MS. Forty-seven volatiles, including n-alkanes, 1-alkenes, aldehydes, ketones, phenolics, olefins, and paraffins from C6 to C18, were identified. The acceptability of the water was correlated inversely with intensity of odor and taste sensory scores, as well as the concentrations of aldehydes and ketones present. Maneesin (2001) [73] reported that storing water in HDPE containers (processed at 204°C with addition of Irganox 1010) for three months imparted significant off-flavors, using nonanal content in water as the off-flavor indicator, along with different-from-control sensory tests and headspace analysis using an electronic nose.

Compared to HDPE, LDPE is in general processed under more vigorous conditions, i.e. higher processing pressures and temperatures [73], and therefore the off-flavors from LDPE pouches and coatings may be more of a concern [72, 74]. Srivastava and Rawat (1978) [75] reported that paper/aluminum/polyethylene pouches tolerated heat (75-90°C in boiling water) but imparted “plastic flavor” to milk, in terms of their consumer acceptability.

Many studies have been conducted to investigate the use of polyethylene as a milk packaging material; however, due to its transparency, quite often light-induced off-flavors are more pronounced than packaging off-flavors.

2.2.1.2. Polyethylene terephthalate (PET)

“Portability improves profitability” [76] and reflects the growing market for single-serve milk packages. Polyethylene terephthalate, an attractive packaging material with high clarity, low oxygen transmission rate, considerable mechanical strength, light weight and versatility [64], is becoming an increasingly popular packaging material for milk. However, an odorous degradation product from PET processing (acetaldehyde) is a concern in PET packaged water and milk.

Van Aardt (2001) investigated the origination and sensory impact of acetaldehyde in milk [12, 77]. Since PET is a clear, transparent material, and acetaldehyde is a contributor to light-oxidized off-flavors, acetaldehyde in milk may be present due to both light-induced oxidation and migration from PET. Sensory detection group thresholds of acetaldehyde in milk containing 3.25%, 2%, and 0.5% fat were determined to be 3939, 4020 and 4040 ppb, respectively,

with no statistically significant difference among differing fat levels. Headspace analysis (SPME-GC) showed that fluorescent light exposure (1100-1300 lx, 4°C, 18 days) resulted in an increase of acetaldehyde in milk. However, a trained panel using a nine-point sensory scale was not able to detect acetaldehyde in either light-exposed or light-protected samples. It was found that acetaldehyde levels in milk stored in various packaging materials (glass, HDPE, clear PET, clear PET with UV absorber and amber PET) were all below the human flavor threshold.

2.2.1.3. Paper cartons

Paper cartons, such as gabletops or Tetra-Pak (Brick-Paks), are widely used for pasteurized milk including ultra-high temperature sterilized (UHT) milk. One or more polymer layers are combined with paperboard, to provide good barrier properties, heat resistance and printability [64]. An aluminum layer may also be added to increase the light and oxygen barrier properties of paper cartons. Mehta and Bassette (1978, 1980) [78, 79] reported that UHT milk in aluminum foil-lined cartons, as judged by a 5-member trained panel and a 24-member untrained consumer panel, was not as good as freshly pasteurized milk, but superior to milk in plain polyethylene-lined cartons. A positive correlation was found between the off-flavor intensity and the n-pentanal concentration.

Off-flavors recognized as “lacks freshness” [80] or “stale” [78] in paper carton packaged milk were found to significantly impair the milk acceptance [13,

81]. Often the off-flavors are the result of oxidative hydrocarbons migrating from the LDPE inner coatings [67].

Leong *et al.* (1992) [13] investigated the packaging off-flavor in water and in homogenized milk with fat contents of 3.25%, 2% or 0.05%, packaged in PE-coated paperboard cartons for one, three or six days at 2.2°C. Paired comparison tests were performed by a 10-member screened panel. It was found that packaging off-flavor in water and milk was recognized within one day of storage, with no significant increase in the off-flavor intensity in the following three days of storage. Smaller size cartons had a more intense packaging off-flavor, since the surface area to volume ratio is larger for smaller containers. Heat sealing did not contribute significantly to the packaging off-flavor.

Gandhi (1996) [81] had elementary school children (2nd through 5th grades) taste reduced fat (2%) milk in half-pint (237 ml) PE-coated paperboard cartons (stored for three days at 2.2°C), and evaluated the results using a two-sided paired preference test and a nine point hedonic scale. The results indicated that the elementary school children had a significantly higher preference and acceptability rating for the control, milk stored in glass containers, than for milk in cartons. The same samples were evaluated by an 11-member trained panel using a paired comparison test, and the flavor difference between milk in glass and cartons was also recognized.

2.2.2. Light barrier properties of packaging materials

To protect milk and other dairy products from photosensitized oxidation, it is critical to filter out the visible light below 500 nm, particularly in the harmful blue-violet visible range of 400-500 nm, using colored or opaque light barriers [56]. Figure 8a shows the light transmission at various wavelengths for different milk packaging materials. Glass allows the highest light transmission through the UV and visible ranges of the spectrum. Compared to the natural (unpigmented) HDPE, the addition of UV absorber eliminates the light transmission below 400 nm but not between 400-500 nm. Yellow pigments significantly reduce the light transmission below 500 nm, and the bright yellow pigment is more effective than the pale yellow pigment. White pigment (titanium oxide, TiO_2) reduces the light transmission but will still allow partial light transmission at 400-500 nm. Paper cartons (Figure 8b) have the least light transmission and offer the best light protection to milk. The light transmission through PE cartons is below the recommendations from IDF (International Dairy Federation) for pasteurized milk [58]. IDF recommends that the maximum permissible light transmission through packaging material should be 8% at 500 nm and 2% at 400 nm [57].

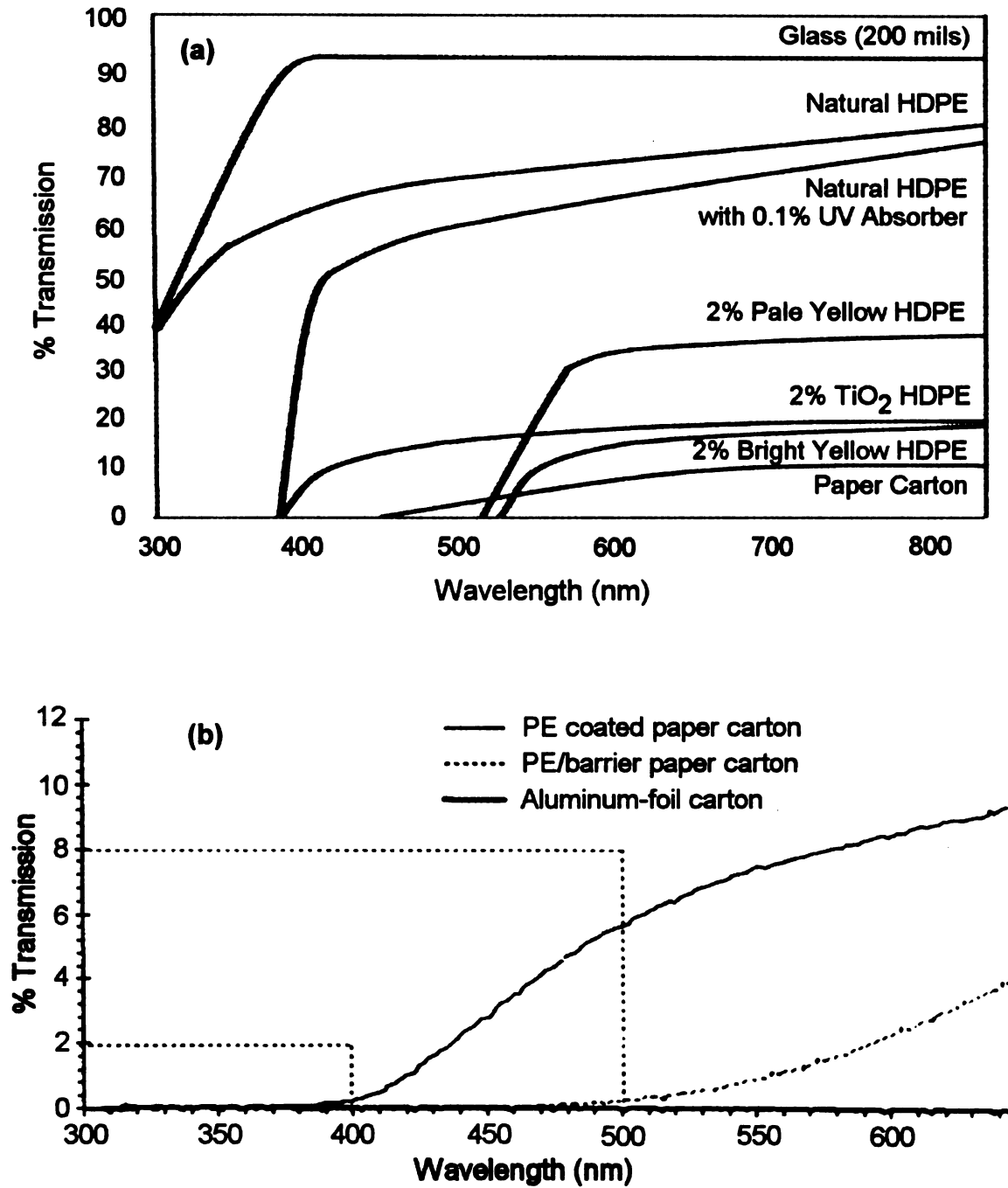


Figure 8 Light transmission through various packaging materials. (a) Glass, unpigmented HDPE and HDPE with yellow or white pigments (20-22 mils), and paper carton (modified from [56], Figure 3); (b) PE, non-foil barrier and aluminum-foil cartons. The dotted lines indicate IDF recommendation limits (modified from [58], Figure 6).

Since the 1960's, the effect of packaging material on light induced quality deterioration of milk has been widely studied [7, 8, 32, 33, 55, 60, 77, 82-86]. Satter and deMan (1973) [60] reported that opaque pouches protected milk from light induced quality changes (24 hours of cool-white fluorescent light, 1076 lx or 2152 lx); paper cartons protected milk up to 12 hours but not longer; HDPE jugs offered less light protection (3 hours at 2152 lx and 12 hours at 1076 lx), and clear pouches provided the least light protection (3 hours at 2152 lx and 6 hours at 1076 lx). Dimick (1973) [7] reported that paperboard containers protected milk from light-oxidized flavor changes up to 48 hours, whereas milk in plastic and glass containers developed the off-flavor following only 12 hours of exposure (1076 lx). Coleman *et al.* (1976) [8] evaluated milk stored in HDPE jugs and unpigmented and colored (yellow, red, blue and black) paper cartons and exposed to cool-white fluorescent (1076 lx). It was found that all paper cartons offered greater protection to light induced flavor changes than did HDPE jugs, and there were no significantly different protection effects for the paper cartons printed in different colors. Pouches of milk packaged in different PE overwraps of varying light transmittances (printed white/yellow, aluminum ink, or coextruded black/white pigments) [83] and aluminum foil shields on the bottom and the top of the HDPE jugs [33] were proposed to provide additional light protection. Van Aardt *et al.* (2001) [77] reported better milk quality retention in amber PET and UV compounded PET than in clear PET bottles.

2.2.3. Other packaging factors affecting milk quality

2.2.3.1. Size and shape

Size and shape directly affect the diffusion rates of the migrants and have an effect on the packaging off-flavors in milk. For example, Leong *et al.* (1992) [13] reported a significantly stronger packaging off-flavor in milk packaged in half-pint (237 ml) paper cartons than milk in quart (946 ml) and half-gallon (1893 ml) containers, after 6 days of storage at 2.2°C. The ratio of surface area to volume can be used as a measurement of the size/shape factor. The higher the ratio, the relatively larger surface area is available for migration per unit volume, and therefore the packaging off-flavor is likely to be more significant.

Light penetration also depends on the ratio of surface area to volume, or more precisely (but also more difficult to define), the ratio of surface area that is exposed to light, e.g. the top surface of a package, to the package volume. Dunkley *et al.* (1963) [54] mentioned in a comparison of glass pint (473 ml), quart (946 ml) and half-gallon (1893 ml) bottles, the intensity of light oxidized off-flavor produced by one hour exposure was inversely related to the container size.

Packaging size also affects the microbial stability of milk. Erickson (1997) [87] compared milk in 1 liter pouches, 2 liter PE-coated paper cartons, and one gallon (3.785 L) HDPE jugs. Slightly higher microbial populations (total and psychrotrophic counts) were found in milk packaged in the larger containers, and in milk whose package had been opened and dispensed. It was suggested that a unit gallon of milk may remain fresher when packaged in multi-unit packages than if packaged in one single container.

2.2.3.2. Oxygen permeability

Good oxygen barrier properties are more critical for long shelf life milk products such as UHT milk. Rysstad *et al.* (1998) [58] evaluated the sensory and chemical shelf life of UHT milk stored in aluminum-foil, non-foil barrier (X-board), and PE cartons, with oxygen transmission rates of ~0, 10-20 and >1000

$\frac{\text{ml}}{\text{m}^2 \cdot 24 \text{ h} \cdot \text{atm}}$, respectively. The light transmission properties of these three

paperboards are shown in Figure 8b. At 6°C with no light exposure, milk in PE cartons had significant off-flavor after 24 weeks, while in the other two materials (which were better oxygen barriers) there was no off-flavor detected in 26 weeks. When exposed to light, off-flavors developed in PE cartons after 2 weeks, in X-board after 8 weeks, and were not detected in milk stored in aluminum-foil cartons.

For fresh pasteurized milk, the oxygen in the packaging headspace, in addition to the oxygen dissolved in the milk, is usually sufficient to induce light oxidation, which usually can be initiated in a relative short period of time (from 15 minutes to 12 hours).

2.3. Light oxidation of cheese

Light-induced oxidation may take place if cheese is exposed to sunlight or fluorescent light, and can lead to quality changes in color and flavor, as well as loss of nutrients or formation of potentially toxic compounds [3]. Cheeses are susceptible to light-induced quality changes, since they are often wrapped in clear transparent packaging materials, in small pieces under fluorescent light in the dairy cases for longer times than milk [34]. Oxidative quality changes are mostly located at the cheese surface [3]. Discoloration and off-flavors caused by light oxidation may lower product quality and marketability [5].

2.3.1. Discoloration of cheese

Color is an important attribute affecting the appearance acceptability of Cheddar cheese. To reinforce natural color and provide appearance to match market preference, annatto extract and β -carotene are the two colorants often used [88]. Annatto is a water-based colorant and more readily dissolves in milk than β -carotene. Discoloration of Cheddar cheese is often associated with annatto, which is susceptible to oxidation and sensitive to processing parameters such as pH and temperature [89].

Hong *et al.* (1995) [90] described the factors affecting light-induced discoloration of annatto-colored cheese. Under light exposure, the surface of Cheddar cheese may experience a slow decrease in redness along with a rapid decrease in yellowness, resulting in a decrease of hue angles (0° for red and 90° for yellow), where the hue angle is defined as $\tan^{-1}(b/a)$ for a (redness) > 0 and b

(yellowness) > 0. Exposure to cool white fluorescent light (vs. warm white), high light intensity, longer light exposure, higher storage temperature (i.e. 8°C vs. 2°C) lower pH (i.e. 4.8 vs. 5.4) reduces the color stability of annatto and results in more severe discoloration. Hong *et al.* (1995) [91] conducted a study to investigate the effects of packaging and lighting. He found that exposure of Cheddar cheese in modified atmosphere packaging (flushed with 99% carbon dioxide prior to sealing) to cool-white fluorescent light (3500 lx) at 8°C for 14 days, resulted in significant decreases in yellowness and hue angles, and the effects were more pronounced when using a packaging film with a higher oxygen transmission rate. Using the same lighting condition, he found that Cheddar cheese in vacuum packaging had slightly lower yellowness values and an increase in redness. Incorporating a UV absorber into the cheese packaging did not improve the color stability, while enclosing it in aluminum foil provided a significantly great protection.

Petersen *et al.* (1999) [88] compared the light sensitivity of annatto and β -carotene, two commercial colorants, to monochromatic light at 313, 366 or 436 nm, in a model system as well as in an industrial scale production. In general, exposure to UV light (313 or 366 nm) caused more color bleaching than exposure to visible light (436 nm). Annatto had higher apparent quantum yields, i.e. more sensitivity to light, than β -carotene, irrespective of wavelength. The light sensitivity of both colorants depended significantly on the combination of pH (5.2 and 5.4) and light wavelength. When exposed to light at 316 nm, annatto was much more unstable at low pH than β -carotene. Lowering the pH increased the

discoloration of Cheddar cheese during light exposure, which may be due to acid-base equilibrium, e.g. between superoxide radical ($O_2^{\bullet-}$) and a more reactive hydroperoxyl radical (HO_2^{\bullet}) with $pK_a \approx 4.8$ [5].

“Pink discoloration” is observed with annatto-colored cheese, has been known and studied since the 1930s. Unlike the light-induced discoloration [90], the pink discoloration is not limited to the surface, but can occur throughout the cheese loaf [92]. Possible causes of this color defect include mold enzymes and acids [93, 94], sulfhydryl compounds [95, 96], precipitation of carotenoids due to hydrogen sulfide [97], fluorescent light exposure [90, 98], and pH [90]. A recent study by Shumaker and Wendorff (1998) [92] reported that cooking temperatures and types of emulsifying salts used had a significant effect on the occurrence of pink color. High cooking temperature resulted in slight decreases in Hunter a and b values, and overall decreases in hue angles. High sodium citrate to disodium phosphate ratio (emulsifying salts) resulted in decreased hue angles. Low cheese pH was expected to accelerate pink discoloration but it did not cause significant color changes in this study.

2.3.2. Light-induced flavor changes of cheese

Oxidation of lipids and proteins contributes to light-induced flavor changes in cheeses. Under fluorescent light exposure, lipids and proteins may experience photosensitized oxidation in the presence of riboflavin, which presents in cheese at levels of 0.30-0.60 mg/100 g [5, 99]. Free radicals and/or singlet oxygen are involved in these oxidative reactions with low activation energies, which can cause further decomposition of lipids and proteins.

Mortensen *et al.* (2004) [5] comprehensively reviewed light induced changes in packaged cheeses, and summarized their work on this topic [36, 100-103] as well as the related work of other researchers [34, 35, 39, 88, 90, 91, 104-107]. Studies related to different cheese products were summarized in terms of various packaging characteristics, light exposure times and intensities, parameters investigated (i.e. instrumental or sensory measurements), and major results [5]. Factors affecting the occurrence of light-induced quality changes, including cheese products, process parameters, packaging materials, and light exposure were reviewed.

Cheese compositional characteristics which affect its photosensitized oxidation include types and amounts of fatty acids, amino acids, prooxidants, and antioxidants. High fat cheeses are more susceptible to oxidative discoloration since more oxidizable substrate is available. High unsaturated fatty acid content cheeses (due to the addition of vegetable oil), are more prone to oxidation than normal saturated fatty acid cheeses. Oxidative decomposition of proteins mainly involves the amino acids and not the peptide backbone, and therefore the

amount of “free” amino acids is more important than the total protein content. Prooxidants include metals, such as copper [108] and iron [109] from processing equipment or nutrient fortification, and sensitizers, such as riboflavin and chlorophyll (e.g. herbs in cream cheese), can accelerate oxidative reactions. Antioxidants found in cheese include carotenoids and tocopherols (mainly in the lipid phase), and small amounts of ascorbic acid in the aqueous phase [110, 111]. β -carotene is the second most light absorbing constituent of cheeses (Figure 9). It may protect riboflavin by absorbing a significant fraction of the harmful light energy in synergy with γ -tocopherol; however, under certain conditions it may function as a prooxidant instead of an antioxidant [112].

Low pH cheeses are more susceptible to discoloration. The physical properties of the cheese matrix, in terms of light penetration and oxygen absorption, directly affect the area and depth of the oxidizable region. Homogenization of milk reduces the particle diameter and increases the number of particles, which has the net result of increasing light reflection. Solid-sample fluorescence spectroscopy [106] has been used to visualize the intensity and propagation of light-induced oxidation in dairy products including Jarlsberg cheese, and 5-6 mm of light penetration was reported.

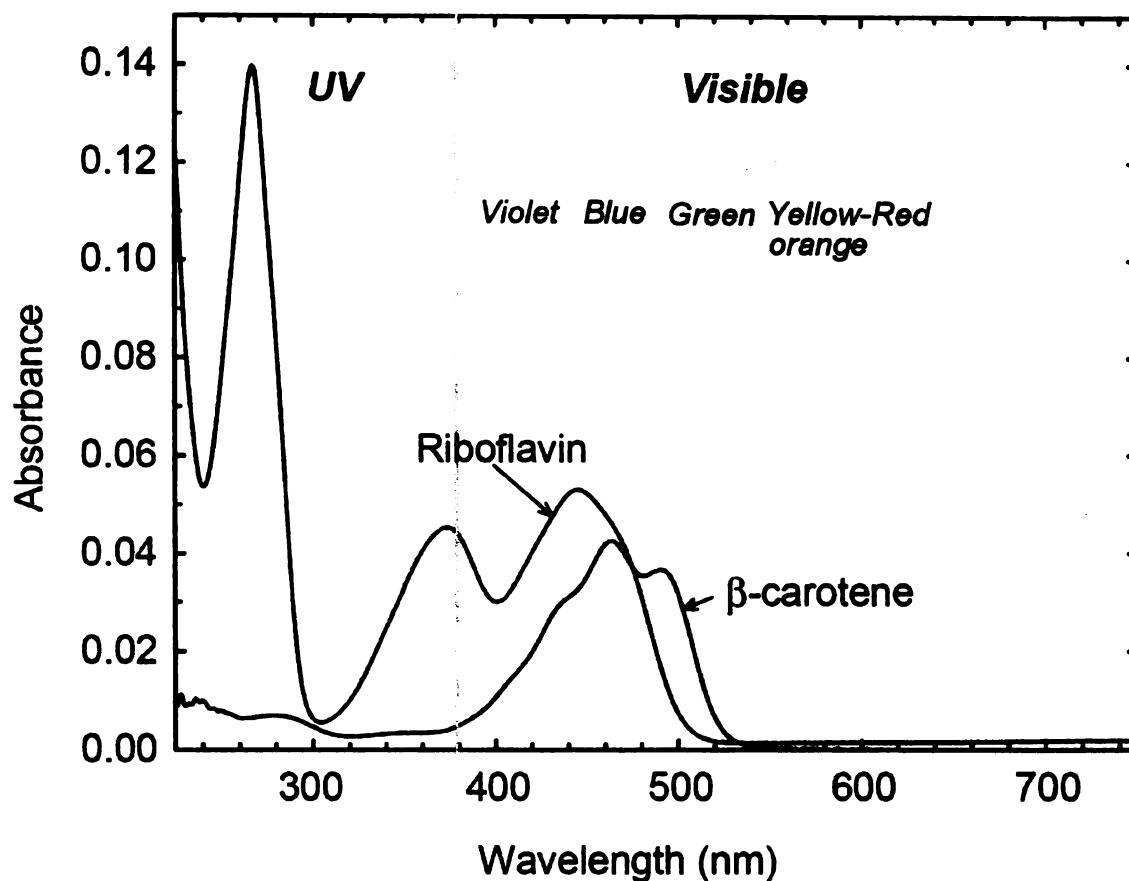


Figure 9 Absorption spectra of the major naturally occurring colorants of cheeses at concentrations found in milk (4.52 mm riboflavin in phosphate-citrate buffer, pH 6.6, and 0.37 mm β -carotene in carbon tetrachloride); from [5], Figure 2.

Packaging materials affect light-induced oxidation because of their light and/or oxygen barrier. Aluminum foil is an excellent barrier to light, and metallization of plastic materials is widely used to improve the oxygen, moisture and light barrier properties. The effect of wall thickness, pigments and titanium oxide has been reviewed previously.

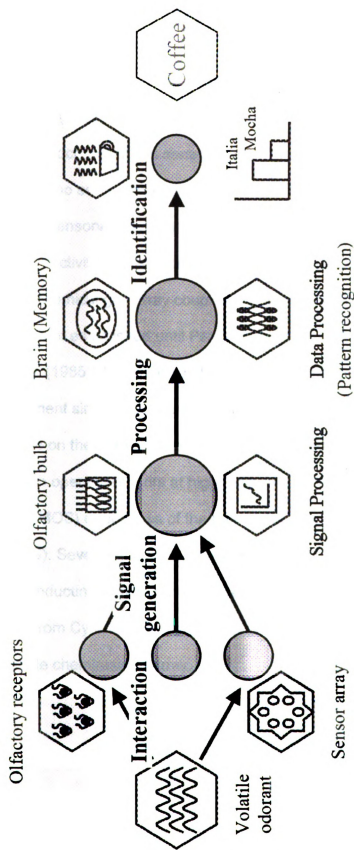
Along with oxygen transmission rate, initial gas composition and product to headspace ratio will affect oxygen availability. Vacuum packaging reduces light-induced oxidation by reducing the oxygen content in the package headspace [91]. Oxidation can still take place, however, because of the oxygen dissolved in the product. Extremely low oxygen levels (e.g. 0.01%) can be achieved using oxygen absorbers [102, 103], which can reduce the amount of secondary oxidative volatiles.

Cool-white fluorescent light can be as harmful to cheeses as it can be to milk. The turnover times are expected to be considerably longer for cheeses than fluid milk, which may be from 8 hours [6, 9] to 2-3 days [10]. In addition, cheeses are often wrapped in transparent packaging and displayed in small pieces with large surface areas exposed to light. Significant quality changes in Harvarti cheese were observed after 12 hours of light exposure, regardless of storage temperature (3°C and 10°C), light source (yellow light and standard fluorescent light), or light intensity (600 lx or 1200 lx).

2.4. Electronic nose

An electronic nose is an instrument, which comprises a headspace sampling system, an array of gas sensors with partial specificity, i.e. differing selectivity, and a computer to perform signal processing and data processing (i.e. pattern recognition), to analyze gaseous samples qualitatively and/or quantitatively, and is often used as an analog of human olfactory responses (Figure 10). A generally accepted definition of an electronic nose from Gardner and Bartlett (1994) [14, 113] is, “an electronic nose is an instrument which comprises an array of electronic chemical sensors with partial specificity and an appropriate pattern recognition system, capable of recognizing simple or complex odors.” It is different from conventional substance-specific chemical sensor systems, because an electronic nose is designed to quantify and characterize all substances present in gaseous samples as a whole, without separating and identifying the individual compounds like a gas chromatograph. The sensor arrays respond to the mixture of substances simultaneously and create unique sensor response profiles. After extracting certain response features at the signal processing step, the extracted features are collected for data processing using multivariate analysis. Differentiation and/or recognition are then performed based on the multivariate models, which may be then used to identify the unknown samples. More of a complementary approach instead of a substitute for reference methods that use sensory panels [15], an electronic nose can be an automated discriminatory analysis tool for odors and flavors in foods, and has the

Biological olfactory system



Artificial electronic nose

Figure 10 Basic diagram showing the analogy between biological and artificial noses (modified from [114], Figure 6.1)

potential for applications such as quality control, process control, and off-flavor detection [16].

Using various combinations of metal electrodes, electrolytes, and applied potentials, Hartman (1954) [115] assembled the very first experimental array of amperometric electrochemical gas sensors to analyze odorous samples, although there was no serious attempt to process the data patterns [113]. Several studies developed sensory arrays based on temperature-sensitive resistors, modulation of conductivity, modulation of the contact potential, etc. However, the concept of using chemical gas array coupled with computer-based odor classification was not established until Persaud and Dodd (1982) [116] in the U.K. and Ikegami *et al.* (1985) [117] in Japan built their systems [113]. After nearly 20 years of development since then, many commercial electronic nose systems are currently available on the market (Table 2). Most are desktop analytical instruments, which operate sensors at high temperature (e.g. Metal Oxide Semiconductors, MOS) or because of the bulk of the sensors (e.g. Mass Spectrometry, MS). Several handheld units based on SAW (Surface Acoustic Wave) or CP (Conducting Polymer) mechanisms are also available, e.g. the Cyranose 320TM from Cyrano Sciences, which uses a 32-channel carbon black polymer composite chemiresistor array.

Table 2 Commercially available electronic nose instruments (modified from [118], [119] Table 4.7 and [120] Table 7.1)

Manufacturer	Chemosensor Type*	Number of Sensors	Pattern Recognition
Agilent Technology	MS	— ²	ANN, PCA, PLS
Alpha M.O.S	MOS, CP, SAW, QCM, MS	6-24	ANN, DFA, PCA
AppliedSensor	MOSFET, MOS, QCM	—	—
AromaScan	CP	32	PCA, ANN
Bloodhound Sensors	CP	14	ANN, CA, PCA
Cyrano Sciences	CP (composite)	32	PCA
EEV Ltd. Chemical Sensor System	CP, MOS, QCM, SAW	8-28	ANN, DFA, PCA
Electronic Sensor Technology	GC, SAW	1	SPR
Element	MOS	—	—
EnviroNics Industries	IMCELL	—	—
HKR Sensorsysteme	QCM	6	ANN, CA, DFA, PCA
Lennartz Electronic	MOS, QCM	16-40	ANN, PCA, PCR
Marconi Applied Technologies	CP, MOS, QCM	—	—
Microsensor Systems	SAW	—	—
Neotronics Science	CP	12	—
Osme'tech	CP	48	—
RST Rostock	MOS, QCM	6-10	ANN, PCA
Sensobi Sensoren	(microsensor)	8-16	—
Shimadzu	MOS	6	PCA
SMart Nose	MS	—	PCA, DFA
Technobiochip	QCM	8	—
Technologies AB	MOSFET, QCM	—	—
WMA Airsense	MOS	10	ANN, DC, PCA, SPR

¹Chemosensor type; Mass Spectrometry- MS; Metal Oxide Semiconductor – MOS, Organic Conducting Polymer – CP, Quartz Resonator Microbalance – QCM, Surface Acoustic Wave – SAW, Gas Chromatography – GC, Quadrupole Mass Spectrometry – QMS, Infrared – IR and Metal-oxide-semiconductor Field Effect Transistor – MOSFET. Pattern recognition; Artificial Neural Network – ANN, Distance Classifiers – DC, Principal Component Analysis – PCA, Statistical Pattern Recognition – SPR, Discriminant Function Analysis – DFA, Cluster Analysis – CA and Principal Components Regression – PCR.

² Information not available.

2.4.1. Sensor arrays

A chemical gas sensor is a device that is capable of converting a chemical quantity into an electrical signal which corresponds to the concentration of specific particles such as atoms, molecules, or ions in gases [119]. It is a reversible process: a dynamic equilibrium develops as volatile compounds are constantly being adsorbed and desorbed at the sensor surface [121]. The types of chemical sensors that are used in the electronic nose applications need to, but may not only, respond to odorous volatiles. Gas sensors respond to a range of organic molecules, depending on the sensor construction, but they also respond to water vapor, which is odorless to humans. In general, CP sensors are the more sensitive to humidity changes than MOS sensors.

Chemical gas sensors that are ideal to be used in electronic noses should have high sensitivity (comparable to the human nose which can smell to 10^{-12} g/ml) and partial specificities, i.e. each sensor responds to a different range of compounds present in the gaseous sample. It is also ideal to have the sensors insensitive to humidity and temperature, with high stability and reproducibility, short reaction and recovery time, easy calibration, durable and inexpensive [121].

The advantages/disadvantages of chemical sensors based on conductometric, capacitive, potentiometric, calorimetric, gravimetric, optical, and amperometric principles are listed in Table 3. The schematic diagrams of the five commercially available sensor mechanisms are shown in Figure 11.

Table 3 Classification of chemosensors that have been used (modified from [119], Table 4.1)

Principle	Measurand	Sensor type		Sensitivity	Advantages	Disadvantages
Conductometric	Conductance	Chemoresistor	Metal oxide semiconductor (MOS)	5-500 ppm	Inexpensive, microfabricated	Operates at high temperature
			Conducting polymer (CP)	0.1-100 ppm	Operates at room temperature, microfabricated	Very sensitive to humidity
Capacitive	Capacitance	Chemocapacitor	Polymer	--	Applicable to CMOS-based chemosensor	Very sensitive to humidity
Potentiometric	Voltage/e.m.f.	Chemdiode	Schottky Diode	--	Integrated, applicable to CMOS-based chemosensor	Needs Pd, Pt, Au, Ir (expensive)
Calorimetric	I-V/C-V	Chemotransistor	MOS field effect transistor (MOSFET)	ppm	Integrated, applicable to CMOS-based chemosensor	Odorant reaction product must penetrate gate
			Thermistor (pyroelectric)	--	Low cost	Slow response
Gravimetric	Piezoelectricity	Mass-sensitive chemosensor	Pellistor	--	Low cost	Slow response
			Thermocouple	--	Low cost	Slow response
Optical	Refractive index	Resonant-type chemosensor	Quartz crystal microbalance (QCM)	1.0 ng mass change	Well understood technology	MEMs fabrication, interface electronics?
			Surface acoustic wave (SAW)	1.0 ng mass change	Differential devices can be quite sensitive	Interface electronics?
Amperometric	Intensity /spectrum	Fiber-optic chemosensor	Surface plasma resonance (SPR)	--	High electrical noise immunity	Expensive
			Fluorescence, chemoluminescence	--	High electrical noise immunity	Restricted availability of light sources
Amperometric	Toxic gas sensor	Toxic gas sensor	Electrocatalyst	ppb-ppm	Low cost	Size
					no RH interference	

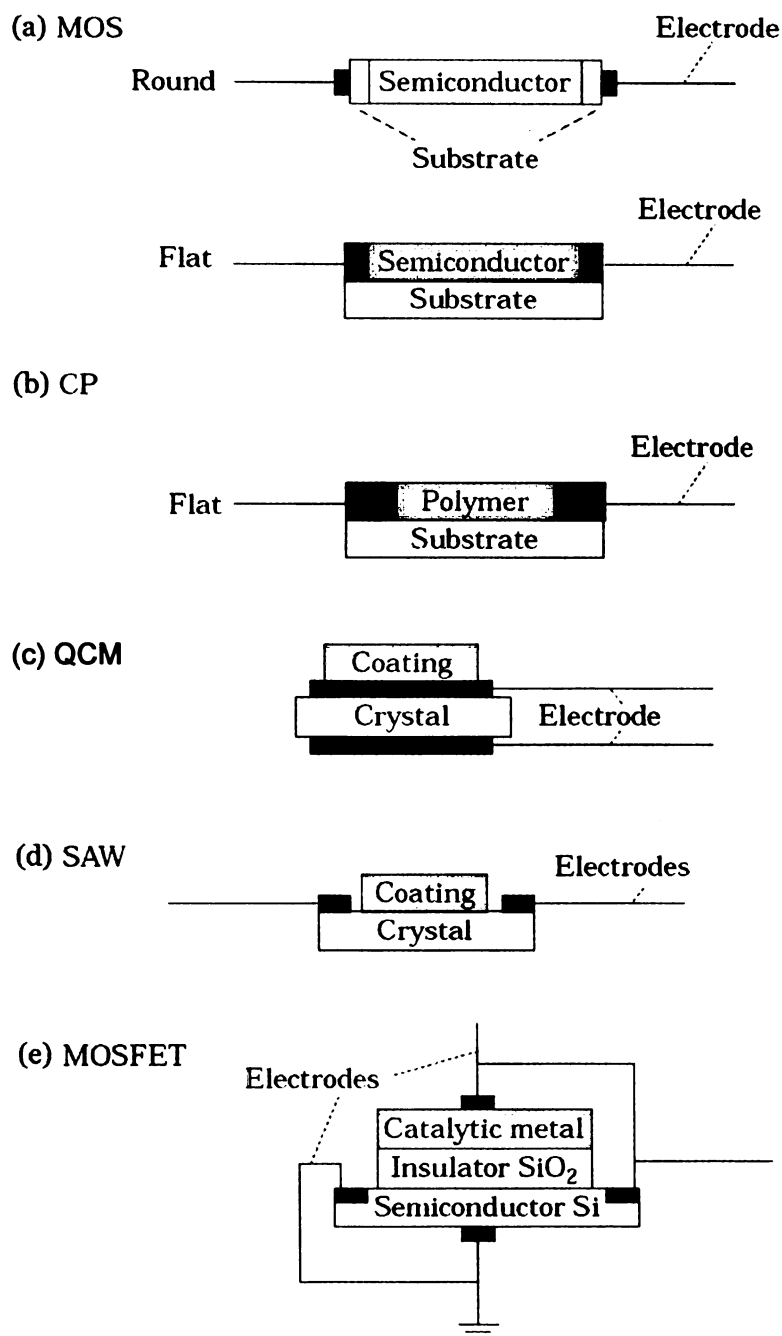


Figure 11 Schematic diagrams of five different kinds of sensors. (a) metal oxide semiconductor (MOS); (b) conductive polymer (CP); (c) quartz crystal microbalance (QCM); (d) surface acoustic wave (SAW); (e) MOS field effect transistor (MOSFET). Modified from [121], Figure 1.

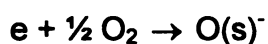
Based on the operating temperatures, these sensors can be categorized as hot sensors (e.g. MOS, MOSFET) and cold sensors (e.g. CP, SAW, QCM). Operating at higher temperatures may make the sensors less sensitive to moisture with less carry over from one measurement to another, and therefore they may have less sensor drift and longer lifetime [15]. On the other hand, the high operating temperature consumes more energy, as well as limits their use as sensors for handheld/portable devices. Comparison of the performance of the MOS, MOSFET, CP, QMB and SAW sensors is shown in Table 4.

Table 4 Comparative properties and performance of the most frequently used gas sensors in electronic nose instruments (from [122], Table 1).

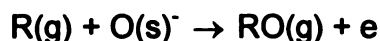
Performance	MOS	MOSFET	CP	QMB	SAW
Selectivity	Poor	Moderate	Moderate	High	High
Sensitivity	> 0.1 ppm	> 0.1 ppm	0.01 ppm	> 0.1 ppm	ppb
Reproducibility	Poor	Good	Good	Moderate	Moderate
Temperature dependence	Low	Low	High	Moderate	High
Carrier gas	Synthetic air (O ₂)	Synthetic air (O ₂)	Inert/ Synthetic air (O ₂)	Inert/ Synthetic air (O ₂)	Inert/ Synthetic air (O ₂)
Humidity dependence	Low	Moderate	High	Low	Low
Operating temperature (°C)	300-400	100-200	Ambient	Ambient	Ambient
Response time (sec.)	(0.5 - 5)	(0.5 - 5)	(20 - 50)	(20 - 50)	(20 - 50)
Recovery time	Fast	Fast	Slow	Slow	Slow
Lifetime (years)	3 - 5	1 - 4	1 - 2	< 2	< 2

2.4.1.1. Metal oxide semiconductors (MOS)

The *n*-type metal oxide semiconductors, e.g. SnO₂, ZnO, and Fe₂O₃, respond to reducible gases such as H₂, CH₄, C₂H₅ or H₂S with increased conductivity at temperatures of 200-500°C [119]. At equilibrium (i.e. baseline), oxygen in the air is adsorbed on the surface [O(s)] by trapping free electrons [e] from *n*-type semiconductors, which consequently produces a high resistive layer.



When the reducible gases [R(g)] are introduced to the system and react with the sensors, they consume the oxygen atoms adsorbed on the surface [RO(g)] and increase free electrons [e], which thus increases their conductivity.



Similarly, *p*-type semiconductors (e.g. CuO, NiO and CoO) respond to oxidizable gases (e.g. O₂, NO₂, Cl₂) which decreases their conductivity during the reaction.

Note that these instruments usually measure the resistance (R) instead of the conductivity (σ), based on the relationship:

$$R = \rho \left(\frac{L}{A} \right) = \frac{1}{\sigma} \left(\frac{L}{A} \right), \quad \text{where} \quad \begin{array}{l} \rho: \text{resistivity,} \\ L: \text{length,} \\ A: \text{cross section area.} \end{array}$$

The reaction between gases and surface oxygen varies depending on the operating temperature of the sensors and the activity of semiconductor materials, including the doped impurities and catalytic metal additives such as palladium (Pd) or platinum (Pt) [119]. The impurities act as additional electron donors (or

acceptors). Controlling the doped amount of impurities can change the conductivity of the sensors, i.e. sensitivity. The catalytic metals doped to the sensors or coated as a thin layer on the sensor surface control the selectivity of the sensors.

MOS sensors have been widely marketed and used in many commercial electronic nose systems, due to their high sensitivity and stability, compared to sensors based on other mechanisms, e.g. CP, QCM, SAW, although MOS sensors have relatively poorer selectivity [123], i.e. are less substance-specific and responding to a wider range of compounds. Redundant information obtained as a result of poor selectivity may be reduced using multivariate methods such as principle component analysis (PCA) or discriminant function analysis (DFA) at the data processing step. Other limitations of MOS sensors include: their high sensitivity to ethanol, CO₂, and moisture, which masks desired responses to aroma compounds, i.e. “blinds” the sensors to other analytes of interest, the baseline recovery may be slow for some high molecular weight compounds, and certain reactive gases such as sulfur compounds or weak acids may have irreversible binding reactions and can permanently “poison” MOS sensors [15].

2.4.1.2. Conductive organic polymer (CP)

CP sensors rely on a change in conductivity when exposed to reducible or oxidizable gases. Reversible changes in conductivity take place when chemical substances (e.g. methanol, ethanol, and ethyl acetate) adsorb and desorb from the polymer [119]. The sensors (Figure 11b) are composed of a substrate (e.g.

fiberglass or silicon), a pair of gold-plated electrodes, and a conducting organic polymer such as polypyrrole, polyaniline, polythiophene, or polyacetylene as a sensing element [15, 123]. The common feature of these electronically conducting materials is a one-dimensional polymer backbone with conjugated double bonds, i.e. alternating single and double bonds, which enables a super-orbital to be formed for electronic conduction [113, 119]. Polypyrrole can be either fully oxidized or doped by different amounts of counter-anions, which balances the charge on the polypyrrole backbone and changes the polymer conductivity. The properties of the resulting conducting polymers depend on the choice of monomer and counter-anions and the polymerization conditions, e.g. solvent used and concentration of the monomer and counter-anions [113].

CP sensors have the following advantages [15, 113, 119]: (1) a wide choice of materials can be synthesized; (2) relatively low cost materials; (3) respond to a broad range of organic vapors; (4) operate at room temperature; (5) allow extreme miniaturization, i.e. small sizes, since the sensor responses are independent of the polymer length. The disadvantages of CP sensors include [15, 123]: (1) sensitive to moisture; (2) relative long response time; (3) short life-time; (4) poor batch-to-batch reproducibility; (5) pronounced sensor drift over time or with changes in temperature.

2.4.1.3. Quartz crystal microbalance (QCM) and surface acoustic wave (SAW)

QCM and SAW sensors are gravimetric odor sensors, using acoustic wave devices that operate by detecting the effect of sorbed molecules on the propagation of acoustic waves [119]. A basic device consists of a piezoelectric substrate, such as quartz, LiNbO_3 or ZnO , with a chemically and thermally stable sorbent coating. Sorption of vapor molecules into the sorbent coating is then detected by the change in resonance frequency and amplitude of oscillation of the propagation of acoustic waves on the piezoelectric materials [15, 113]. The sensitivity and selectivity of a sensor depends on the thickness of the quartz crystal and the choice of sorbent coating materials, which must take into consideration the solubility parameter of the sorbent coating and detecting gases [113]. QCM sensors (Figure 11c) propagate the acoustic waves inside the crystal (e.g. quartz). SAW sensors (Figure 11d) comprise a relatively thick plate of piezoelectric material with electrodes, usually of gold, to excite the oscillation of the surface, i.e. the acoustic waves transmitted at the surface of the crystal [15, 113].

Both QCM and SAW sensors can be operated at room temperature, and can be modified for a higher degree of specificity by choosing different sorbent coatings. The main problems with QCM and SAW sensors are their relatively poor long-term stability and high sensitivity to moisture, poor batch-to-batch reproducibility, and pronounced sensor drift over time or with changes in temperature.

2.4.1.4. Metal-oxide semiconductors field-effect transistors (MOSFET)

MOSFET sensors rely on a change of electrostatic potential to respond to gases [123]. A MOSFET sensor consists of a silicon semiconductor, a silicon oxide insulator and a catalytic metal “gate”, e.g. palladium, platinum, iridium or rhodium (Figure 11e). In the case of the palladium (Pd) MOSFET transistor, the applied voltage on the metal gate (i.e. palladium) and the drain (where the current flows out) contact creates an electric field, which influences the conductivity of the transistor. When the metal gate reacts to the substances which can generate hydrogen atoms (H^{\bullet}), such as hydrogen, ethanol, and hydrogen sulfide [113], the electric field and thus the current flowing through the sensor are modified. The changes in voltage necessary to keep a constant current flow are then recorded as the sensor responses [123].

The selectivity and sensitivity of MOSFET sensors are influenced by the operating temperature (50-200°C), the composition of the metal gate, and the microstructure of the catalytic metal [123]. MOSFET sensors have similar advantages and disadvantages as those reported for MOS sensors, such as high sensitivity and robustness. To achieve good quality and reproducibility the MOSFET sensors may require higher levels of manufacturing expertise [123].

2.4.2. Signal processing

Prior to entering the data processing step for pattern recognition, signal processing is required to extract the feature(s) of the sensor responses. Each sensor in the sensor array gives a dynamic response over time while reacting to the injected gaseous samples. An ideal first order sensor response to a step odor input, i.e. an instantaneous step change in odor concentration at $t = 0$ over a specified period of time (until the end of region III), is shown in Figure 12a. The steady-state region III is the region that is commonly used to estimate the sensor parameter because it eliminates any variability in the flow delivery system, e.g. dead-time and flow rate [113]. The MOS sensors in this study used the sensor parameter in the steady-state region (Figure 12b), $\max(\frac{R-R_0}{R_0})$, the rescaled maximum value of the resistance R to the baseline resistance R_0 . Since the injected volatile concentrations decreased gradually instead of the ideal step input, the steady-state region III may not end as a sharp slope as shown in Figure 12a.

If the response time of the sensors to odors is relatively long, the initial slope (i.e. the slope of the linear portion in region I) may be used as a predictor of the final steady-state value [113]. If there is no significant variability in the dynamic behavior of the sampling system, e.g. using an automated sampling system instead of manual sampling, parameters in the dynamic regions II and IV may be useful in data processing.

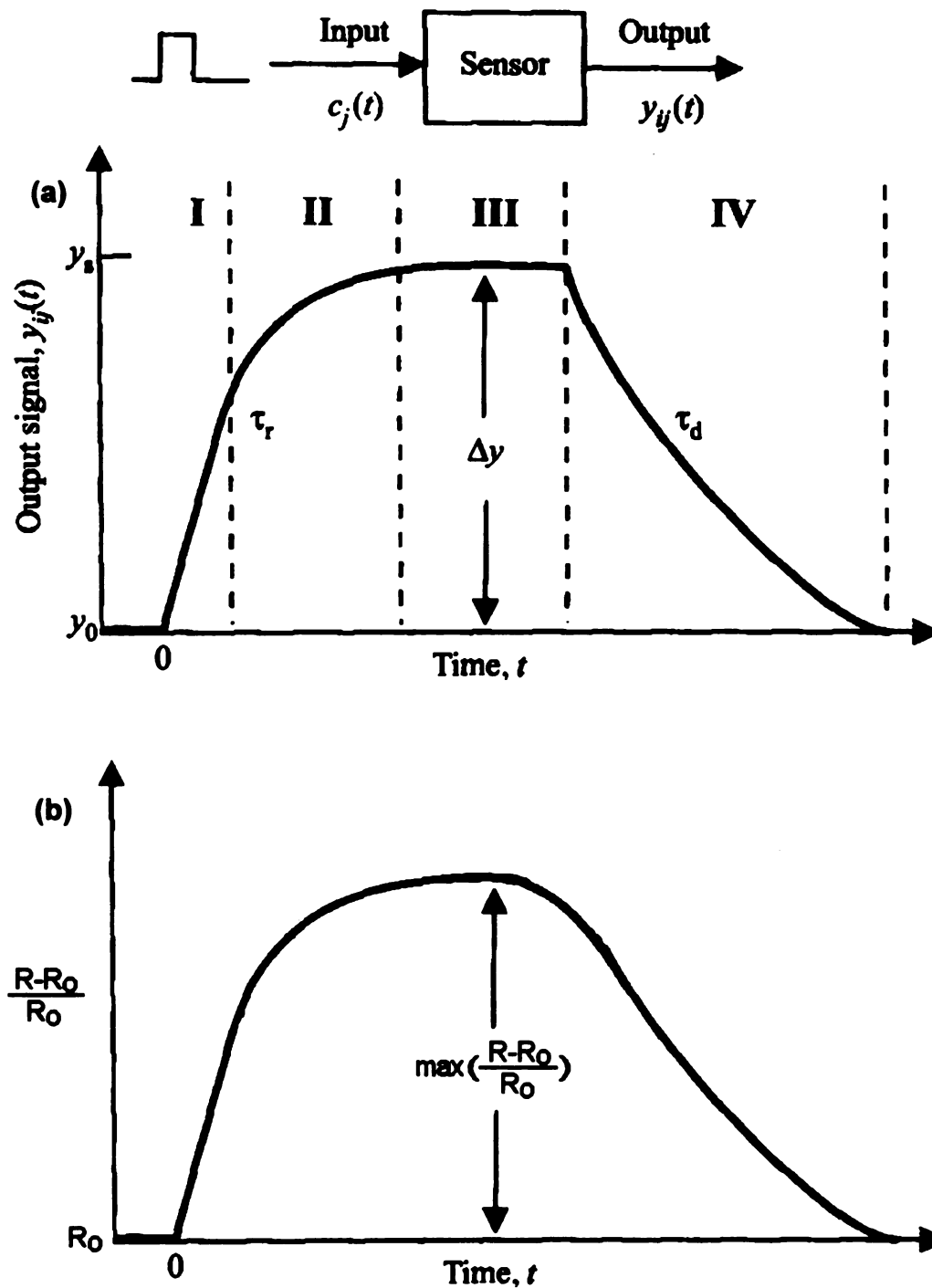


Figure 12 Sensor responses of (a) an ideal first order odor sensor responding to a step odor input (b) MOS sensors in this study (R: resistance). Figures modified from [113], Figure 6.13.

To remove or reduce the irrelevant sources of variation (either random or systematic), a data preprocessing step is often applied before the data, i.e. the extracted feature(s) described above, are entered into the multivariate analysis. Preprocessing changes the data which will either positively or negatively influence the results [124]. Several common preprocessing techniques are described below.

Normalization of a sample vector is accomplished by dividing each variable by a constant [124]. Amine *et al.* (1998) [125] compared the performance of three types of normalization applied to MOS sensor responses (FOX 4000 system, AlphaMOS), and concluded that the sum normalization

(normalizing to unit area by dividing $\sum_{j=1}^{nvars} |x_j|$, where the x_j is the j^{th} sensor

response of sample x in the experimental set) gave the best differentiation in principle component analysis (PCA) and discriminant function analysis (DFA).

Mean centering is a common preprocessing tool that is applied to account for an intercept in the data. Variable scaling is achieved by dividing each element in a variable vector by the standard deviation of the variable. Autoscaling is the application of both mean centering and variable scaling [124]. These are common tools for variable preprocessing. For example, mean centering is always used in PCA. As shown in Figure 13, without mean centering, the first principle component (PC1) describes the direction from the origin to the cloud of data, instead of the variance of the data (Figure 13b).

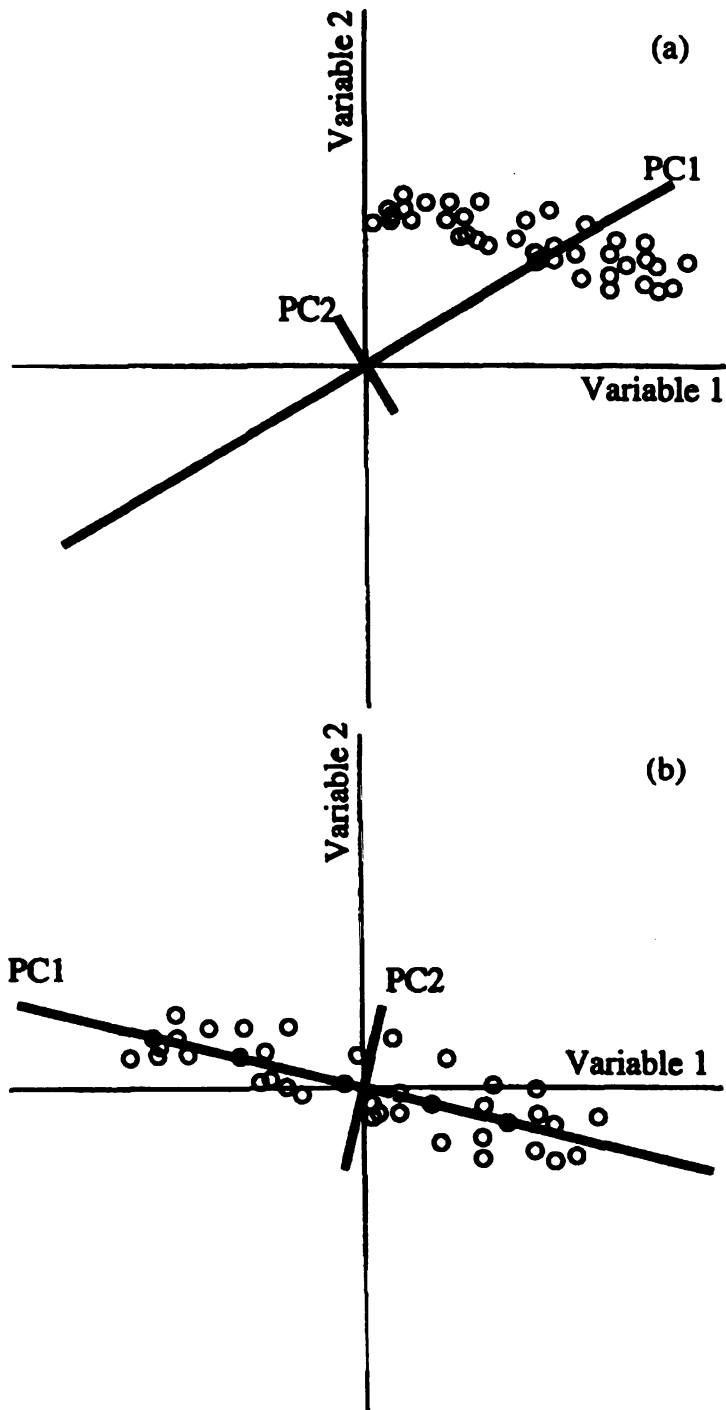


Figure 13 Example of PCA (a) without mean centering and (b) after mean centering.

2.4.3. Data processing

Pattern recognition (PARC) is the second most critical element of an electronic nose, after the design of sensor arrays. A more generalized definition of electronic nose was used for techniques using multivariate analysis techniques to analyze any multiple instrumental measurements, such as the area responses on a chromatogram [126] or peaks on a mass spectrum (e.g. HP 4440A from Agilent Technologies and SMart Nose™ from SMart Nose).

Figure 14 shows the multivariate analysis techniques applied to electronic nose data, including statistical chemometric methods and biologically inspired methods [114]. “Unsupervised” learning routinely separates the different classes from the response vectors, by discriminating between unknown odor vectors without being presented with the corresponding descriptors. On the other hand, in “supervised” learning a known set of odors is systematically introduced to build a model, which is then evaluated by testing/predicting the class membership of an unknown odor. Based on the data distribution assumption (e.g. normal distribution), the classical statistical methods can be categorized as parametric (e.g. discriminant function analysis, DFA) and non-parametric (e.g. nearest neighbor, NN) methods.

The biologically inspired methods are more capable of handling non-linear data, and have further advantages such as learning capabilities, self-organizing, generalization and noise tolerance. Since electronic noses are designed to simulate human noses, it may be more desirable to apply biologically motivated algorithms that imitate the human brain by learning from patterns.

More detailed description of the multivariate analysis techniques used in this study are discussed in Chapter 2.6.

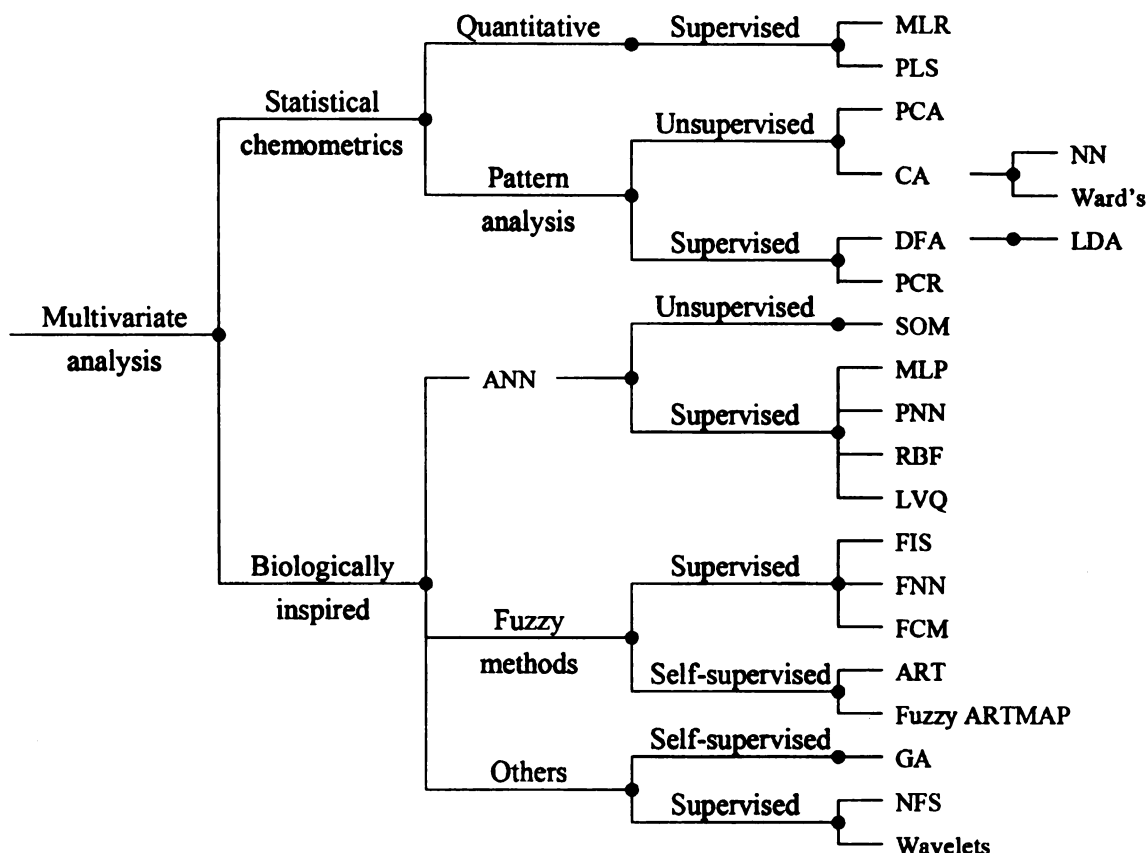


Figure 14 Classification scheme of the multivariate pattern analysis techniques applied to the electronic nose data, including multiple linear regression (MLR), partial least squares (PLS); principle component analysis (PCA), cluster analysis (CA) including nearest neighbor (NN), discriminant function analysis (DFA) including linear discriminant analysis (LDA), principle component regression (PCR), artificial neural networks (ANN) including self-organizing map (SOM), multi-layer perceptron (MLP), probabilistic neural networks (PNN), radial basis function (RBF), learning vector quantization (LVQ), fuzzy inference systems (FIS), fuzzy neural networks (FNN), fuzzy c-means clustering (FCM), adaptive resonance theory (ART), fuzzy ARTMAP, genetic algorithms (GA), neuro-fuzzy systems (NFS) and wavelets (from [114], Figure 6.3).

2.4.4. Applications of the electronic nose

2.4.4.1. Electronic nose in milk applications

Electronic nose systems have been widely applied in many different areas, such as environmental monitoring, medical diagnostics and health monitoring, natural product identification, process monitoring, food and beverage quality assurance, automotive and aerospace applications, detection of explosives, cosmetics and fragrances [127]. Table 5 shows some examples of electronic nose applications in natural products including foods, and the sensors and pattern recognition methods that have been applied. Of main interest in this study are the cases involving dairy products and their packaging. These are reviewed below.

Heating time and temperature control of the pasteurization process affect milk quality. Cooked off-flavor in pasteurized milk was the first flavor defect in milk that was analyzed using an electronic nose. Sulfur containing volatiles such as hydrogen sulfide, which is generated during pasteurization, give a “cooked or sulfurous taint” in milk. Further overheating may produce carbonyl compounds, nonenzymatic browning or Maillard reaction byproducts [128]. Sberveglieri *et al.* (1998) [129] showed promising results using a lab-made electronic nose, with an array of four MOS sensors, to discriminate (using principle component analysis, PCA, and cluster analysis, CA) the heat treatments of whole milk, i.e. pasteurization, direct ultra high temperature (UHT) method and “in bottle” sterilization. The result was then verified by the headspace volatile contents quantified using DH (dynamic headspace using absorbent Tenax).

Table 5 Recent electronic nose applications in natural products (modified from [130], Table 19.1).

Application	Sensor	Data Analysis
Toasting level of oak wood barrels	6 MOS	PCA, DFA, NN
Fermentation- Bioprocess monitoring	eNOSE 4000 (Neotronics)-12 CP	DA
Freshness of soybean curd	6 MOS	PCA
Cheese ripening	eNOSE 5000 (12CP 8 MOS); 6QMB; 10MOS-FET + 5MOS; Smart Nose (MS)	CDA
Milk spoilage (yeast/bacteria)	14 CP (Bloodhound)	BP-NN, DFA, PCA, CA
Espresso (7 blends)	Pico-1 (5 Thin Film MOS)	PCA, ANN
Espresso	4 thin film Tin Oxide	PCA, MLP ANN, data is drift corrected
Beans/Ground/liquid		Fuzzy ARTMAP
Coffee	12 MOS	PCA, DFA
Vanillin fortified Grapefruit Juice	ion-trap MS chemical sensor	
Fruit Ripeness monitoring	Tin Oxide	NN
Fruit Quality	thickness shear mode quartz resonators (TSMR) coated with pyrrolic macrocycle	PCA and Learning Vector Quantization (LVQ) neural network
Tomato Aroma	e-NOSE 4000 (12 CP)	MVDA (CDA)
Soft rot detection in potato tubers	2 MOS and 3 MOS (2 experiments)	Threshold
Oatmeal oxidation	Fox 3000 (Alpha MOS)	PCA, SIMCA
Barley Grain Quality	10 MOSFET, 6 MOS, 1 CO ₂ monitor	PCA, PLS, PLS-DA, SIMCA
Cereal quality	BH114, Blood hound, 14surface-responsive polymer array	PCA, DA, CA
Wheat classification by grade	16 electrochemical	K-NN, NN
Wheat quality	CP array	RBF-ANN (92 samples in training)
Rice Quality	10 MOSFET and 12 MOS	PCA
Capelin spoilage for fishmeal production	FreshSense (9 electrochemical gas sensors)	PLS1, saturated generalized linear model
Mahi-mahi freshness	AromaScan (32 CP)	MDA using AromaScan A32S Windows software v. 1.3
Chicken Freshness	8 MOS	Neural net
Minced Meat Rancidity	HP 4440	PCA
Swine Products	FOX 2000, 6 MOS	LDA, SIMCA
Olive oil quality	8 CP	PCA
Frying Fat Quality	4 MOS	Compared results of MOS sensors to reference food oil sensor using line plots.
Corn oils	AromaScan (32 CP)	PCA
Maize Corn oil rancidity	MOSES II- 8 MOS, 8 QMB's	PCA
Tansy Essential Oil	32 CP	PCA
Golden Rod Essential Oil	32 CP	PCA
Wood Chip Sorting	32 CP	PCA

Visser and Taylor (1998) [131] tested the performance of a commercial electronic nose, Aromascan A32S equipped with 32 CP sensors, by analyzing varieties of food products. The fresh and cooked milk samples were differentiated using a sensory panel (triangle test), and the headspace volatiles of salt-added samples (to reduce relative humidity) were clearly discriminated in PCA analysis. However, the electronic nose was not capable of differentiating aromas from cheese, coffee and banana. This was due to the high moisture sensitivity of CP sensors, and the sensor responses were mainly influenced by the water vapor instead of the volatiles from the product. Mulville (2000) [132] reported that an electronic nose equipped with MOSFET, MOS and IR sensors was able to differentiate boiled/non-boiled milk mixtures in ratios of 0/100, 10/90 and 50/50 using PCA analysis.

Zondervan *et al.* (1999) [133] used an electronic nose (Neotronics eNOSE 4048) equipped with 12 CP sensors and an autosampler to analyze 8 blockmilks (obtained by heating and drying/concentrating a mixture of milk and sugar to ca. 98% dry matter) at various stages of processing, and associated the results with the sensory scores given by a trained panel of 23 members using quantitative descriptive analysis. Volatiles generated in the Maillard reaction during the caramelization step are the main contributors of the product flavors. The results showed that the electronic nose was capable of differentiating samples (PCA and DFA) and predicting the sensory scores (ANN).

Since off-flavors in milk comprise a mixture of numerous volatiles, a gas chromatograph can be used to determine the volatile contents, which then can

be analyzed using the same multivariate analysis techniques. Vallejo-Cordoba and Nakai (1993, 1994, 1995) [134-137] developed pattern recognition techniques to differentiate pasteurized milk with different shelf-lives, which were determined by sensory evaluation based on ADSA guidelines. The shelf life was ended whenever a score of 5 or lower was recorded by three of the five judges. Incubation for 18 hours at 24°C produced headspace volatiles from milk samples which were then quantified by DH-GC (chapter 2.5) and analyzed using multivariate analysis. Principle component regression (PCR) based on the DH-GC peak areas was capable of predicting the milk shelf life within an accuracy of ± 2 days, which was much better than that obtained using psychotropic bacteria counts (PBC). An artificial neural network (ANN) was also used for shelf-life prediction and it performed better than PCR. Linear discriminant analysis (LDA) was able to classify the milk with different shelf-life and identify the spoilage-associated volatiles. Marsili (1999, 2000) [126, 138] investigated cooked (UHT milk), light-oxidized, lipid-oxidized (added copper), and microbial spoiled UHT milk via a similar approach, using SPME-GC instead of DH-GC.

2.4.4.2. Electronic nose in cheese applications

Electronic noses analyze the mixture of volatiles directly, as typical cheese flavors do not depend upon a single key component, but originate from a variety of aroma compounds, i.e. component balance theory [139]. Most studies in this field focus on either differentiating the types or origins of cheese samples, correlating to the sensory quality, or monitoring the aging processes of cheese

manufacturing. Similarly, DH-GC or SPME-GC coupled with pattern recognition techniques may also be generalized as an “electronic nose” [140].

Wijesundera and Walsh (1998) [141] analyzed various cheeses using an electronic nose fitted with 18 MOS sensors (FOX 3000 from AlphaMOS). Six varieties of cheese (Edam, Gouda, Parmesan, Pecorino, Jarlsberg and Cheddar) were cut into 3 x 1 x 1 cm pieces, sealed in 20 ml headspace vials, and equilibrated at 40°C for 15 minutes. Using PCA, most of the six varieties were discriminated except for two overlapping pairs: Edam/Gouda and Parmesan/Pecorino. Cheddar cheeses at different aging times (1, 3, 7, and 22 months) were also fully discriminated with PCA.

Drake *et al.* (2003) [142] exploited a mass spectrometer (MS) based electronic nose (HP 4400, Agilent Technology) to differentiate aged Cheddar cheeses from different locations, using PCA and CA (cluster analysis). Pillonel *et al.* (2003) [143] differentiated 20 Emmental cheese samples from Switzerland, Germany, France, France, Austria and Finland using DH-GC and PCA analysis.

Schaller *et al.* (1999) [144] tested five sensor technologies and four instruments: eNose 5000 (EEV Chemical Sensor Systems) with 12 CP and 8 MOS sensors, QMB6 (HKR-Sensorsysteme) with 6 QMB sensors, NST 3220 (Nordic Sensor Technologies) with 10 MOSFET and 5 MOS sensors, and SMart Nose (SMart Nose Ltd.) based on a mass spectrometer (MS), to analyze the Swiss Emmental cheese samples at different stages of ripening. The results of PCA and DFA showed that MOS sensors gave the best discrimination, but the MOS sensors seem to be damaged by short-chain fatty acids released from the

Emmental cheese [15]. The CP sensors had pronounced sensor drift and resulted in poor selectivity. The QCM sensors had relatively lower sensitivity and were not capable of detecting the differences between cheese samples, and neither did the MS system. The MOSFET sensors did not give good discrimination between samples. Their attempt [145] to detect the rind taste off-flavor due to inadequate ripening and/or storage in Emmental cheese was not successful using the NST 3220 system. Schaller *et al.* (2000) [146] then applied preconcentration techniques (purge-and-trap or SPME) and significantly improved the performance of the SMart Nose system (MS based) to differentiate Emmental cheese samples ripened for 1, 21, 98 and 180 days.

Squibb (2001) [147] evaluated two handheld electronic nose systems, ppbRAE (RAE Systems) and Cyranose 320TM (Cyrano Sciences). The ppbRAE uses a photoionization detector and was able to detect differences between rancid and normal rapeseed oil samples and to detect the spiking of cardboard and tissue paper with disinfectant. The Cyranose 320TM instrument was able to distinguish mature Cheddar cheese from the other cheese samples, but could not differentiate between mild and medium cheese.

Trihaas *et al.* (2002) [148-150] focused on the microbiological quality of Danish blue cheese and Camembert cheese, and analyzed them using the two electronic nose systems: BH-114 (Bloodhound) employing 14 CP sensors and aFOX-3000 (AlphaMOS) was equipped with 6 MOS, 4 CP and 2 QCM sensors. Both systems proved to be capable of defining the ripening stage of the cheese samples.

O'Riordan and Delahunty (2003) [151, 152] evaluated cheese-grader-classified (based on market specification of sensory characteristics) Cheddar cheese samples using an electronic nose system fitted with 8 MOS sensors. Electronic nose discrimination (PCA) between cheeses was related to composition, the profile and abundance of headspace volatiles, and the descriptive sensory characteristics of the cheeses.

2.4.4.3. Electronic nose in packaging applications

Several studies have used electronic noses to study off-flavors from packaging materials, e.g. HDPE, PET, and paper cartons. As discussed previously (Chapter 2.2.1), migrants such as oxidative hydrocarbons and residual solvent or additives may cause packaging off-flavors in the food contents.

Maneesin (2001) [73] investigated the packaging off-flavor from one-gallon HDPE water containers. The electronic nose (12 MOS sensors, FOX 3000, AlphaMOS) was capable of discriminating the volatiles from HDPE produced with different antioxidants (Irganox 1010 and α -tocopherol), but not the water contained in the HDPE containers. Similarly, Das (2003) [66] used the same electronic nose to analyze 8 HDPE resin samples, and also found that the instrument was capable of discriminating the resins but not the water samples containing the resins at 40°C for one week.

To detect retained solvents on printed packaging films, van Deventer and Mallikarjuna (2002) [153, 154] evaluated the performance of three electronic nose systems: FOX3000 (AlphaMOS) equipped with 12 MOS sensors, Cyranose

320™ (Cyrano Sciences) equipped with 32 CP sensors, and QMB6 (HKR Sensorsysteme) equipped with 6 QCM sensors. The results of linear discriminant analysis (LDA), which were displayed on two-dimensional canonical discriminants plots, indicated that all three systems correctly identified 100% of the unknown samples, while the FOX3000 and Cyranose 320™ were superior based on discriminatory power and practical features.

For quality control purposes, Poling *et al.* (1997) [155] constructed multivariate models of volatiles from various qualities of PET pellets and paperboard, based on the sensor responses of the electronic nose FOX 4000 (AlphaMOS) fitted with 18 MOS sensors. The models were then used to successfully predict the qualities of unknown samples.

To monitor taints related to printed solid boards, Heiniö and Ahvenainen (2002) [156] utilized an electronic nose NST 3320 (Nordic Sensor Technologies) equipped with 10 MOSFET, 12 MOS, one CO₂ sensor and one humidity sensor, to differentiate 20 solid board samples that were unprinted, lacquered, and offset-printed in 14 different colors. The electronic nose succeeded (PCA) in grouping these materials according to their coloring agents or lacquering, despite slight overlapping of replicates, and showed some of the off-flavor intensities obtained from sensory tests.

2.5 Solid-phase microextraction (SPME)

Solid-phase microextraction is a solvent-less extraction technique developed in 1990 [157], which involves the exposure of a fused silica fiber with a thin layer of polymer coating, to isolate and concentrate analytes (volatiles or semivolatiles) from a gaseous or liquid sample, or the headspace of a liquid or solid sample. Analytes are absorbed or adsorbed by the fibers, and later thermally desorbed in the injection port of a gas chromatograph (Figure 15), or dissolved into the mobile phase of a SPME/HPLC interface, and then delivered to the HPLC column for separation [158].

At equilibrium, the amount of an analyte extracted by the coating is determined by the thickness of the polymer coating [159], and the magnitude of the partition coefficient of the analyte between the sample matrix and the coating materials [160]. Although SPME is an equilibrium sampling method, it can still be highly reproducible through proper calibration and precise control of the exposure time (Figure 16). Temperature can also affect the equilibrium during extraction since the partition coefficient of the analyte is temperature dependent. Other factors which can affect SPME precision [160] include: agitation conditions, sample volume, headspace volume, vial shape, conditions of the fiber coating (e.g. cracks, adsorption of high molecular weight species), geometry of the fiber (thickness and length of the coating), sample matrix components (e.g. salt, organic material, humidity), time between extraction and analysis, analyte losses (adsorption on the walls, permeation through Teflon, absorption by septa), geometry of the injector, fiber positioning during injection, condition of the injector

(pieces of septa), stability of the detector response, and moisture in the needle, etc. These experimental parameters should be kept constant to ensure good reproducibility of the SPME extraction.

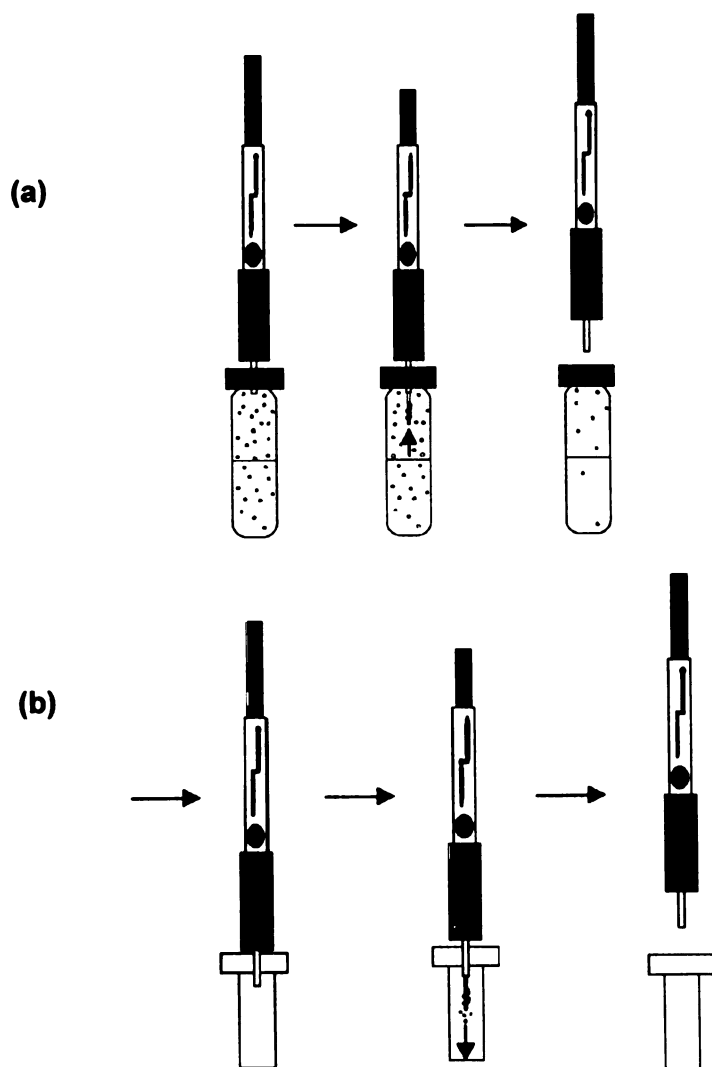


Figure 15 Solid phase microextraction (SPME) to concentrate headspace volatiles: (a) extraction; (b) desorption [159].

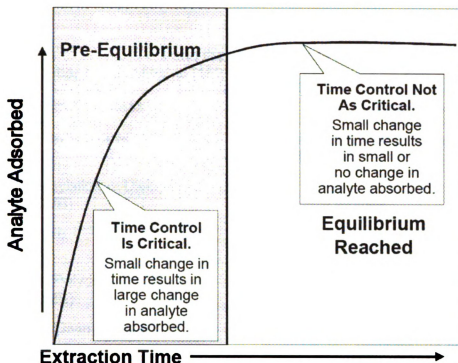


Figure 16 Effect of time on amount of analyte absorbed (modified from [161]).

Based on the characteristics (e.g. volatility and polarity) of target analytes, polymer coatings and/or coating thickness should be selected. In general, highly volatile compounds require a thick coating, and a thin coating is most effective for adsorbing/desorbing semivolatile analytes. Table 6 lists the types of SPME fibers available (Supelco, Bellefonte, PA) and recommended use.

A technical document from Supelco Inc. [162] gives a detailed review of SPME applications up to the year 2001 in the areas of foods, polymers/coatings, natural products, pharmaceuticals, biological matrices, toxicology, forensics, and environmental (water, pesticides, soil and air). Applications using SPME-GC to analyze the headspace volatiles of milk and cheese are reviewed below.

Table 6 Types of SPME fibers and their recommended use (modified from the table "SPME Fiber Assemblies" in [162]).

Film Thickness	Recommended use
Polydimethylsiloxane (PDMS)	Considered nonpolar for nonpolar analytes
Polydimethylsiloxane/Divinylbenzene (PDMS/DVB)	Ideal for many polar analytes, especially amines
Polyacrylate (PA)	Highly polar coating for general use, ideal for phenols
Carboxen/Polydimethylsiloxane (CAR/PDMS)	Ideal for gaseous/volatile analytes, high retention for trace analysis
Carbowax/Divinylbenzene (CW/DVB)	For polar analytes, especially for alcohols, low temperature limit
Carbowax/Templated Resin (CW/TPR)	Developed for HPLC applications, e.g. surfactants
Divinylbenzene/Carboxen/PDMS (DVB/CAR/PDMS)	Ideal for broad range of analyte polarities, good for C3-C20 range

Marsili (1999) [126] quantified the light-induced headspace volatiles in 2% milk and skim milk. Spiked pentanal and hexanal in milk were analyzed by SPME (75 μ m CAR/PDMS fiber, 45°C, 15 minutes) and DH (dynamic headspace, i.e. purge-and-trap and thermal desorption using the absorbent Tenax), to compare the method performance. It was found that the SPME method showed significantly better repeatability, i.e. a lower coefficient of variation (%CV), and had comparable detection limits (0.3 ng/ml pentanal and 0.8 ng/ml hexanal in 2% milk) and linear least squares correlation coefficients. A study conducted by Contarini and Povo (2002) [163] using a DVB/CAR/PDMS fiber concluded that SPME and DH had similar repeatability.

Marsili (1999) [126] used the same SPME method to develop a rapid technique to study the off-flavors in milk. A mass spectrometer (MS) and multivariate statistical analysis (MVA), which was PCA in the study, were used to identify and differentiate the headspace volatiles from abused milk samples with detectable malodor or off-flavors, including cooked (UHT milk), light-oxidized, lipid-oxidized (added copper), and microbial spoiled UHT milk. Furthermore, Marsili (2000) [138] collected commercial 2% milk and chocolate milk and stored them at $7.2 \pm 0.5^\circ\text{C}$ until the end of shelf-life, which was determined when 3 of the 4 judges gave a score below 5, followed the ADSA guidelines. A SPME-MS-MVA technique, using partial least squares (PLS), was utilized to correlate the headspace volatiles and the shelf-life as determined by sensory evaluation. It was found that the SPME-MS-MVA technique was a viable alternative to current

commercial electronic nose instruments, and capable of differentiating off-flavored milk, and also could predict the milk shelf-life.

Van Aardt *et al.* (2001) [12, 77] used a SPME technique (75 μ m CAR/PDMS fiber, 45°C, 15 minutes) to quantify the acetaldehyde in milk, which can originate from both light-induced oxidation and through migration from PET bottles. González-Córdova and Vallejo-Córdova (2003) [164] using SPME (85 μ m PA fiber, 70°C, 30 minutes equilibrium time, and 60 minutes exposure time) to determine the hydrolytic rancidity, i.e. amounts of free fatty acids (FFA), and was able to correlate this to the rancid flavor intensity sensory scores using stepwise multiple linear regression. Piero *et al.* (2003) quantified the short chain saturated aldehydes (C₅-C₉) in the headspace of infant formula (powder) using SPME (65 μ m PDMS/DVB fiber, 25°C, 15 minutes) coupled with GC-MS. Hexanal, a potential marker of milk powder oxidation, was quantified in the ppm level using an isotope dilution technique.

SPME coupled with GC or HPLC has been widely used to analyze aroma [140, 146, 165-173], off-flavors [107] and contaminants [174, 175] in cheese. Frank *et al.* (2004) collected the headspace volatiles of Cheddar, blue-mold, and hard-grating (Parmesan, Pecorino and *Grana Padano*) styles of cheese varieties using a CAR/PDMS fiber (22°C, 16 hours), and analyzed them using GC-olfactometry and GC-MS. Sulfur compounds such as dimethyl trisulfide and methionol played an important role in cheese aroma. Pionnier *et al.* (2004) [173] studied the aroma release during eating *in vivo*, using a 100 μ m PDMS fiber to collect headspace volatiles of stirred cheese slurries at 25°C over time. Pérès *et*

al. (2001) [166] used different SPME fibers (PDMS, PA, PDMS/DVB, and CAR/PDMS) to extract the headspace volatiles of Camembert cheese samples (20°C, 10 minutes), and a model was constructed using CAR/PDMS fiber coupled with GC-MS and stepwise discriminant analysis (SDA). Pinho *et al.* (2002, 2003) [168, 170, 171] quantified volatile free fatty acids (FFA) in Terrincho ewe cheese, and compared the performance of the six fibers: PDMS, PDMS/DVB, CW/DVB, DVB/CAR/PDMS, PA, and CAR/PDMS. It was concluded that the CAR/PDMS fiber (20°C, equilibrium time of 20 minutes, and exposure time of 30 minutes) gave the most complete cheese volatile profiles. Kim *et al.* (2003) studied the light-oxidized volatile compounds in goat's milk cheese using a 65 µm PDMS/DVB fiber (40°C, equilibrium time of 30 minutes and exposure time of 30 minutes), and concluded that fluorescent light can increase the headspace volatile compounds including 1-heptanol, heptanal, nonanal, and 2-decenal [107]. Zambonin *et al.* (2001 and 2002) [174, 175] extracted two types of mycotoxins, cyclopiazonic acid (CPA) and mycophenolic acid (MPA), from the surface of semi-soft cheeses and blue-veined cheeses, respectively, using a 60 µm PDMS/DVB fiber (room temperature, pH 3 buffered solution, 30 minutes) coupled with HPLC-UV.

2.6. Multivariate statistical techniques

2.6.1. Unsupervised learning techniques

2.6.1.1 Hierarchical clustering analysis (HCA)

Hierarchical clustering analyses (HCA) proceeding by either a series of successive mergers (agglomerative hierarchical methods) or a series of successive divisions (divisive hierarchical methods), can be used to examine the interrelationships between all observations in a two-dimensional plot and is known as a dendrogram [124, 176]. It is a measure of dissimilarity between group observations, based on the pairwise dissimilarities among the observations in the two groups [177]. Three linkage criteria for agglomerative hierarchical procedures are illustrated in Figure 17, including single linkage (minimum distance or nearest neighbor), complete linkage (maximum distance or farthest neighbor), and average linkage. A single linkage dendrogram is generated based on their nearness in row space; in this each sample is initially treated as an individual cluster, then joined to the “nearest neighbors” to create fewer numbers of clusters, as the analysis proceeds. This continues until only one cluster remains (Figure 17d). Cutting the dendrogram horizontally at a particular height partitions the data into disjointed clusters represented by the vertical lines that intersect it. Groups that merge at high distance values, e.g. objects (1, 2) and (3, 4, 5) (Figure 17d), are candidates for natural clusters. It is interesting to compare the actual class membership, if available, with the natural clustering. If they are not coincident, the measurements (X 's) might not be sufficient to differentiate different groups, and clustering might be affected by factors not considered.

In brief, samples which are more 'similar', e.g. milk or Cheddar cheese subjected to the same duration of light exposure, are expected to be naturally clustered, i.e. in the same or nearby clusters.

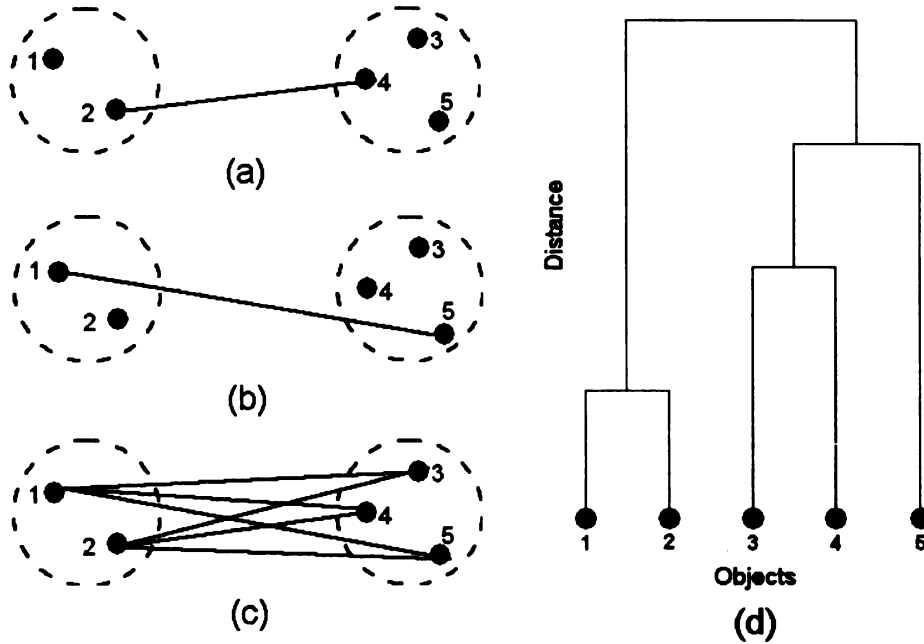


Figure 17 An example of hierarchical clustering analysis (HCA). The intercluster distances can be defined as (a) single linkage, d_{24} , (b) complete linkage, d_{15} , and (c) average linkage, $\frac{d_{13} + d_{14} + d_{15} + d_{23} + d_{24} + d_{25}}{6}$, (d) single linkage dendrogram for distances between 5 objects [176].

2.6.1.2 Principle component analysis (PCA)

Principle components are the linear combinations of the p random variables X_1, X_2, \dots, X_p , which represent a new coordinate system with maximum variability [176]. The first principle component (PC1) is the projection of the p -dimensional data that explains the most variance of the original variance-covariance structure. The second principle component (PC2) is orthogonal to PC1 and explains the maximum amount of the remaining variation, and so on. Let Σ be the covariance matrix associated with the random vector

$\mathbf{X}^T = [X_1, X_2, \dots, X_p]$ with the mean $\boldsymbol{\mu} = E(\mathbf{X})$ such that

$$\Sigma = \text{Cov}(\mathbf{X}) = E(\mathbf{X} - \boldsymbol{\mu})(\mathbf{X} - \boldsymbol{\mu})^T.$$

Using singular value decomposition (SVD), Σ can be written as

$$\Sigma = \mathbf{P} \Lambda \mathbf{P}^T,$$

where

$$\mathbf{P} = [\mathbf{e}_1, \mathbf{e}_2, \dots, \mathbf{e}_p],$$

$$\Lambda = \begin{bmatrix} \lambda_1 & 0 & \dots & 0 \\ 0 & \lambda_2 & \vdots & \vdots \\ \vdots & \dots & \ddots & 0 \\ 0 & \dots & 0 & \lambda_p \end{bmatrix},$$

eigenvectors $\mathbf{e}_i = [e_{i1}, \dots, e_{ip}]^T$, and eigenvalues $\lambda_1 \geq \lambda_2 \geq \dots \geq \lambda_p \geq 0$.

The i^{th} principle component PC_i is given by

$$PC_i = \mathbf{e}_i^T \mathbf{X},$$

$$\text{or } PC_i = e_{i1}X_1 + e_{i2}X_2 + \dots + e_{ip}X_p \quad i = 1, 2, \dots, p,$$

where

$$\text{Var}(PC_i) = \mathbf{e}_i^T \Sigma \cdot \mathbf{e}_i = \lambda_i \quad i = 1, 2, \dots, p$$

$$\text{Cov}(PCi, PCi') = \mathbf{e}_i^T \Sigma \cdot \mathbf{e}_{i'} = 0, \quad i \neq i'.$$

Computationally, let $\tilde{\mathbf{x}}$ be a $n \times p$ data matrix representing n observations for the p variables. Assume $\tilde{\mathbf{x}}$ is mean-centered ($\mu = 0$), i.e. the estimated mean has been subtracted from each column:

$$\tilde{\mathbf{x}} = \begin{bmatrix} \tilde{x}_{11} & \tilde{x}_{12} & \dots & \tilde{x}_{1p} \\ \tilde{x}_{21} & \vdots & \dots & \vdots \\ \vdots & \vdots & \dots & \vdots \\ \tilde{x}_{n1} & \tilde{x}_{n2} & \dots & \tilde{x}_{np} \end{bmatrix}_{n \times p} \quad \text{where} \quad \frac{\sum_{i=1}^n \tilde{x}_{ij}}{n} = 0$$

$$\begin{aligned} \Sigma &= \begin{bmatrix} E(X_1 - 0)^2 & E(X_1 - 0)(X_2 - 0) & \dots & E(X_1 - 0)(X_p - 0) \\ E(X_2 - 0)(X_1 - 0) & \vdots & \dots & \vdots \\ \vdots & \vdots & \ddots & \vdots \\ E(X_p - 0)(X_1 - 0) & \dots & \dots & E(X_p - 0)^2 \end{bmatrix} \\ &= \begin{bmatrix} \frac{\tilde{x}_{11}^2 + \dots + \tilde{x}_{n1}^2}{n-1} & \frac{\tilde{x}_{11}\tilde{x}_{12} + \dots + \tilde{x}_{n1}\tilde{x}_{n2}}{n-1} & \dots & \frac{\tilde{x}_{11}\tilde{x}_{1p} + \dots + \tilde{x}_{n1}\tilde{x}_{np}}{n-1} \\ \frac{\tilde{x}_{12}\tilde{x}_{11} + \dots + \tilde{x}_{n2}\tilde{x}_{n1}}{n-1} & \vdots & \dots & \vdots \\ \vdots & \vdots & \ddots & \vdots \\ \frac{\tilde{x}_{1p}\tilde{x}_{11} + \dots + \tilde{x}_{np}\tilde{x}_{n1}}{n-1} & \dots & \dots & \frac{\tilde{x}_{1p}^2 + \dots + \tilde{x}_{np}^2}{n-1} \end{bmatrix} = \frac{\tilde{\mathbf{x}}^T \tilde{\mathbf{x}}}{n-1} \end{aligned}$$

The principle components $PC1, \dots, PCk$ can be obtained using the singular value decomposition of $\Sigma = \frac{\tilde{\mathbf{x}}^T \tilde{\mathbf{x}}}{n-1}$ using the same procedure described on the previous page.

Notice that the total population variance $\sum_{i=1}^p \text{Var}(X_i)$ equals the total variance of the principle components,

$$\sum_{i=1}^p \text{Var}(X_i) = \text{tr}(\mathbf{\Sigma}) = \text{tr}(\mathbf{P}\mathbf{\Lambda}\mathbf{P}^T) = \text{tr}(\mathbf{\Lambda}) = \lambda_1 + \lambda_2 + \dots + \lambda_p = \sum_{i=1}^p \text{Var}(PC_i) ,$$

and the proportion of total population variance explained by each PC_i is

$$\frac{\lambda_i}{\lambda_1 + \lambda_2 + \dots + \lambda_p} \quad i = 1, 2, \dots, p .$$

Principle component analysis can be used for data reduction. Since the algorithm used to select each PC explains the maximum amount of the remaining variance of \mathbf{X} , most variation is expected to be represented by PC_1, \dots, PC_k , $k \leq p$. Scatter plots of the first two or three PC's ($k = 2$ or 3) are useful for observing p -dimensional data on two dimensional (Figure 18) or three dimensional plots, which will explain most of the variation of the original data matrix explained.

Geometrically, PCA involves rotation of the original coordinates (dimension p) to the new coordinates (dimension $k \leq p$):

$$\mathbf{X} = \mathbf{T}\mathbf{P}^T + \mathbf{e} .$$

\mathbf{T} is called the score matrix, with columns as latent vectors. \mathbf{P} , the loading matrix, contains the information about how the original measurements are related to the principle components. In PCA, the columns of \mathbf{P} are simply the eigenvectors of the covariance matrix $\mathbf{\Sigma}$. Error $\mathbf{e} = \mathbf{0}$ when all principle components are included in the model ($k = p$). Dimension reduction ($k < p$) is achieved when most of the

variation can be represented by fewer principle components so that ϵ is small and can be ignored.

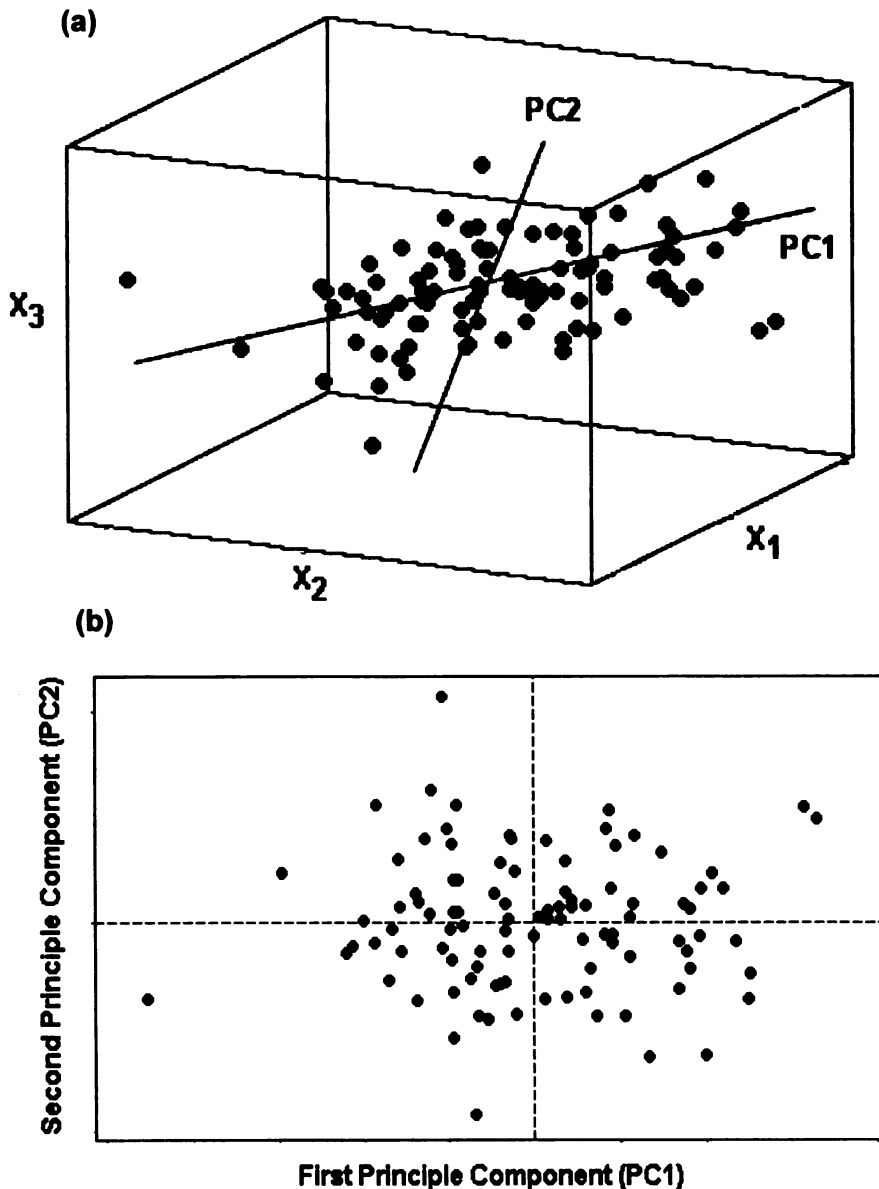


Figure 18 An example of principle component analysis (PCA). (a) Principle components PC1 and PC2 in the original three dimensional space composed by variables X_1 , X_2 and X_3 ; (b) scatter plot of the first two principle components PC1 and PC2. Diagrams were generated using Minitab R13 (Minitab Inc., PA).

2.6.2. Supervised learning techniques

2.6.2.1 Linear/quadratic discriminant function analysis (LDA/QDA)

Discrimination and classification involves defining decision boundaries so as to separate observations from different populations. R. A. Fisher (1938) first introduced the linear discrimination method described above, for two or more populations [178]. Let \mathbf{x} be a $p \times 1$ data vector which represents one observation of the p variables. From Bayesian decision theory, the posterior probabilities of assigning \mathbf{x} to class ω_i is

$$P(\omega_i | \mathbf{x}) = \frac{p(\mathbf{x} | \omega_i)P(\omega_i)}{\sum_{j=1}^c p(\mathbf{x} | \omega_j)P(\omega_j)} \quad i = 1, \dots, c.$$

where $P(\omega_i)$ is the prior probabilities of class ω_i , and $p(\mathbf{x} | \omega_i)$ is the conditional densities of \mathbf{x} given ω_i . A set of discriminant functions is defined as

$g_i(\mathbf{x}), i = 1, \dots, c$, which allocates \mathbf{x} to class ω_i if $g_i(\mathbf{x}) > g_{i'}(\mathbf{x})$, for all $i \neq i'$. To minimize the error rate of classification, \mathbf{x} should be assigned to the group with the highest posterior probability [179],

$$\text{thus } g_i(\mathbf{x}) = P(\omega_i | \mathbf{x}) = \frac{p(\mathbf{x} | \omega_i)P(\omega_i)}{\sum_{j=1}^c p(\mathbf{x} | \omega_j)P(\omega_j)}.$$

If $g_i(\mathbf{x})$ is redefined by ignoring the scale factor $\sum_{j=1}^c p(\mathbf{x} | \omega_j)P(\omega_j)$ and taking its

natural logarithm, it will become

$$g_i(\mathbf{x}) = \ln p(\mathbf{x} | \omega_i) + \ln P(\omega_i) \quad i = 1, \dots, c,$$

and random variables X_1, X_2, \dots, X_p are multivariate normal distributed

$$p(\mathbf{x} | \omega_i) \sim N_p(\boldsymbol{\mu}_i, \boldsymbol{\Sigma}_i),$$

and the discriminant functions are

$$g_i(\mathbf{x}) = -\frac{1}{2}(\mathbf{x} - \boldsymbol{\mu}_i)^T \boldsymbol{\Sigma}_i^{-1}(\mathbf{x} - \boldsymbol{\mu}_i) - \frac{p}{2} \ln 2\pi - \frac{1}{2} \ln |\boldsymbol{\Sigma}_i| + \ln P(\omega_i) \quad i = 1, \dots, c.$$

Moreover, if it assumes all classes have identical covariance matrices, $\boldsymbol{\Sigma}_i = \boldsymbol{\Sigma}$, the discriminant functions are simplified as,

$$g_i(\mathbf{x}) = -\frac{1}{2}(\mathbf{x} - \boldsymbol{\mu}_i)^T \boldsymbol{\Sigma}^{-1}(\mathbf{x} - \boldsymbol{\mu}_i) + \ln P(\omega_i),$$

which involves measuring the squared Mahalanobis distance $(\mathbf{x} - \boldsymbol{\mu}_i)^T \boldsymbol{\Sigma}^{-1}(\mathbf{x} - \boldsymbol{\mu}_i)$

from \mathbf{x} to the nearest group mean $\boldsymbol{\mu}_i$. Dropping the quadratic term $\mathbf{x}^T \boldsymbol{\Sigma}^{-1} \mathbf{x}$

which is independent of i , the discriminant functions then are linear:

$$g_i(\mathbf{x}) = (\boldsymbol{\Sigma}^{-1} \boldsymbol{\mu}_i)^T \mathbf{x} + \left[-\frac{1}{2} \boldsymbol{\mu}_i^T \boldsymbol{\Sigma}^{-1} \boldsymbol{\mu}_i + \ln P(\omega_i) \right] \quad i = 1, \dots, c.$$

Linear decision boundaries can be used to separate groups with the same covariance matrices, with the assumption of equal and unequal $P(\omega_i)$'s, and which are demonstrated in Figure 19a and Figure 19b, respectively.

For cases where we have unequal group covariance matrices, $\boldsymbol{\Sigma}_i \neq \boldsymbol{\Sigma}$, the quadratic term $\mathbf{x}^T \boldsymbol{\Sigma}^{-1} \mathbf{x}$ cannot be dropped, and the discriminant functions are quadratic:

$$g_i(\mathbf{x}) = \mathbf{x}^T \left(-\frac{1}{2} \boldsymbol{\Sigma}_i^{-1} \right) \mathbf{x} + (\boldsymbol{\Sigma}_i^{-1} \boldsymbol{\mu}_i)^T \mathbf{x} + \left[-\frac{1}{2} \boldsymbol{\mu}_i^T \boldsymbol{\Sigma}_i^{-1} \boldsymbol{\mu}_i + \ln P(\omega_i) \right] \quad i = 1, \dots, c.$$

A quadratic decision boundary used to separate two groups with different covariance matrices is demonstrated in Figure 19c.

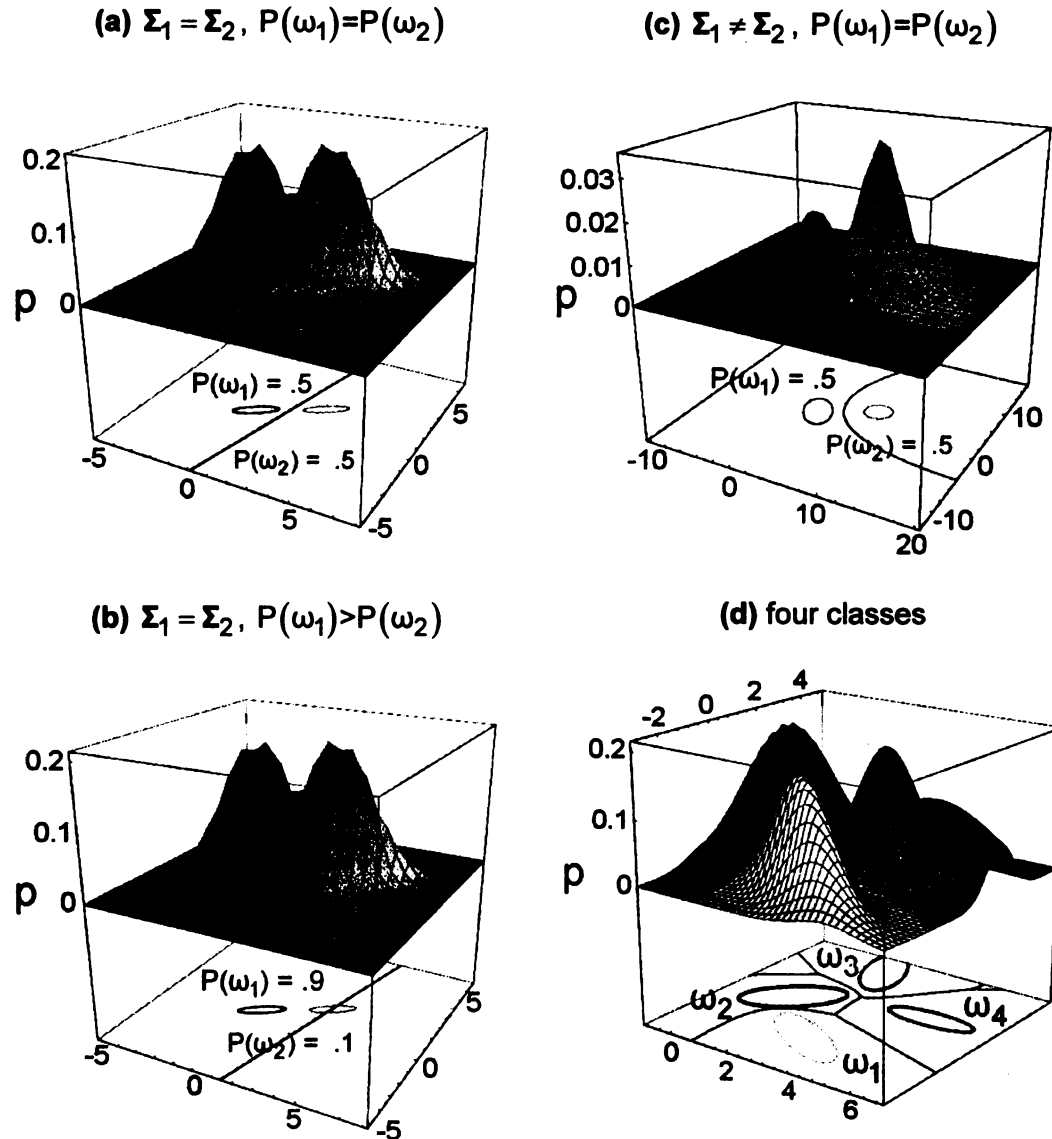


Figure 19 Decision boundaries defined based on the discriminant functions. (a) linear boundaries of two classes with identical covariance and equal prior probabilities; (b) linear boundaries of two classes with identical covariance and unequal prior probabilities; (c) quadratic boundaries of two classes with different covariance and equal prior probabilities; (d) decision boundaries for four normal distributions [179].

In short, linear discriminant function analysis (LDA) can be used to separate classes that are normally distributed using the equal covariance assumption. This can be evaluated using the “test of homogeneity” on the group covariance matrices [180]. Quadratic discriminant function analysis (QDA) can be applied when covariances are assumed or tested unequal. Figure 19d shows an example of decision boundaries for multiple group discrimination.

For visual inspection or graphical description of LDA, canonical discriminant analysis (CDA) may be used to reduce the dimension from a large number p to a relatively few (2 or 3) linear combinations, such that the between-class variance \mathbf{B} is maximized relative to the within-class variance \mathbf{W} [176, 177]. The between-class covariance matrix is,

$$\mathbf{B} = \sum_{i=1}^c \pi_i (\boldsymbol{\mu}_i - \boldsymbol{\mu})(\boldsymbol{\mu}_i - \boldsymbol{\mu})^T ,$$

where c is the number of classes,

π_i is the percentage of class i samples in the entire data set,

$\boldsymbol{\mu}_i$ is a column vector denoting the mean vector of class i , and

$\boldsymbol{\mu}$ is the overall mean vector such that $\boldsymbol{\mu} = \sum_{i=1}^c \boldsymbol{\mu}_i / c$.

The within-class variance \mathbf{W} is the common covariance matrix $\hat{\boldsymbol{\Sigma}}$. Note that $\mathbf{B} + \mathbf{W}$ equals the total covariance of \mathbf{X} . To obtain the linear combination of \mathbf{X} that maximizes the ratio of between-class variance and within-class variance, the singular value decomposition (SVD) is applied to $(\mathbf{W}^{-\frac{1}{2}})^T \mathbf{B} \mathbf{W}^{-\frac{1}{2}}$, to find its

eigenvectors $\mathbf{v}_1, \mathbf{v}_2, \dots, \mathbf{v}_s$, corresponding to the nonzero eigenvalues. We then obtain the discriminant coordinates

$$\mathbf{a}_i = \mathbf{W}^{-\frac{1}{2}} \mathbf{v}_i \quad i = 1, 2, \dots, s \leq \min(c-1, p).$$

Therefore, the k^{th} canonical discriminant ($\text{CAN } k$) can be written as

$$\text{CAN } k = \mathbf{a}_k^T \mathbf{X}, \quad k = 1, 2, \dots, s$$

or $\text{CAN } k = a_{k1}X_1 + a_{k2}X_2 + \dots + a_{kp}X_p, \quad \text{where } \mathbf{a}_i = [a_{i1}, \dots, a_{ip}]^T.$

Figure 20a is an example of the first canonical discriminant (CAN1), which is the linear combination of the original variables X_1, X_2 and X_3 that maximizes the difference between groups “•” and “◦”. It is not necessary that the canonical discriminants are the same as the principle components, which are the linear combinations of the original variables that maximize the total variance. When the total variance is mainly contributed by the between-group variance, the canonical discriminants are expected to be similar to the principle components. Figure 20b shows an example when the first canonical discriminant (CAN1) is very different from the first principle component (PC1).

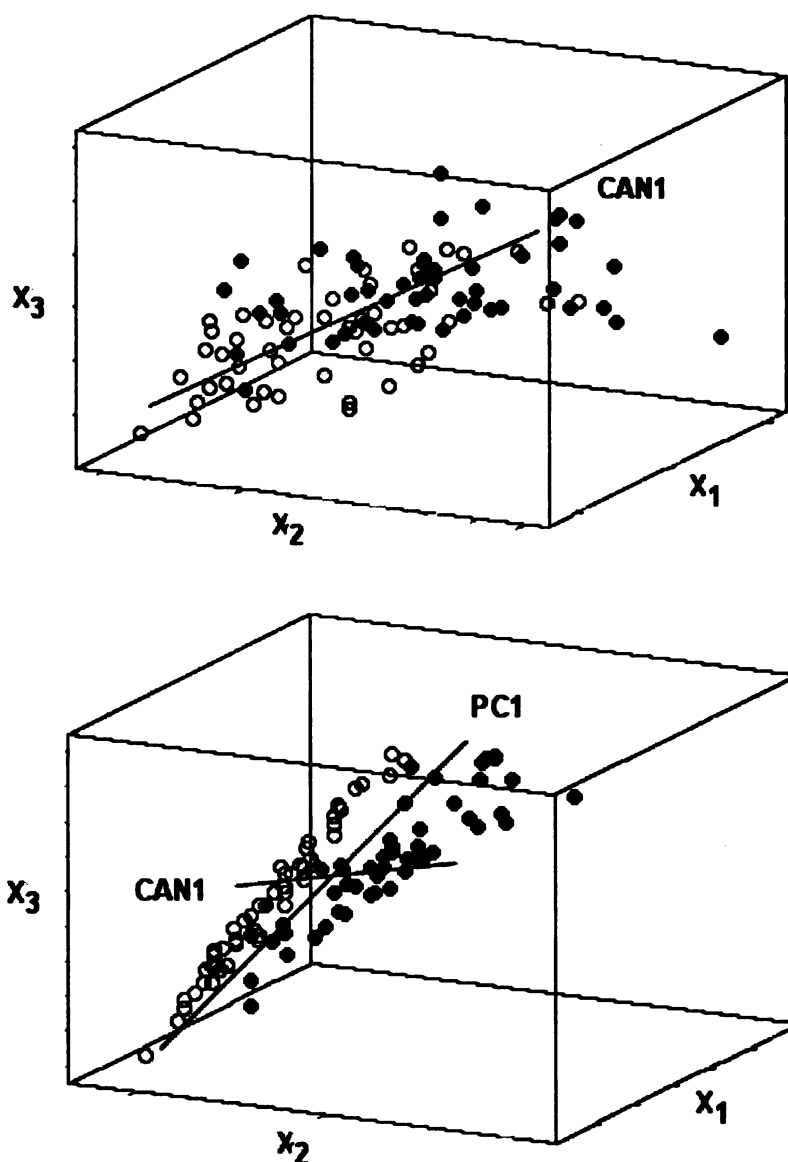


Figure 20 Examples of canonical discriminant analysis. (a) The first canonical discriminant (CAN1) in the three dimensional space composed by variables X_1 , X_2 and X_3 ; (b) a case where the CAN1 is very different from PC1, the first principle component. Diagrams were generated using Minitab R13 (Minitab Inc., PA).

2.6.2.2. k-nearest neighbor (k-NN)

The k-nearest neighbors (k-NN) method is a nonparametric classification technique, which classifies unknown observations based on their similarity with observations in “training” data. That is, for a given unlabeled object x , the method finds k closest labeled objects in the training data set, and assigns x to the class that appears most frequently within the k “neighbors”. For example, using Euclidean distances and $k = 3$ to measure the similarity between unknown and training data in a two dimensional space is illustrated in Figure 21a.

The selection of k and the metric to define closest “neighbors” are critical to the performance of k-NN. Considering

$$1 \leq k \leq \min(n_i) \quad i = 1, \dots, c,$$

where n_i is the number of training samples in class ω_i , and c is the number of the classes. If the classes are well separated, the one nearest neighbor has a high probability to be in the same class, thus $k=1$ provides a good classification rule [124]. If classes are not clearly separated, using $k>1$ may yield smoother decision regions and provide probabilistic information, though it may also destroy the locality of the estimation and increase the computational burden. Weighted distances may be applied instead of Euclidean distances for higher dimensional data, to reduce the severe requirements for computation time and storage, as a result of lack of data reduction in such a nonparametric procedure [179].

In k-NN, the identification of an unknown observation depends on the “majority votes”, if the closest k neighbors of an unknown observation do not

have a majority class, a “tie” occurs and the unknown data cannot be assigned to any group (Figure 21b).

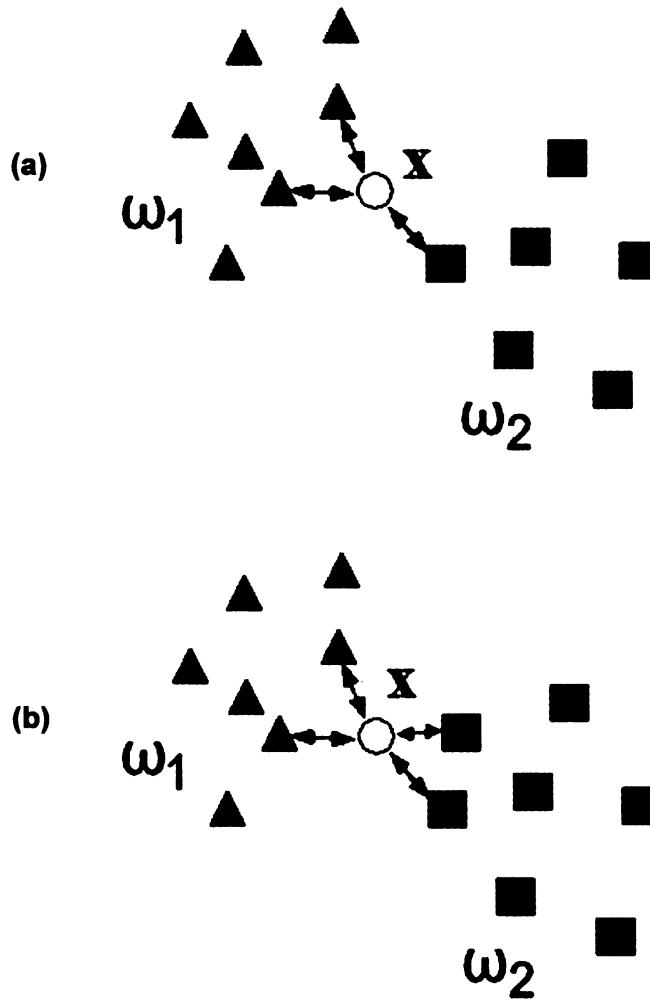


Figure 21 Examples of k-nearest neighbor (k-NN). (a) 3-NN, the k-nearest neighbor such that $k = 3$, where the unknown observation x is assigned to the class ω_1 , since two out of the three “neighbors” from the training set belong to ω_1 . (b) A “tie” occurs in 4-NN, where the unknown observation x cannot be assigned to either ω_1 or ω_2 .

2.6.3. Quantitative analyses

2.6.3.1 Partial least square (PLS) regression

Partial least square regression generalizes and combines the features from principle component analysis and multiple linear regression, to predict dependent variables (Y) from independent variables ($X^T = [X_1, X_2, \dots, X_p]$) and to describe their common structure [181], for example, to predict sensory scores (Y) from the instrumental measurements (X). When Y is a vector and X is full rank, the prediction can be accomplished using ordinary multiple linear regression (MLR). MLR is not applicable if X 's are highly correlated, or the number of observations are smaller than the number of X 's ($n < p$). Principle component regression (PCR) applies multiple linear regression using principle components of X as predictors, to eliminate the multicollinearity problem by using the orthogonality of the principle components. However, PCR does not choose an optimum subset of predictors for Y . Principle components are selected to explain X and not necessary to be the best subsets to explain Y .

The PLS approach is an indirect modeling technique (Figure 22) which finds components from X that are also relevant for Y , using simultaneous decomposition of X and Y . The selection of these components, called latent vectors, is to explain as much as possible the covariance between X and Y .

The decomposition of X and \hat{Y} (the estimator of Y) are

$$X = TP^T, \text{ and}$$

$$\hat{Y} = TBC^T,$$

where T is the score matrix and P is the loading matrix.

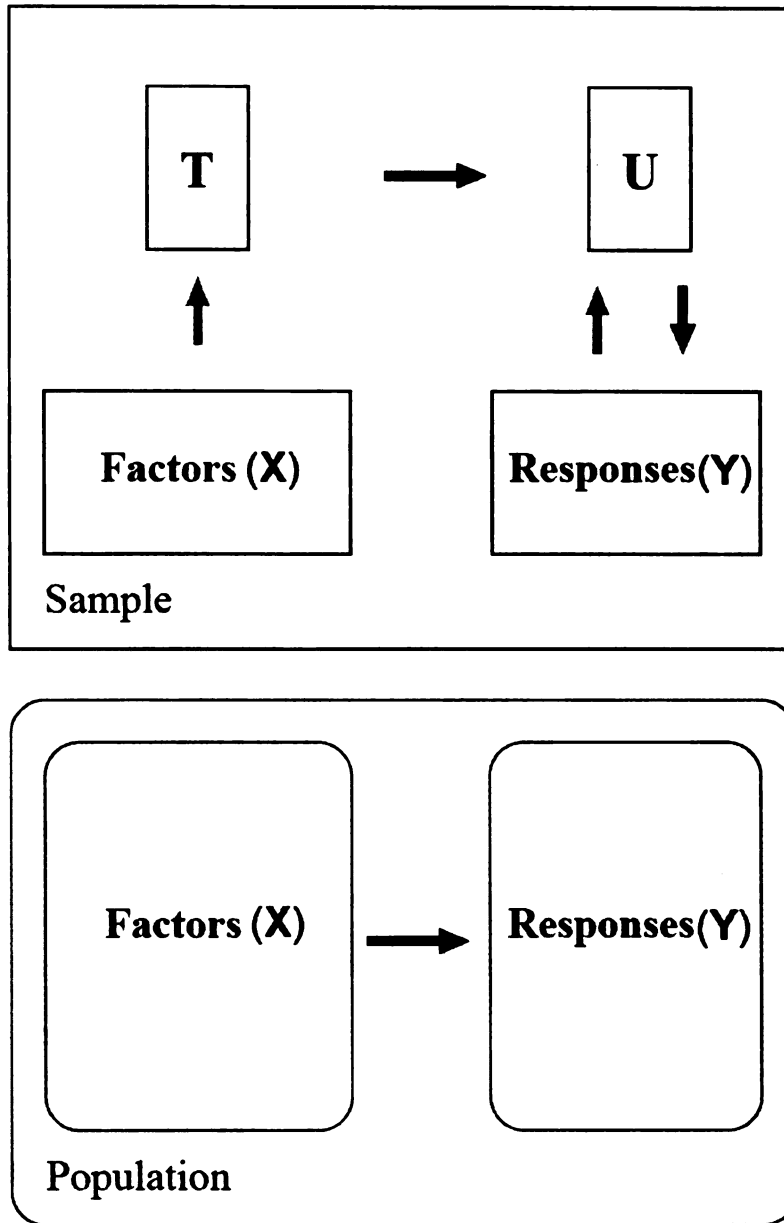


Figure 22 The indirect modeling concept of partial least squares (PLS) approach (modified from [182], Figure 3).

The columns of **P** are the latent vectors, which are not orthogonal in PLS (note that the loading matrix **P** in PCA is orthogonal). **B** is a diagonal matrix with the regression weights as diagonal elements. The PLS is to find two sets of weights (**w** and **c**), which can be used to create linear combinations of the columns of **X** and **Y** such that their covariance is maximum, i.e., to find the first pair of vectors **t** and **u** such that

$$\left\{ \mathbf{t} = \mathbf{X}\mathbf{w}, \mathbf{u} = \mathbf{Y}\mathbf{c} \mid \mathbf{w}^T \mathbf{w} = 1, \max[\text{cov}(\mathbf{t}, \mathbf{u})] \right\}.$$

When the first latent vector is found, it is subtracted from both **X** and **Y** and the procedure is re-iterated. PLS can be performed using the iteration algorithm above [181] or singular value decomposition [124].

2.6.3.2. Multilayer perceptron (MLP)

Neural networks are adaptive computer architectures based on an analogy of the biological neural system, and are used to learn or discover the association between input and output patterns, and to analyze the structure of the input patterns. The basic neural network units of neurons (Figure 23a), are connected by weighted connections (synapses), and arranged in layers. Values of the parameters (i.e. the synaptic weights) of the networks are modified iteratively as a function of the model performance. Mean square error (MSE), the average squared error between the network outputs and the target outputs, is a common criterion function for feedforward networks such as multilayer perceptrons [183].

Multilayer perceptrons (MLP, Figure 23b) are used in a supervised manner with an error back-propagation algorithm. Network learning starts with an untrained network, and a training pattern is presented to the input layer. The signal is passed through hidden layers, and the output obtained at the output layer. Synaptic weights and biases are then adjusted based on an error-correction rule, e.g. to minimize the MSE [184]. Back-propagation learning updates the network weights and biases in the direction in which the MSE decreases most rapidly:

$$\mathbf{x}_{k+1} = \mathbf{x}_k - \alpha_k \mathbf{g}_k$$

where \mathbf{x}_k is a vector of current weights and biases, \mathbf{g}_k is the current gradient, and α_k is the learning rate [179, 185].

Neural network transfer functions are denoted by f in Figure 23, and can be any differentiable functions which generate outputs. They are required to be differentiable since the back-propagation algorithm calculates the derivatives of any transfer functions used. A typical MLP contains one or more non-linear sigmoidal functions (e.g. log-sigmoid or tan-sigmoid functions) in the hidden layers, and a linear function in the output layer [185].

Training the MLP using gradient decent in the criterion function (e.g. MSE) ultimately reaches the lower bound of the error when having infinite training data. The choice of learning rate (α_k) and number of weights affects the asymptotic error value, as well as how fast the training error decreases, since in practice we do not have infinite data points for training. Also, when the lower bound of training error is reached, it often makes the models too optimistic, i.e. the models

may not be applicable for another independent data set. Therefore, an early stop criterion based on a validation data set, is usually needed. Network training stops when the error reaches a minimum for the validation set [179].

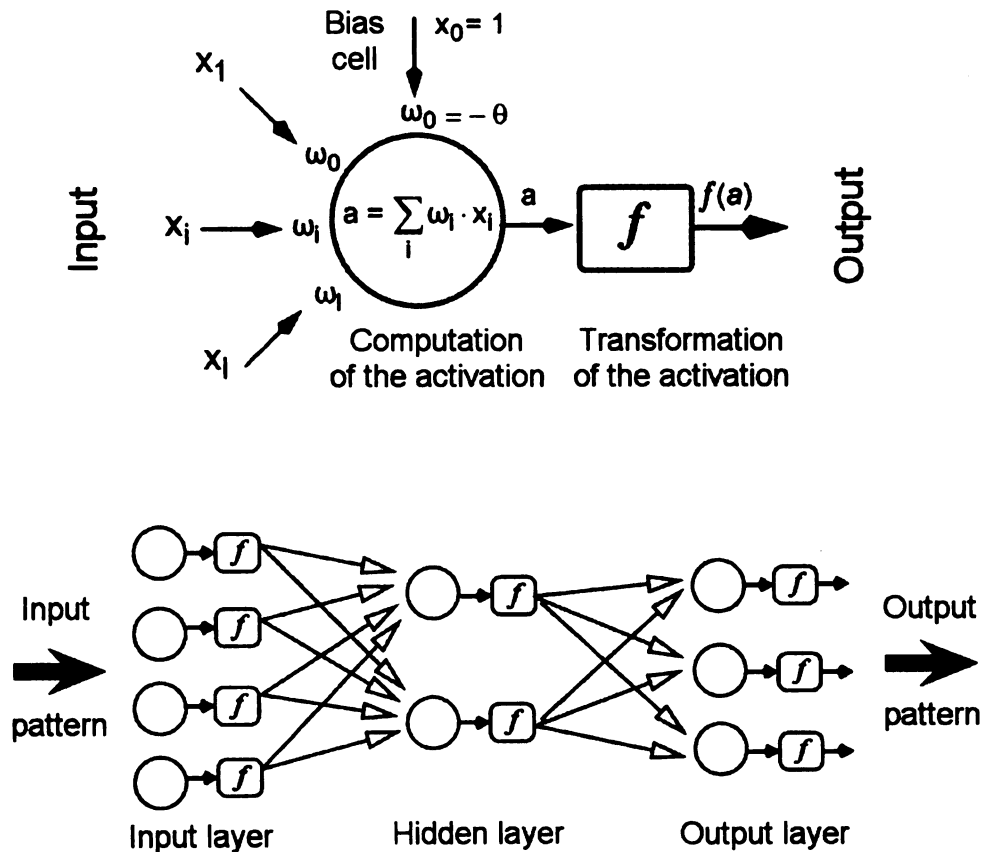


Figure 23 Multilayer perceptron (MLP) structure. (a) A neuron, the basic neural unit; (b) a multilayer perceptron [183].

CHAPTER 3

MATERIALS AND METHODS

3.1. Sample preparation

Milk in one gallon clear HDPE containers (3.785 L) was obtained from a local retail store (Meijer, Okemos, MI) and distributed into the glass or other milk packaging materials on the same day. At Meijers, the milk was displayed on open stainless steel shelves at ~5°C, with lighting by fluorescent bulbs covered by yellow plastic tubes, i.e. gold shield [54, 55]. Milk samples, within 10-14 days of sell-by dates, were picked from the middle of the bottom shelves, immediately wrapped in brown paper bags, transported to the laboratory, and stored in a 5°C refrigerator within 15 minutes. A fan was installed inside of the refrigerator to help reduce the temperature fluctuation to within $\pm 1^\circ\text{C}$.

3.1.1. Light-oxidized off-flavors in 2% milk

Reduced fat (2%) milk was distributed into glass bottles (nominal capacity 8 oz, clear, Boston Rounds, Qorpak, Bridgeville, PA) in a 5°C environmental chamber. Samples were then exposed to cool-white fluorescent light (4 bulbs of Light of America F15 T8 CW OP11 15W) for 48 hours at 5°C. The light intensity was measured from the top of the sample bottles using a digital light meter (Model SLM 110, A.W. Sperry Instruments, NY), and the average light intensity was recorded as ~1000 lx. All sample bottles were wrapped in aluminum foil prior to light exposure. The aluminum foil wraps of randomly selected sample bottles

were removed for 2, 4, 8, 12, 24, 36 and 48 hours. Two controls (“0” and “d”) were prepared using the same type of glass bottles that were wrapped in aluminum foil and stored in the dark for 0 or 48 hours. Milk was light exposed for specified times, immediately removed from each container, and prepared for use in sensory evaluation and headspace analyses using SPME or the electronic nose (experimental flowchart in Figure 24). For sensory evaluation, 20 ml of the milk samples were distributed into glass vials (nominal capacity 20 ml, screwed top with foil-lined cap) in a 5°C environmental chamber, covered with aluminum foil and stored at 5°C. Milk samples were moved to ambient temperature (~21°C) approximate one hour prior to each sensory session. The milk temperature was maintained at 10-15°C for all sensory testing [186]. For instrumental analyses, 1 ml of the milk sample was removed from each container using a 1 ml serological glass pipet, sealed in a 10 ml headspace vial, and stored below -18°C.

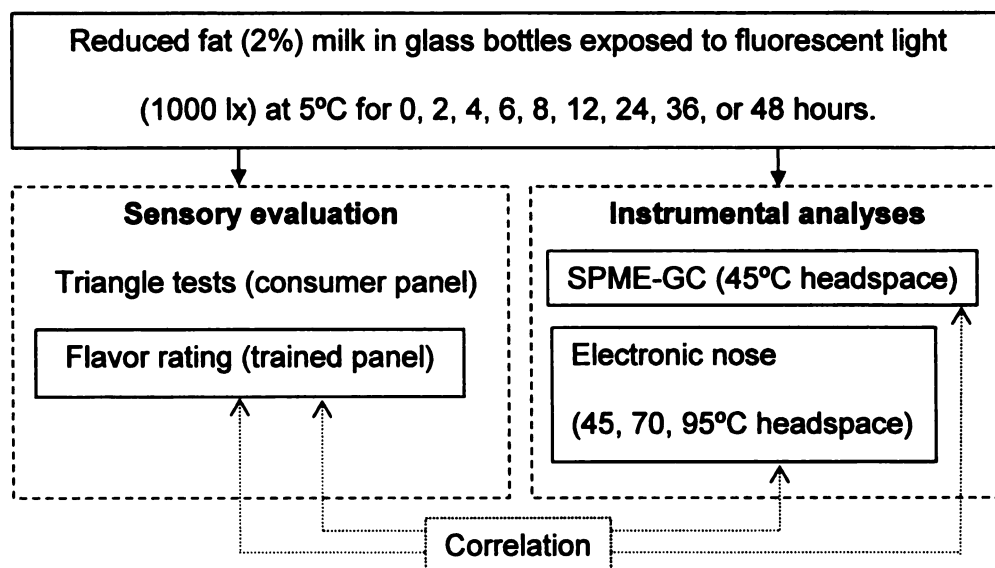


Figure 24 Experimental flowchart to investigate the light-oxidized off-flavors in 2% milk, using sensory evaluation and instrumental analyses.

3.1.2. Packaging off-flavors in 2% milk

Samples of HDPE, HDPE compounded with TiO_2 (HDPE- TiO_2), and PET bottles (food grade, nominal capacity 8 oz., Boston Rounds, eBottles.com, Woodbridge, CT) were purchased from an internet store (eBottles.com). PE-coated paper cartons (nominal capacity 8 oz., Gable top) were obtained from a local dairy plant (Melody Farms, Lansing, MI); the empty cartons were erected and sealed using equipment at Melody Farms. The empty cartons were opened, filled manually with milk or water, and resealed using binder clips (Figure 25). Glass bottles (nominal capacity 8 oz., clear, Boston Rounds, Qorpak, Bridgeville, PA) filled with milk or water were used as the control.



Figure 25 Packaging materials used for milk and/or water. Front row left to right: a PE-coated paper carton, a HDPE- TiO_2 bottle, and a PET bottle. Back row left to right: a HDPE bottle, a glass bottle, and a glass bottle wrapped in aluminum foil.

To investigate the effects of packaging off-flavors, samples of various packaging materials were analyzed using the electronic nose. Water and 2% milk stored in various packaging materials at 5°C for 3 days were analyzed using the electronic nose, and sensory evaluation performed using a consumer and/or trained panel. The experimental flowchart is shown below (Figure 26).

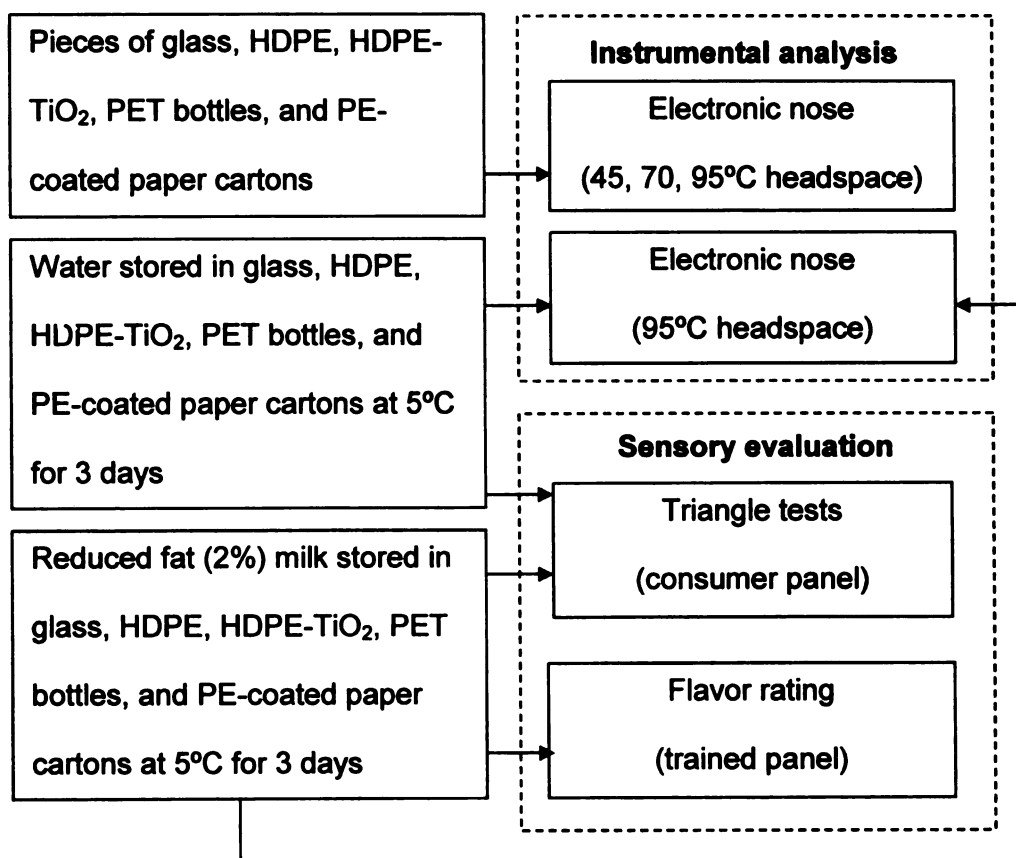


Figure 26 Experimental flowchart to investigate packaging off-flavors in 2% milk, using sensory evaluation (triangle tests and flavor rating based on ADSA guidelines) and instrumental analysis (electronic nose).

One gram of the HDPE, HDPE-TiO₂, PET bottles, or PE-coated paper cartons cut into pieces of ~1 cm² were sealed in 10 ml headspace vials for electronic nose analysis. One gram of glass from broken glass bottles was used as the control. The headspace samples of various packaging materials were generated at 45, 70 or 95°C for 15 minutes, using the oven located on the autosampler of the electronic nose.

Water (HPLC grade in 4 L amber glass jugs, J.T. Baker, Phillipsburg, NJ) stored in various packaging materials at 5°C for 3 days, was analyzed using a series of triangle tests and the electronic nose. Twenty ml of the water samples were distributed into 20 ml glass vials and evaluated at ambient temperature (~21°C) using a consumer panel. One ml of water samples was removed from each container using a 1 ml serological glass pipet, sealed immediately in a 10 ml headspace vial, and stored at ambient temperature prior to electronic nose analysis. Water in the original 4L jugs was used as the control.

Reduced fat (2%) milk was stored in the glass, HDPE, HDPE-TiO₂, PET bottles, and PE-coated paper cartons at 5°C for 3 days. One ml milk sample was removed from each container using a 1 ml serological glass pipet, sealed in a 10 ml headspace vial immediately, and stored below -18°C for electronic nose analysis at a later time. Twenty ml of the milk samples that had been stored in glass, HDPE, and PET bottles, and PE-coated paper cartons was distributed into 20 ml glass vials in a 5°C environmental chamber and evaluated at 10-15°C by a consumer panel or a trained sensory panel.

3.1.3. Light-oxidized and packaging off-flavors in 2% milk

Reduced fat (5%) milk stored in glass, HDPE, HDPE-TiO₂, PET bottles, and PE-coated paper cartons were exposed to fluorescent light (1000 lx) at 5°C for 12 hours (Figure 27). One ml milk sample was removed from each container using a 1 ml serological glass pipet, sealed immediately in a 10 ml headspace vial, and stored below -18°C for electronic nose analysis at a later time. Twenty ml milk samples was distributed into 20 ml glass vials in a 5°C environmental chamber and evaluated at 10-15°C by a consumer or a trained sensory panel.

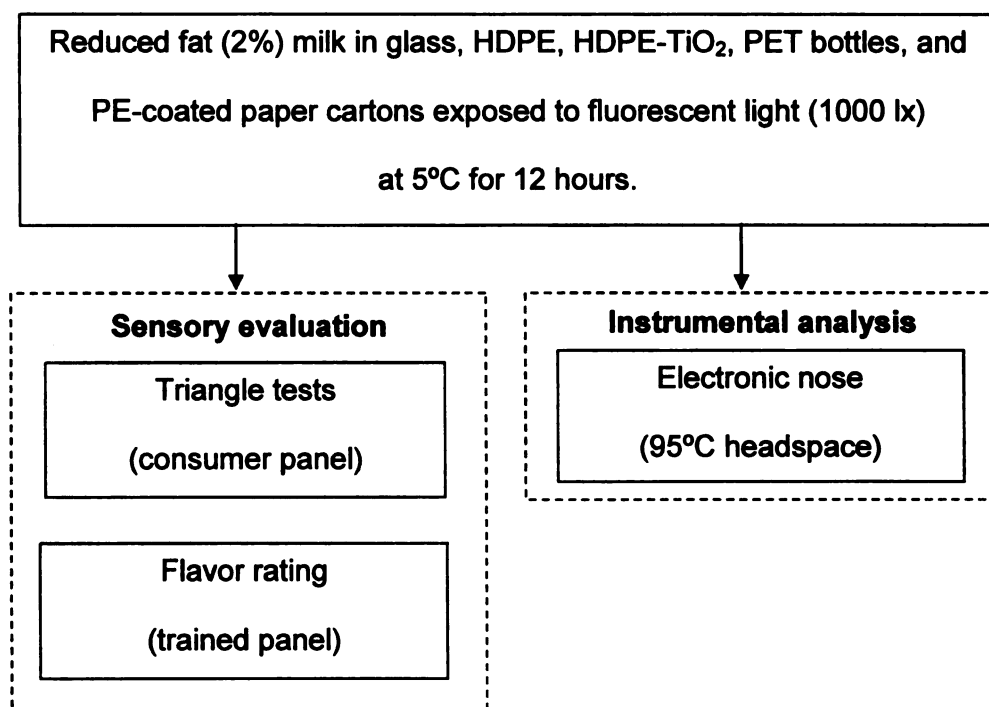


Figure 27 Experimental flowchart to investigate the light-oxidized and packaging off-flavors in 2% milk, using sensory evaluation and instrumental analysis (electronic nose).

3.1.4. Cheddar cheese samples

A block of cheddar cheese (21.3 kg, medium sharpness, aged at 5°C for 7 months) was obtained from the Michigan State University Dairy Plant. The outer layer (~ 5 cm) of the cheese block was trimmed off and discarded. The cheese block was then cut into one-pound (454 g) blocks and vacuum-sealed in transparent shrink bags (Cryovac® B-series, Cryovac, Duncan, SC), which were characterized as high gloss and low oxygen permeability. Table 7 lists the oxygen and water vapor transmission rates of the Cryovac® B-series bags.

Table 7 Oxygen and water vapor transmission rates of the Cryovac® B-series bags, given the temperature (°C) and relative humidity (%RH).

Transmission rate	Value	Source
Oxygen transmission rate at 4.4°C, 0% RH	$3 - 6 \frac{\text{cc}}{\text{m}^2 \cdot \text{day}}$	Product specification from the supplier
Oxygen transmission rate at 5°C, 60% RH	$2.4 \frac{\text{cc}}{\text{m}^2 \cdot \text{day}}$	Measured using an Oxtran ¹
Water vapor transmission rate at 37.8°C, 100% RH	$0.5 - 0.6 \frac{\text{g}}{100\text{in}^2 \cdot \text{day}}$	Product specification from the supplier

¹ A modified Oxtran 100 - Twin (Mocon Inc., Minneapolis, MN), operated inside of an environmental chamber controlled at 5°C, 60% RH.

The Cheddar cheese in 1-lb vacuum-sealed blocks was arranged randomly in the environmental chamber and exposed to fluorescent light (2 bulbs of Philips F48T12/CW/HO 60W) for 0, 2, 4 and 6 weeks. The relative humidity fluctuated between 50-70% RH due to the malfunctioning relative humidity control of the chamber. The oxygen transmission rates of the vacuum bag did not vary significantly at different relative humidity (Table 7), thus the fluctuation of relative humidity was not expected to affect the results. The light intensity was measured from the top of the cheese blocks using a digital light meter (Model SLM 110, A.W. Sperry Instruments, NY), and the average light intensity was recorded as ~2000 lx. All cheese blocks were wrapped in aluminum foil prior to placement to the chamber, and the foil wraps were removed for 0, 2, 4 or 6 weeks for randomly selected samples. To avoid deviations in light exposure, all cheese blocks were rearranged followed a random sequence generated using Matlab 6.1 (The MathWorks Inc., Natick, MA) every 3 days, during the 6 weeks of light exposure. Figure 28 shows the arrangement of the Cheddar cheese blocks in the 5°C environmental chamber equipped with the light fixture.

Two samples, i.e. surface slabs (the top surface) and interior slabs (~1 cm below the top surface), were taken from the Cheddar cheese samples exposed for a specified duration of light. For color measurement and sensory evaluation, 3mm thick slabs were sliced off using a cheese cutter (Model CC-12, Nelson-Jameson, Marshfield, WI), vacuum-sealed in Nylon/PE bags (0.75 mil nylon/ 2.25 mil polyethylene, Koch, Kansas City, MO), and stored at 5°C until one-hour prior to sensory evaluation. All samples were evaluated at ambient temperature

(~21°C). For headspace analysis, 1 mm thick slabs were removed using a razor blade, and cut into a disk-like specimen (0.15 ± 0.01 g, i.d. = 11 mm) using a test tube. Each specimen was sealed in a 10 ml headspace vial and stored below -18 °C for analysis at a later time.

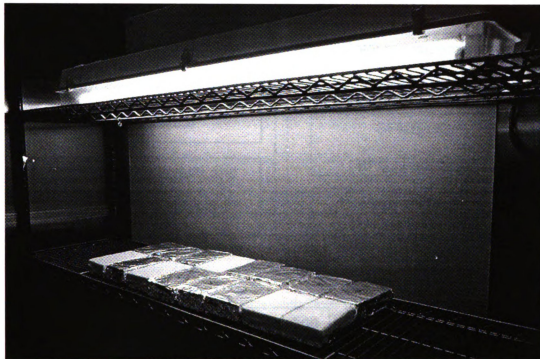


Figure 28 The arrangement of the Cheddar cheese samples exposed to fluorescent light (2000 lx) at 5°C for 0, 2, 4, or 6 weeks. The aluminum foils were unwrapped at the specified weeks. Cheese blocks were rearranged randomly every 3 days.

Figure 29 shows the experimental flowchart to investigate the light-induced deterioration of Cheddar cheese and its effect on color, body/texture, and flavor, using sensory (different-from-control and ADSA rating) and instrumental methods (color measurement, SPME-GC and the electronic nose).

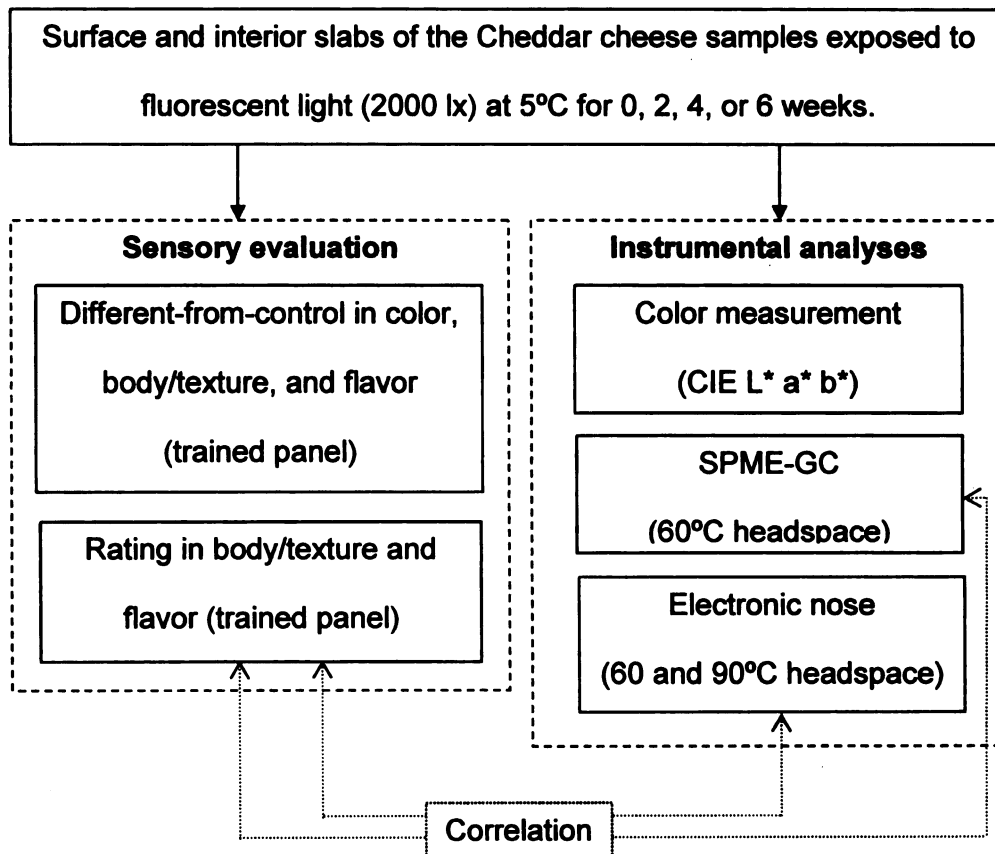


Figure 29 Experimental flowchart to investigate the light-induced deterioration of Cheddar cheese in color, body/texture, and flavor, using sensory evaluation and instrumental analyses.

3.2. Sensory evaluation

Triangle tests were performed by a 24-member consumer panel, which was recruited mainly from the students and faculty members of the School of Packaging and Department of Food Science & Human Nutrition, Michigan State University. A rating based on the ADSA guidelines and different-from-control tests were performed using a trained panel of 8-9 members, which consisted of the coach and members of the Michigan State University dairy judging team for Collegiate Dairy Products Evaluation Contest, 2002. The trained panelists received training on the ADSA guidelines for six types of dairy products: milk, Cheddar cheese, creamed cottage cheese, Swiss type yoghurt, butter and ice cream, for 4-6 hours per week for a 6-8 week period.

Panelists were told to spit out all test specimens after judging (foam cup was provided), and rinse their mouth with deionized water between specimens if necessary. A three-digit random number was assigned to each milk, water or cheese specimen. Random number codes and permutations were generated using Matlab 6.1 (Mathworks Inc., Natick, MA). The sensory evaluation designs and test forms for all sensory tests are shown in Appendix 6.2.

3.2.1. Triangle tests performed by a consumer panel

Triangle tests were conducted in the sensory laboratory using a consumer panel of 24 panelists, to determine the overall flavor difference between samples and the control. Each panelist evaluated samples in an individual booth and recorded the results on the data sheet provided. For each sample set, a series of

four triangle tests were presented sequentially and randomly. Each triangle test contained a total of three specimens of two samples (treatment and control), with two identical and one “odd” specimen. Panelists were told to determine the odd specimen, and had to guess even if no difference was apparent.

3.2.2. Rating based on ADSA guidelines performed with a trained panel

Numerical sensory scores of milk flavor (from 1: pronounced off-flavor to 10: no criticism) were obtained from an 8-member trained panel. Evaluation was performed using the scoring guidelines from the American Dairy Science Association (Table 8 and Appendix 6.2.2). No criticisms were assigned a score of “10”. Sixteen milk flavor criticisms were evaluated, and an overall flavor score assigned based on the existence and intensities of the off-flavor(s). Eight milk specimens were presented simultaneously in each sample set, and the panelists were asked to rate the specimens from left to right. Milk from the original one gallon HDPE containers was provided as a reference, panelists were not asked to give a sensory score to the control.

Rating the body/texture and flavor of the Cheddar cheese was performed using a 9-member trained panel, following the ADSA guidelines, which assigned scores according to the perceived defects of cheese samples (Table 9). Rating on body/texture (from 1: defective to 5: no criticism) was given based on the criticisms listed in Table 9. The criticisms “gassy” and “open” were excluded since they are not expected as a result of light exposure. For flavor, all 13 criticisms were evaluated (from 1: pronounced off-flavors to 10: no criticism).

Table 8 Product attributes and scores of the ADSA guideline for scoring off-flavors in milk (S: slight, D: definite, P: pronounced). No criticism is assigned a score of 10. Pronounced acid, rancid and unclean off-flavors are not acceptable and denoted as "*" [80].

Flavor	S	D	P
Acid	3	1	*
Bitter	5	3	1
Cooked	9	8	6
Feed	9	8	5
Fermented/ Fruity	5	3	1
Flat	9	8	7
Foreign	5	3	1
Garlic/onion	5	3	1
Lacks Freshness	8	7	6
Malty	5	3	1
Oxidized - Light	6	4	1
Oxidized - Metal	5	3	1
Rancid	4	1	*
Salty	8	6	4
Unclean	3	1	*

Table 9 Product attributes and scores of the ADSA guideline for scoring flavor and body/texture defects of Cheddar cheese (S: slight, D: definite, P: pronounced) [80].

Flavor	S	D	P
Bitter	9	7	4
Feed	9	8	6
Fermented	7	5	3
Flat/Low Flavor	9	8	7
Fruity	7	5	3
Heated	9	8	7
High Acid	9	7	5
Oxidized	8	6	3
Rancid	6	4	1
Sulfide	9	7	4
Unclean	8	6	3
Whey Taint	8	7	5
Yeasty	6	4	1

Body/Texture			
Corky	4	3	2
Crumbly	4	3	2
Curdy	4	3	2
Gassy	3	2	1
Mealy	4	3	2
Open	4	3	2
Pasty	4	3	1
Short	4	3	2
Weak	4	3	2

3.2.3. Difference-from-control tests using a trained panel

Evaluation was performed by a 9-member trained panel. A different-from-control test using a rating of 0 (no difference) to 5 (extreme difference) was applied to determine the difference in color, body/texture, and flavor, between the test samples and the control, i.e. the sample slabs of ~1 cm below the Cheddar cheese having no light exposure.

3.3. Electronic nose analysis

Headspace volatiles generated from 2% milk, water, packaging materials (glass, HDPE, HDPE-TiO₂, PET bottles, and PE-coated paper cartons) or cheese samples were analyzed using the electronic nose (Fox 3000, Alpha-MOS, Toulouse, France) equipped with 12 metal oxide semiconductor sensors (chamber A: T30/1, P10/1, P10/2, P40/1, T70/2, PA2; chamber C: LY/LG, LY/G, LY/AA, LY/Gh, LY/gCTI, LY/gCT). Liquid or solid samples were sealed in 10 ml headspace vials and placed in the sample trays (Figure 30c). The autosampler was programmed to move the sample vials to the oven (Figure 30b) to generate headspace volatiles, which were then injected into the injection port (Figure 30e) of the sensor chamber (Figure 30b) using a 5 ml gas-tight syringe (Figure 30d).

Twelve MOS sensors reacted simultaneously to the injected headspace sample, which was a mixture of volatiles, which resulted in a change in resistance (R) from the resistance at equilibrium R_0 . Maximum values of $\frac{R-R_0}{R_0}$ were recorded for preprocessing and multivariate statistical analysis. Four replicates of each sample set were analyzed in a semi-random order. Each

sample set was independently evaluated twice; one for building a supervised model and the other for testing model generalization.

Each sample vial was taken directly from -18°C storage and placed on the tray of the autosampler (HS 100) immediately before each injection. Headspace was generated at specified temperatures for 15 minutes, and then 2.5 ml of the static headspace was taken by syringe and directly injected by the autosampler into the sensor chambers. Sensor responses (the scaled sensor resistance change, $R-R_0$, divided by the equilibrium sensor resistance prior to injection R_0) were recorded and processed using a personal computer and the acquisition software (Alpha SOFT version 8.0, Alpha-MOS, Toulouse, France).

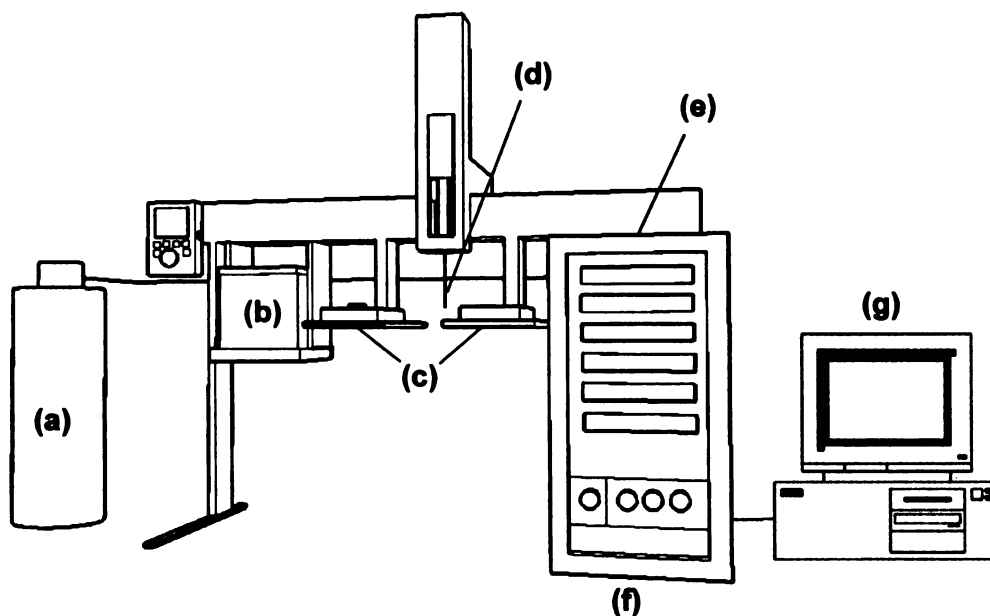


Figure 30 The electronic nose system (Fox 3000, Alpha-MOS): (a) compressed air; (b) oven, used to generate headspace volatiles at specified temperatures and times; (c) sample trays to hold vials; (d) gas-tight syringe; (e) injection port; (f) sensor chamber containing the 12 MOS sensors; (g) computer, to collect and analyze data. The parts (b), (c), (d) belong to the autosampler (HS 100).

3.4. Solid-Phase Microextraction-Gas Chromatography (SPME-GC)

Headspace analysis was performed using a gas chromatograph coupled with solid-phase microextraction (SPME) sampling [159]. A 75 μm Carboxen/Polydimethyl Siloxane (CAR/PDMS) fiber, or a 65 μm Polydimethylsiloxane/Divinylbenzene (PDMS/DVB) fiber was mounted in a manual holder (Supelco, Bellefonte, PA) and used to collect the headspace volatiles generated by heating milk or Cheddar cheese specimens in 10 ml headspace vials, using an oven with precise temperature control (gas chromatograph HP 5890). A Hewlett-Packard gas chromatograph (HP 6890) equipped with FID detector and integrator (HP 3395) was used to separate the headspace volatiles desorbed from SPME fibers.

To select the proper analytical condition, a standard solution of 10 ng/ml of pentanal, hexanal, dimethyl disulfide, methional (3-methylthiopropionaldehyde), and 20 ng/ml of internal standard 4-heptanone was prepared in HPLC grade water and sampled using two different SPME fibers (CAR/PDMS and DVB/PDMS). One ml standard solution was sealed in a 10 ml crimp-top headspace vial and stored at 5°C. Sampling temperature was controlled using a refrigerator (5°C) or GC oven (30 and 45°C). Five minutes of preheating was followed by sampling times at 5, 15 or 25 minutes. A complete randomized design was applied to 27 specimens, at three sampling temperatures (5, 30 and 45°C) and times (5, 15 and 25 minutes). Three replicates were performed for each combination. Reproducibility was evaluated by comparing the coefficient of variation (%CV), which is a measure of the deviation of a variable from its mean,

$$\%CV = \frac{\text{standard deviation}}{\text{mean}} \times 100\% .$$

Normalization of the peak areas using the peak area of the internal standard [28, 126] was also evaluated.

3.4.1. SPME-GC for milk samples

One ml milk sample was taken using a 1 ml serological glass pipet, transferred to a 10 ml sealed crimp-top headspace vial, and stored below -18°C for analysis at a later time. Headspace sampling was performed using a CAR/PDMS fiber at 45°C for 15 minutes with 5 minutes of preheating. The separation of volatiles from milk was accomplished using a 30 m x 0.32 mm x 0.25 µm HP5 column. Column temperature was initially set at 35°C for 12 minutes, which allowed all target volatiles to pass through the column, and then heated to 220°C at a rate of 20°C/min, to clean up the volatiles generated by degradation of the fiber.

External standards were prepared by spiking analytical grade pentanal, hexanal and dimethyl disulfide into 2% milk, at levels of 0, 0.5, 1, 2, 4 and 10 ng/ml. Four replicates of each concentration were analyzed. Three replicates were used to build the correlation models, i.e. training data, and one replicate was used to test the model performance. Initial levels of pentanal, hexanal, and dimethyl disulfide in the 2% milk were estimated by extrapolating the regression line to the x-axis. Quantification was based on the linear regression equations of the calibration curves, with the addition of the estimated initial concentration of the volatile components.

3.4.2. SPME-GC for Cheddar cheese samples

Cheddar cheese specimens (disk-shaped solid, 0.15 ± 0.01 g) were sealed in 10 ml vials and stored below -18°C for analysis at a later time. Separation of the volatiles from Cheddar cheese was accomplished using a 60 m x 0.25 mm x 0.25 μm Supelcowax 10TM column (Supelco, Bellefonte, PA). Column temperature was set initially at 35°C , and then heated to 220°C at a rate of $2^{\circ}\text{C}/\text{min}$. Headspace of cheese samples were generated at 60°C for 15 minutes, and four replicates were performed for each sample. Volatiles were identified by comparing the peak retention times of the standards, and the peaks with better reproducibility were selected for further multivariate analyses. Three replicates were used to build the correlation models, i.e. training data, and one replicate was used to test the model performance.

3.5. Light transmission of milk packaging materials

Percent light transmission of the various packaging materials (HDPE, HDPE-TiO₂, PET, and PE-coated paper cartons in white or blue) in the 200-1100 nm range was measured using a UV-visible spectrophotometer (Lambda 25, PerkinElmer, Wellesley, MA) equipped with an integrating sphere (RSA-PE-20). Samples were cut into 4 cm x 4 cm pieces, mounted on a sample holder with a window (i.d. = 1 cm) and aligned perpendicular to the light path.

3.6 Color measurement of cheese

Surface slab (top 3 mm surface) and interior slab (3 mm slices of ~1 cm below the top surface) color (CIE $L^* a^* b^*$) of the of the Cheddar cheese exposed to fluorescent light were measured using a spectrophotometer (Hunterlab ColorQuest 45°/0° Spectrophotometer, Hunter, VA). Sample slabs packaged in Nylon/PE bags were placed on top of the sample holder with a window (i.d.= 1 cm), and the color measured reflectively in a 45°/0° geometry (Figure 31a).

The CIE $L^*a^*b^*$ color space (Figure 31b) is the color standard developed by the International Commission on Lighting (Commission Internationale d'Eclairage, CIE) in 1976 [187]. It defines the color perceived by human eyes using three parameters: L^* indicates lightness or luminosity, from white to black. The chromaticity coordinates a^* and b^* indicate color directions: $+a$ to $-a$ is from red to green, and $+b$ to $-b$ from yellow to blue, and the center is achromatic, hues of gray. As the values of a^* and b^* increase, such that the point moves out from the center, the chroma or purity of the color increases. The Euclidean distance between two color points (ΔE) is

$$\Delta E = \sqrt{(\Delta L^*)^2 + (\Delta a^*)^2 + (\Delta b^*)^2}$$

where ΔL^* , Δa^* , Δb^* are the differences in lightness, redness and yellowness. It is a convenient way of presenting color differences between the standard and the samples [188].

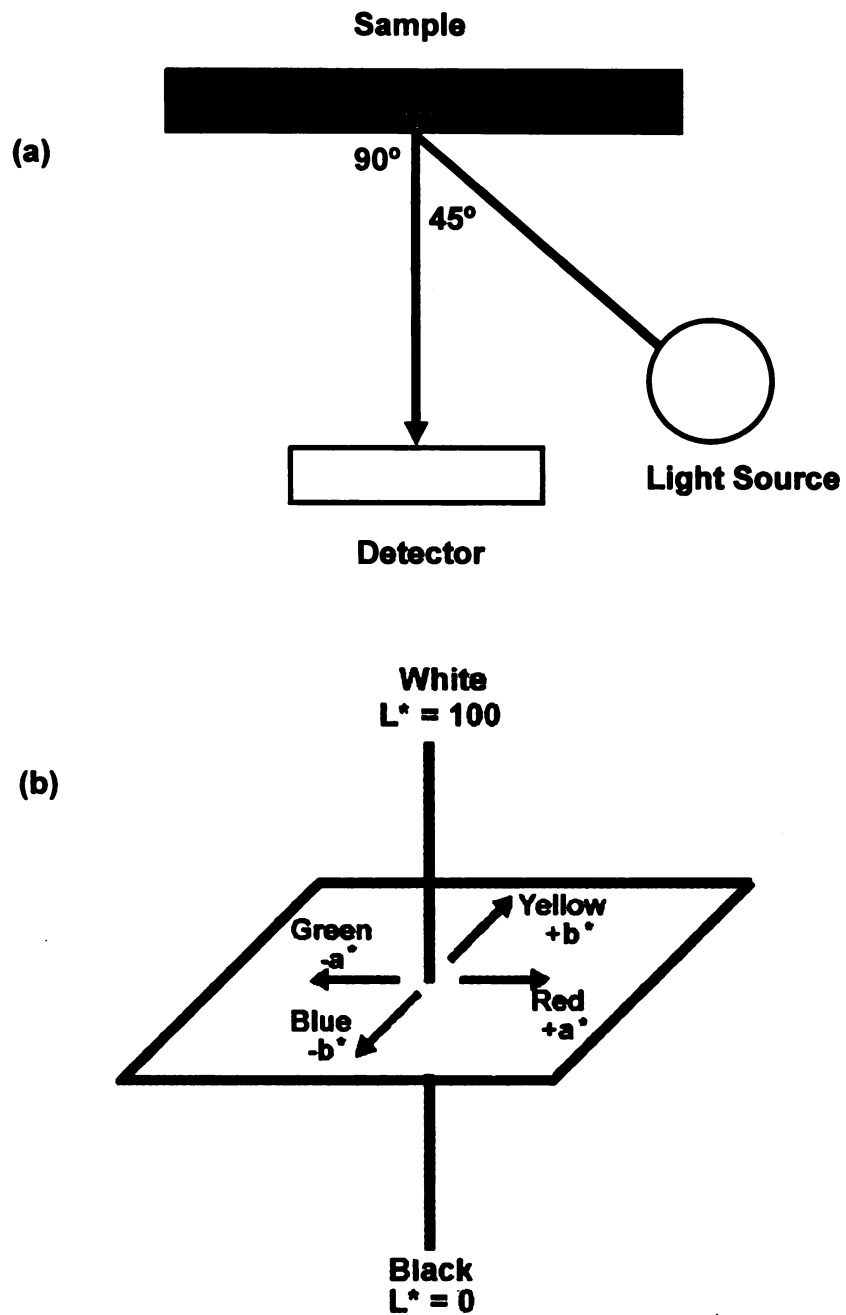


Figure 31 Schematic diagram of (a) 45°/0° geometry of the spectrophotometer [189]; (b) the CIE $L^* a^* b^*$ color space [187].

3.7. Multivariate statistical techniques

3.7.1 Data preprocessing

Maximum values of the relative sensor resistance changes, $\max(\frac{R-R_0}{R_0})$,

were recorded and mean centered, i.e. subtracting the average from each sensor among different samples. Mean centering was applied to account for an intercept term in the regression models [124]. The mean values of the training sets were used for mean centering of both training and test sets.

3.7.2. Unsupervised learning techniques

Hierarchical clustering analysis (HCA) and principle component analysis (PCA) were performed using PROC CLUSTER and PROC PRINCOMP procedures (SAS 8.0, SAS Institute, Cary, NC), respectively. In HCA, single linkage (nearest neighbor) was used as the algorithm for similarities, with the computation of eigenvalues and normalizing of distances suppressed. Results of HCA were presented in a dendrogram, where each step in the clustering process is illustrated by a join of the tree. In PCA, principle components were calculated from the covariance matrix, and scatter plots of the first two or three principle components were generated for visual inspection of the data points. The scree plots (PROC FACTOR) may also be plotted to examine the fraction of total variance in the data as explained or represented by each principle component.

3.7.3. Supervised learning techniques

Linear/quadratic discriminant function analysis (LDA/QDA), and k-nearest neighbor (k-NN) were performed using PROC DISCRIM procedure (SAS 8.0, SAS Institute, Cary, NC). In LDA/QDA, “testing of the equality of normal population parameters” [180] was carried out prior to the analysis. If there is a strong evidence of unequal variances among the groups, QDA is expected to have a better performance of defining the decision boundaries. On the other hand, LDA is used to separate classes that are normally distributed with equal covariance. A parametric method, based on a multivariate normal distribution within each class, was used to derive the LDA or QDA. Models were cross-verified by the leave-one-out method, i.e. each observation was classified using a discriminant function computed from the other observations in the training set. An independent test data set was used to test the model generalization. Canonical discrimination plots with the first two or three LDA discriminants were generated for visual inspection of the sample discrimination. Nonparametric classification was based on a k-NN algorithm ($k \leq$ number of replicates), i.e. no assumption of multivariate normal distributed data was required. Cross-validation and testing of the model generalization was performed using similar procedures as used in LDA/QDA analyses.

The correct identification rates (i.e. hit rates) were calculated at the steps of training (model building), validation (cross validation of training set using leave-one-out method), and testing (applying an independent test data set). Correct identification rates of training data are usually the highest for the

“training” step, as the models are built using the same data set. The “validation” step, which is used to verify the model stability, may have lower correct identification rates: cross validation was performed by leaving out one data point at a time and verifying its “identified” group using the reduced models built by the rest of the training data set. The “test” step is applied to test the model generalization, i.e. how well the model works when applied to an independent data set. It may have either a higher or lower correct identification rate than the validation step. A model is considered to be unstable if the correct identification rate is extremely high for training but low for validation, or to be “optimistic” when the rate is high for training but low for the test step.

3.7.4. Quantitative analyses

Partial least squares analysis (PLS) was performed using PROC PLS (SAS 8.0, SAS Institute, Cary, NC). The singular value decomposition (SVD) algorithm was used to compute extracted PLS factors. Models were verified using cross validation (leave-one-out method in training set) for PLS, along with the test set validation. A SAS macro “plsplot.sas” (available at <http://www.sas.com>) was used to generate scatter, loading and residual plots for visual inspection of model performance.

Multilayer perceptrons (MLP) was performed using the Neural Network Toolbox 4.0 of Matlab 6.1 (The MathWorks Inc., Natick, MA). A feed-forward backpropagation network was constructed, with a tan-sigmoid function in the hidden layer, and a linear function in the output layer (Figure 32). An independent

data set was applied for validation (early stopping to avoid over-fitting) as well as for testing (estimating a network's ability to generalize), with the following training parameters (Figure 33).

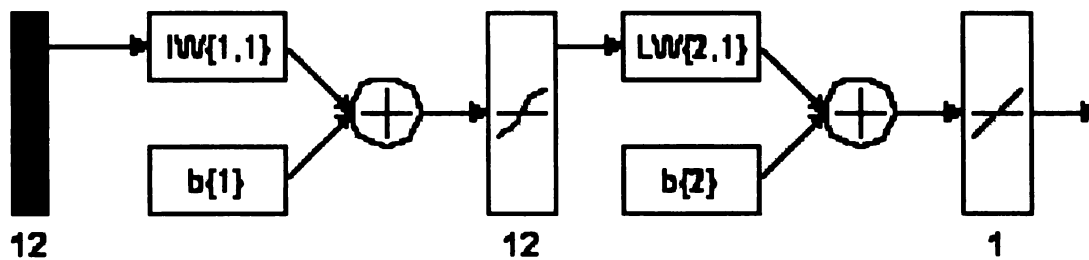


Figure 32 The feed-forward backpropagation network with 12 input nodes, which correspond to the mean-centered 12 sensor responses), and one output node, i.e. numerical sensory score (figure modified from Matlab output).

Training Parameters			
epochs	100	mu_dec	0.1
goal	0	mu_inc	10
max_fail	5	mu_max	10000000000
mem_reduc	1	show	25
min_grad	1e-010	time	Inf
mu	0.001		

Figure 33 Training parameters of the feed-forward backpropagation network (figure modified from Matlab output).

Root mean square error (RMSE) was used to evaluate the performance of the models. RMSE values are determined by calculating the deviations of predicted responses from their expected ones, summing up the measurements, and then taking the square root of the sum:

$$\text{RMSE} = \sqrt{\frac{\sum_{i=1}^n (\hat{F}(x_i) - F(x_i))^2}{n}},$$

where $\hat{F}(x_i)$ is the predicted response based on the model, $F(x_i)$ is the expected response, n is the number of specimens. The smaller the RMSE, the better the performance of the model.

CHAPTER 4

RESULTS AND DISCUSSION

4.1. Light-oxidized off-flavors in 2% milk

4.1.1. Sensory evaluation

Using a 24-member consumer panel, a series of four triangle tests were conducted sequentially, to determine if milk exposed for 2, 4, 8, or 12 hours could be differentiated from the control, i.e. milk stored in aluminum foil-wrapped glass bottles (Table 10). It showed that light exposure (1000 lx, 5°C) resulted in a subtle olfactory change in reduced fat milk after 4 hours ($p < 0.20$). A significant overall difference was detected after 8 hours ($p < 0.05$), and 13 out of 24 consumer panelists had the correct responses. The flavor change was more noticeable after 12 hours ($p < 0.01$).

The “occurrence” of light-oxidized off-flavors in milk is dependant on the light exposure conditions and sensory techniques. The light-oxidized off-flavors were reported to appear in milk as soon as 15 minutes to 12 hours (Chapter 2.1.3, [6-8, 54, 60, 62]). Fluid milk in clear transparent packages has been shown to be highly susceptible to consumer-detectable light-induced quality changes due to retail display. Fluid milk is often displayed for times ranging from at least 8 hours [6, 9] to 2-3 days [10].

Table 10 Triangle test results on light-oxidized 2% milk in glass bottles against control, i.e. 2% milk stored in aluminum foil-wrapped glass bottles. Tests were performed by a 24-member consumer panel.

Duration of light exposure	Number of correct responses from 24 subjects	p
2 hours	9	—
4 hours	11	0.20
8 hours	13	0.05
12 hours	15	0.01

Milk samples with differing levels of light oxidation were then evaluated by an 8-member trained panel, based on ADSA guidelines. The test was performed in a semi-ascending sequence, such that samples were presented to the panelists from short to long light exposure times, to avoid the carry-over effect of light-oxidized off-flavors. The sensory scores of 2% milk in glass bottles decreased with increase in the duration of light exposure, to a score of ~5.5 in 24 hours (Table 11 and Figure 34). Compared to the control sample (no light exposure), the decrease in sensory scores of the milk samples was not statistically significant until after 36 hours of light exposure (Table 11). However, the sensory scores of 2% milk decreased after 4 hours of light exposure and were further reduced in milk exposed to light for 8 hours or longer (Figure 34). The variances were significantly greater for milk samples exposed to light for 8 hours and longer, which was evidence of the off-flavor “detection” on the part of the trained panel. Increased variance among different treatments limits the application of analysis of variance (ANOVA) and multiple comparisons (e.g. Tukey’s studentized range test) to indicate a change in sensory scores. The

ADSA guidelines are designed to monitor various off-flavors in milk from different sources and not specific for light-oxidized off-flavor. Milk samples with “slight”, “definite” or “pronounced” light-oxidized off-flavors should receive a score of “8”, “6” or “3”, respectively (chapter 3.3.3). Oxidized but not highly oxidized milk samples tended to receive a “6” as they contained a “definite” but not quite “pronounced” off-flavor. Thus similar ratings may be given to milk samples with slightly different intensities of light oxidized off-flavors. Due to the large variation and more “clustered” rating scale, light-oxidized quality change was not statistically significant until after 36 hours of light exposure (1000 lx), although the detection of off-flavors by some members of the trained panel was observed in 4 or 8 hours.

The consumers picked up a moderate light-oxidized flavor change after 4 hours of fluorescent light exposure (1000 lx, 5°C), and the change was significant after 8 hours and more pronounced after 12 hours. The trained panel gave significantly lower sensory scores to milk exposed to light for 36 hours or longer, although the reduction in average sensory scores and increased sensory score variances indicated that the off-flavor development was occurring in 4 or 8 hours.

Table 11 Sensory scores of light-oxidized 2% milk based on ADSA guidelines. Scores were given by an 8-member trained panel.

Duration of light exposure (hours)	Sensory score		
0	8.50	±0.54	a ¹
2	8.38	±1.06	a, b
4	7.75	±0.89	a, b, c
8	6.63	±1.60	a, b, c
12	6.38	±2.20	a, b, c
24	5.63	±2.93	a, b, c
36	5.38	±2.62	c
48	5.50	±1.77	b, c

¹ Means with the same letter are not statistically different at $\alpha=0.05$ (Tukey's studentized range test).

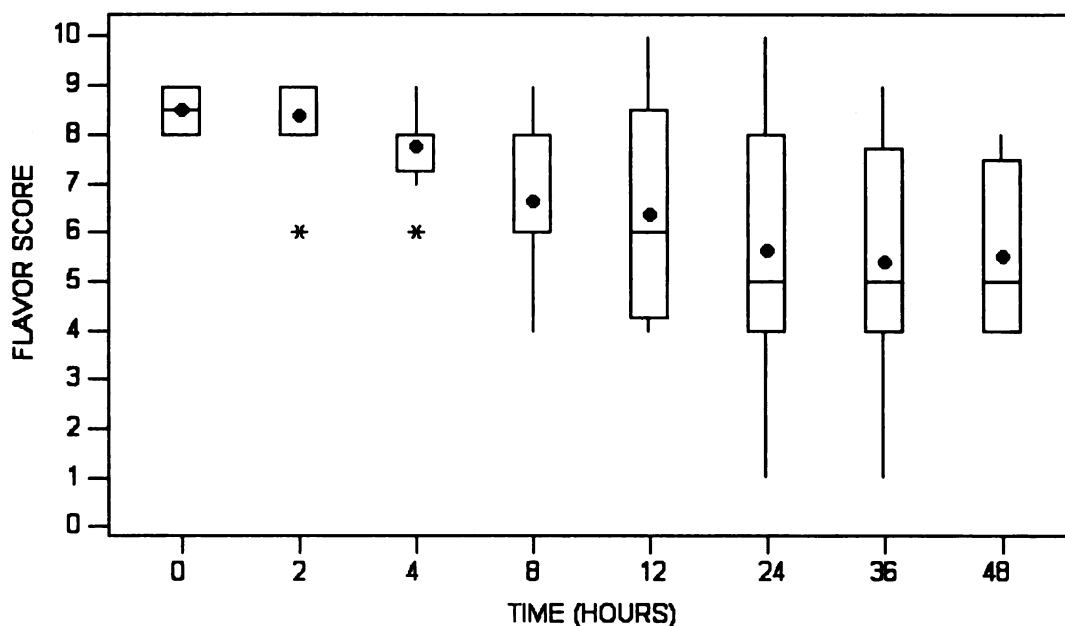


Figure 34 Flavor sensory scores based on ADSA guidelines of 2% milk in glass bottles exposed to 0, 2, 4, 8, 12, 24 or 48 hours of fluorescent light (1000 lx, 5°C). •: mean values of each treatment; *: possible outliers.

4.1.2. Headspace analysis using SPME-GC

4.1.2.1. Optimizing the headspace sampling parameters

Two different SPME fibers (CAR/PDMS and DVB/PDMS) were used to collect the headspace volatiles of the standard aqueous solution (pentanal, hexanal, dimethyl disulfide, methional, and 20 ng/ml of internal standard 4-heptanone) at 5, 30 or 45°C for 5, 15 or 25 minutes. Pentanal, hexanal, dimethyl disulfide and internal standard 4-heptanone can be clearly identified and quantified from the GC chromatograms, while the peak for methional had very poor resolution and reproducibility (data not shown). Methional is not stable in aqueous solutions and tends to decompose to lower molecular weight sulfur compounds such as methyl mercaptan and dimethyl sulfide [1, 20]. Preliminary testing showed that volatized methional can be collected using a CAR/PDMS fiber, along with decomposed products including dimethyl disulfide.

High temperature may increase SPME volatile adsorption by increasing the headspace volatile content, or decreasing the adsorption by reducing the partition coefficient of volatiles between the fiber and vial headspace. Sampling temperatures (5, 30 and 45°C) had the opposite effect on CAR/PDMS and DVB/PDMS fibers, such that higher temperature resulted in more volatile adsorption by the CAR/PDMS fiber (Figure 35a, b and c), but less volatile adsorption by the DVB/PDMS fiber ((Figure 35, f and g).

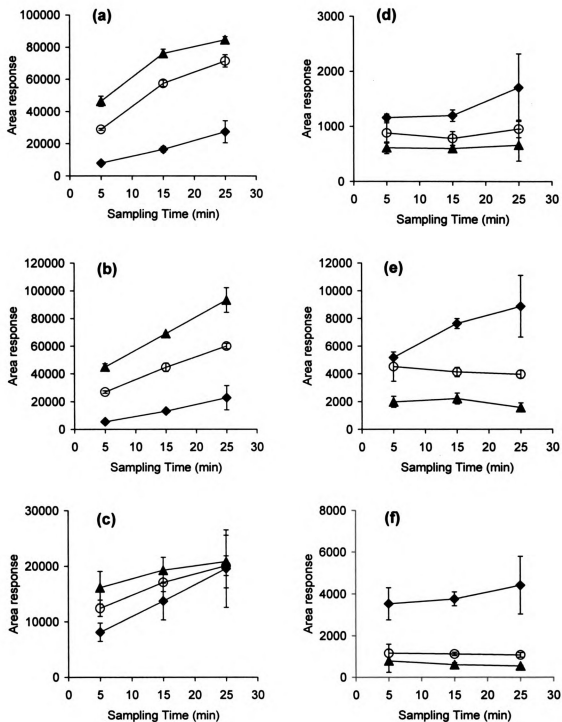


Figure 35 Area responses for (a) pentanal, (b) hexanal and (c) dimethyl disulfide sampling using CAR/PDMS, or DVB/PDMS fiber (d, e, f, respectively), at different sampling temperatures (◆: 5°C, ○: 30°C, ▲: 45°C). Error bars show the standard deviations of three replicates.

Table 12 Coefficient of variation (%CV) for the CAR/PDMS fiber used to quantify volatiles in the standard aqueous solution.

Temperature (°C)	Time (min.)	Without Normalization			Normalized Using I.S. ¹		
		PEN	HEX	DMDS	PEN	HEX	DMDS
5	5	11.50	21.19	20.22	19.96	12.99	18.43
	15	10.95	11.54	24.72	24.21	21.98	10.87
	25	25.23	38.27	35.71	20.37	11.43	15.74
30	5	2.01	3.45	11.86	13.78	9.24	18.35
	15	3.43	6.92	9.57	4.77	3.22	16.32
	25	5.34	3.17	8.86	3.30	4.53	6.50
45	5	6.71	5.41	18.09	5.07	4.26	18.07
	15	3.55	0.68	12.03	5.36	6.13	9.65
	25	2.24	9.55	22.72	16.00	10.61	12.18

¹ normalized using the area response of the internal standard 4-heptanone

Table 13 Coefficient of variation (%CV) for the DVB/PDMS fiber used to quantify volatiles in the standard aqueous solution.

Temperature (°C)	Time (min.)	Without Normalization			Normalized Using I.S. ¹		
		PEN	HEX	DMDS	PEN	HEX	DMDS
5	5	5.69	2.10	21.80	2.57	2.35	19.13
	15	8.75	4.70	8.99	12.30	2.38	4.91
	25	35.87	25.11	31.24	39.84	8.81	12.67
30	5	20.96	23.40	37.63	17.54	9.97	21.96
	15	15.83	8.18	7.15	11.78	10.59	9.19
	25	16.79	6.97	10.08	22.48	11.73	10.81
45	5	17.40	19.70	70.28	34.16	11.23	59.68
	15	9.09	17.52	16.73	16.78	9.37	6.05
	25	44.11	20.64	6.53	29.62	26.99	8.54

¹ normalized using the area response of the internal standard 4-heptanone

Sampling methods with higher adsorption may provide better sensitivity and reproducibility (lower %CV if the standard deviations are similar). The CAR/PDMS fiber, which is designed to analyze trace volatiles and to have high affinity to volatiles in general, had much higher area responses than the DVB/PDMS fiber (Figure 35).

The amounts of pentanal and dimethyl disulfide absorbed by the CAR/PDMS fiber were closer to the equilibrium at higher temperatures (30°C and 45°C), as the increments of adsorbed volatiles over time were decreasing (Figure 35), while the adsorption was still linearly dependent on sampling time at 5°C. More time was required for hexanal adsorption to reach equilibrium. SPME may be used as a pre-equilibrium or an equilibrium sampling technique. If the sampling time is long enough for a system (among liquid phase, headspace, and fiber) to reach equilibrium, the area response will not increase with sampling time (Figure 16). In general, the higher the sampling temperature, the sooner the system reaches equilibrium. With accurate timing, quantification using SPME is repeatable, even though equilibrium is not reached. Therefore, sampling using the CAR/PDMS fiber at 45°C for 15 minutes was selected to be used in this study based on its more reproducible pentanal and hexanal contents, i.e. lower %CV (Table 12).

The use of an internal standard, 4-heptanone, was suggested [28, 126] to improve reproducibility. However, normalizing the area responses of pentanal, hexanal, and dimethyl disulfide with the internal standard did not always reduce the coefficients of variation (Table 12 and Table 13). The amount of 4-heptanone

absorbed varied similarly as did the other volatiles, and the variation was not always cancelled out by normalization. Different volatiles have different affinity to SPME fibers, which can also be affected by the other volatiles in the system. Since the internal standard did not always improve the reproducibility of the process, it was eliminated to simplify the sample preparation and to avoid unnecessary variation.

4.1.2.2. Quantifying the headspace volatiles of light-oxidized milk

Under fluorescent light exposure (1000 lx, 5°C), pentanal content increased rapidly in 2% milk over time, while no significant increase in pentanal occurred in samples in the dark (Figure 36). It has been reported that [28, 190] formation of pentanal increased with a second-order polynomial correlation, and that riboflavin plays an important role in the formation of pentanal. Hexanal content also increased with increased exposure time, but not as rapidly as pentanal during the first 12 hours. Marsili (1999) [28] exposed 2% milk to 200 ft-c (2152 lx) fluorescent light in half-gallon (1.89 L) HDPE jugs, and found that the amount of pentanal and hexanal continuously increased, with a more rapid increase of pentanal for the first 12 hours.

Hexanal, a secondary product of lipid oxidation, has often been used as an indicator of lipid oxidation. In this study 2% milk exposed to light for 4 hours had a very mild flavor change (Table 10), and the hexanal level was 2.5 ± 1.0 ng/ml (i.e. ppm). The light-oxidized off-flavor was detected by consumers when light exposure time reached 8 hours ($p < 0.05$), whereas the hexanal content

remained at about the same level, 2.5 ± 1.1 ng/ml (Figure 36). Pentanal, which is also a secondary oxidative product of lipid oxidation but is generated via different mechanisms than hexanal, had concentrations of 3.7 ± 0.6 and 6.2 ± 0.5 ng/ml in 2% milk exposed to light for 4 and 8 hours, respectively. Lee (2002) [190] found that the antioxidants ascorbic acid and BHA (hydrogen atom donors as antioxidants) decreased the formation of pentanal but that sodium azide (singlet oxygen quencher) increased the formation of pentanal. Both antioxidants and the singlet oxygen quencher reduced the formation of hexanal and heptanal.

Dimethyl disulfide has been reported as being mainly responsible for the light oxidized off-flavors in skim milk, as a major byproduct from milk protein deterioration [20]. However, the expected increase in dimethyl disulfide was not detected (Figure 36). Marsili (1999) [28] was not able to quantitatively determine the concentration of dimethyl disulfide, since the dimethyl disulfide peak response was very small on the GC chromatograms, obtained using a CAR/PMDS fiber or Tenax trap system coupled with a thermal desorption unit for headspace sampling. Conversely, Jung *et al.* (1998) claimed that in skim milk, dimethyl disulfide content increased significantly within 8 hours of light exposure (2400 lx, 20°C) in a 150 ml Erlenmeyer flask. He quantified the amount of DMDS using a Tenax trap coupled with a thermal desorption unit for headspace sampling.

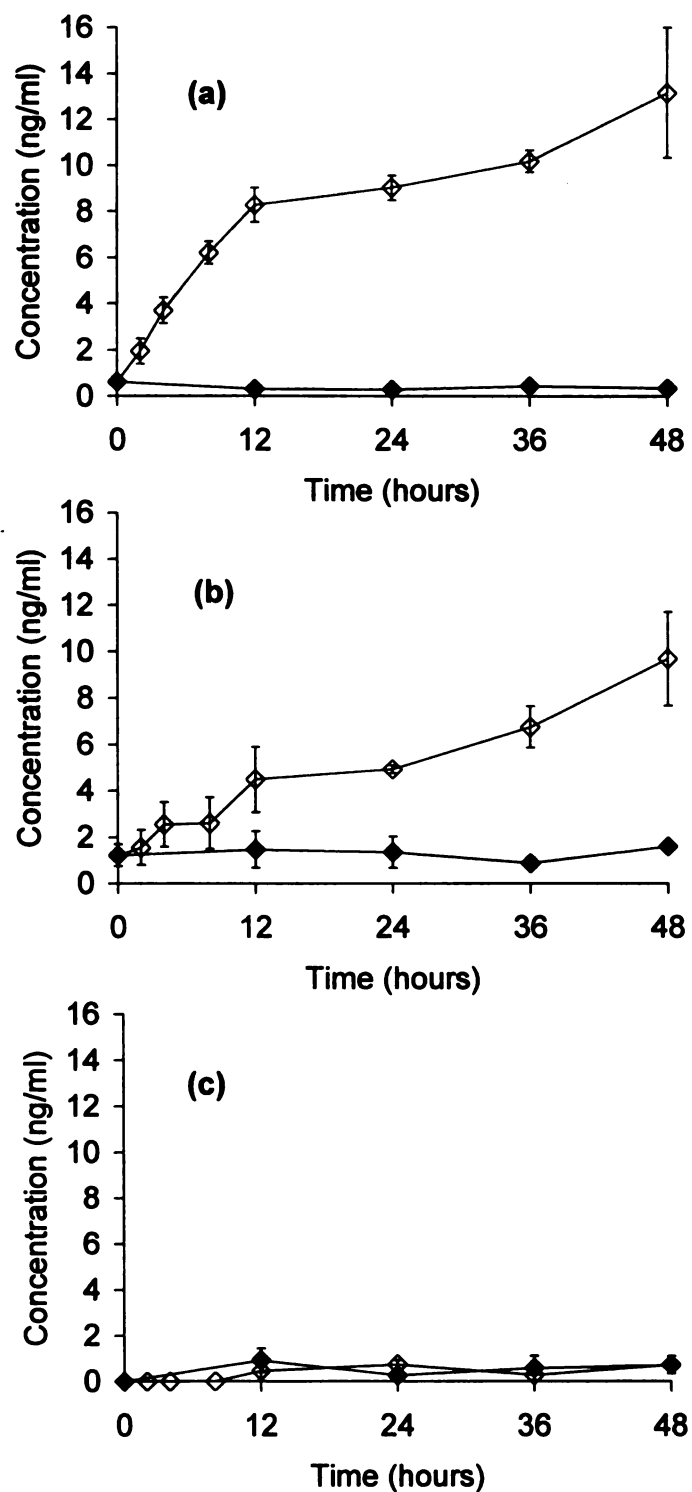


Figure 36 The amount of (a) pentanal (b) hexanal, and (c) dimethyl disulfide in 2% milk with (◇) and without (◆) light exposure for 0 to 48 hours. Error bars show the standard deviations of three replicates.

4.1.3. Headspace analysis using the electronic nose

Figure 37 shows the profiles of sensor response over time, to the 95°C headspace samples of 2% milk exposed to fluorescent light for 0 or 48 hours. The differences between sensor profiles of the two samples were not distinct and difficult to visually justify by comparing the 12 MOS sensor responses directly.

Therefore the steady-state parameter, $\max(\frac{R-R_0}{R_0})$, was recorded (Figure 12) and analyzed using multivariate statistical methods for pattern recognition (Chapter 3.7).

Unsupervised learning techniques, hierarchical clustering analysis (HCA) and principle component analysis (PCA), did not show an obvious pattern or separation among the headspace volatiles generated at 45, 70 or 95°C, for 2% milk exposed to light for 0, 2, 4, 8, 12, 24, 36 or 48 hours (Figure 38, Figure 39 and Figure 40). Although an unclear pattern with few “outliers” was observed in the 45°C headspace sample set (Figure 38), the milk samples exposed to 36 and 48 hours of fluorescent light were partially clustered within the group in HCA as well as PCA. However, it was difficult to define a clear separation boundary.

The first two principle components (PC1 and PC2) were able to explain 88.63% (i.e. 52.44% + 36.19%), 94.21%, and 92.14% of the total data variation of the 12 sensor responses for 45, 70, and 95°C headspace volatiles, respectively. That is, after projecting the 12 data dimensions into the two dimensional space constructed by the PC1 and PC2, most of the total variance was preserved in the two dimensional models.

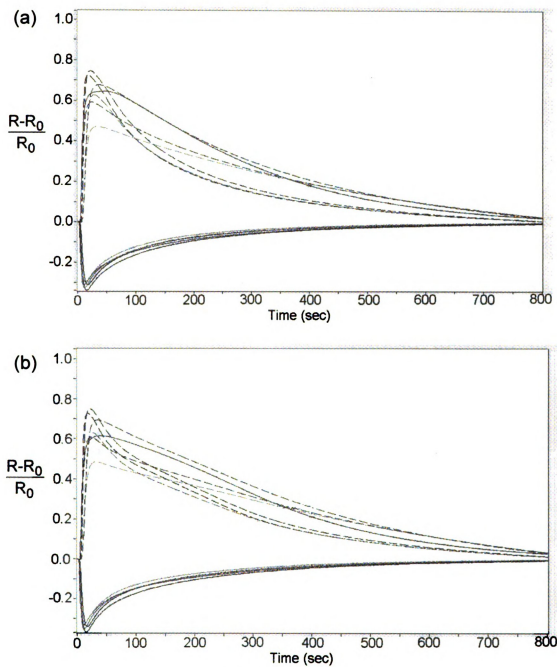


Figure 37 Sensor responses ($\frac{R-R_0}{R_0}$) of the electronic nose to 95°C headspace of 2% milk (a) without (b) with 48 hours of light exposure at 5°C.

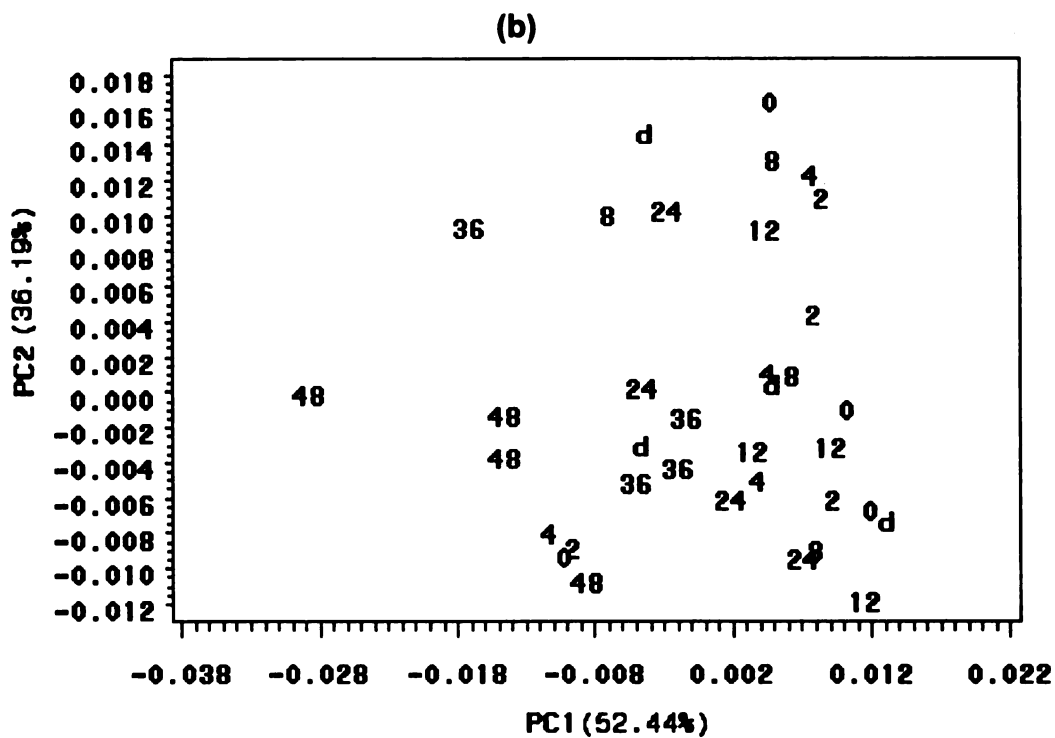
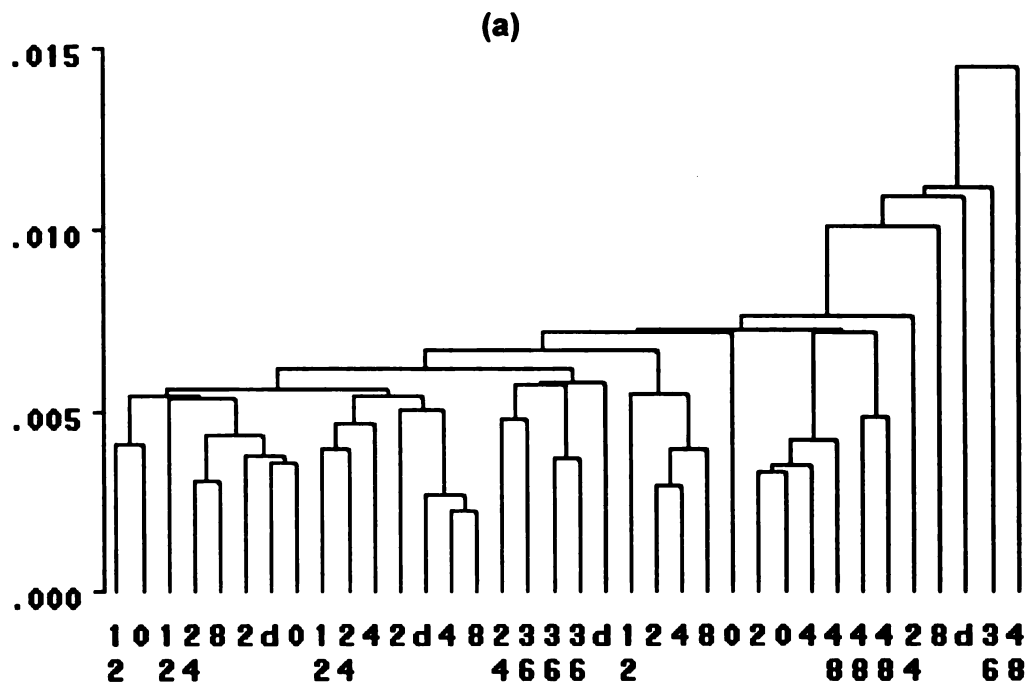


Figure 38 (a) HCA and (b) PCA of the sensor responses for 45°C headspace of 2% milk exposed to 0, 2, 4, 8, 12, 24, 36, or 48 hours of light at 5°C. Sample “d” was stored in the dark for 48 hours.

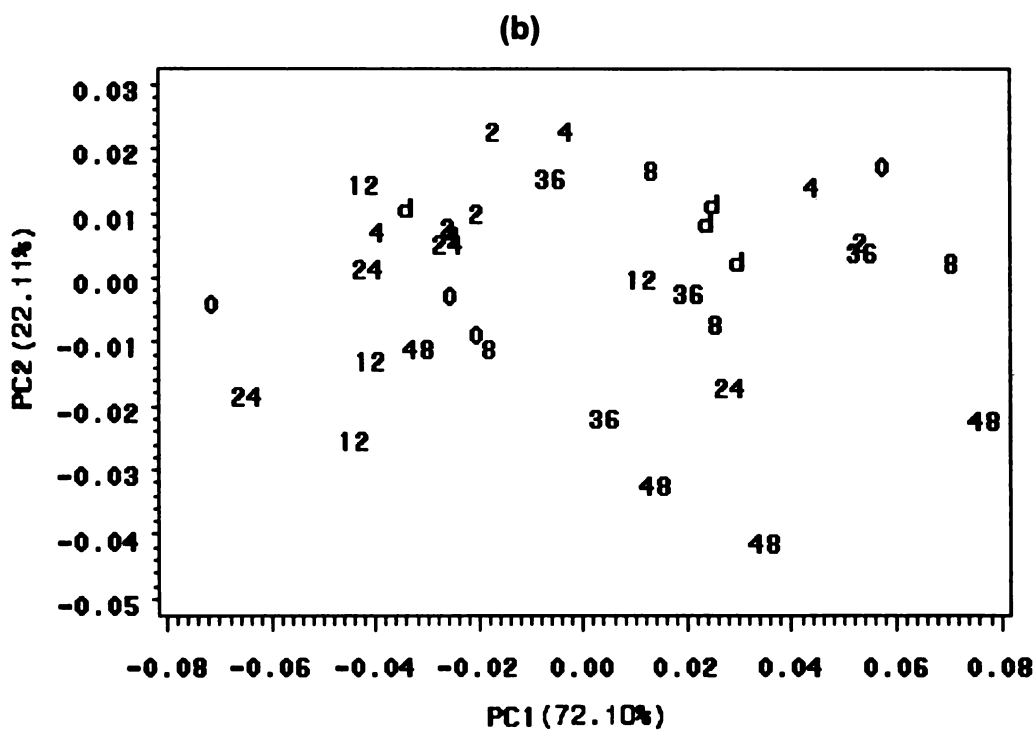
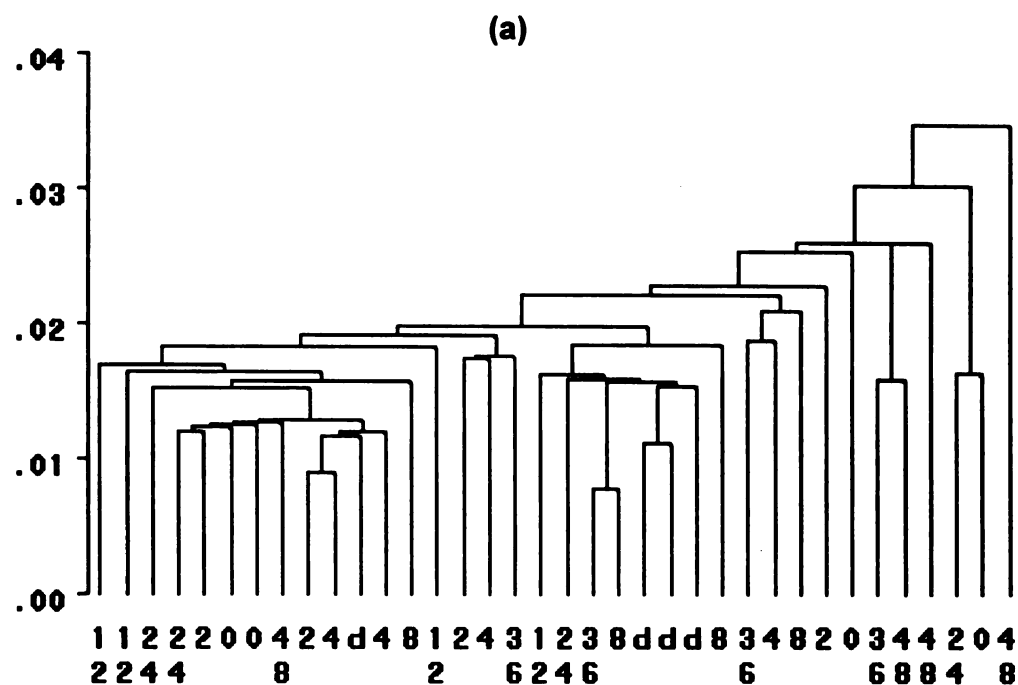


Figure 39 (a) HCA and (b) PCA of the sensor responses for 70°C headspace of 2% milk exposed to 0, 2, 4, 8, 12, 24, 36, or 48 hours of light at 5°C. Sample “d” was stored in the dark for 48 hours.

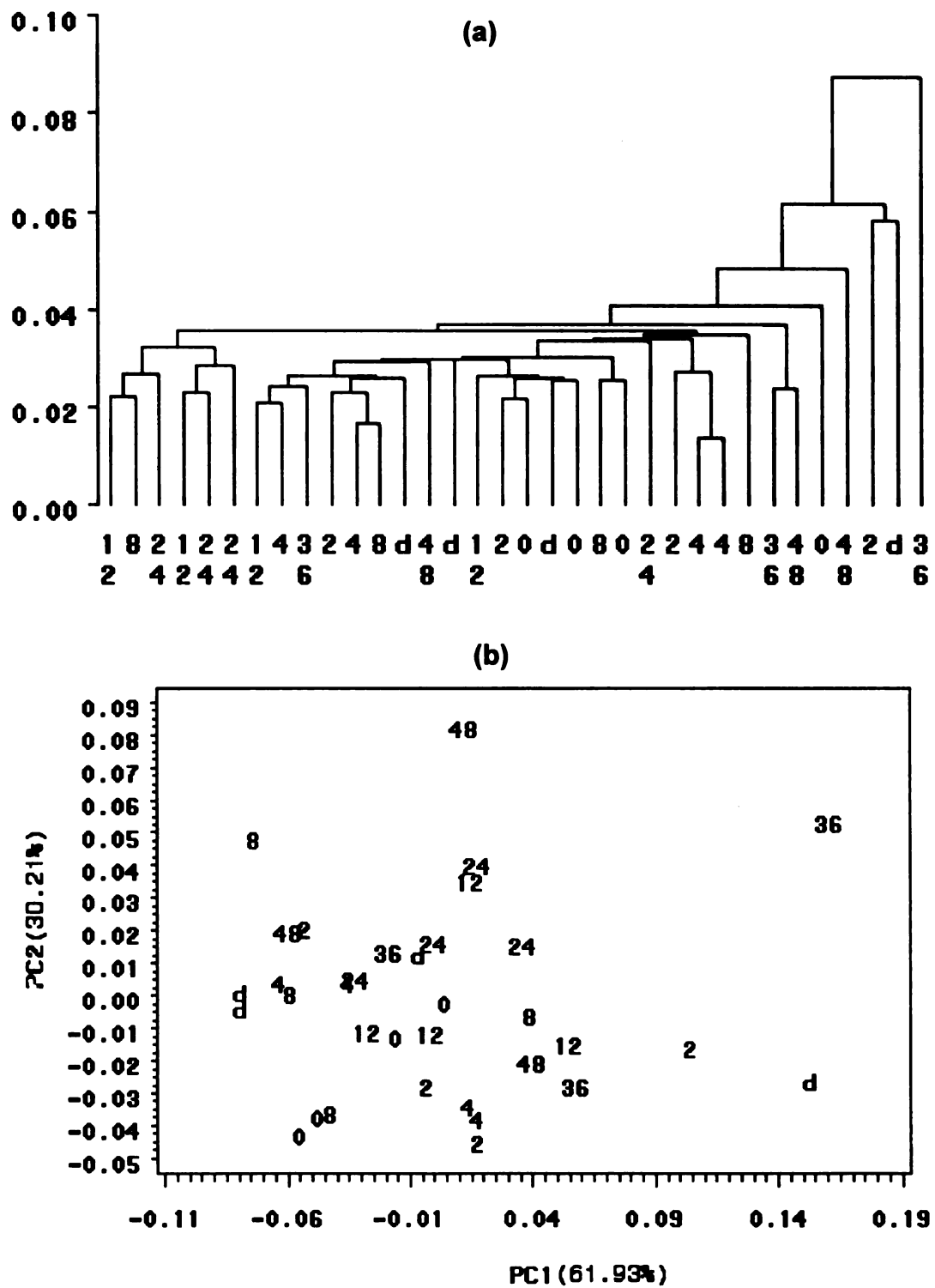


Figure 40 (a) HCA and (b) PCA of the sensor responses for 95°C headspace of 2% milk exposed to 0, 2, 4, 8, 12, 24, 36, or 48 hours of light at 5°C. Sample “d” was stored in the dark for 48 hours.

Supervised learning techniques (LDA/QDA and k-NN) were applied to discriminate the sensor responses for 45, 70 and 95°C headspace volatiles of light oxidized 2% milk (Figure 41, Figure 42, and Figure 43). Discriminatory methods were evaluated by comparing the correct classification rates (i.e. hit rates) to the training, validation and test steps. As discussed in Chapter 2.6.2, the LDA linear approach is more applicable for data with equal group variances, while QDA may work better for data with unequal group variances (Figure 19). The equality of normal population parameters was tested, and the results $p > 0.05$ (data not shown) indicated there was no strong evidence of unequal group variances. LDA had a comparable or higher correct identification rate than QDA at the test steps (Figure 41, Figure 42, and Figure 43). The QDA identification rates were higher for training and lower for the validation and test steps, which implied that QDA models might be too optimistic; the quadratic functions were not necessary for separating groups with equal variances and therefore more classification mistakes occurred in predicting the group identities of the unknown samples at the test steps.

Among the k-NN methods with various k, 1-NN had the most correct identification rate at the test step. When unknown samples were subjected to the model, their identities were determined by their closest one “neighbor” in the training data. In 2-NN, 3-NN or 4-NN, taking the closest two, three or four points did not improve the identification. It is mainly the occurrence of “ties” that prevents better identification, thus the model is not able to identify the unknown sample if the two “neighbors” belong to different groups in 2-NN. This also

implies that the groups were fairly close to each other in the models, so counting more “neighbors” resulted in lower correct identification rates.

Only one third or less of the light-oxidized milk samples in the test data set were correctly identified in terms of their exact light exposure duration. Poor differentiation among the milk samples with similar extent of light oxidation was mainly responsible for the low identification rates.

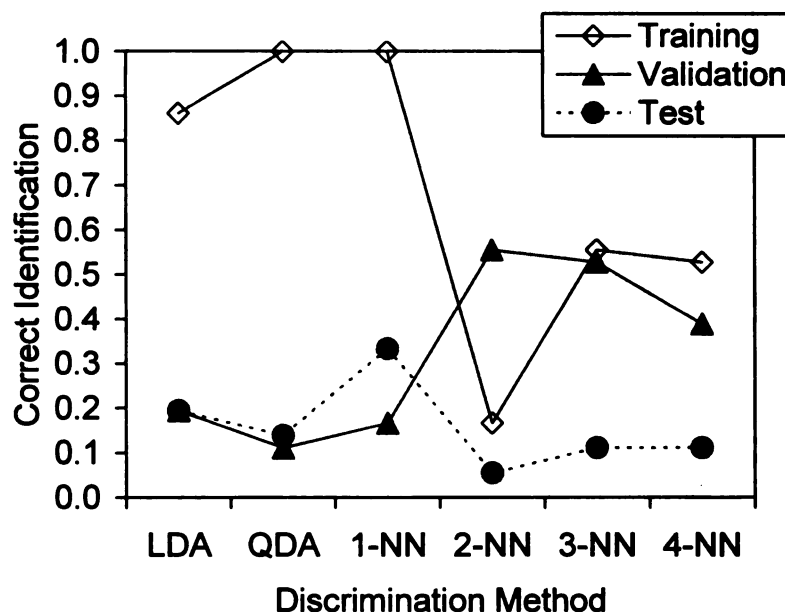


Figure 41 Classification rates for discrimination methods applied to the sensor responses using a headspace temperature of 45°C for 2% milk exposed to 0, 2, 4, 8, 12, 24, 36, or 48 hours of light, using LDA, QDA, and k-NN for k = 1, 2, 3, and 4.

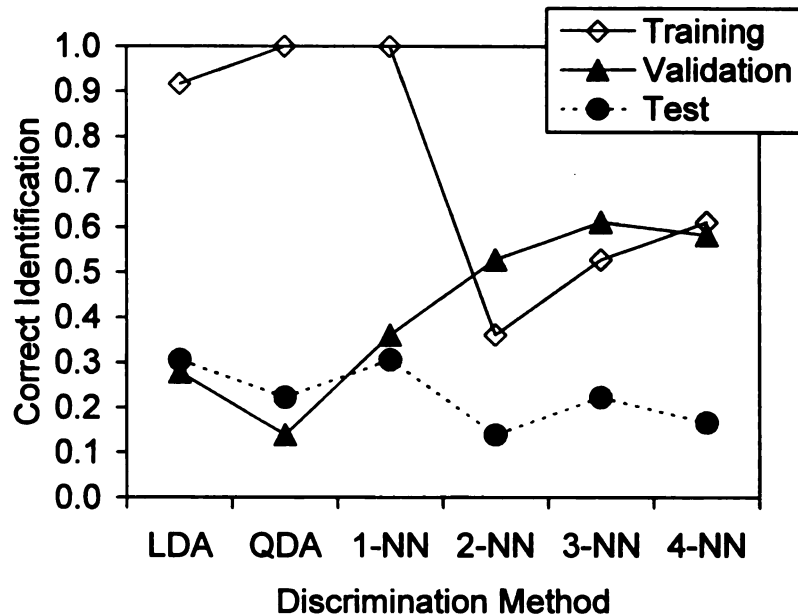


Figure 42 Classification rates for discrimination methods applied to the sensor responses using a headspace temperature of 70°C for 2% milk exposed to 0, 2, 4, 8, 12, 24, 36, or 48 hours of light, using LDA, QDA, and k-NN for k = 1, 2, 3, and 4.

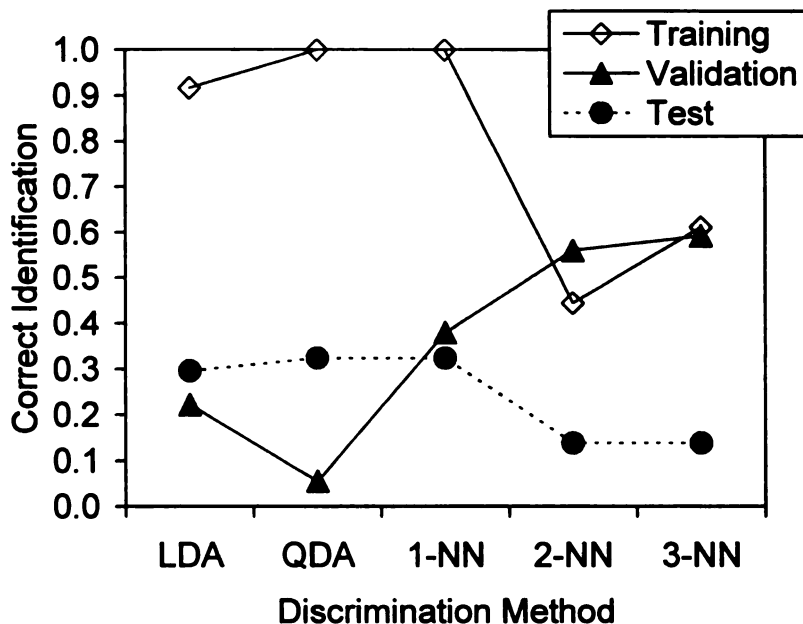


Figure 43 Classification rates for discrimination methods applied to the sensor responses using a headspace temperature of 95°C for 2% milk exposed to 0, 2, 4, 8, 12, 24, 36, or 48 hours of light, using LDA, QDA, and k-NN for k = 1, 2, and 3.

The LDA models can be graphically displayed as canonical discrimination scatter plots (Figure 44a, Figure 45a, and Figure 46a). Independent test data sets were then evaluated by the models (Figure 44b, Figure 45b, and Figure 46b). The first two canonical discriminants CAN1 and CAN2 were able to explain 86.20% (i.e. 71.23% + 14.97%), 78.75% and 91.53% of the total variances of the 12 sensor responses for the 45, 70 and 95°C headspace volatiles of the light oxidized milk, respectively, which means most of the total variance was preserved in the two dimensional models constructed by CAN1 and CAN2. Milk samples with the same duration of light exposure were not differentiated completely, but samples with similar extent of light oxidation still tended to be closer to each other. This trend was more obvious at 95°C (Figure 46) rather than 70°C or 45°C.

The goodness of the model generalization, i.e. the ability of the models to be applicable for unknown sample prediction, can be evaluated by comparing the group regions on the discriminant scatter plots at the training and test steps. The 95°C training and test data had a more consistent group distribution. The test data belongs to the same group (i.e. same light exposure duration) as was projected as shown by their similar group territories, compared to the 45°C and 70°C samples. For both training and test data, the groups arranged along the CAN1 coordinate with the levels of light exposure (Figure 46). It reflected the fact that all sensors responded to the light oxidized volatiles in a similar way, the more volatiles, the higher the sensor responses.

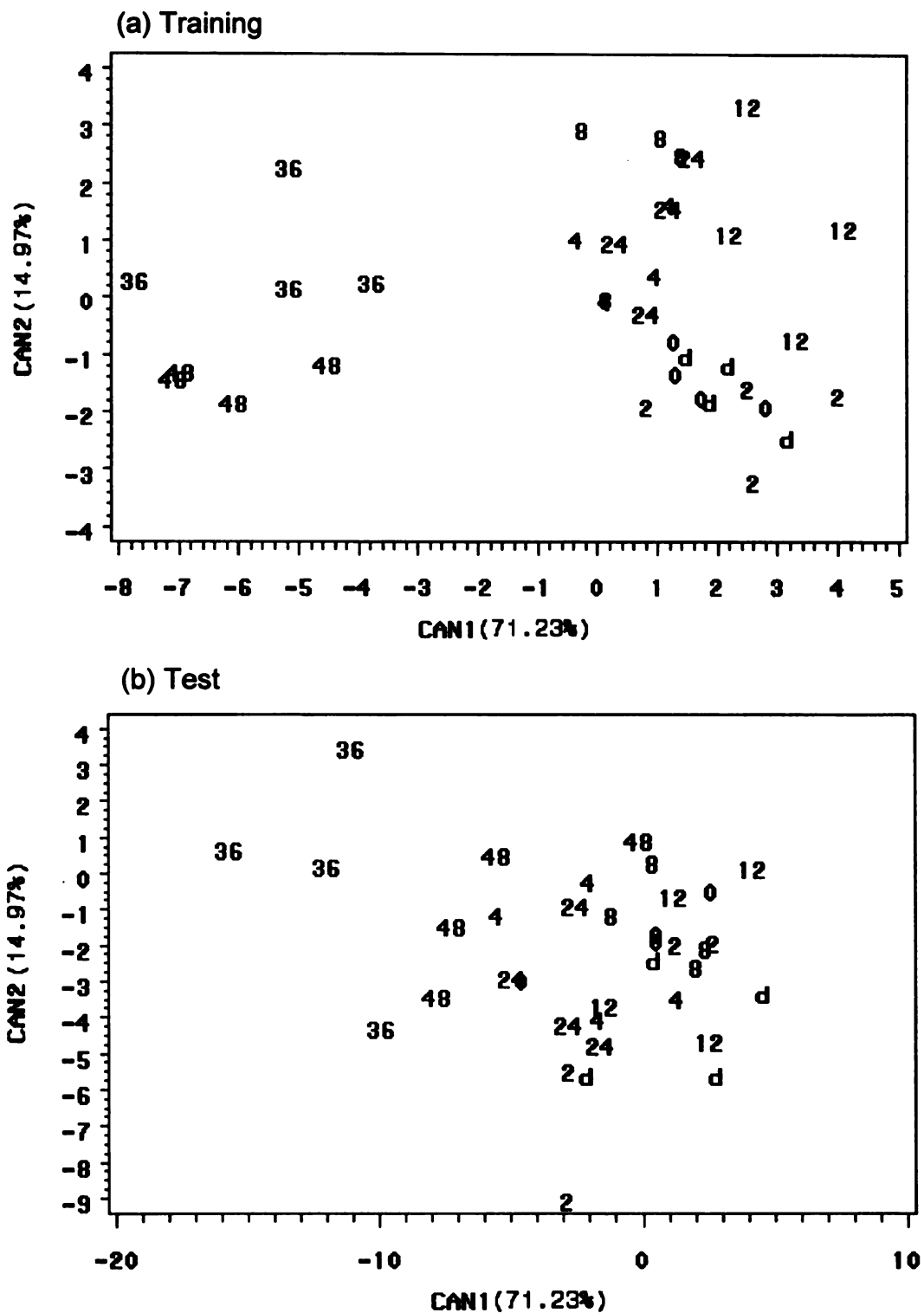


Figure 44 Canonical discriminant scatter plots of the (a) training (b) test data sets. Headspace of 2% milk samples exposed to 0, 2, 4, 8, 12, 24, 36, or 48 hours of light was generated at 45°C.

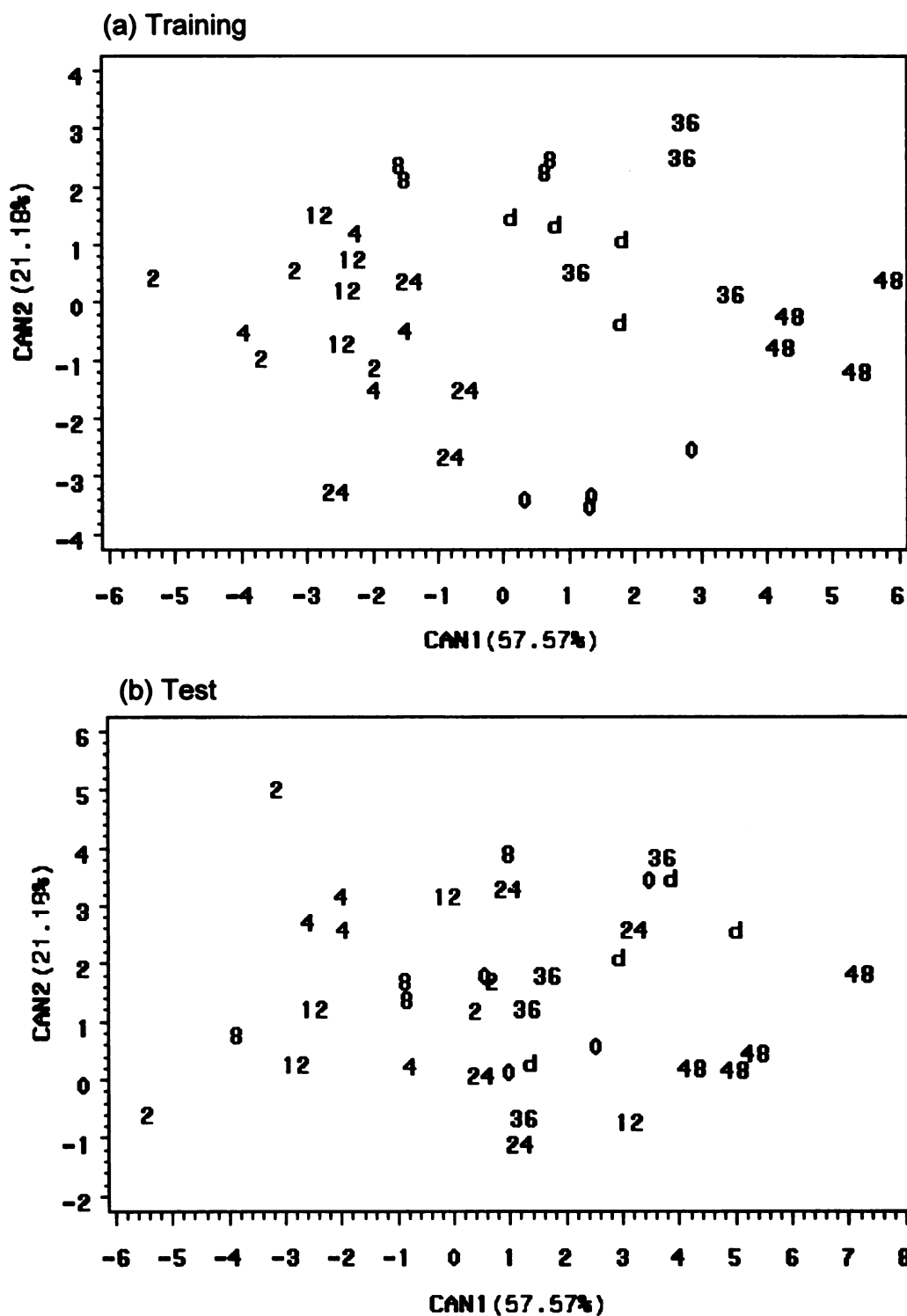


Figure 45 Canonical discriminant scatter plots of the (a) training (b) test data sets. Headspace of 2% milk samples exposed to 0, 2, 4, 8, 12, 24, 36, or 48 hours of light was generated at 70°C.

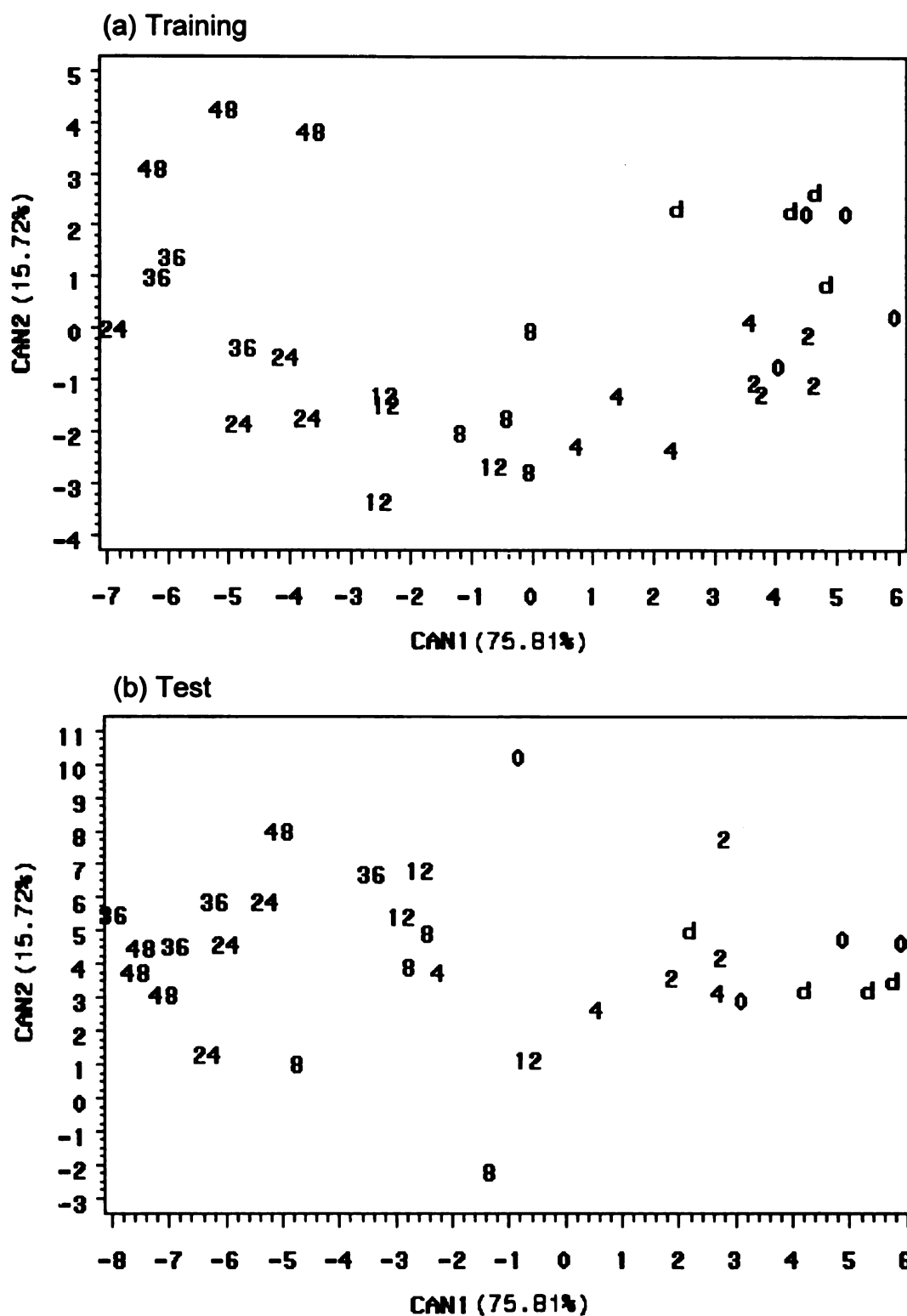


Figure 46 Canonical discriminant scatter plots of the (a) training (b) test data sets. Headspace of 2% milk samples exposed to 0, 2, 4, 8, 12, 24, 36, or 48 hours of light was generated at 95°C.

The data were then evaluated by “pooling” the results. Instead of assigning off-flavor samples to their exact light exposure duration, a “harmful light exposure time” was defined as the “threshold” point for milk deterioration, i.e. the differentiation between the two categories “good” and “bad” which was then tested. For instance, the LDA or 1-NN model based on the 45°C headspace samples was able to recognize 89% of 2% milk exposed to light for 24 hours or longer at the test step (Figure 47). The LDA and 1-NN models based on the 70°C headspace samples identified 83% of the 2% milk exposed to light for 24 hours or longer (Figure 48). More importantly, the LDA model based on 95°C headspace samples correctly recognized 97% of the 2% milk exposed to light for 8 hours or longer (Figure 49), which had comparable sensitivity to the consumer triangle sensory testing (Table 10).

The electronic nose provided better discrimination at 95°C than at 70°C and 45°C. Higher headspace temperature increased the amount of volatiles and resulted in higher sensitivity and better discrimination. Although undesired volatiles may also be generated due to overheating the milk, it will not be an issue if the volatiles from overheated milk are consistent or generated in a similar manner.

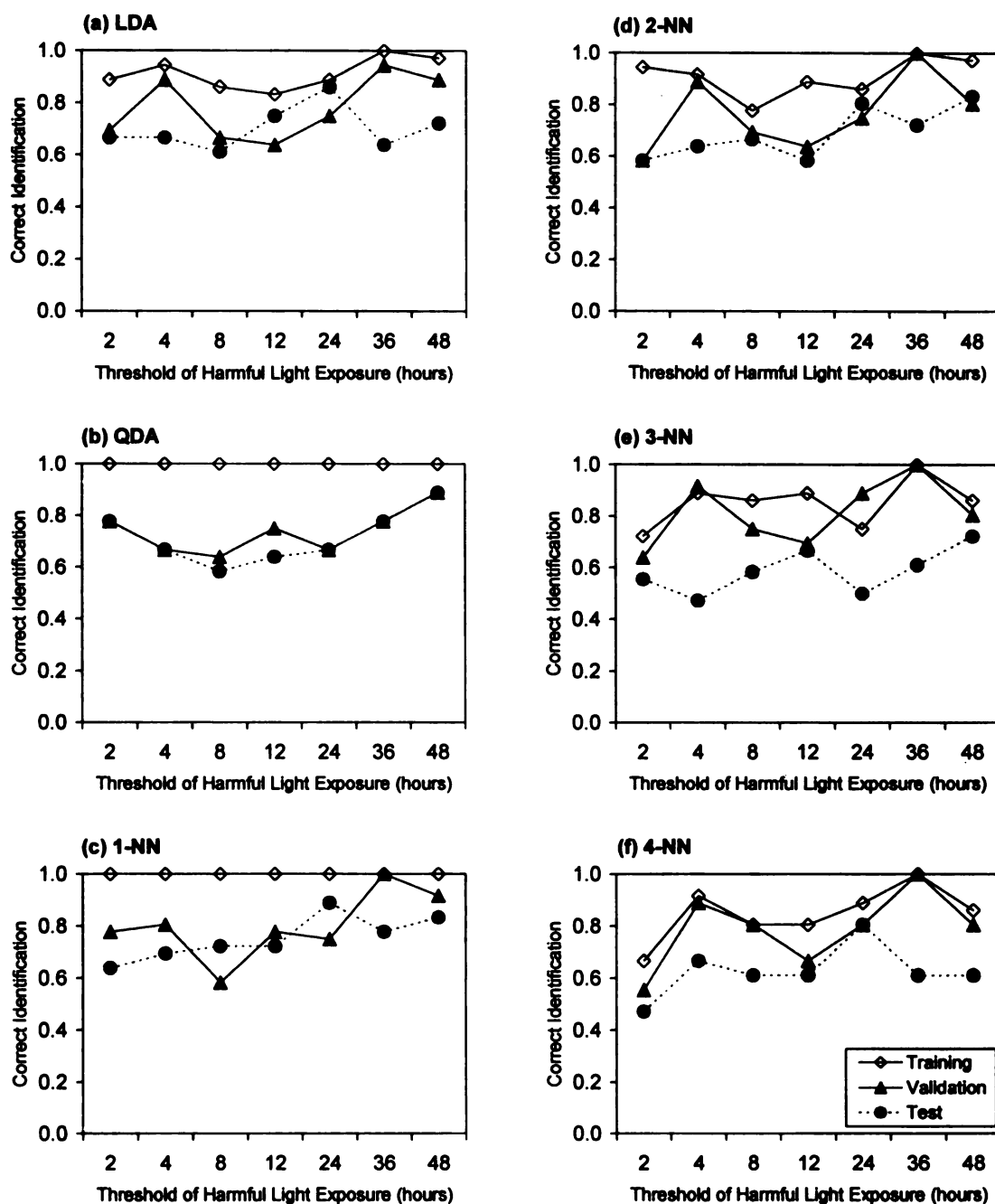


Figure 47 Classification rates of the defined threshold of harmful light exposure for discrimination methods applied to the sensor responses using a headspace temperature of 45°C using LDA, QDA, and k-NN for k = 1, 2, 3, and 4.

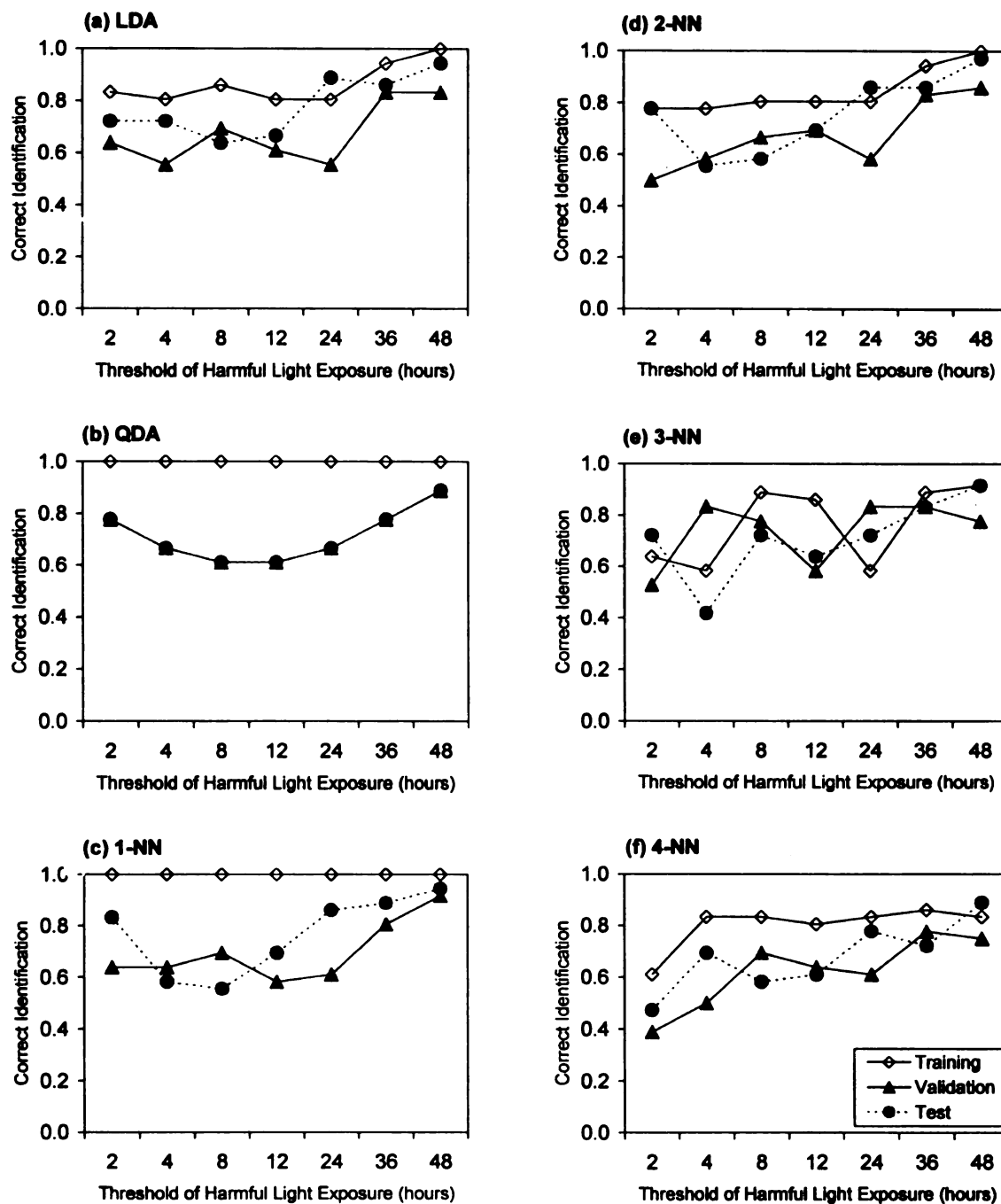


Figure 48 Classification rates of the defined threshold of harmful light exposure for discrimination methods applied to the sensor responses using a headspace temperature of 70°C using LDA, QDA, and k-NN for k = 1, 2, 3, and 4.

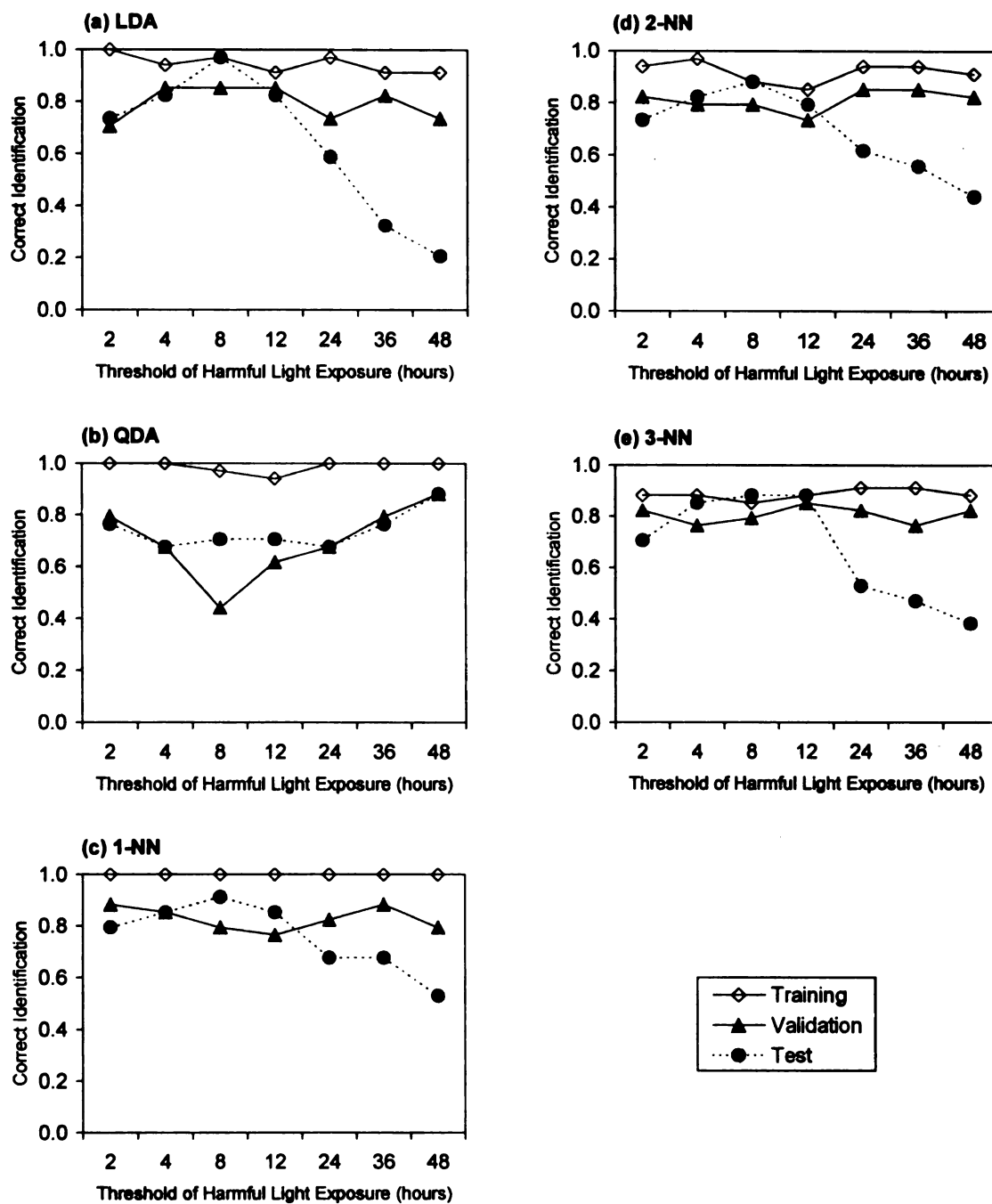


Figure 49 Classification rates of the defined threshold of harmful light exposure for discrimination methods applied to the sensor responses using a headspace temperature of 95°C using LDA, QDA, and k-NN for k = 1, 2, 3.

4.1.4. Correlation of results from sensory and instrumental analyses

Since light oxidized milk received lower sensory scores and had higher levels of oxidative byproducts in the headspace, a negative correlation is expected between sensory quality and headspace volatiles, analyzed using the electronic nose or SPME-GC. The goal is to set up an instrumental method which can be applied in a rapid quality evaluation of milk and which has high correlation to sensory scores.

Headspace pentanal, hexanal, and dimethyl disulfide in 2% milk were quantified using SPME-GC. Correlation between their headspace volatile contents and the numerical sensory scores was investigated using PLS (Figure 50) and MLP (Figure 51). The predicted sensory scores and the root mean square error (RMSE) were used to evaluate the performance of the models. The smaller the RMSE, the better the performance of the model.

The MLP model, which was based on a non-linear backpropagation algorithm, gave more precise predicted sensory scores and lower root mean square error (RMSE) than the PLS model. The PLS model is a linear statistical method and was used to find latent component(s) of the independent variables, i.e. headspace levels of pentanal, hexanal, and dimethyl disulfide.

Similar RMSE values at the training and test steps in both models indicated the models were not over-fitted.

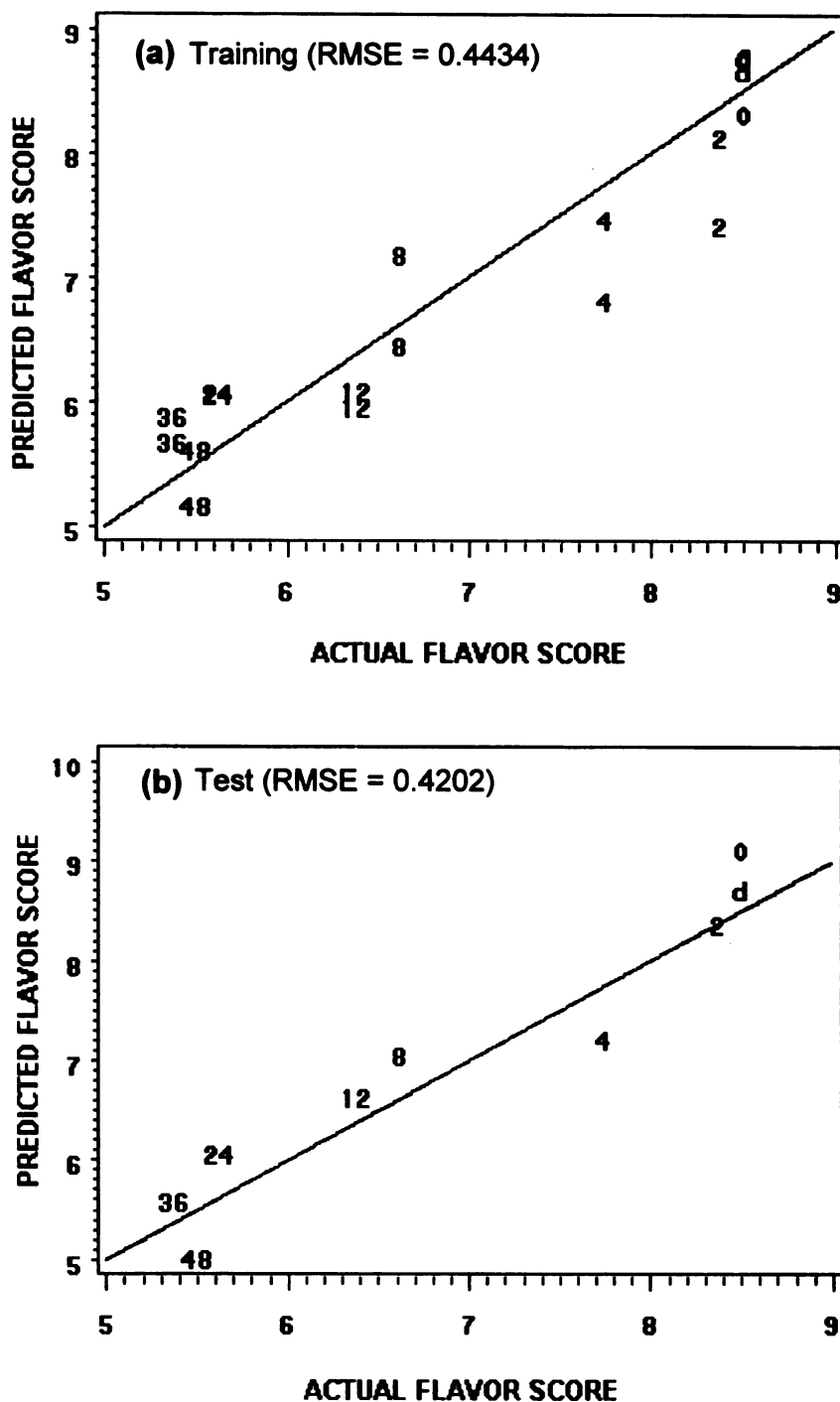


Figure 50 PLS predicted versus actual flavor scores of 2% milk exposed to 0, 2, 4, 8, 12, 24, 36, or 48 hours of light, based on levels of pentanal, hexanal and dimethyl disulfide quantified using SPME-GC. Models were applied to (a) training data and (b) test data. The reference line indicates equal values of predicted and actual sensory scores.

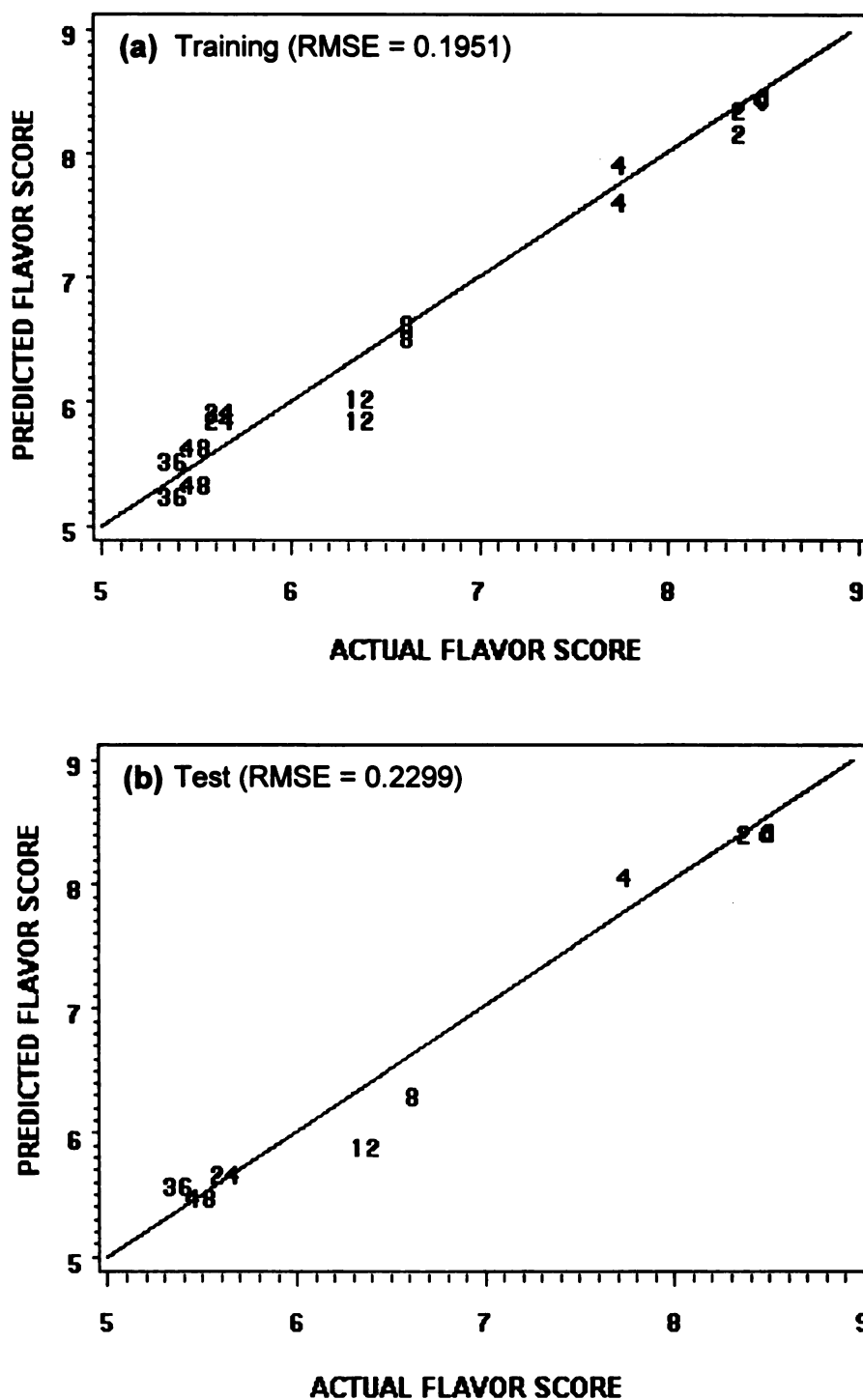


Figure 51 MLP predicted versus actual flavor scores of 2% milk exposed to 0, 2, 4, 8, 12, 24, 36, or 48 hours of light, based on levels of pentanal, hexanal and dimethyl disulfide quantified using SPME-GC. Models were applied to (a) training data and (b) test data. The reference line indicates equal values of predicted and actual sensory scores.

PLS and MLP models were also used to investigate the correlation between sensory scores and electronic nose sensor responses for the 45, 70 and 95°C headspace samples of light oxidized 2% milk (Figure 52 to Figure 57). It showed that the electronic nose was not able to provide an effective prediction of sensory scores at 45°C or 70°C headspace, whether the applied model was PLS or MLP. The 45°C or 70°C headspace temperature was not high enough to generate sufficient volatiles in the headspace and resulted in low sensitivity and poor prediction, regardless of the applied multivariate technique.

On the other hand, the sensor responses for 95°C headspace samples resulted in a relatively more precise prediction (Figure 54 and Figure 57). The 95°C PLS model (RMSE = 0.3828) had predicted sensory scores varied with a range ~1, which increased slightly but was still reasonable when applying to the test data set (RMSE = 0.5470). The 95°C MLP model had a low RMSE (0.0040) and narrower ranges on predicted sensory scores, compared to the 95°C PLS model (Figure 54a) at the training step. However, it gave a poor prediction at the test steps (RMSE = 1.0748) which indicates over-fitting by the MLP model. Training loops based on a backpropagation algorithm may have proceed too long, which resulted in an over-fitted model. The MLP model was too optimistic for the training data and failed to be adapted for an independent data. The model did not cover the reasonable variation among future unknown samples.

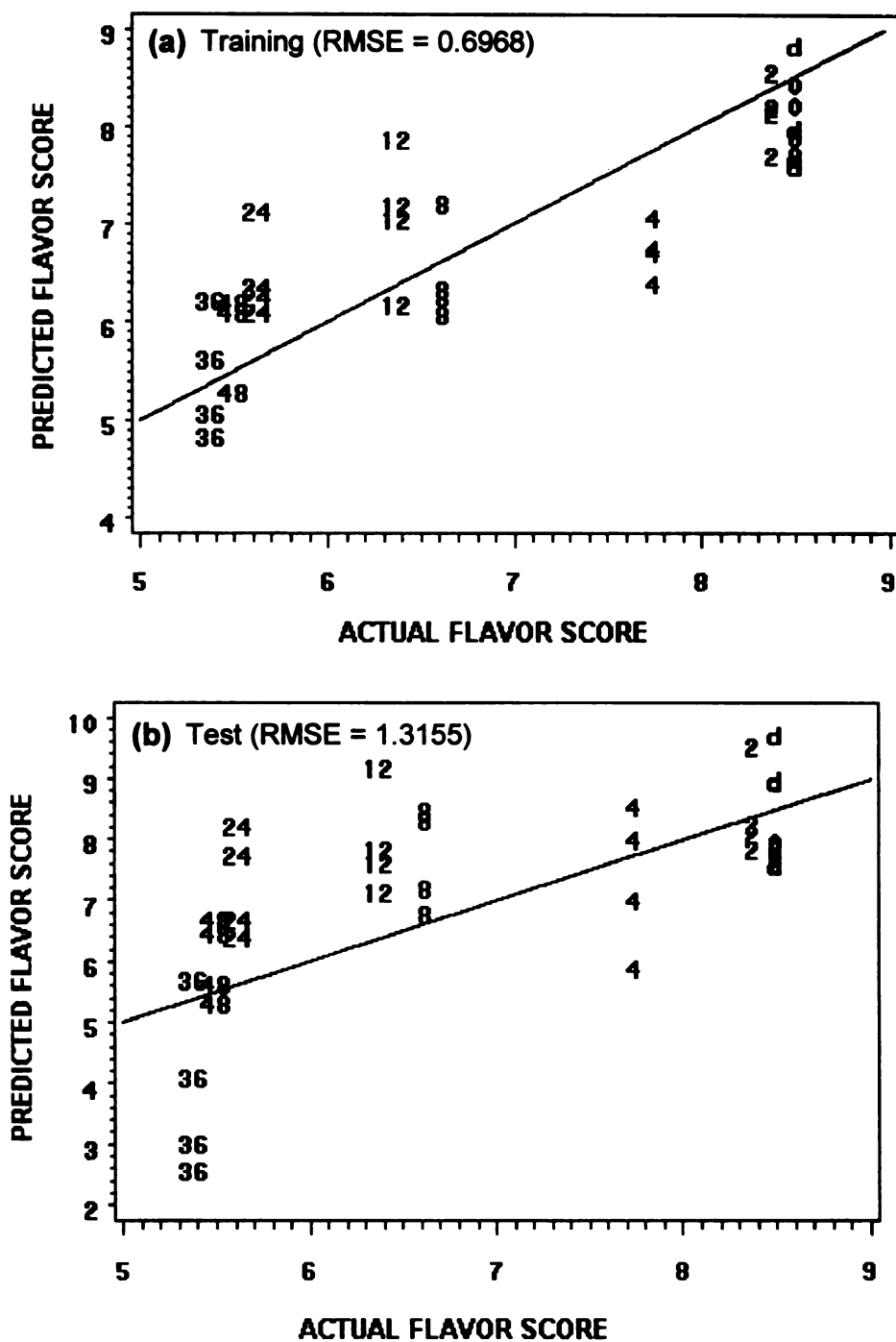


Figure 52 PLS predicted versus actual flavor scores of 2% milk exposed to 0, 2, 4, 8, 12, 24, 36, or 48 hours of light, based on the sensor responses using a headspace temperature of 45°C. Models were applied to (a) training data and (b) test data. The reference line indicates equal values of predicted and actual sensory scores.

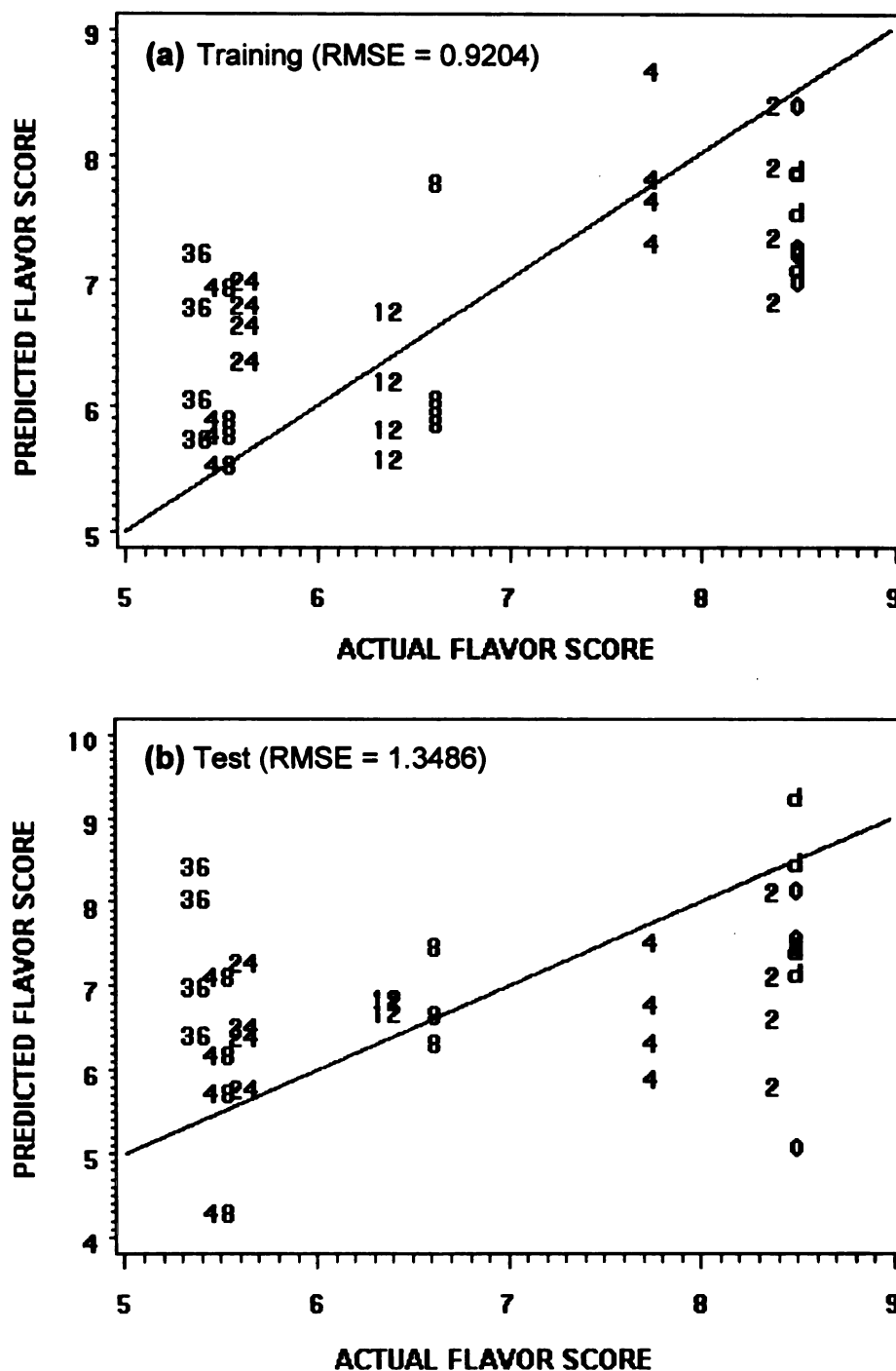


Figure 53 PLS predicted versus actual flavor scores of 2% milk exposed to 0, 2, 4, 8, 12, 24, 36, or 48 hours of light, based on the sensor responses using a headspace temperature of 70°C. Models were applied to (a) training data and (b) test data. The reference line indicates equal values of predicted and actual sensory scores.

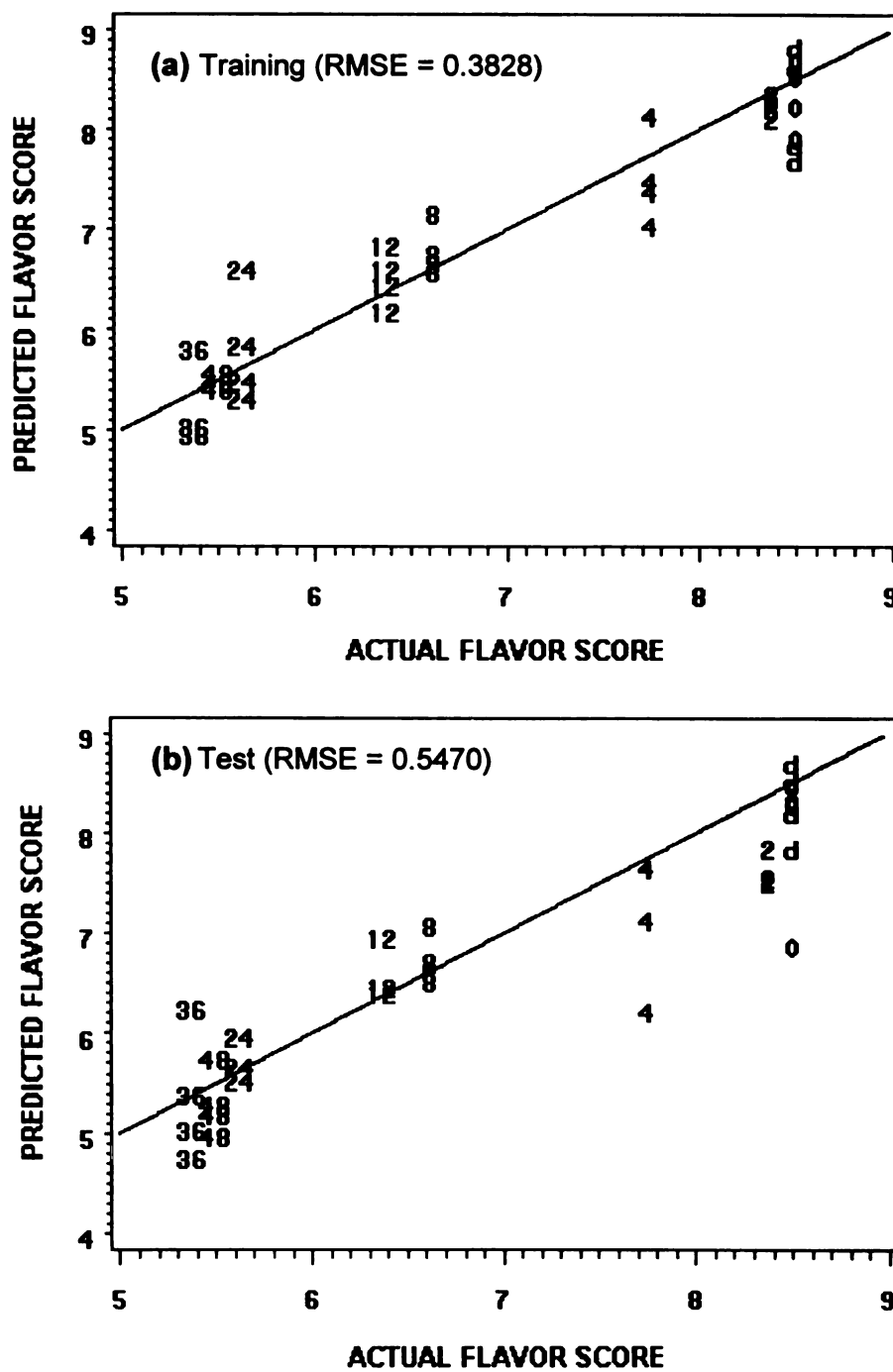


Figure 54 PLS predicted versus actual flavor scores of 2% milk exposed to 0, 2, 4, 8, 12, 24, 36, or 48 hours of light, based on the sensor responses using a headspace temperature of 95°C. Models were applied to (a) training data and (b) test data. The reference line indicates equal values of predicted and actual sensory scores.

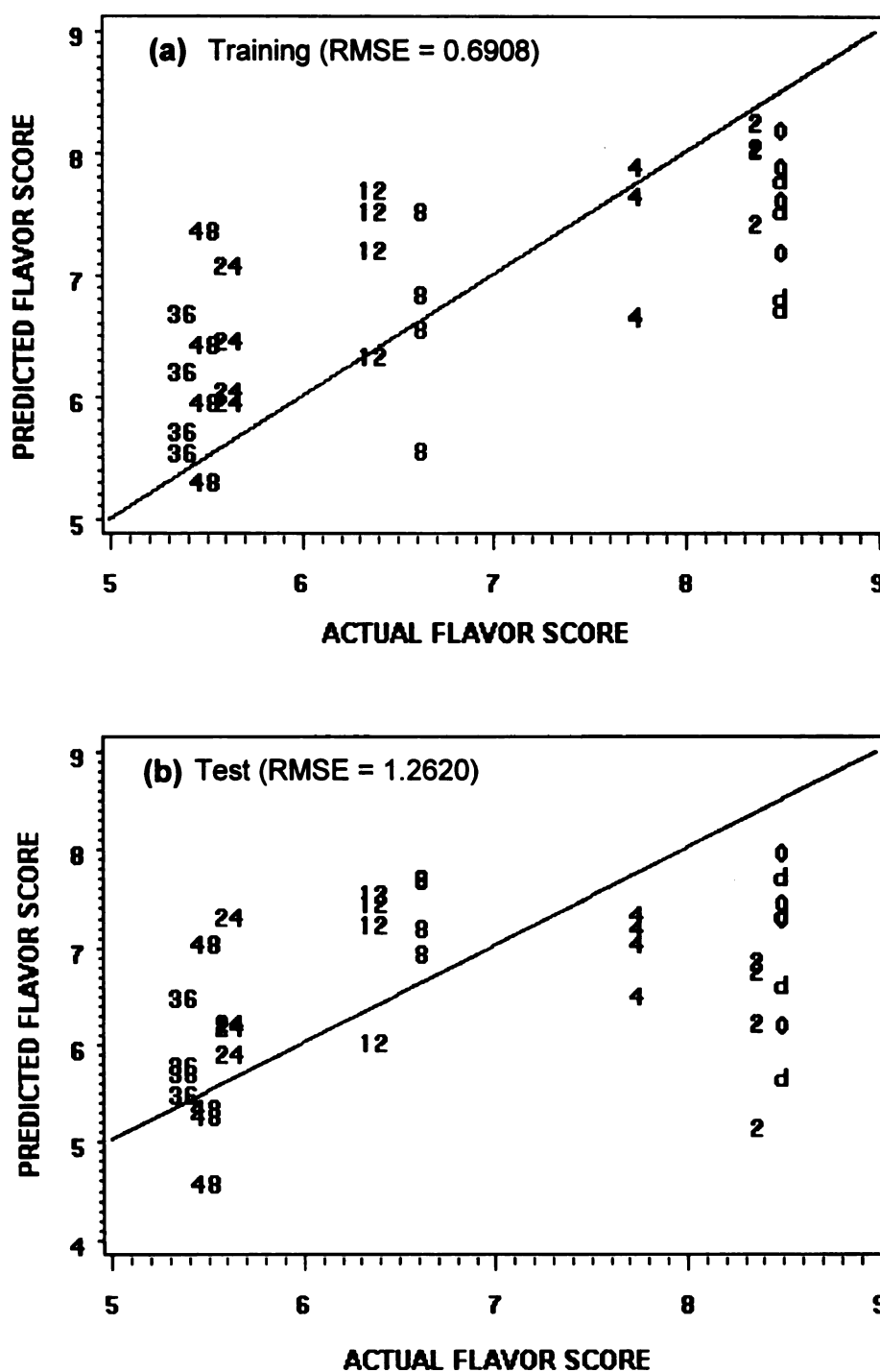


Figure 55 MLP predicted versus actual flavor scores of 2% milk exposed to 0, 2, 4, 8, 12, 24, 36, or 48 hours of light, based on the sensor responses using a headspace temperature of 45°C. Models were applied to (a) training data and (b) test data. The reference line indicates equal values of predicted and actual sensory scores.

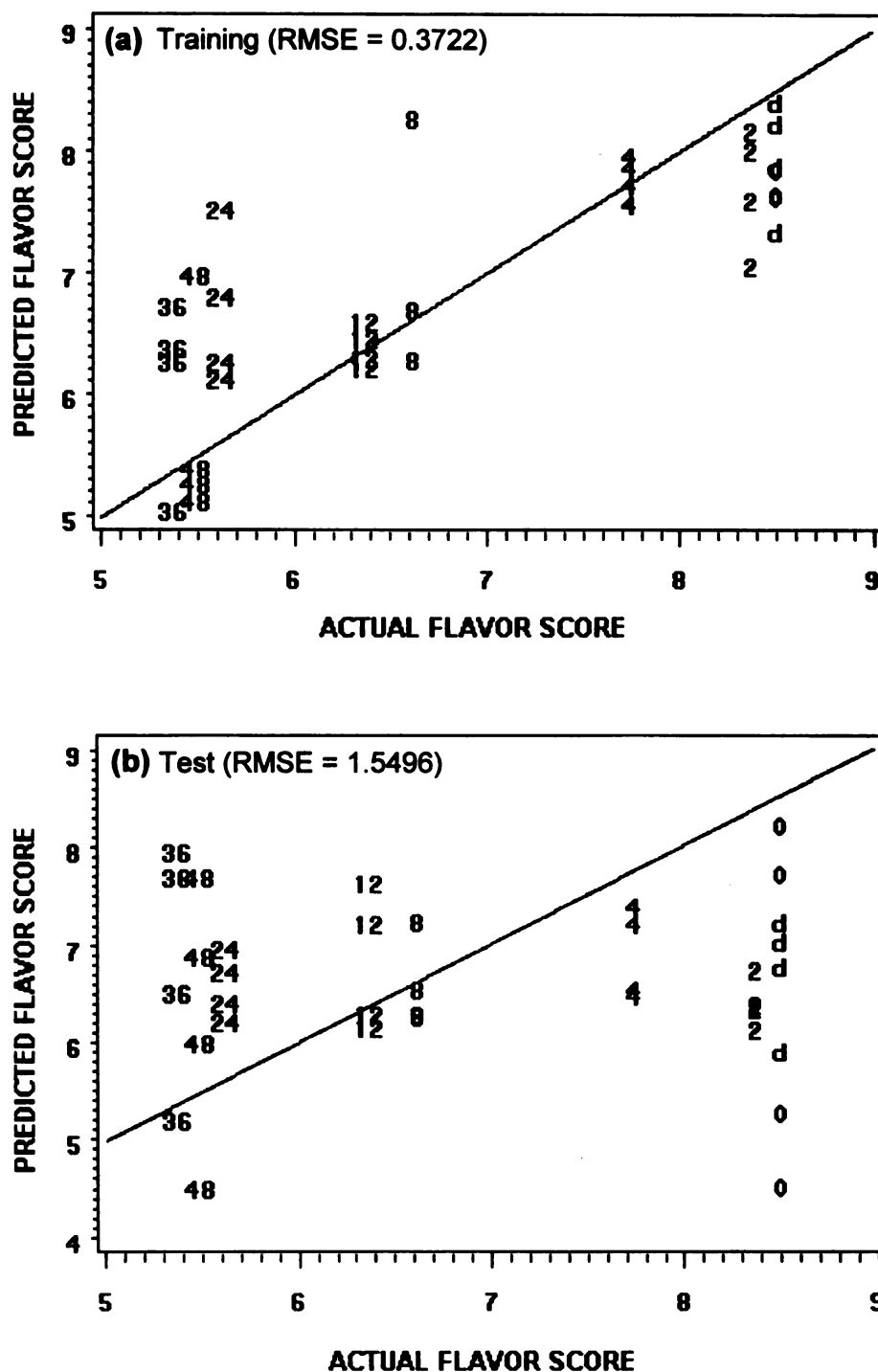


Figure 56 MLP predicted versus actual flavor scores of 2% milk exposed to 0, 2, 4, 8, 12, 24, 36, or 48 hours of light, based on the sensor responses using a headspace temperature of 70°C. Models were applied to (a) training data and (b) test data. The reference line indicates equal values of predicted and actual sensory scores.

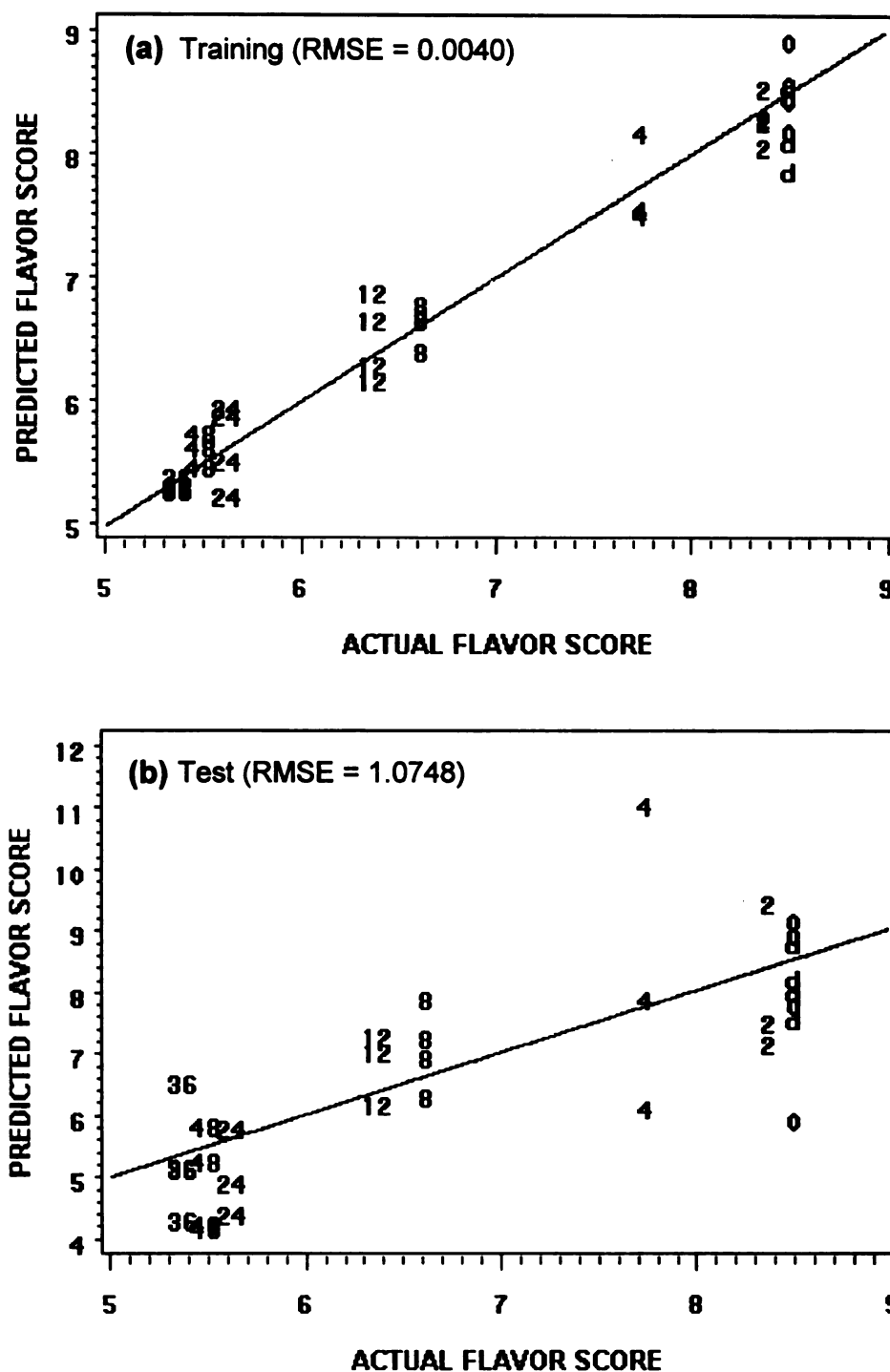


Figure 57 MLP predicted versus actual flavor scores of 2% milk exposed to 0, 2, 4, 8, 12, 24, 36, or 48 hours of light, based on the sensor responses using a headspace temperature of 95°C. Models were applied to (a) training data and (b) test data. The reference line indicates equal values of predicted and actual sensory scores.

The PLS approach was to find latent component(s) from the sensor responses that were also relevant to the sensory scores. It was expected that some of these would be well defined since higher volatile contents or sensor responses were expected from light-oxidized samples with lower sensory scores. The MLP was a better model than PLS when over-fitting was not a concern. The models, developed based on training data, should cover potential variation in both training and future unknown samples. This usually depends on the reproducibility of the instrumental measurements or the selection of training data.

4.2. Packaging and light-oxidized off-flavors

4.2.1. Off-flavors from packaging materials

The milk packaging materials, glass, HDPE, HDPE-TiO₂, PET, and PE-coated paper cartons, were cut into ~1 cm² pieces, sealed in 10 ml headspace vials, and analyzed using the electronic nose. The sensor responses for the 45, 70 or 95°C headspace samples were then analyzed using the unsupervised (HCA and PCA) and supervised (LDA/QDA and k-NN) learning techniques.

A natural clustering and clear separation among various packaging materials were observed on HCA dendrograms and PCA score plots (Figure 58 to Figure 60). PE-coated paper carton (denoted as “P”) headspace samples were more separated from glass, HDPE and HDPE-TiO₂ samples at all headspace temperatures. This implies that PE-coated carton material, which contains additives from both paper and PE layers, had a distinctively different headspace volatile composition than that of the glass and plastic materials.

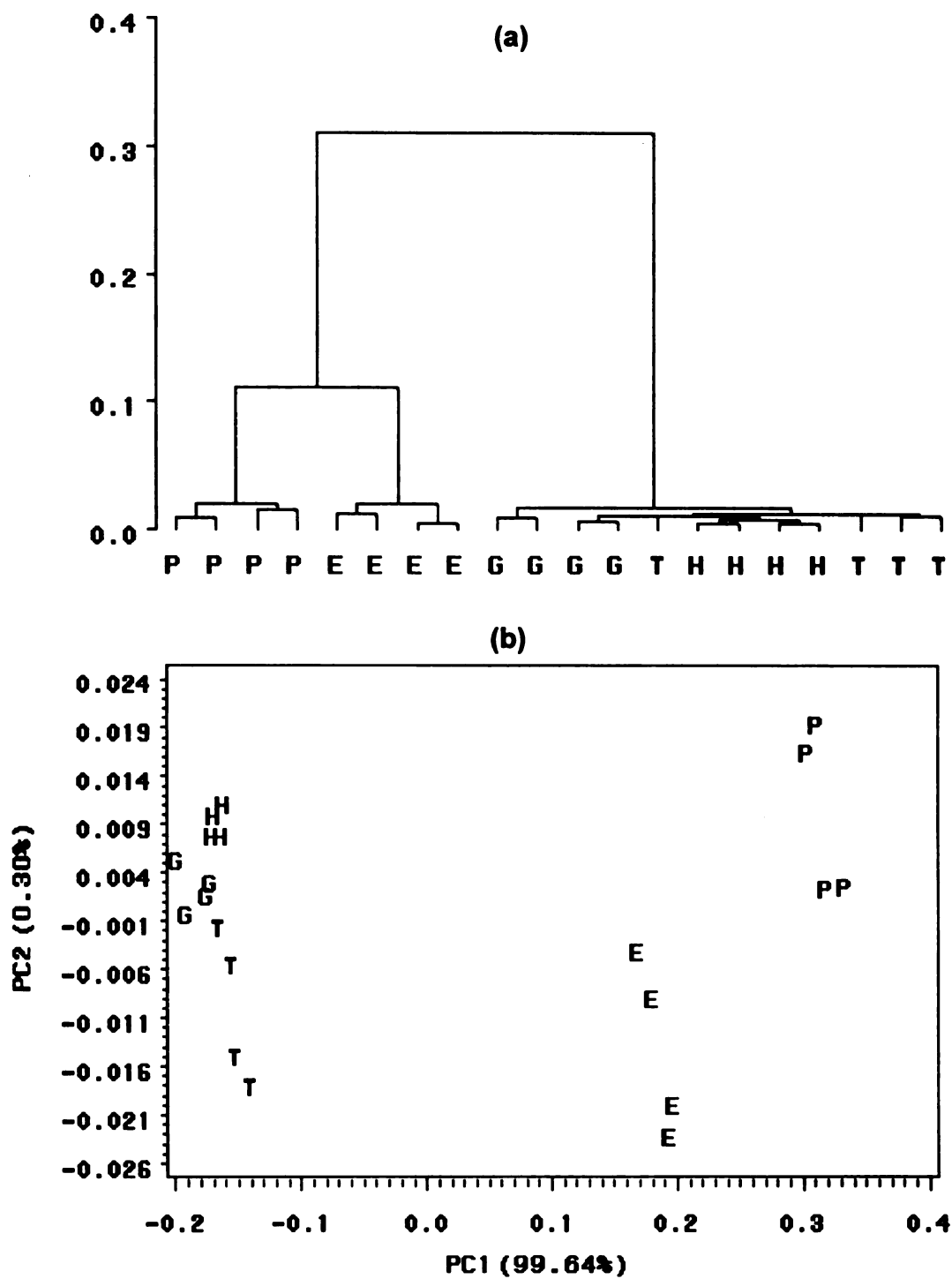


Figure 58 (a) HCA and (b) PCA of sensor responses for 45°C headspace of various packaging materials: glass (G), HDPE (H), HDPE-TiO₂ (T), PET (E), and PE-coated carton material (P).

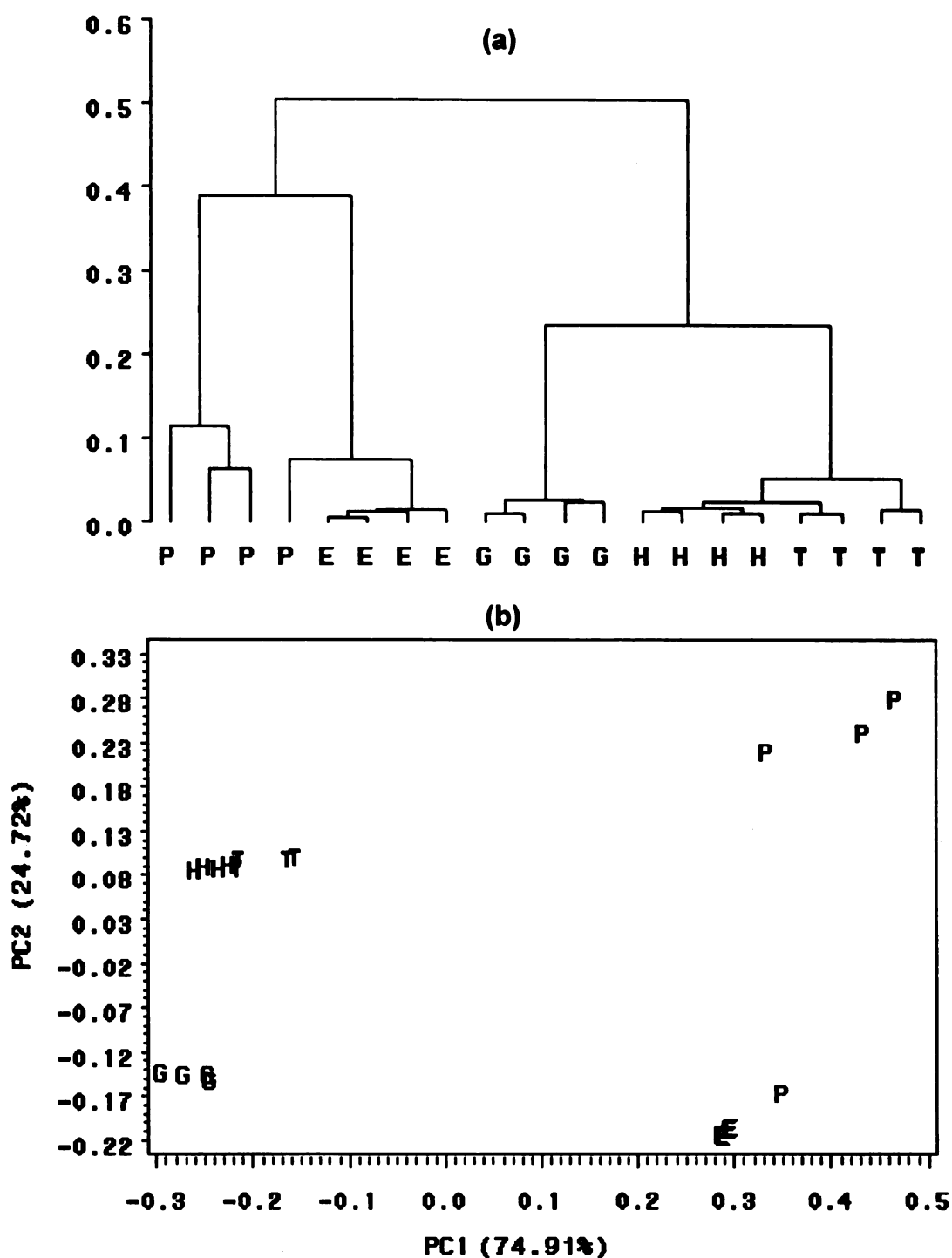


Figure 59 (a) HCA and (b) PCA of sensor responses for 70°C headspace of various packaging materials: glass (G), HDPE (H), HDPE-TiO₂ (T), PET (E), and PE-coated carton material (P).

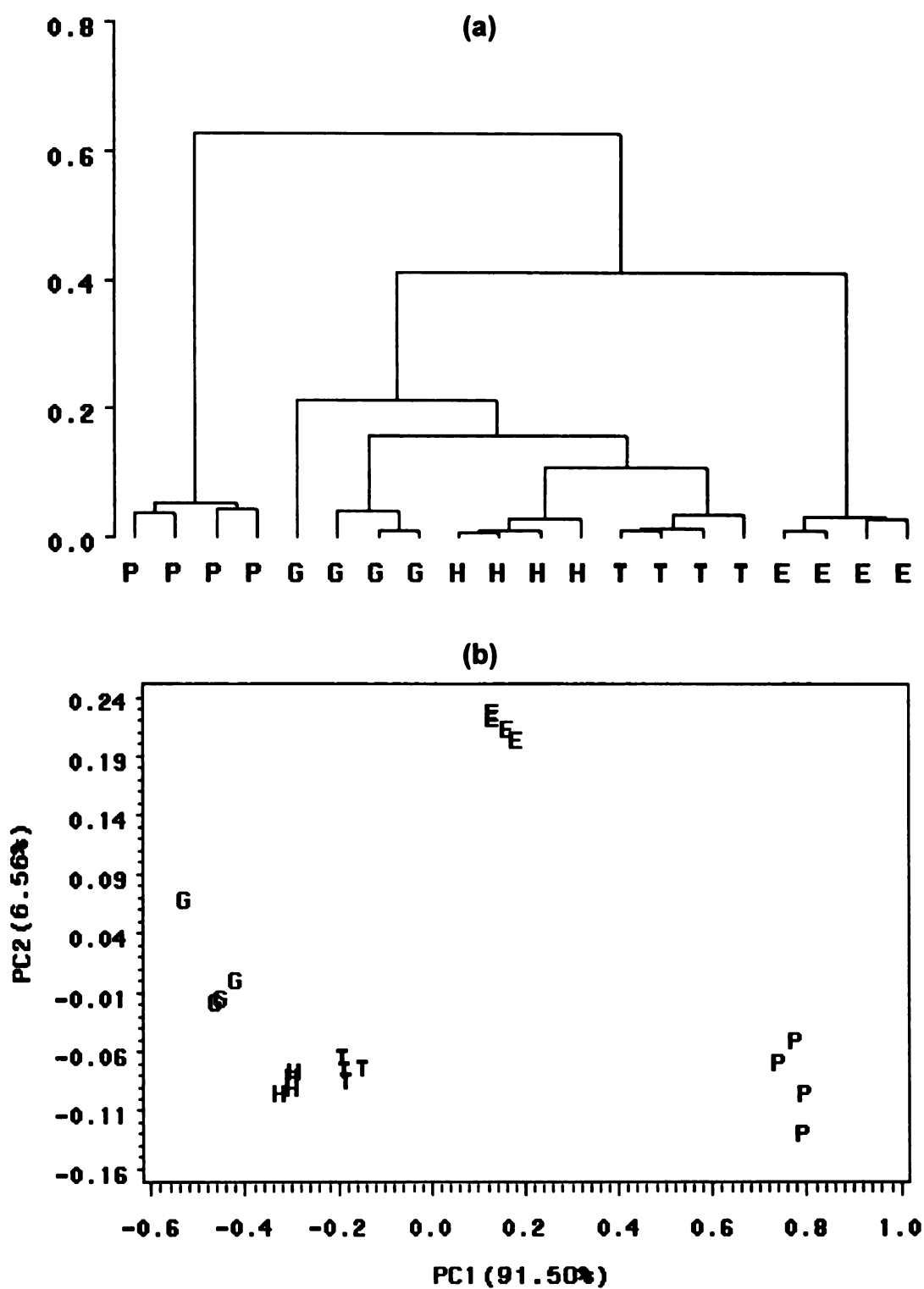


Figure 60 (a) HCA and (b) PCA of sensor responses for 95°C headspace of various packaging materials: glass (G), HDPE (H), HDPE-TiO₂ (T), PET (E), and PE-coated carton material (P)

Supervised learning techniques, LDA/QDA and k-NN for $k = 1$ to 4, were used to build differentiation and recognition models (Figure 61 to Figure 63). The training data did not have significant evidence of unequal variance among groups, i.e. testing the equality of normal population parameters had $p > 0.05$ (data not shown), thus using the quadratic approach (QDA) was not necessary and may have overfitted, which resulted in lower correct identification rates. Instead, the linear boundaries (LDA) provided better recognition for the unknown samples at the test step. The nonparametric k-NN approach had the same correct identification rates at all k 's as did the LDA. The high and constant correct identification rates indicated that the groups were well-separated in the models, therefore, the classification did not depend on the discriminant methods.

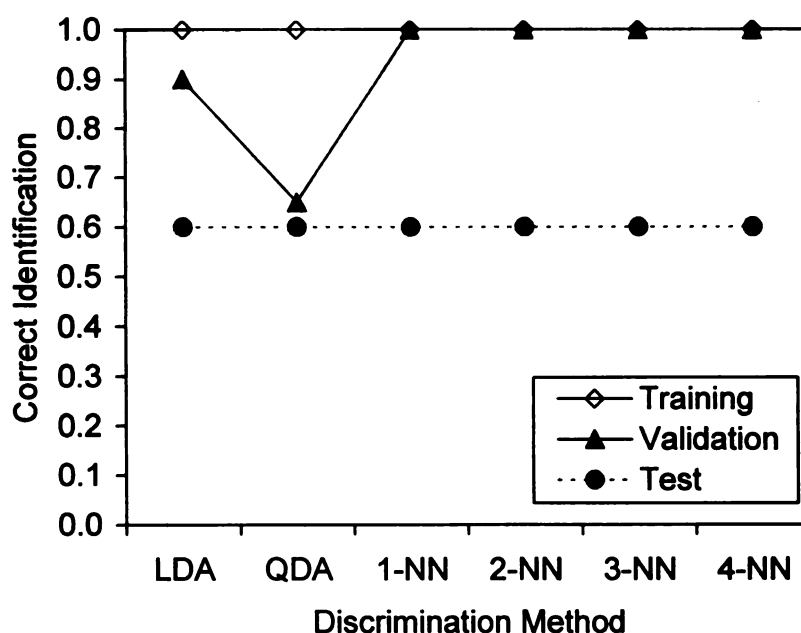


Figure 61 Correct classification of various discrimination methods applied to sensor responses for the 45°C headspace of various packaging materials, using LDA/QDA and k-NN for $k = 1, 2, 3, 4$.

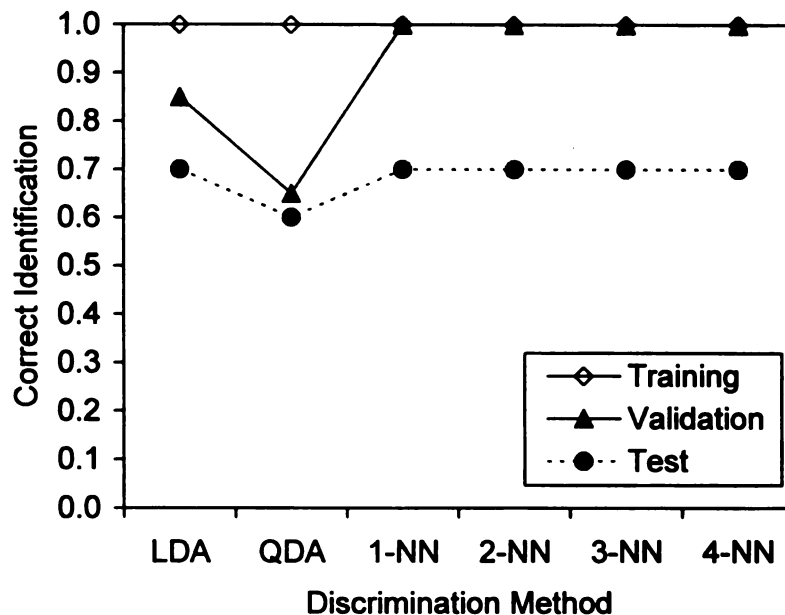


Figure 62 Correct classification rates of various discrimination methods applied to sensor responses for the 70°C headspace of various packaging materials, using LDA/QDA and k-NN for k = 1, 2, 3, 4.

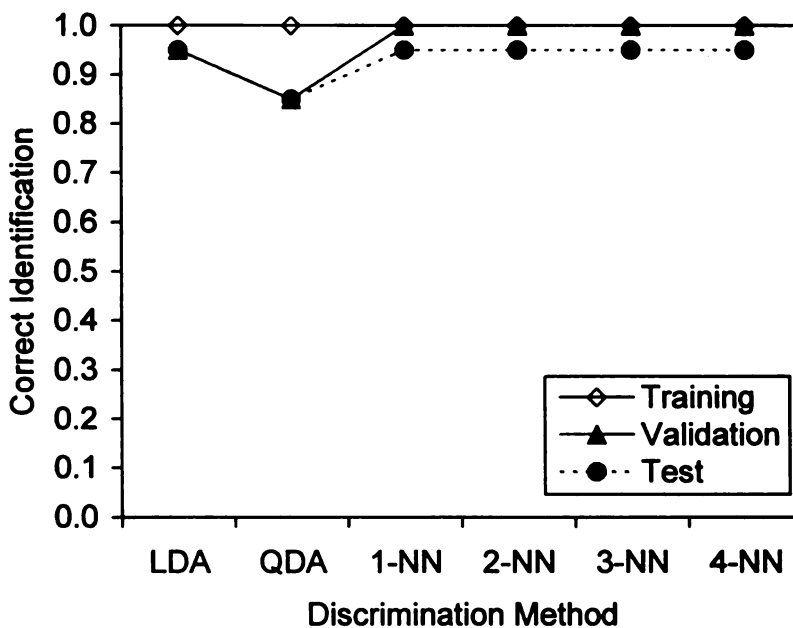


Figure 63 Correct classification rates of various discrimination methods applied to sensor responses for the 95°C headspace of various packaging materials, using LDA/QDA and k-NN for k = 1, 2, 3, 4.

The correct identification rates at the test steps for the LDA and k-NN models were 0.6, 0.7 and 0.95 for models based on 45, 70 and 95°C headspace samples, respectively (Figure 61 to Figure 63). More volatiles were released at higher headspace temperature, which resulted in more intense sensor responses, and gave more clearly defined regions for correct recognition of unknown samples.

Linear discriminant models can be graphically displayed in two-dimensional canonical discriminant scatter plots (Figure 64 to Figure 66). The first two discriminants, CAN1 and CAN2, explained 99.73%, 99.05% and 96.42% of the total variance of the sensor responses for 45, 70, and 95°C headspace samples, respectively. It showed clear separation among the different packaging materials. Unknown samples (i.e. an independent test data set), while being projected to the models, were mostly located at the expected regions, with slightly larger group variances. The PE-coated carton material and PET were well separated from the other packaging materials, and all PE-coated carton material and PET samples in the test data set were fully recognized using LDA or k-NN (data not shown).

The closeness of glass, HDPE and HDPE-TiO₂ headspace samples was responsible for the incorrect identification. This implies that the headspace volatiles from HDPE (and HDPE-TiO₂) were relatively low, which resulted in similar sensor responses to glass, which is an inert material and no or little headspace volatiles were expected under the test conditions.

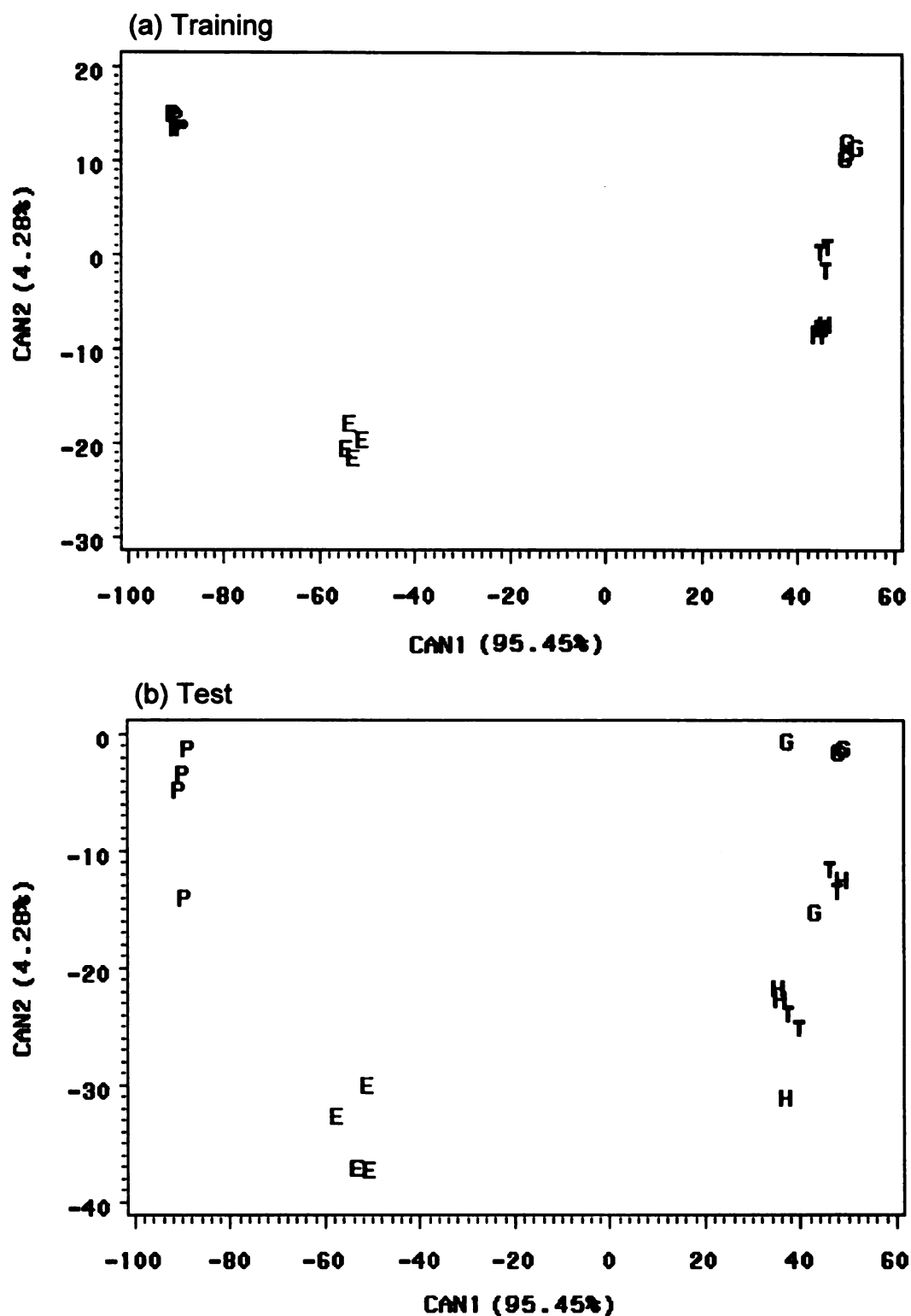


Figure 64 Canonical discriminant scatter plots of the (a) training (b) test data sets. Headspace samples of various packaging materials: glass (G), HDPE (H), HDPE-TiO₂ (T), PET (E), and PE-coated carton material (P), were generated at 45°C.

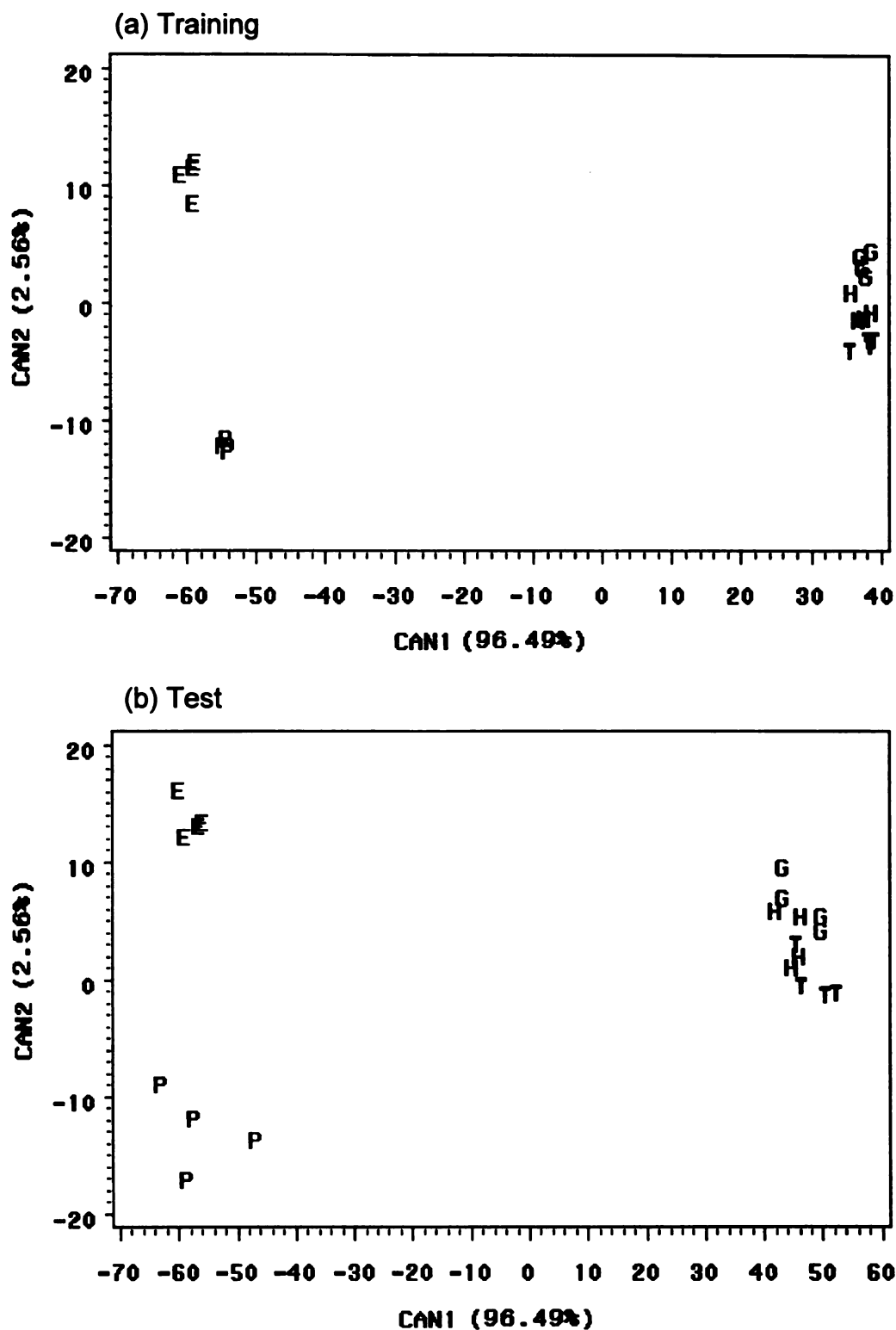


Figure 65 Canonical discriminant scatter plots of the (a) training (b) test data sets. Headspace samples of various packaging materials: glass (G), HDPE (H), HDPE-TiO₂ (T), PET (E), and PE-coated carton material (P), were generated at 70°C.

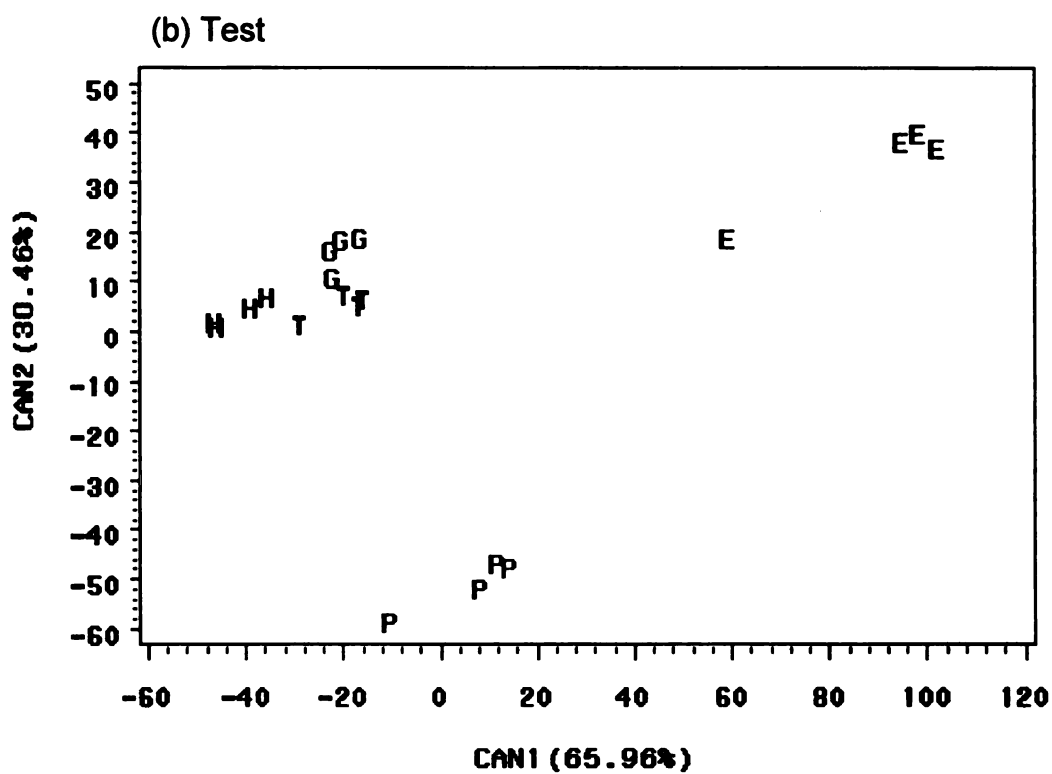
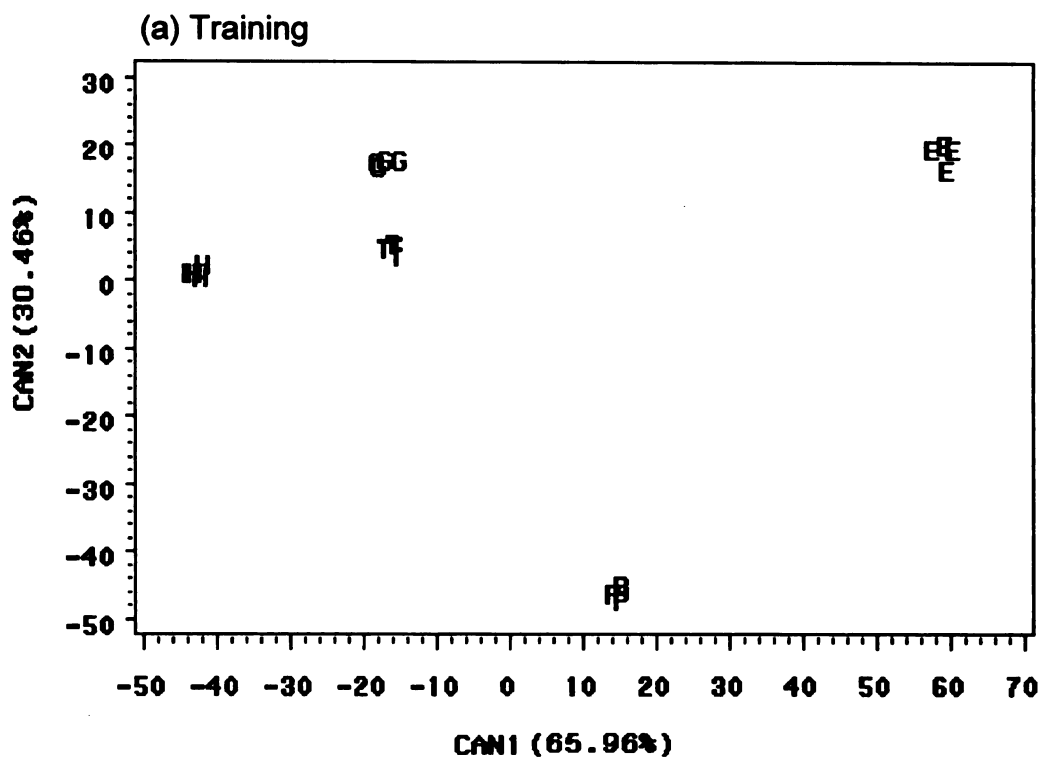


Figure 66 Canonical discriminant scatter plots of the (a) training (b) test data sets. Headspace samples of various packaging materials: glass (G), HDPE (H), HDPE-TiO₂ (T), PET (E), and PE-coated carton material (P), were generated at 95°C.

Direct analysis of the packaging materials led to more intense sensor responses from the more concentrated headspace volatiles and resulted in clear differentiation. In addition, significantly less interference from water vapor was expected, since MOS sensors also respond to water vapor, which is odorless. However, not all types of volatiles in packaging materials will migrate to food contents; when the migration takes place, not all amounts will migrate to the food matrix. Quantifying the volatiles from packaging materials directly may not correctly reflect the actual impact of migration of packaging off-flavors, which were mostly not detected by consumers.

4.2.2. Packaging off-flavors in water and 2% milk

4.2.2.1. Sensory evaluation

Two series of triangle tests, each performed by 24 consumer panelists, were conducted to investigate if the direct contact of packaging materials (glass, HDPE, PET and PE-coated paper cartons) resulted in detectable flavor changes in water or 2% milk at 5°C for 3 days. It was found that water stored in HDPE bottles had a very mild flavor difference ($p < 0.10$) from the control, i.e. deionized water (Table 14). No significant packaging off-flavors in 2% milk were detected (Table 15).

Packaging off-flavors from HDPE bottles were very subtle but still had the most correct responses from the consumers among the tested packaging materials, in both water and 2% milk (Table 14 and Table 15). Oxidative hydrocarbons generated during plastic processing are responsible for the

packaging off-flavors [11-13], and the intensities vary dependent on the severity of the processing conditions (temperature and/or pressure).

Table 14 Triangle test results on HPLC grade water in glass, HDPE, PET bottles and PE-coated paper cartons at 5°C for 3 days; HPLC grade water stored in a 4 L amber glass jug was used as the control. Tests were performed by a 24-member consumer panel.

Packaging Material	Number of Correct Responses from 24 Subjects	p
Glass	9	--
HDPE	12	0.10
PET	8	--
Paper Cartons	7	--

Table 15 Triangle test results on 2% milk in glass, HDPE, PET bottles and PE-coated paper cartons, at 5°C for 3 days; 2% milk stored in a 4 L amber glass jugs was used as the control. Tests were performed by a 24-member consumer panel.

Packaging Material	Number of Correct Responses from 24 Subjects	p
Glass	6	--
HDPE	10	--
PET	9	--
Paper Cartons	6	--

The results are contrary to those from analysis of the packaging materials using the electronic nose, where HDPE was found to have less headspace volatiles than PET and PE-coated carton material (Figure 64 to Figure 66). Qualitatively, the volatiles in the high temperature headspace (45, 70 or 95°C for the electronic nose analysis) of packaging materials were not necessarily odor-active migrants causing packaging off-flavors in water or 2% milk after storage at 5°C for 3 days. In addition, the responses and threshold levels of volatiles are different for the human nose and the electronic nose. Quantitatively, analysis of the potential migrants in packaging materials directly may overestimate the concentrations of the actual migrants. In addition, the migrants which cause packaging off-flavors may have low volatility and mostly exist in the liquid phase instead of the headspace.

An 8-member trained panel evaluated 2% milk in glass, HDPE, HDPE-TiO₂, PET bottles and PE-coated paper cartons, and was not able to show a significant flavor change, when stored at 5°C for 3 days (Table 16 and Figure 67). 2% milk samples in glass bottles received a slightly lower score (6.38 ± 2.07) than 2% milk in HDPE (7.00 ± 1.77) and HDPE-TiO₂ (7.75 ± 1.39), which have been a result of the large variance of the sensory scores. Statistically, 2% milk in glass, HDPE, HDPE-TiO₂ and PET bottles did not have significant flavor difference (Table 16). Samples in PE-coated cartons had a slightly lower absolute sensory score (4.63 ± 2.26). However, there was no strong evidence of a significant flavor change in PE-coated cartons, due to the highly diverse sensory scores (two outliers at score 1 and 9).

Table 16 Sensory scores of 2% milk in glass, HDPE, HDPE-TiO₂, PET bottles and PE-coated paper cartons at 5°C for 3 days. Scores were given by an 8-member trained panel.

Duration of light exposure (hours)	Sensory Score (average \pm standard deviation)		
Glass	6.38	± 2.07	a b
HDPE	7.00	± 1.77	a b
HDPE-TiO ₂	7.75	± 1.39	a
PET	5.88	± 2.90	a b
Paper Carton	4.63	± 2.26	b

¹ Means with the same letter are not statistically different at $\alpha = 0.05$ (Tukey's studentized range test).

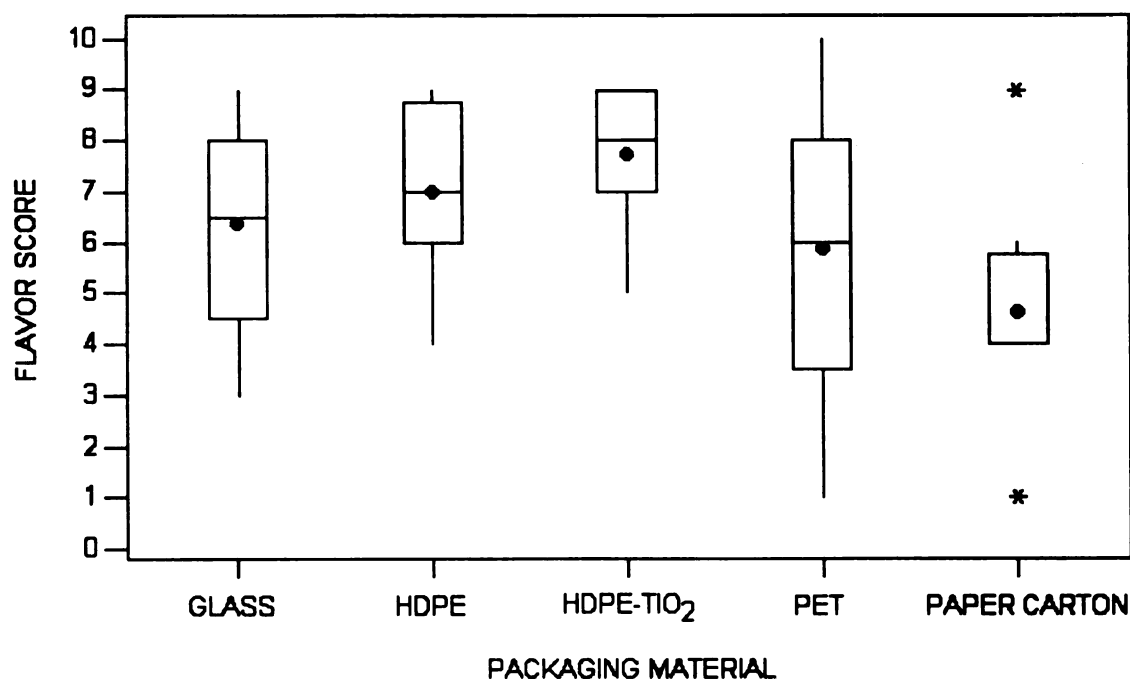


Figure 67 Sensory scores of reduced fat milk stored in glass, HDPE, HDPE-TiO₂, PET bottles, and PE-coated paper cartons, at 5°C for 3 days.

The highly diverse sensory score, especially for the samples stored in PET and PE-coated cartons, might indicate detection of packaging off-flavors by part of the trained panel. The same trained panel (but not conducted on the same day) gave a sensory score of 8.50 ± 0.54 to the 2% milk in glass bottles and stored in the dark for 48 hours (Table 11), which was unexpectedly different from the score assigned to the 2% milk in glass bottles and stored in the dark for 3 days (6.38 ± 2.07). Several panelists commented that there was long lasting aftertaste in water and 2% milk stored in various packaging materials (data not shown). Since the samples were evaluated in random order, the aftertaste of packaging off-flavors may have interfered with the evaluation of further samples, and led to the large variance in sensory scores.

4.2.2.2. Headspace analysis using the electronic nose

The 95°C water and 2% milk headspace samples were analyzed using the electronic nose. Unsupervised learning techniques, HCA and PCA, did not show an obvious pattern or separation among the water or 2% milk samples stored in various packaging materials at 5°C for 3 days (Figure 68 and Figure 69).

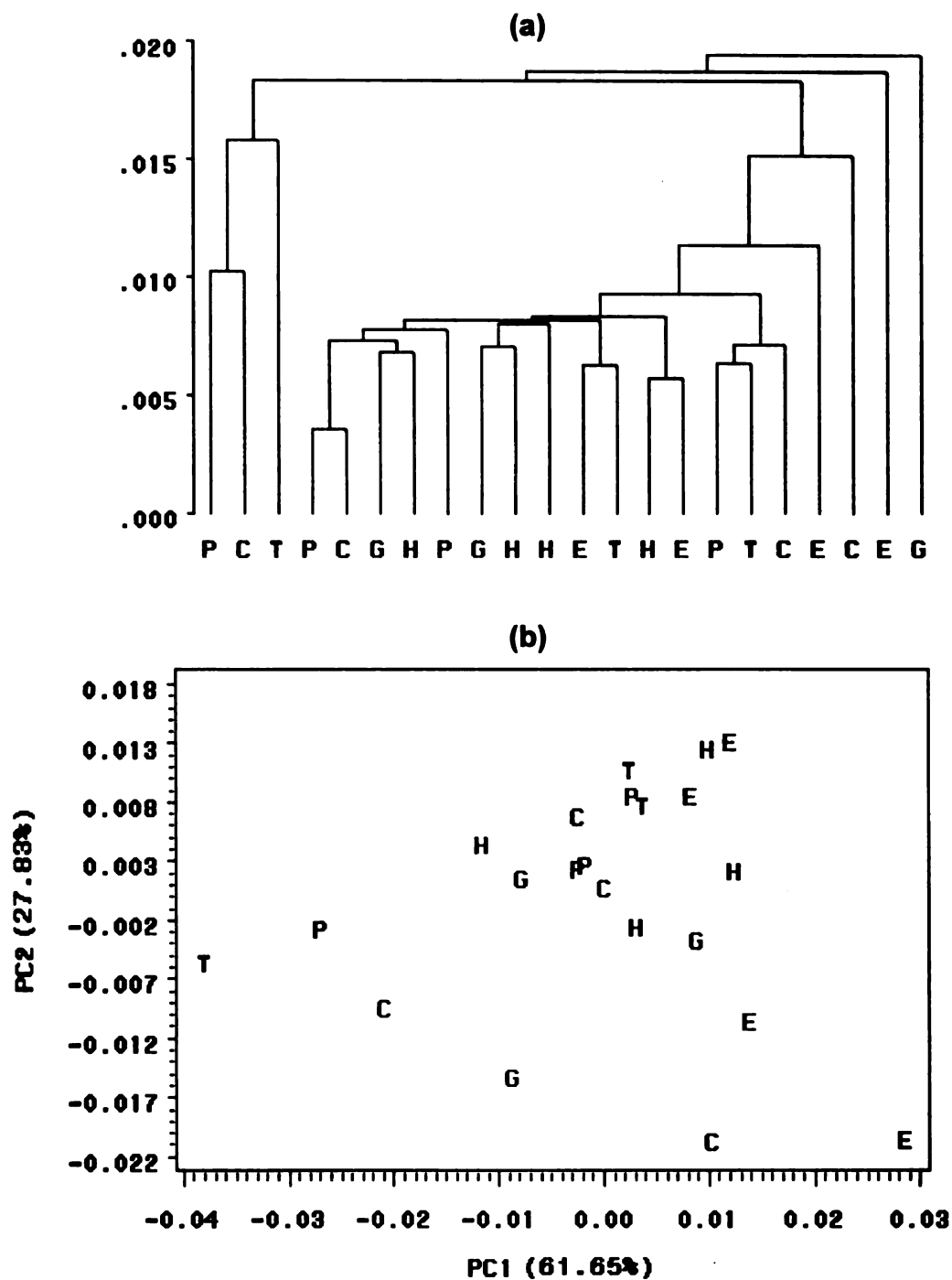


Figure 68 (a) HCA (b) PCA of sensor responses for the 95°C headspace of water stored in various packaging materials: glass (G), HDPE (H), HDPE-TiO₂ (T), PET (E), and PE-coated paper cartons (P), at 5°C for 3 days. Control (C) is water from the original 4L amber glass jug.

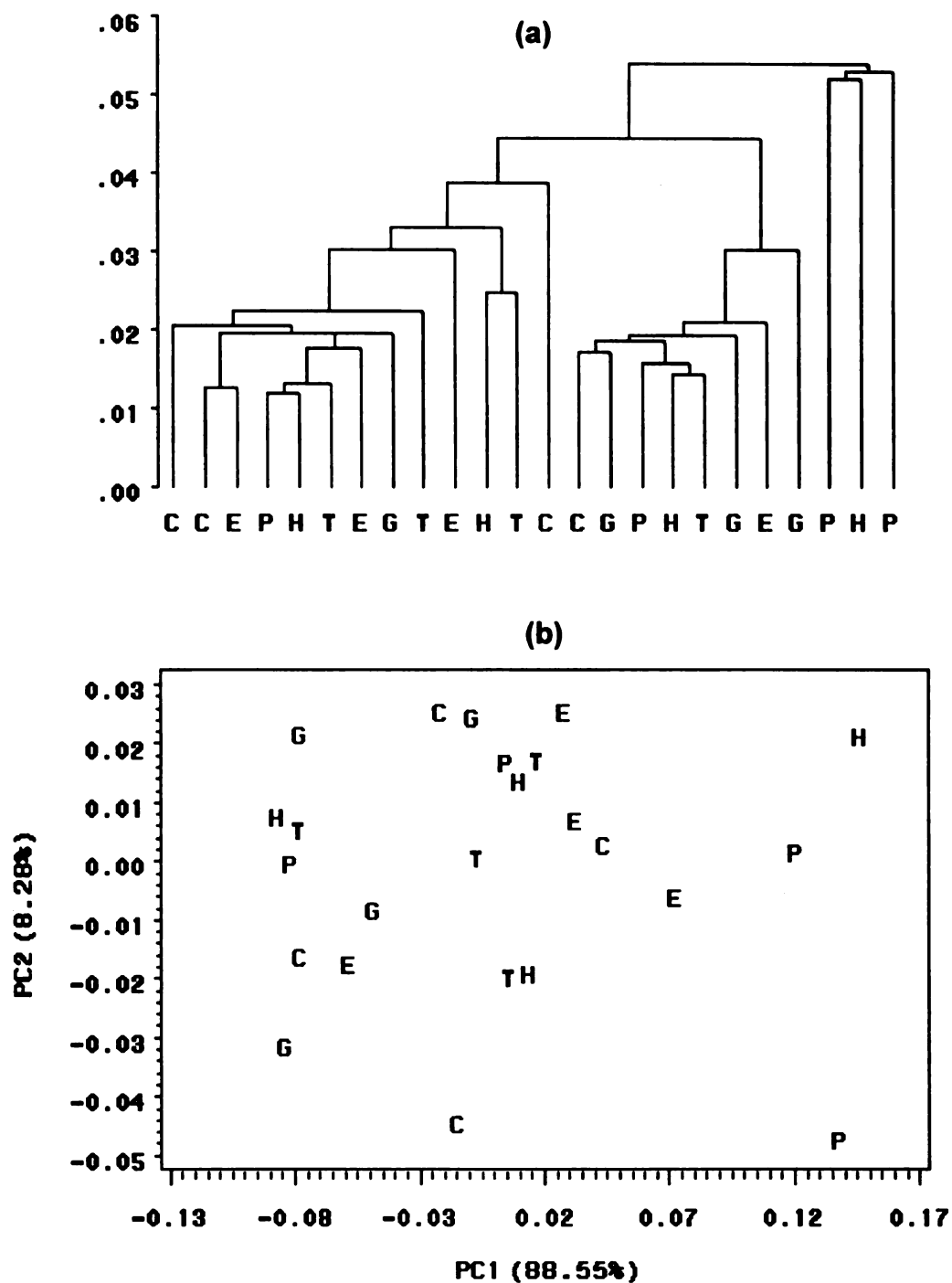


Figure 69 (a) HCA (b) PCA of sensor responses for the 95°C headspace of 2% milk stored in various packaging materials: glass (G), HDPE (H), HDPE-TiO₂ (T), PET (E), and PE-coated paper cartons (P), at 5°C for 3 days. Control (C) is milk from the original gallon HDPE jug.

Supervised learning techniques, LDA/QDA and k-NN for $k = 1$ to 4, had poor correct identification rates at the test step, for water and 2% milk stored in various packaging materials less than 0.3 and 0.2, respectively (Figure 70 and Figure 71). A graphical display of LDA results as canonical discriminant scatter plots showed a grouping trend, but no group separation in the models can be clearly defined (Figure 72a and Figure 73a). When projecting unknown samples on the models, it showed poor recognition for both water and 2% milk samples (Figure 72b and Figure 73b). The headspace volatiles of each packaging material were clearly differentiated by the electronic nose (Figure 66), while the water or 2% milk samples were not able to be differentiated based on their packaging materials. It was probably a result of low concentration of the migrants in the water and 2% milk headspace, and the interference of water vapor, which MOS sensors respond to. Maneesin (2001) [73] and Das (2003) [66] found that the electronic nose (FOX 3000, AlphaMOS) was capable of discriminating volatiles originated from different HDPE jugs or resins, but the water samples having direct contact to the HDPE or resins were not fully differentiated.

In conclusion, packaging off-flavors did not prove to be a concern from storing 2% milk in glass, HDPE, HDPE-TiO₂ and PET bottles, and PE-coated paper cartons (half-pint, 237 ml) at 5°C for 3 days. Both sensory and instrumental analyses did not indicate any strong evidence of significant packaging off-flavors.

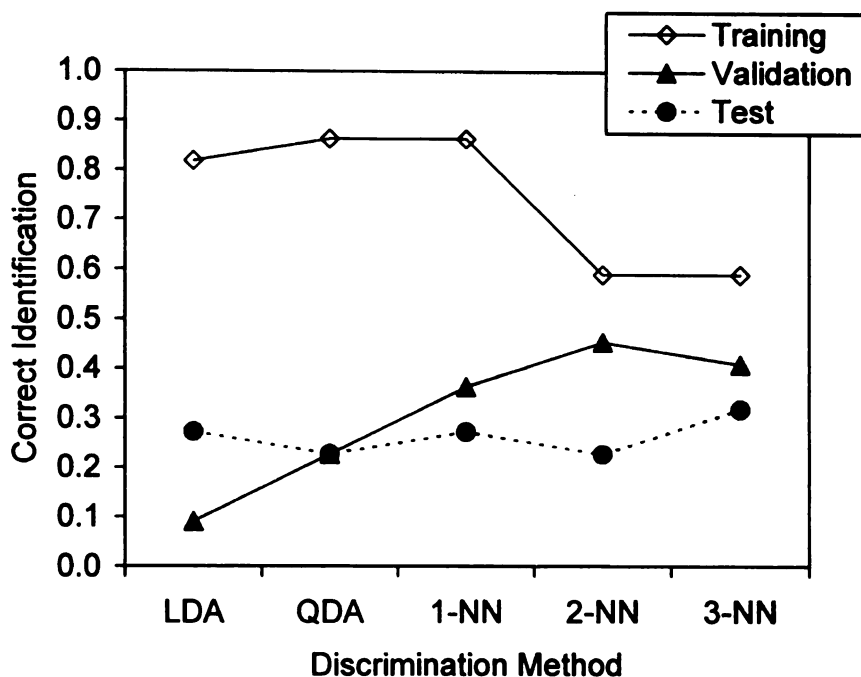


Figure 70 Correct classification rates of various discrimination methods applied to sensor responses for 95°C headspace of water in various packaging materials, using LDA/QDA and k-NN for k = 1, 2, 3, 4.

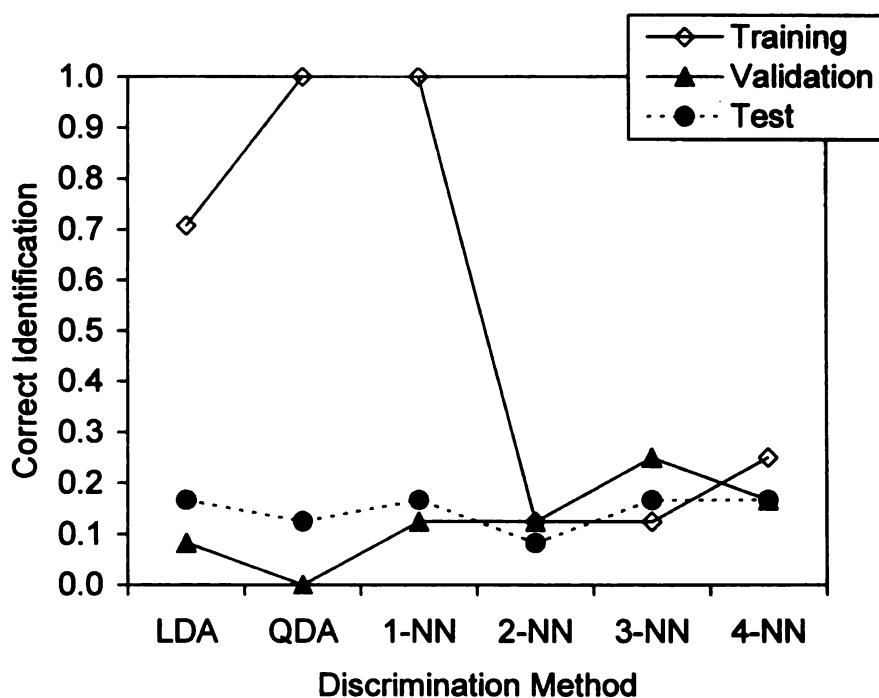


Figure 71 Correct classification rates of various discrimination methods applied to sensor responses for 95°C headspace of 2% milk in various packaging materials, using LDA/QDA and k-NN for k = 1, 2, 3, 4.

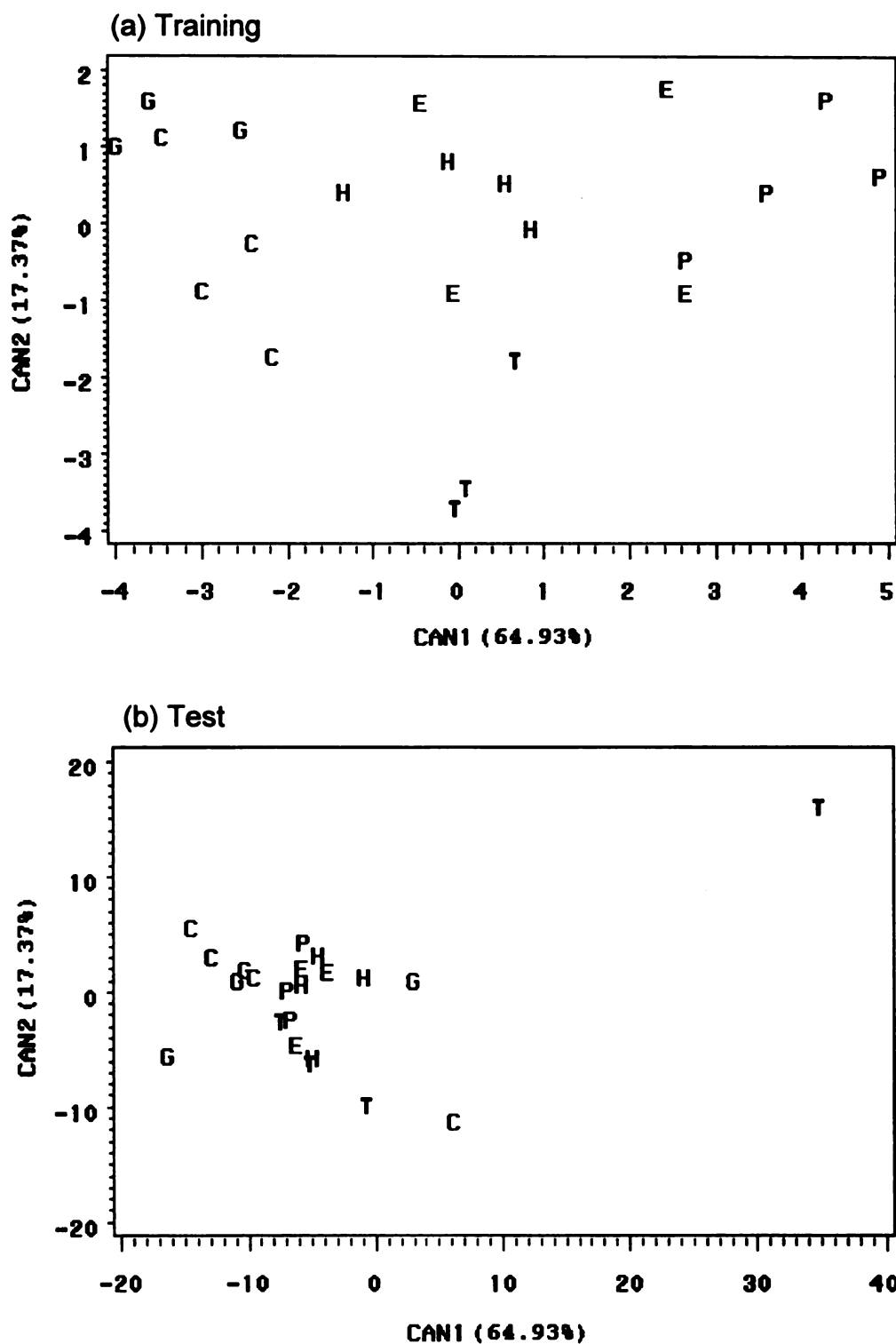


Figure 72 Canonical discriminant scatter plots of the (a) training (b) test data sets. Headspace samples of water stored in various packaging materials: glass (G), HDPE (H), HDPE-TiO₂ (T), PET (E), and PE-coated paper cartons (P), were generated at 95°C.

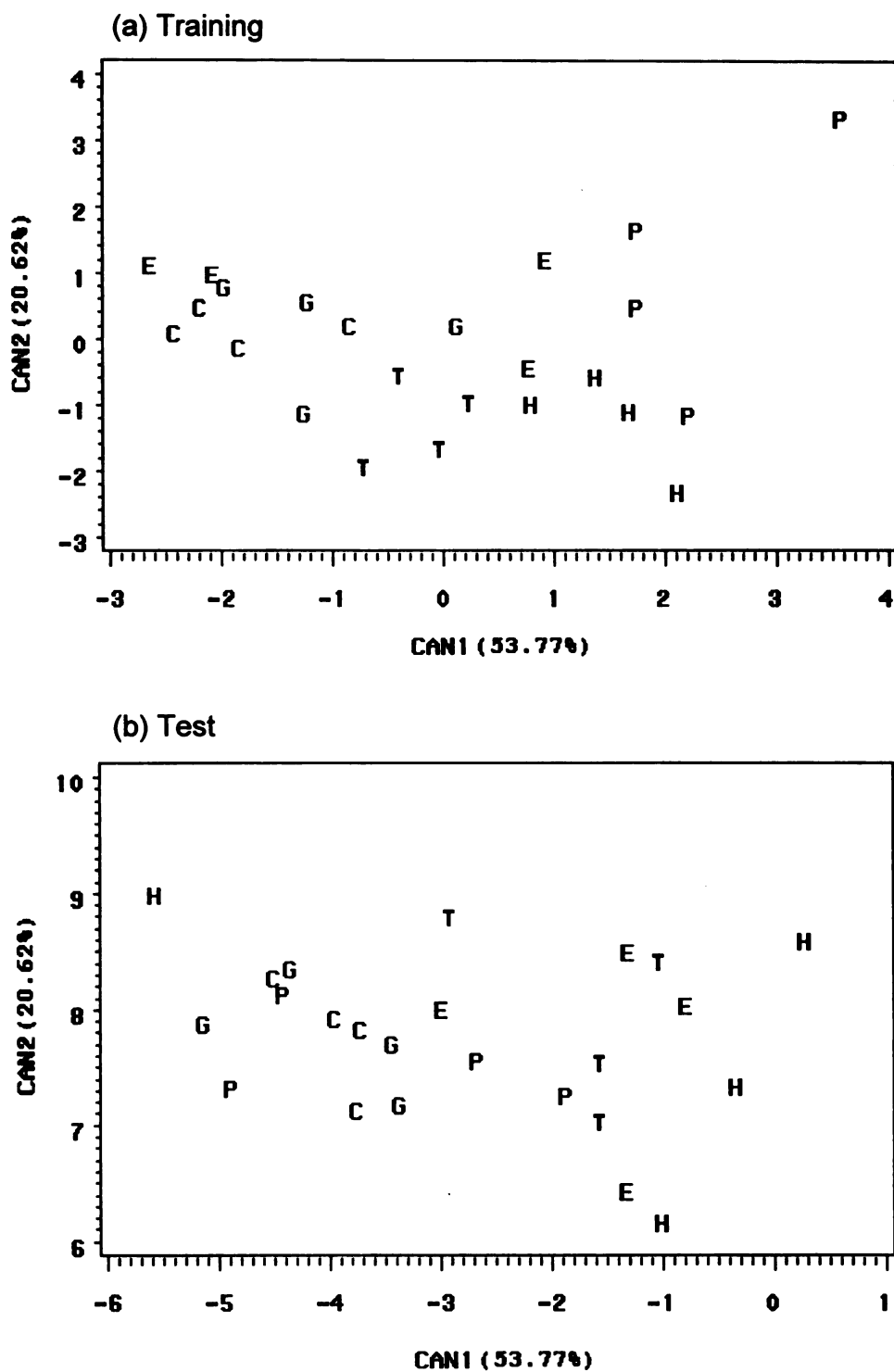


Figure 73 Canonical discriminant scatter plots of the (a) training (b) test data sets. Headspace samples of 2% milk stored in various packaging materials: glass (G), HDPE (H), HDPE-TiO₂ (T), PET (E), and PE-coated paper cartons (P), were generated at 95°C.

4.2.3. Packaging and light oxidized off-flavors in 2% milk

Packaging materials also have different light barrier properties and thus offer different protection for milk against light-induced oxidation, which can be induced by light in both the UV and visible ranges (chapter 2.1.1). Glass is a very poor light barrier and allows light in the higher UV range (300- 400 nm) and throughout the visible range (400-700 nm) to pass through (Figure 8). Clear transparent PET also allows light transmission in the higher UV range (320- 400 nm) as well as 90% of the visible light (400-700 nm) to transmit into the product (Figure 74). Translucent, unpigmented HDPE has up to 70% light transmission at 400-700 nm. Addition of TiO_2 to HDPE reduces light transmission significantly, from ~ 70% to < 20% of visible light. PE-coated paper cartons have the lowest visible light transmission ~ 10%, and the blue colored portion provides additional light protection at 550-750 nm. Table 17 shows the thickness of the tested packaging materials.

To protect milk and other dairy products from photosensitized oxidation in the presence of riboflavin, it is critical to reduce the UV and visible light transmission, especially at 500 nm and below (Figure 7). Addition of white (TiO_2) and/or yellow pigment results in substantial reduction in light transmission [84]. Paper cartons had the lowest light transmission, and more protection can be expected from the paper cartons printed in deep yellow or orange [1], although it has been reported that similar protection is provided by paper cartons printed in different colors (unpigmented, yellow, red, blue, and black) [8].

Table 17 Thickness of the tested packaging materials.

Packaging material	Thickness ¹ (mil)	Thickness (mm)
HDPE	30.7±3.4	0.779±0.086
HDPE-TiO ₂	29.2±1.5	0.741±0.037
PET	19.6±1.9	0.499±0.048
PE-coated paper carton	17.0±0.1	0.432±0.002

¹ measured using a micrometer (Model 549, Testing Machines, Inc., Amityville, N.Y.).

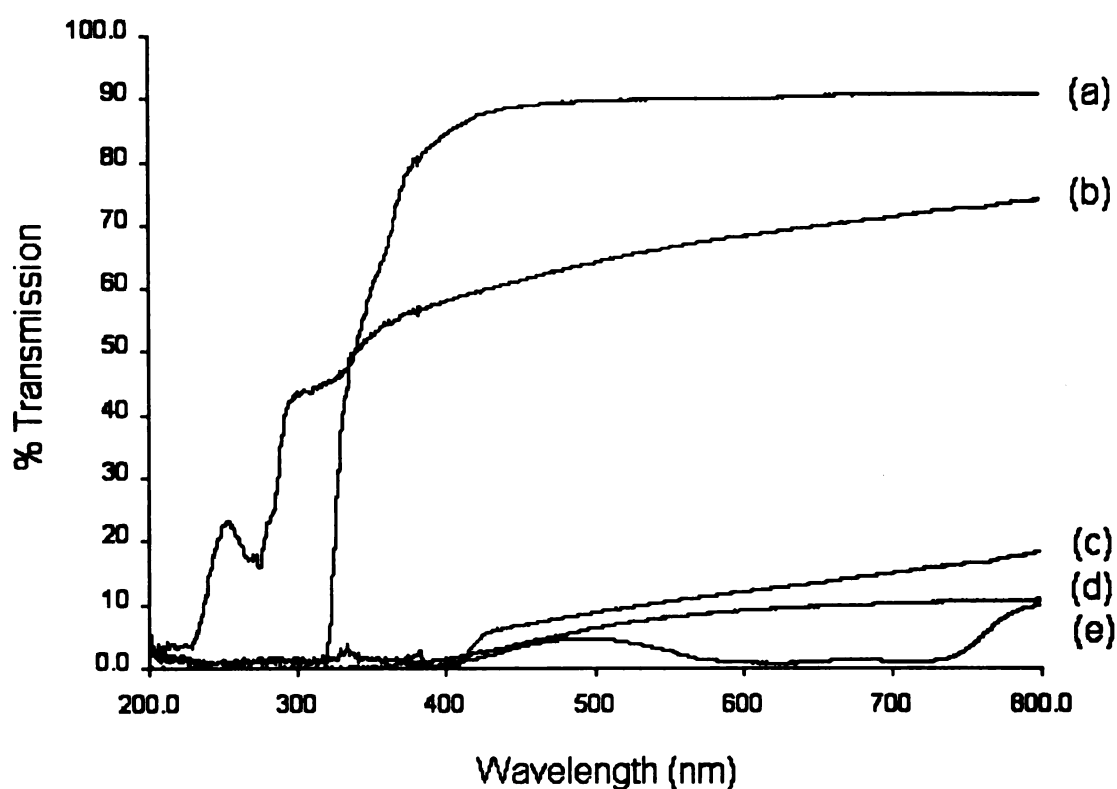


Figure 74 Percent light transmission (200-1100 nm) of various packaging materials: (a) PET; (b) HDPE; (c) HDPE-TiO₂; (d) PE-coated paper cartons in white; (e) PE-coated paper cartons (blue).

4.2.3.1. Sensory evaluation

A series of triangle tests (Table 18) showed that 2% milk in PE-coated paper cartons had no significant olfactory quality change after exposure to 12 hours of fluorescent light (1000 lx) at 5°C, while light-induced quality change in milk stored in other packaging materials (HDPE, HDPE-TiO₂ and PET) was detectable by consumers. Incorporation of the pigment TiO₂ into HDPE (HDPE-TiO₂) reduced but did not eliminate flavor changes ($p < 0.01$), compared to HDPE and PET ($p < 0.001$). The light protection offered by milk packaging was closely related to their light barrier properties (Figure 74). Paper cartons allowed the least light transmission and provided the best light protection among the packaging materials tested, followed by HDPE-TiO₂.

Table 18 A series of triangle tests on 2% milk stored in HDPE, HDPE-TiO₂, PET bottles and PE-coated paper cartons, and exposed to 12 hours of fluorescent light at 5°C; 2% milk stored in aluminum foil wrapped glass bottles was used as the control. Tests were performed by a 24-member consumer panel.

Packaging Material	Number of Correct Responses from 24 Subjects	p
HDPE	17	0.001
HDPE-TiO ₂	15	0.01
PET	17	0.001
Paper Carton	9	--

The sensory scores, from an 8-member trained panel, of 2% milk in paper cartons and HDPE-TiO₂ bottles were slightly, but not significantly, higher than others (Table 19 and Figure 75).

Table 19 Sensory scores of 2% milk stored in glass, HDPE, HDPE-TiO₂, PET bottles, and PE-coated paper cartons, and exposed to 12 hours of fluorescent light at 5°C. Scores were given by an 8-member trained panel.

Packaging material	Sensory score (average \pm standard deviation)		
Glass	5.75	± 2.55	a
HDPE	5.25	± 2.92	a
HDPE-TiO ₂	6.50	± 1.41	a
PET	5.25	± 2.19	a
Paper Carton	6.88	± 2.36	a

¹ Means with the same letter are not statistically different at $\alpha = 0.05$ (Tukey's studentized range test).

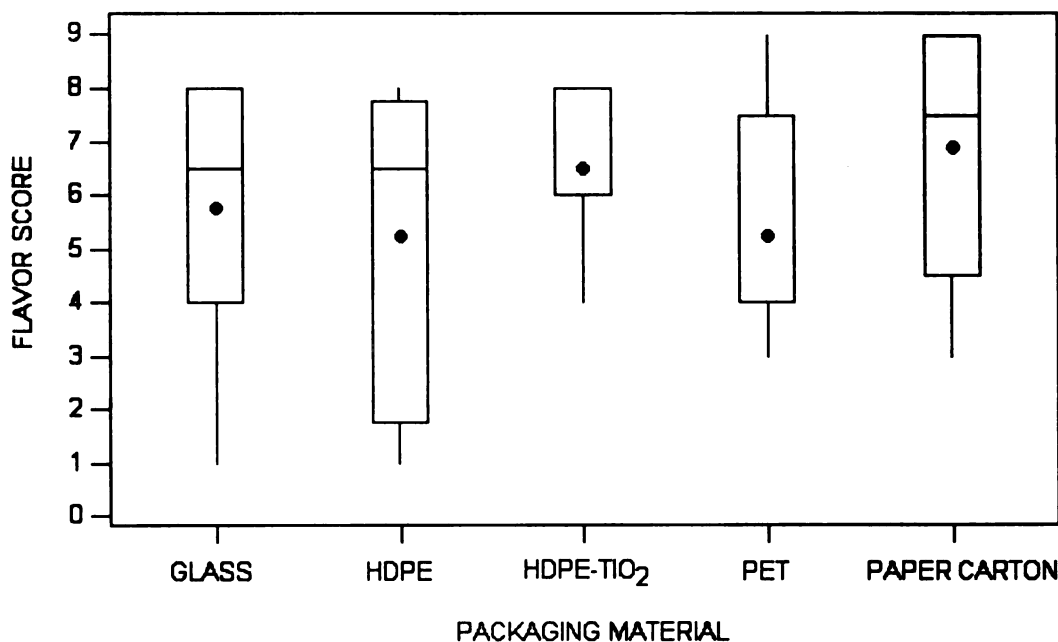


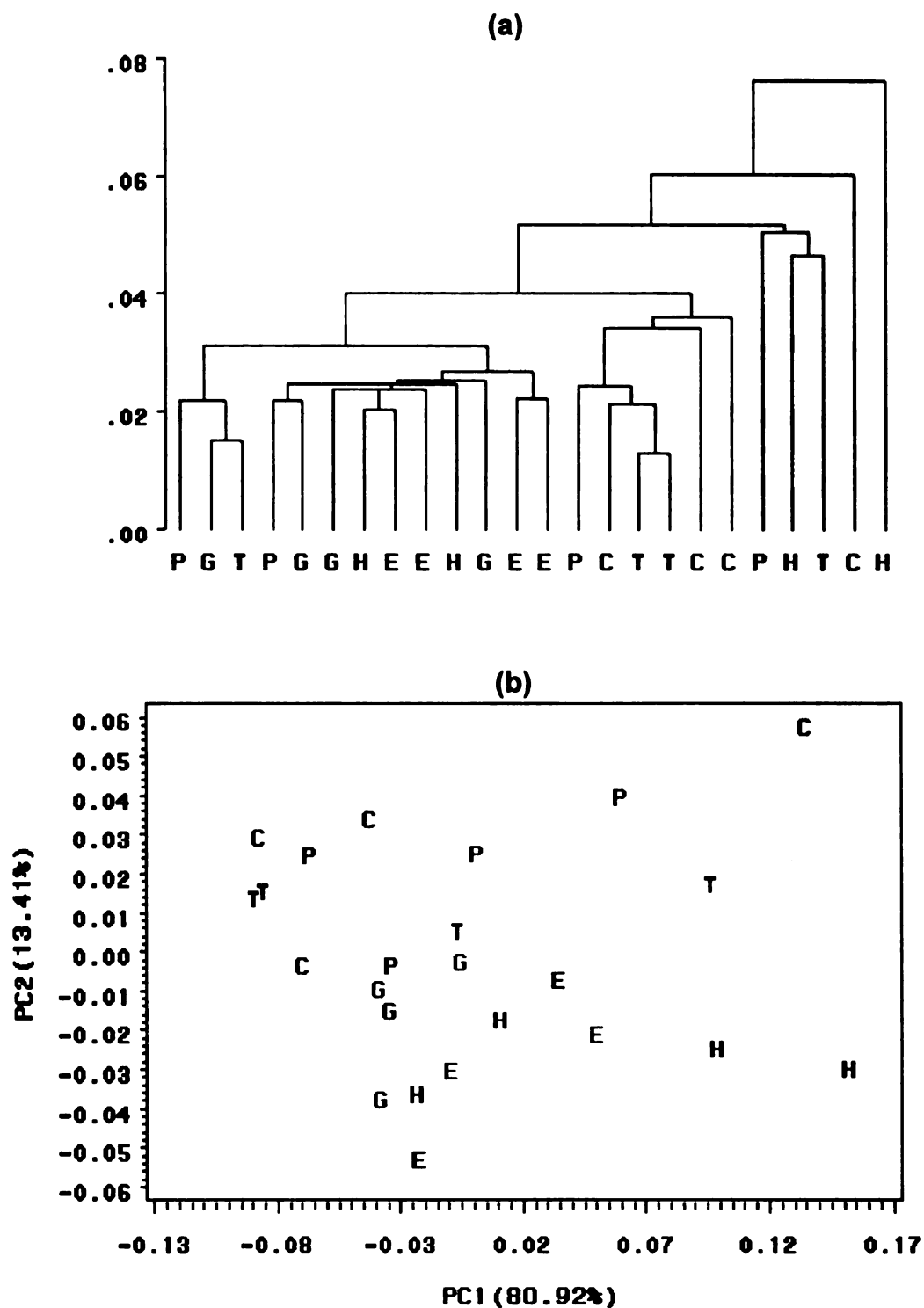
Figure 75 Sensory scores using a trained panel of 2% milk stored in glass, HDPE, HDPE-TiO₂, PET bottles, and PE-coated paper cartons exposed to 12 hours of light at 5°C.

Milk exposed to light for 12 hours in glass bottles received similar sensory scores of 6.38 ± 2.20 (Table 11) and 5.75 ± 2.55 (Table 19) in different tasting sessions. It indicates a reproducible sensory ability of the trained panel for light oxidized off-flavors.

4.2.3.2. Headspace analysis using the electronic nose

Unsupervised learning techniques, HCA and PCA, did not show an obvious pattern or separation among the light oxidized 2% milk samples stored in various packaging materials (Figure 76).

Supervised learning techniques, LDA and 1-NN, had correct identification rates at the test step, 0.54 and 0.63, respectively (Figure 77). Graphical display of LDA results as canonical discriminant scatter plots showed a grouping trend and partial differentiation (Figure 78a), when samples with no or moderate light-oxidized off-flavors (control, paper cartons and HDPE-TiO₂) were clearly differentiated from oxidized samples (glass, HDPE and PET). The first canonical variable (CAN 1) explained 97.09% of the total variance. Along the CAN1 coordinate, the control (milk in aluminum foil wrapped glass bottles), PE-coated paper cartons and HDPE-TiO₂, glass, HDPE and PET, were roughly aligned in the order of expected “good milk” to “light-oxidized milk”, based on light barrier properties of the packaging materials. The distribution was less distinct when projecting unknown samples on the models (Figure 78b). A similar trend was also observed among the light oxidized 2% milk prepared in glass bottles for 0 to 48 hours (Figure 46).



PE-coated paper cartons provided the best light barrier and resulted in the least light-oxidized off-flavors in 12 hours of light exposure, compared to glass, HDPE, HDPE-TiO₂ and PET, although the potential for packaging off-flavors in paper cartons has been reported [13, 81] and recognized as a flavor defect “lacks freshness” in the ADSA sensory guidelines (Table 8). Since the amounts of migrants, e.g. oxidative hydrocarbons, at the surface of the PE coating depend on the processing conditions, the intensity of packaging off-flavors varies. In this study the packaging off-flavors were not significantly perceived by either consumer or trained panels. Compared to light-oxidized off-flavors, the packaging off-flavors were less intense and more difficult to detect.

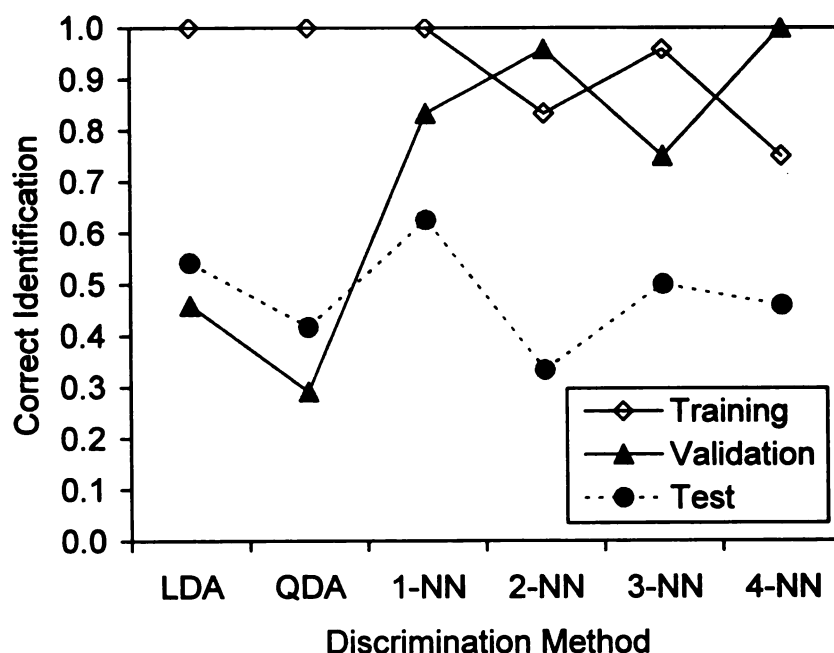


Figure 77 Correct classification rates of various discrimination methods (LDA/QDA and k-NN for k = 1, 2, 3, 4) based on sensor responses for 2% milk stored in various packaging materials and exposed to fluorescent light at 5°C for 12 hours.

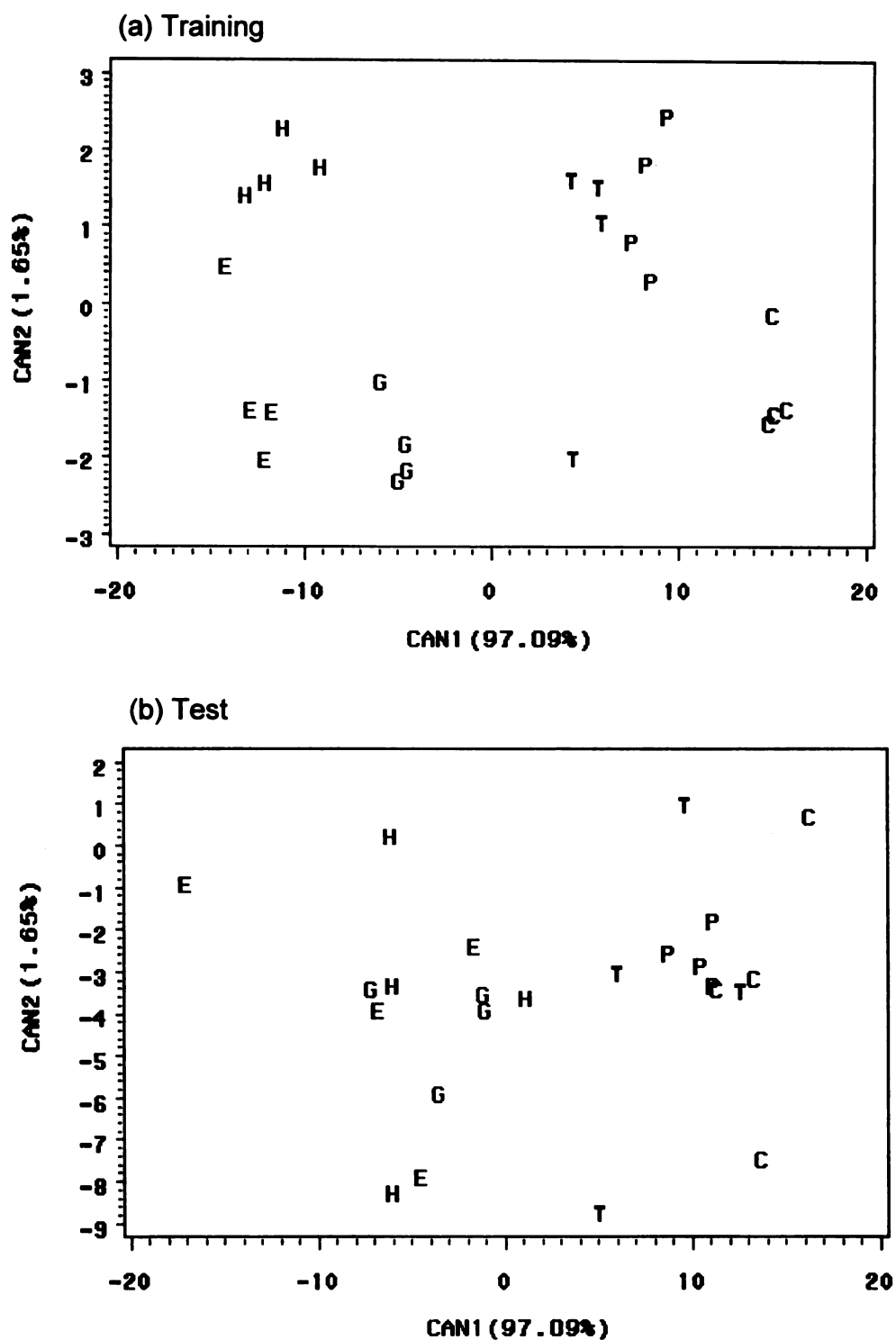


Figure 78 Canonical discriminant scatter plots of the (a) training (b) test data sets. Headspace of 2% milk stored in glass (G), HDPE (H), HDPE-TiO₂ (T), PET (E), and PE-coated paper cartons (P) and exposed to light for 12 hours was generated at 95°C.

4.3. Light oxidation of Cheddar cheese

A Cheddar cheese block (21.3 kg) was cut into one pound (454 g) pieces, vacuum sealed in Nylon/PE bags, and exposed to cool-white fluorescent light (2000 lx) at 5°C for 0, 2, 4 or 6 weeks. The surface slabs (top surface) and interior slabs (1 cm below the top surface) were sampled and evaluated by both sensory and instrumental analyses, to determine any quality changes in color and flavor.

4.3.1. Discoloration of Cheddar cheese

Annatto extract, the water based colorant, was used to enhance the color appearance of the Cheddar cheese, however, it is also susceptible to oxidation and sensitive to processing parameters such as pH and temperature [89]. A 9-member trained panel using a different-from-control test was used to investigate the color change in Cheddar cheese due to light exposure (Table 11 and Figure 79). Cheddar cheese had a significant color change on the top surface in 2 weeks, and a more pronounced discoloration when exposed to light for 4 and 6 weeks. Visual examination revealed that color bleaching was responsible for the differences in color. The Cheddar cheese surface slab which was wrapped in aluminum foil, i.e. no light exposure, had the same color as the interior slabs of all cheese samples, regardless of the light exposure duration of the cheese samples. The interior slabs did not show significant change in flavor or color, which shows that the light-induced discoloration only took place at the top surface, which was the portion exposed to light.

Table 20 Difference-from-control sensory scores in color¹ of Cheddar cheese samples. Interior and surface slabs were taken from Cheddar cheese blocks at 0, 2, 4 or 6 weeks of light exposure (2000 lx). Scores were given by a 9-member trained panel.

Time (weeks)	Color (different-from-control)					
	Interior			Surface		
0	0.22	± 0.44	c	0.33	± 0.50	c
2	0.44	± 0.53	c	2.00	± 0.71	b
4	0.22	± 0.44	c	3.00	± 0.87	a
6	0.22	± 0.44	c	3.00	± 0.87	a

¹ Ranged from 0: no difference to 5: extreme difference.

² Means with the same letter are not statistically different at $\alpha = 0.05$ (Tukey's studentized range test).

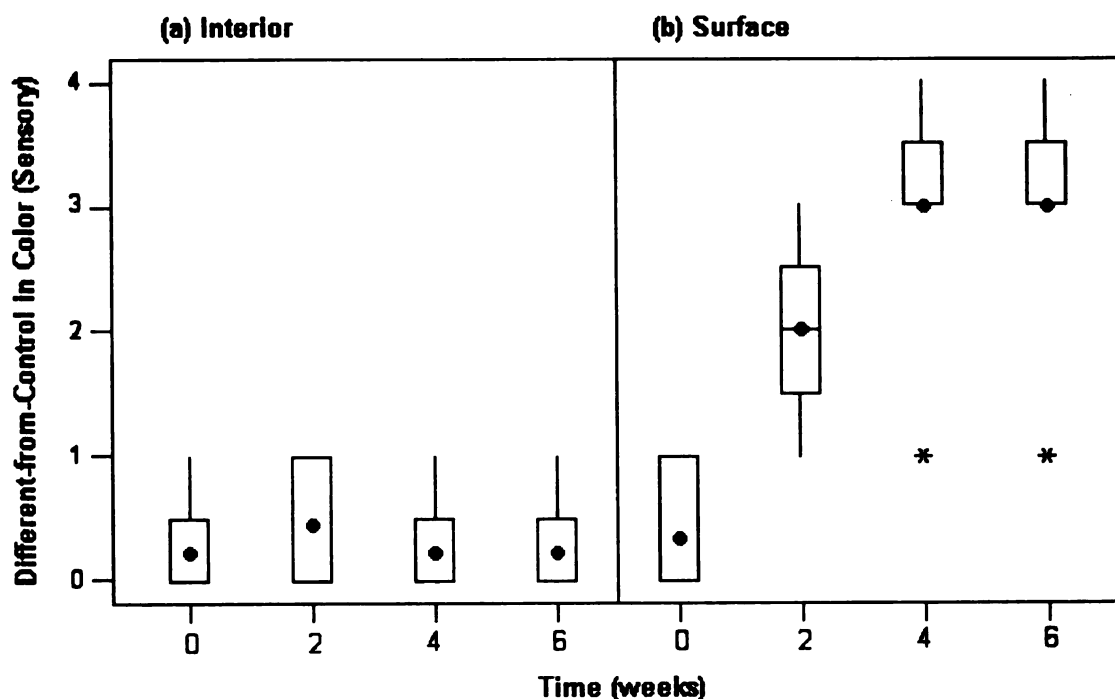


Figure 79 Difference-from-control sensory scores in color of Cheddar cheese samples. (a) Interior and (b) surface slabs were taken from Cheddar cheese blocks at 0, 2, 4 or 6 weeks of light exposure (2000 lx). •: mean values of each treatment; *: possible outliers.

Color measurements using a spectrophotometer (CIE L* a* b*) showed a significant increase in lightness (L*) and decrease in redness (a*) and yellowness (b*), on the top surface of Cheddar cheese exposed to light (Table 21).

Yellowness decreased continuously over the 6 weeks of the light exposure (2000 lx), from 45.36 ± 0.82 to 30.60 ± 0.73 . Redness started to drop after 4 weeks.

Lightness had a relatively small increase over the 6 weeks period.

The overall color change (ΔE) represents the color differences between the sample and control, i.e. vacuum packed Cheddar cheese wrapped in aluminum foil. The ΔE values showed a similar trend as the different-from-control sensory scores, with smaller variation (Figure 79). The color change of the top surface took place in 2 weeks, and developed further in 4 and 6 weeks.

Hong *et al.* (1995) [90] suggested using hue angles (0° for red and 90° for yellow) to measure the color change of Cheddar cheese, to evaluate “pink discoloration”, a common problem that is normally a result of several processing factors such as cooking temperature, emulsifying salts [92], pH or light exposure [90]. They reported that Cheddar cheese exposed to fluorescent light (3500 lx, cool-white) at 8°C for 14 days had significant decreases in yellowness and hue angles as the oxygen transmission rates of the packaging films increased. Table 22 shows the hue angles of the Cheddar cheese samples. The top surface of the Cheddar cheese that was exposed to fluorescent light (2000 lx) had a significant decrease in hue angles (i.e. more “pink” in color visually) in 2 weeks, while no further decrease in hue angles was observed in 4 or 6 weeks.

Table 21 Color measurements (CIE L* a* b*) of the Cheddar cheese samples exposed to 0, 2, 4 or 6 weeks of the fluorescent light (2000 lx).

Time (weeks)	Lightness (L*)			
	Interior		Surface	
0	75.14± 0.25	b, c ¹	74.81± 0.40	c
2	75.16± 0.46	b, c	75.53± 0.35	a, b
4	75.00± 0.43	b, c	75.70± 0.32	a
6	74.94± 0.32	c	76.00± 0.45	a

¹ Means with the same letter are not statistically different at $\alpha = 0.05$ (Tukey's studentized range test).

Time (weeks)	Redness (a*)			
	Interior		Surface	
0	12.06± 0.27	b ¹	11.80± 0.30	b
2	12.59± 0.21	a	11.70± 0.40	b
4	12.52± 0.26	a	10.29± 0.28	c
6	12.75± 0.13	a	9.89± 0.24	d

¹ Means with the same letter are not statistically different at $\alpha = 0.05$ (Tukey's studentized range test).

Time (weeks)	Yellowness (b*)			
	Interior		Surface	
0	46.89± 0.55	a ¹	45.36± 0.82	b
2	46.20± 0.59	a, b	37.57± 0.76	c
4	45.78± 0.44	b	32.81± 0.72	d
6	45.73± 0.76	b	30.60± 0.73	e

¹ Means with the same letter are not statistically different at $\alpha = 0.05$ (Tukey's studentized range test).

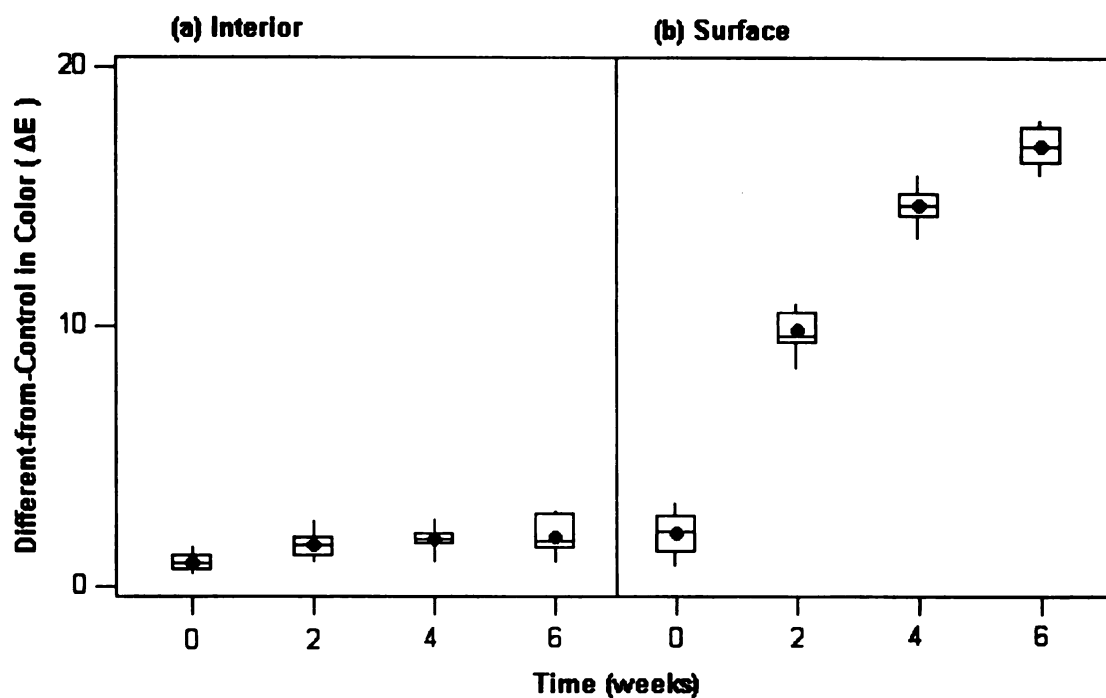


Figure 80 Color difference (ΔE) of Cheddar cheese samples. (a) Interior and (b) surface slabs were taken from Cheddar cheese blocks with 0, 2, 4, 6 weeks of light exposure (2000 lx). •: mean values of each treatment; *: possible outliers.

Table 22 Hue angle, $\tan^{-1}(b/a)$, of the Cheddar cheese samples exposed to 0, 2, 4 or 6 weeks of the fluorescent light (2000 lx).

Time (weeks)	Hue angle (degree)					
	Interior			Surface		
0	75.57	± 0.27	a ¹	75.42	± 0.35	a
2	74.76	± 0.26	b	72.71	± 0.31	c
4	74.71	± 0.31	b	72.59	± 0.47	c, d
6	74.42	± 0.33	b	72.08	± 0.68	c, d

¹ Means with the same letter are not statistically different at $\alpha = 0.05$ (Tukey's studentized range test).

4.3.2. Body and texture of Cheddar cheese

Sensory tests were conducted to evaluate if there was a change in the body and texture of the Cheddar cheese, due to the light exposure. A different-from-control test (from 0: no difference to 5: extreme difference) showed no significant changes occurred (Table 11 and Figure 81). There was a slight but not significant increase in the “differences” in body and texture of the top surface slabs exposed to light for 4 or 6 weeks.

“Body and texture” is part of the sensory quality evaluation of Cheddar cheeses, based on ADSA guidelines (Table 9). A score from 5 (no criticisms) to 1 (poor quality) was assigned based on the sample defects in body and texture, e.g. crumbly, pasty or weak. The results were in agreement with the different-from-control test. No significant deterioration in body and texture, and slight but not significant decreases in the sensory scores of the top surface of the Cheddar cheese occurred for cheese exposed to light (Table 11 and Figure 81).

Table 23 Difference-from-control sensory scores of body and texture¹ of Cheddar cheese samples. Interior and surface slabs were taken from Cheddar cheese blocks with 0, 2, 4 or 6 weeks of light exposure (2000 lx). Scores were given by a 9-member trained panel.

Time (weeks)	Body and Texture (different-from-control)					
	Interior			Surface		
0	0.44	± 0.73	a	0.11	± 0.33	a
2	0.22	± 0.44	a	0.56	± 1.01	a
4	0.56	± 0.88	a	1.44	± 1.33	a
6	0.56	± 0.73	a	1.44	± 1.42	a

¹ Ranged from 0: no difference to 5: extreme difference.

² Means with the same letter are not statistically different at $\alpha = 0.05$ (Tukey's studentized range test).

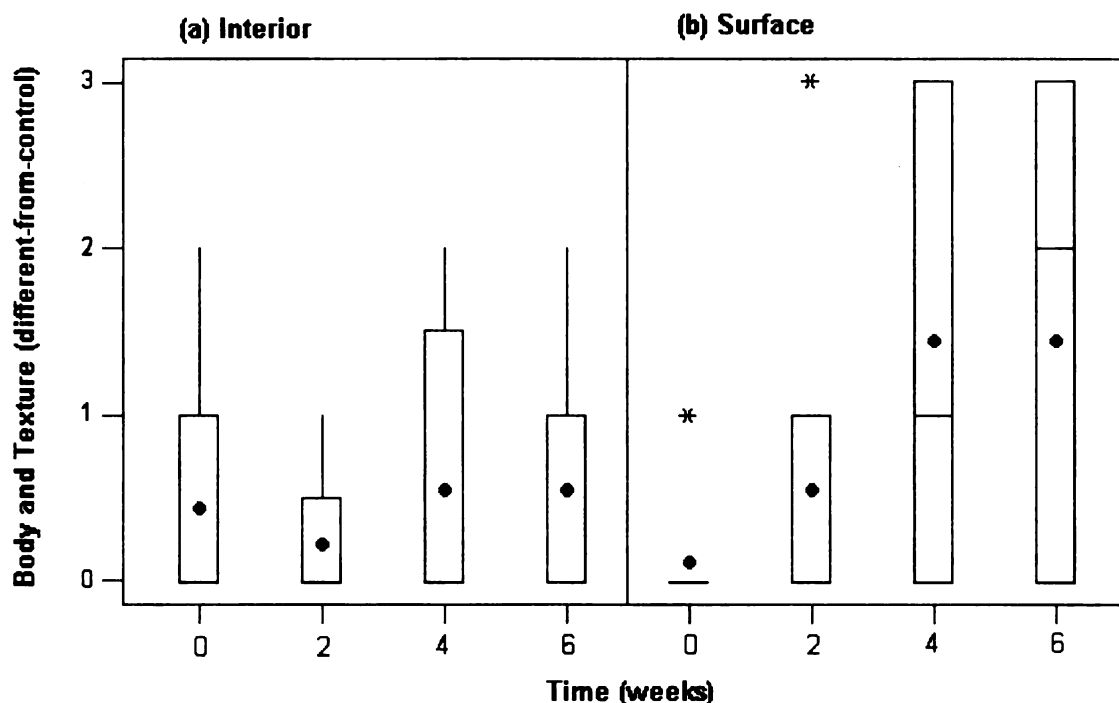


Figure 81 Difference-from-control sensory scores for body and texture of Cheddar cheese samples. (a) Interior and (b) surface slabs were taken from Cheddar cheese blocks with 0, 2, 4 or 6 weeks of light exposure (2000 lx). •: mean values of each treatment; *: possible outliers.

Table 24 Sensory scores of body and texture of Cheddar cheese samples, based on ADSA guidelines¹. Interior and surface slabs were taken from Cheddar cheese blocks with 0, 2, 4 or 6 weeks of light exposure (2000 lx). Scores were given by a 9-member trained panel.

Time (weeks)	Body and Texture (ADSA)				
	Interior			Surface	
0	4.56	± 0.53	a	4.89	± 0.33 a
2	4.44	± 0.53	a	4.78	± 0.44 a
4	4.56	± 0.53	a	4.22	± 0.67 a
6	4.44	± 0.73	a	4.11	± 0.78 a

¹ Ranged from 1: poor quality to 5: no criticisms.

² Means with the same letter are not statistically different at $\alpha = 0.05$ (Tukey's studentized range test).

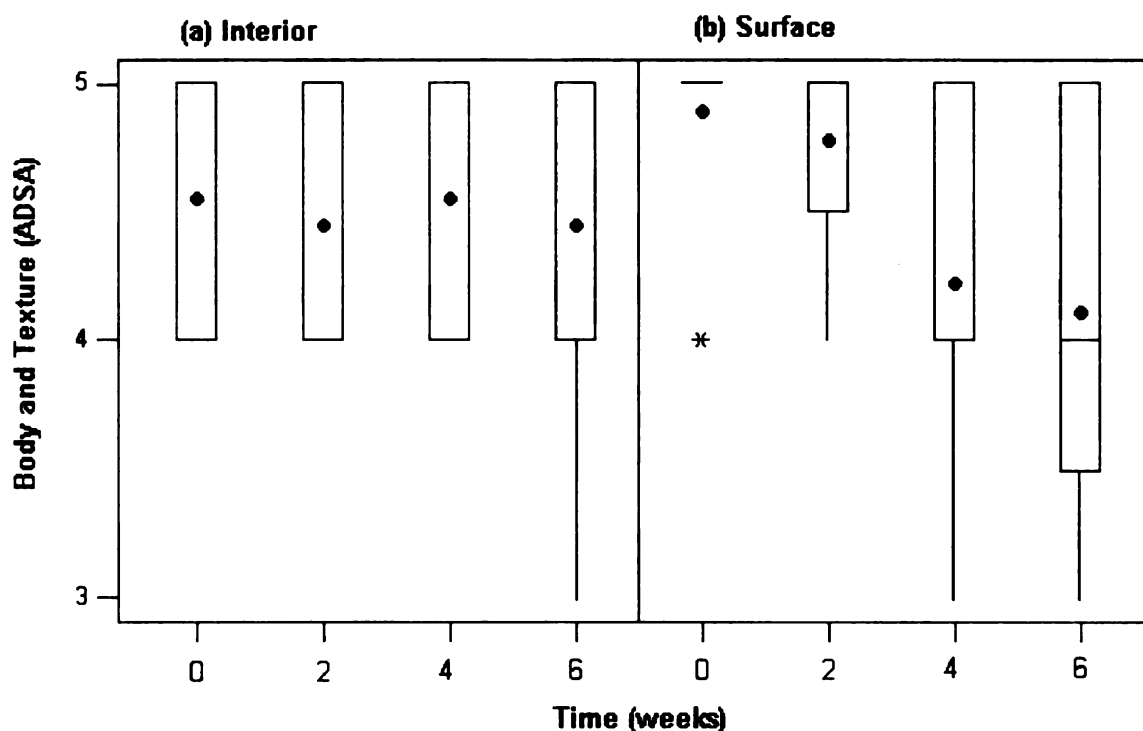


Figure 82 Sensory scores for body and texture of Cheddar cheese samples, based on ADSA guidelines. (a) Interior and (b) surface slabs were taken from Cheddar cheese blocks with 0, 2, 4, 6 weeks of light exposure (2000 lx). •: mean values of each treatment; *: possible outliers.

4.3.3. Light-induced flavor changes of cheese

4.3.3.1. Sensory evaluation

Different-from-control evaluation (Table 11 and Figure 81) showed a significant flavor difference from the control, on the top surface of the Cheddar cheese exposed to light for 2 weeks. After 4 weeks of light exposure, differences were slightly but not significantly higher, and remained almost constant at 6 weeks. The sensory scores from the trained panel (Table 26 and Figure 84) were in agreement with the different-from-control test. The scores were assigned to samples based on the flavor criticisms of Cheddar cheese, e.g. bitter, high acid or rancid, etc. (Table 9). From the listed 13 criticisms, the top surface of Cheddar cheese exposed to light for 2, 4, or 6 weeks received lower sensory scores due to the criticisms such as “oxidize”, “rancid” and “unclean” (data not shown).

4.3.3.2. Headspace analysis using SPME-GC

Using the CAR/PDMS fiber coupled with GC, 24 volatiles were identified by comparing the peak retention times of the samples to standards (Table 27). The volatiles identified in the Cheddar cheese headspace included aldehydes, ketones, alcohols, acids and sulfur compounds. It was reported [105] that aldehydes and ketones were the major constituents of the volatile fraction of shredded Cheddar cheese packaged under CO₂ and N₂, respectively. Acetic acid and sulfur compounds were also quantified. High concentrations of lipid oxidation products, e.g. aldehydes, appeared in light-oxidized shredded Cheddar cheese.

Table 25 Difference-from-control sensory scores in flavor¹ of Cheddar cheese samples. Interior and surface slabs were taken from Cheddar cheese blocks at 0, 2, 4 or 6 weeks of light exposure (2000 lx). Scores were given by a 9-member trained panel.

Time (weeks)	Flavor (different-from-control)			
	Interior		Surface	
0	0.56	± 0.73 b	0.56	± 0.73 b
2	1.11	± 1.05 b	2.44	± 1.01 a
4	0.78	± 0.97 b	3.67	± 1.00 a
6	0.56	± 0.73 b	3.56	± 0.88 a

¹ Ranged from 0: no difference to 5: extreme difference.

² Means with the same letter are not statistically different at $\alpha = 0.05$ (Tukey's studentized range test).

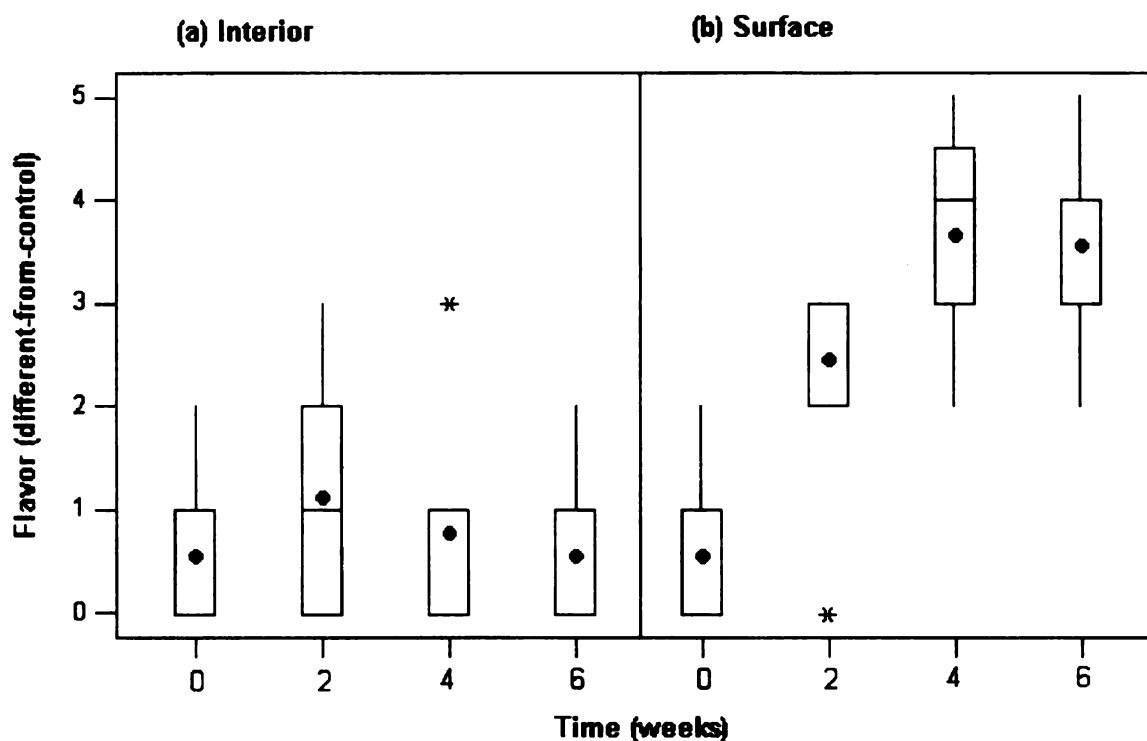


Figure 83 Difference-from-control sensory scores in flavor of Cheddar cheese samples. (a) Interior and (b) surface slabs were taken from Cheddar cheese blocks at 0, 2, 4, or 6 weeks of light exposure (2000 lx). •: mean values of each treatment; *: possible outliers.

Table 26 Flavor sensory scores of Cheddar cheese samples based on ADSA guidelines¹. Interior and surface slabs were taken from Cheddar cheese blocks with 0, 2, 4 or 6 weeks of light exposure (2000 lx). Scores were given by a 9-member trained panel.

Time (weeks)	Flavor (ADSA)			
	Interior		Surface	
0	8.89	± 0.60 a, b	8.89	± 0.93 a, b
2	8.89	± 0.60 a, b	7.22	± 1.56 b
4	8.44	± 1.33 a, b	5.22	± 1.48 b
6	9.11	± 0.33 a	5.11	± 2.03 b

¹ Ranged from 1: poor quality to 10: no criticism.

² Means with the same letter are not statistically different at $\alpha = 0.05$ (Tukey's studentized range test).

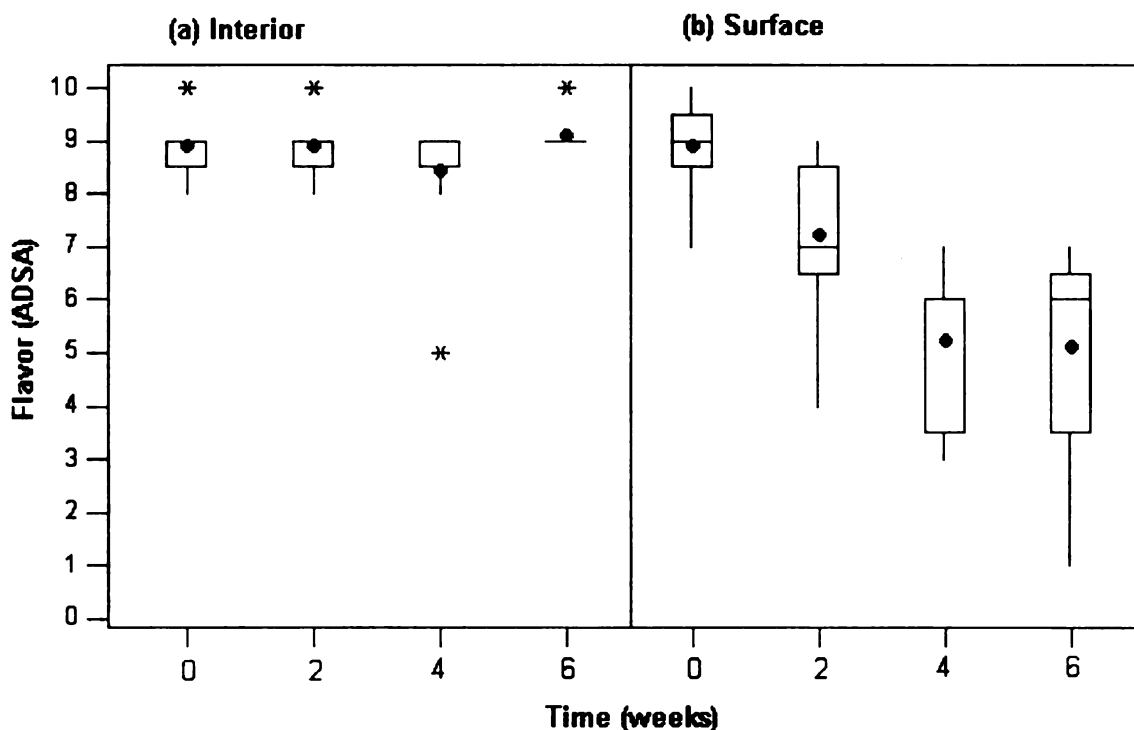


Figure 84 Flavor sensory scores of Cheddar cheese samples based on ADSA guidelines. (a) Interior and (b) surface slabs were taken from Cheddar cheese blocks with 0, 2, 4, or 6 weeks of light exposure (2000 lx). •: mean values of each treatment; *: possible outliers.

Table 27 Volatiles identified¹ in the headspace (60°C, 15 minutes) of Cheddar cheese.

Peak	Compound	Retention time (min)	Selected ²
1	pentane+hexane	5.80	*
2	heptane	6.61	*
3	acetaldehyde	6.80	*
4	carbon disulfide	6.93	
5	methyl sulfide	7.40	*
6	acetone	8.60	*
7	ethyl acetate	9.28	*
8	methanol	9.85	*
9	2-butanone	9.94	
10	2-propanol	10.29	
11	ethanol	10.58	*
12	pentanal	11.76	*
13	2-butanol	12.92	
14	1-propanol	13.27	
15	dimethyl disulfide	14.75	
16	2-methyl-1-propanol	14.84	
17	hexanal	14.88	*
18	1-butanol	16.64	*
19	heptanal	18.10	*
20	2-heptanone	18.16	
21	1-pentanol	20.10	*
22	acetic acid	26.95	*
23	propionic acid	29.47	*
24	butanoic acid	31.73	*

¹ Comparing retention time of the standards.

² Peaks with better reproducibility were selected for further multivariate analyses

Peak compounds with good reproducibility were selected for further multivariate analyses, i.e. HCA/PCA to investigate the sample differences. LDA/QDA and k-NN were used to build models for unknown sample recognition, and PLS/MLP to correlate the area responses of the selected volatiles to the flavor sensory scores from the trained panelists (Table 26 and Figure 84).

Using the unsupervised learning techniques, HCA and PCA, showed clear separation (Figure 85) between the surface slabs (S0, S2, S4, and S6) and interior slabs (I0, I2, I4, and I6), except for two “outliers” (S2 and S4). Further group separation among the group of surface slabs (i.e. the top surface of the Cheddar cheese samples) showed changes in the headspace volatile contents due to light exposure, whereas the interior slabs (i.e. 1 cm depth from the top surface) were relative close to each other on the PCA score plot (Figure 85b).

Supervised models using LDA/QDA and k-NN for $k = 1$ to 3 (Figure 86) showed high correct identification rates at the training and test steps. Considering the overall model performance, 1-NN provided the best discrimination (Figure 86). Its correct identification rates were the highest at the training and test steps, and relatively higher than LDA/QDA at the validation step. Clear discrimination between different samples and an accurate identification of unknown samples was shown for the LDA model graphically presented on the canonical discriminant plots (Figure 87). The first two discriminants, CAN1 and CAN2, explained 99.74% of the total variance. Note that CAN1 explained most of the variation between interior and surface slabs, and CAN2 was able to identify samples with different light exposure times.

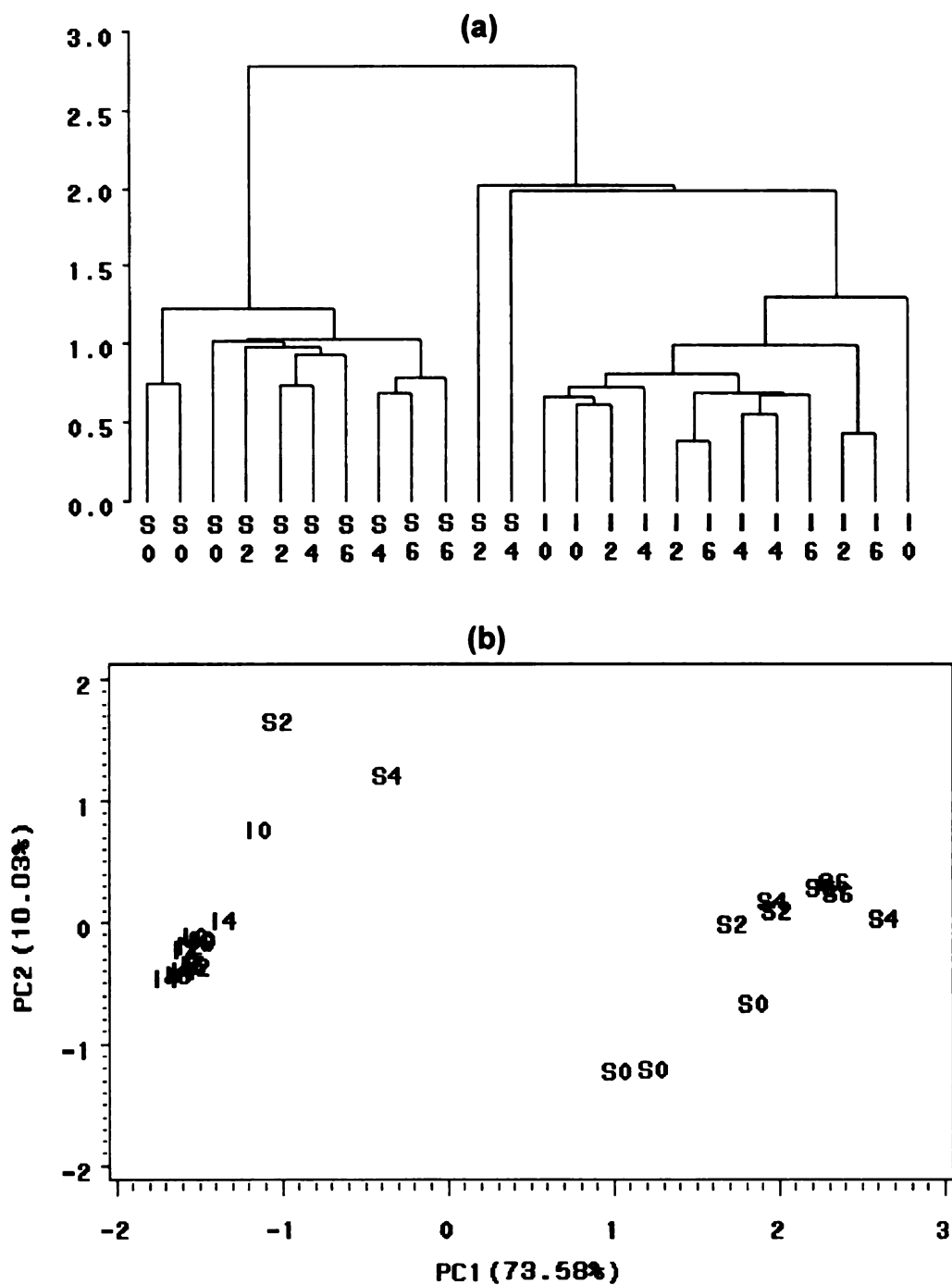


Figure 85 (a) HCA and (b) PCA of area response of SPME-GC. Headspace samples were the interior (I0, I2, I4 and I6) and surface slabs (S0, S2, S4, S6) of the Cheddar cheese samples exposed to fluorescent light for 0, 2, 4, or 6 weeks.

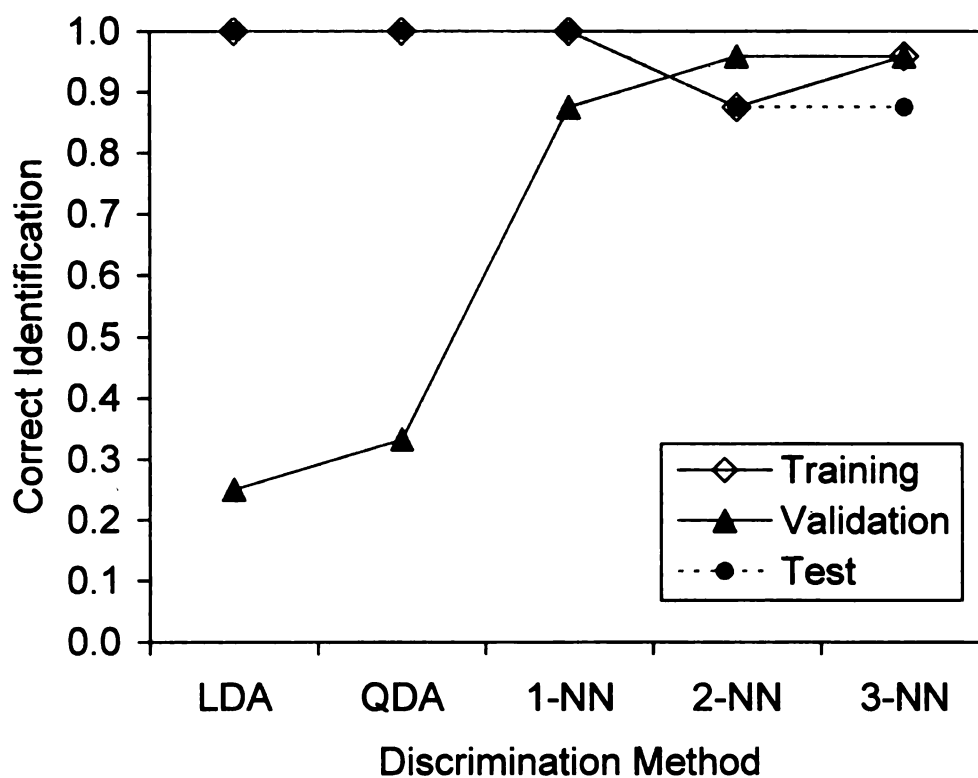


Figure 86 Correct classification rates of various discrimination methods (LDA/QDA and k-NN for k = 1, 2, 3, 4) based on headspace volatiles of interior and surface slabs of the Cheddar cheese samples exposed to fluorescent light for 0, 2, 4 or 6 weeks, quantified using SPME-GC.

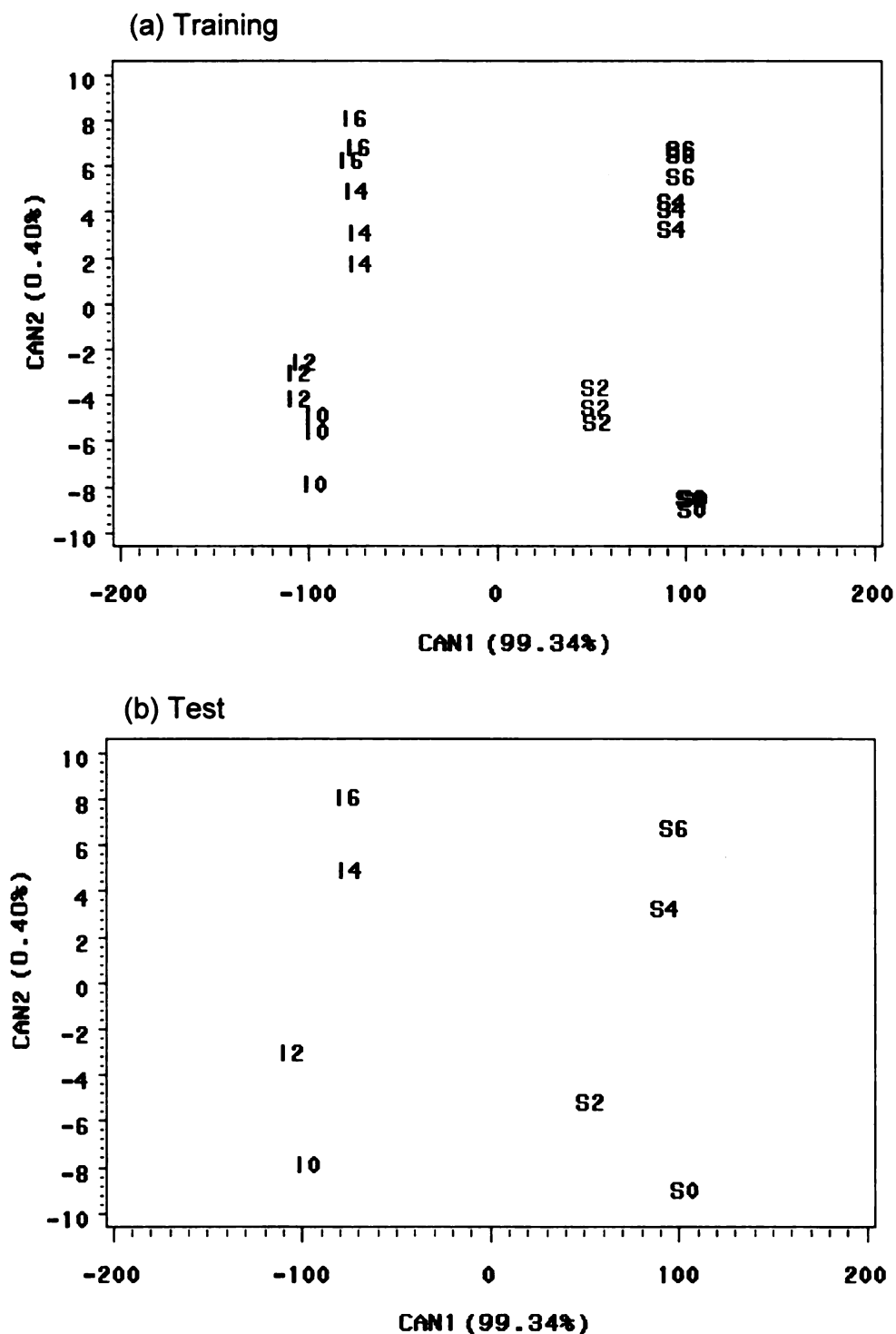


Figure 87 Canonical discriminant scatter plots of headspace volatile contents quantified using SPME-GC of (a) training (b) test data, Headspace samples of interior (I0, I2, I4, I6) and surface (S0, S2, S4, S6) slabs of the Cheddar cheese, were generated at 60°C.

Although the discriminant models showed clear group separation (Figure 87) and high correct identification rates (Figure 86), they may not be useful to identify the light-oxidized Cheddar cheese. The separation among the samples with different extents of light oxidation was much smaller than the separation between the surface and interior slabs. CAN1 accounted for 99.34% of the total variance, while only 0.40% for CAN2. Moreover, the sample S0 (top surface with no light exposure) had similar sensory scores as the interior slabs (I0, I2, I4 and I6), but was separated from the interior slabs on the canonical discriminant scatter plot (Figure 87). All interior slabs had similar sensory scores but were positioned separately on the scatter plot, in a similar manner as the surface slabs which were light-oxidized. It appears that the discrimination was more based on where the samples were taken from than the light-induced flavor changes. The collection of reproducibly identified volatiles may not cover all volatiles that were responsible for the light induced flavor changes, and may have caused the misleading results.

Quantitatively, PLS and MLP models were applied to investigate the correlations between the sensory scores and the area responses of headspace volatiles quantified using the SPME-GC (Figure 88 and Figure 89). The MLP model performed better than the PLS model, in terms of both the ranges of predicted sensory scores and the RMSE. However, the models may not be reliable for predicting light-oxidized Cheddar cheeses for the same reasons discussed previously.

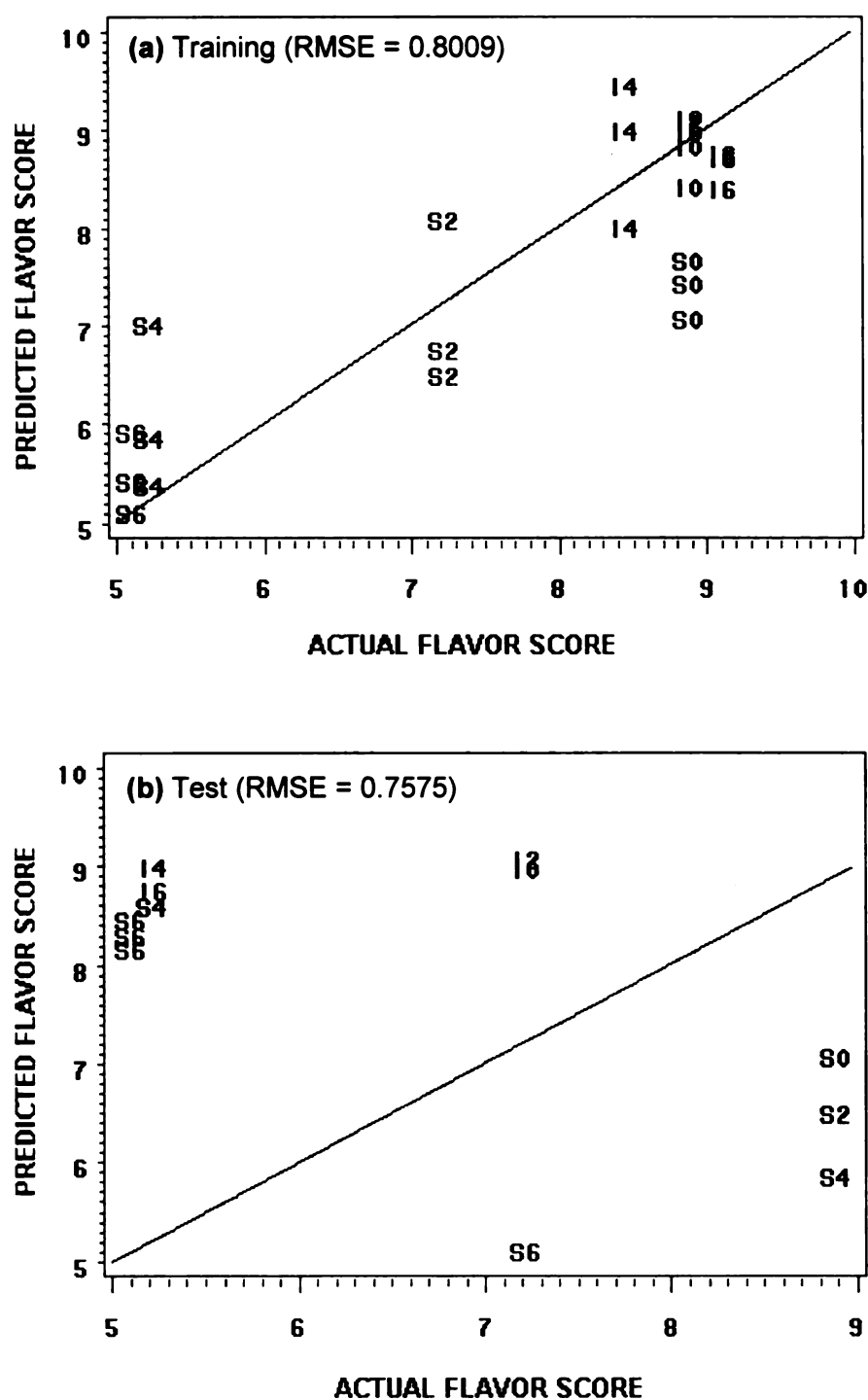


Figure 88 PLS predicted versus actual flavor scores of interior (10, 12, 14, 16) and surface (S0, S2, S4, S6) slabs of the Cheddar cheese, based on area response of SPME-GC to 60°C headspace. Models were applied to (a) training and (b) test data. The reference line indicates equal values of predicted and actual sensory scores.

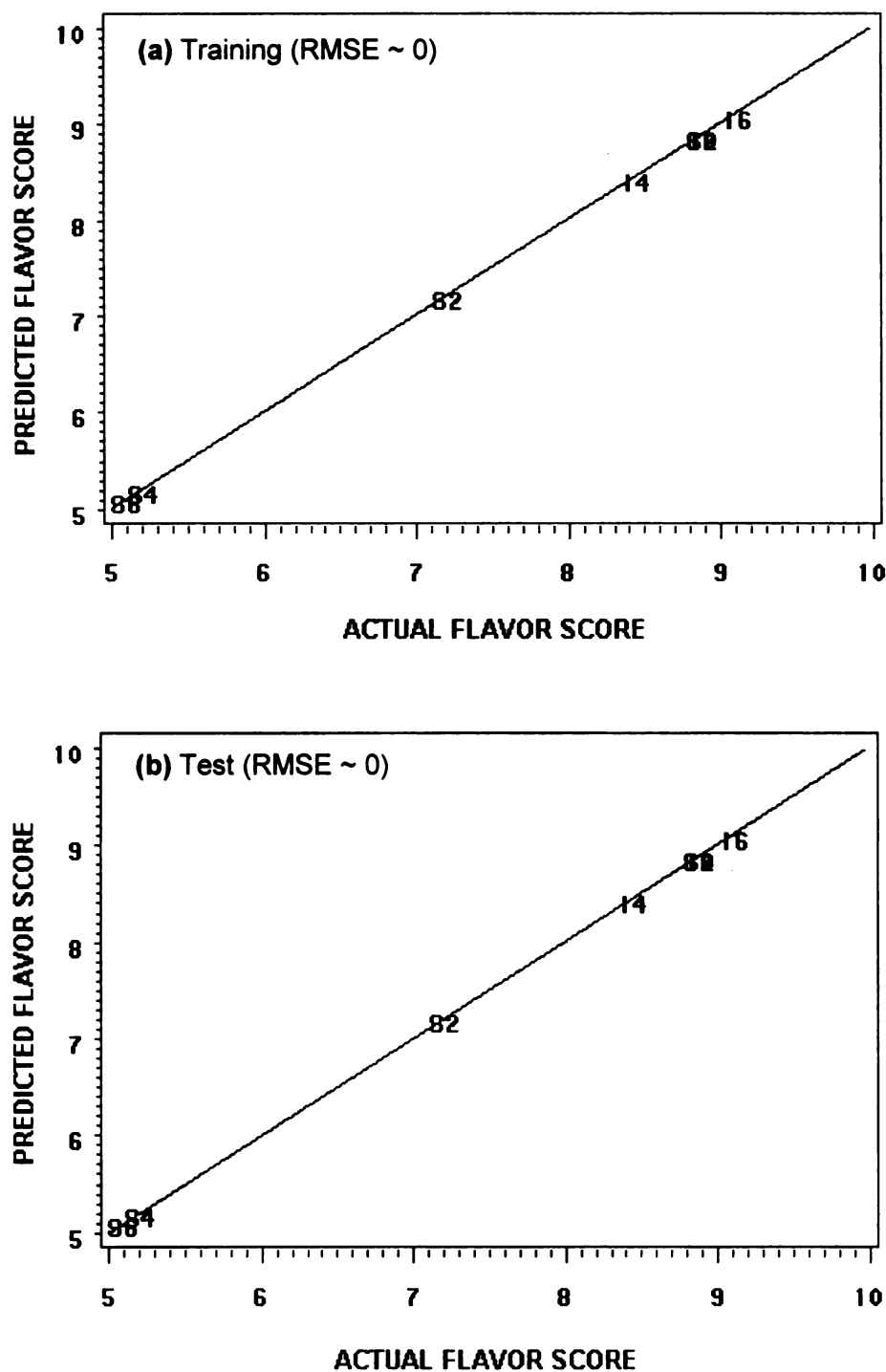


Figure 89 MLP predicted versus actual flavor scores of interior (I0, I2, I4, I6) and surface (S0, S2, S4, S6) slabs of the Cheddar cheese, based on area response of SPME-GC to 60°C headspace. Models were applied to (a) training and (b) test data. The reference line indicates equal values of predicted and actual sensory scores.

4.3.3.3. Headspace analysis using the electronic nose

Headspace samples of light-oxidized Cheddar cheese were generated at 60 or 95°C for 15 minutes and then analyzed using the electronic nose. Figure 90 shows the profiles of sensor response over time, to the 60°C headspace samples of the top surface of Cheddar cheese exposed to light for 0 and 6 weeks. The differences between sensor profiles of the two samples were not distinct by comparing the 12 MOS sensor responses directly. This may be due to the high sensitivity of MOS sensors to ethanol and other alcohols, such that the intense response may mask the sensor responses for other analytes of interest.

Unsupervised learning techniques, HCA and PCA, were applied to view the discrimination and natural grouping of the headspace samples of Cheddar cheese generated at 60°C and 90°C (Figure 91 and Figure 92). No clear separation was apparent in the 60°C PCA score plot (Figure 91b). A partial grouping in the 90°C PCA score plot roughly followed the extent of light oxidation (Figure 92b). Samples with no light exposure (I0, I2, I4, I6 and S0) formed a cluster (around $PC1 = \pm 0.2$ and $PC2 = -0.01$), and the top surface samples (S2, S4 and S6) then partially grouped and gradually moved away from this cluster as the light exposure time increased.

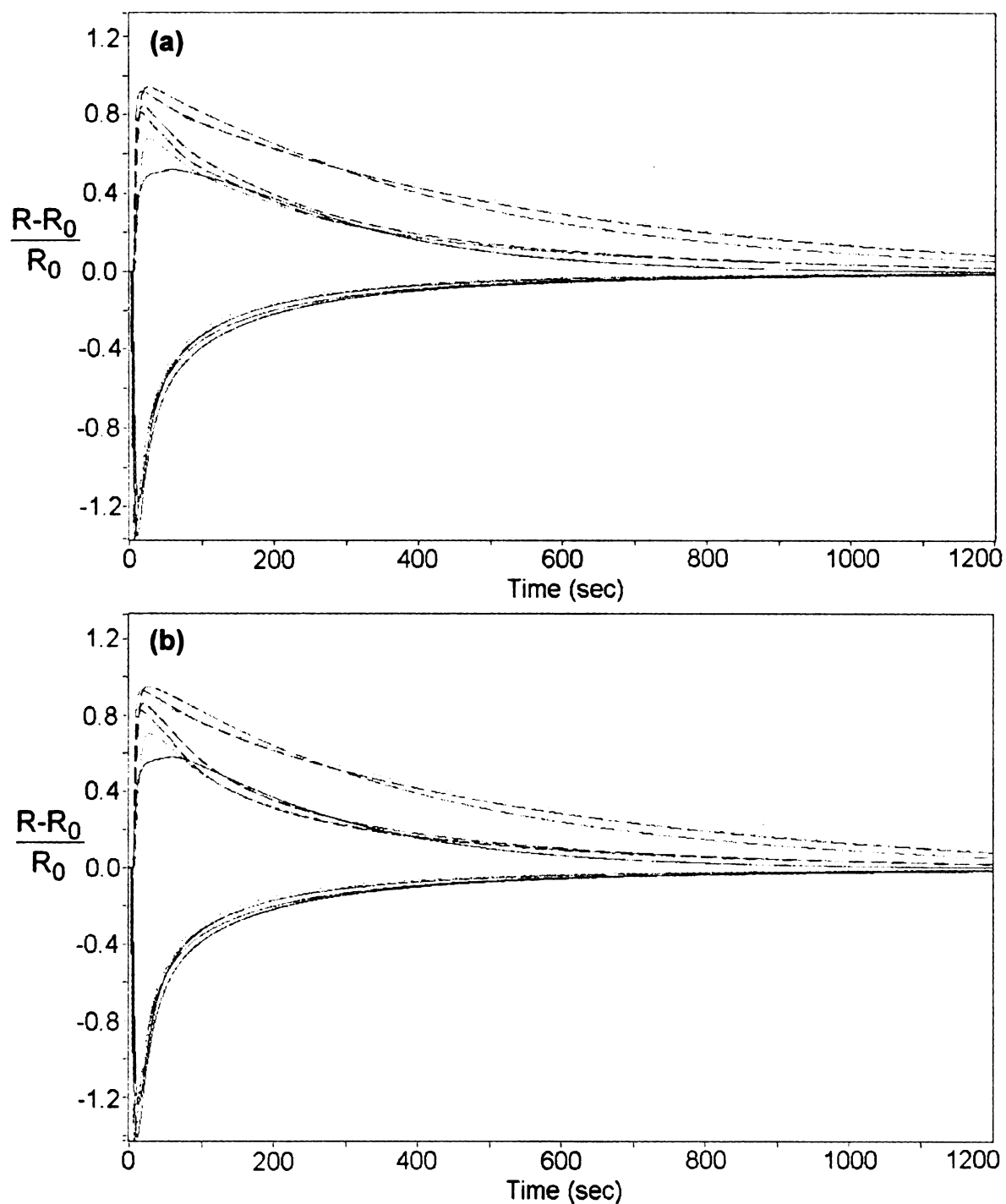


Figure 90 Sensor responses of the electronic nose to 90°C headspace of the top surface samples of Cheddar cheese (a) without (b) with 6 weeks of light exposure at 5°C.

Supervised learning techniques, LDA/QDA and k-NN for $k = 1$ to 4, were applied to training data, which contained four replicates of the surface slabs (S0, S2, S4, and S6) and interior slabs (I0, I2, I4, and I6). The models were cross-validated using the leave-one-out method, and the models were then used to identify the “unknown” samples from an independent test data set, which contained three replicates of the surface slabs S0, S2, S4, and S6.

LDA and 1-NN had the highest correct identification rates (0.4 and 0.5, respectively) at the test steps, for both 60°C and 90°C headspace samples (Figure 93 and Figure 94). A more distinct group separation for the 90°C headspace samples of the Cheddar cheese with differing light oxidation was apparent on the canonical discriminant scatter plot (Figure 96), while the 60°C headspace samples were only partially separated (Figure 95). The Cheddar cheese samples without light exposure, i.e. I0, I2, I4, I6 and S0, grouped at the negative CAN1 (the first canonical discriminant) region (Figure 95a and Figure 96a). Along the CAN1 coordinate, Cheddar cheese top surface samples exposed to light for 2, 4, and 6 weeks were aligned. While subjecting an independent test data set to the models, the 90°C headspace samples stayed at similar group territories (Figure 96b). The 60°C headspace samples from the test set were scattered and shifted to a very different range, which implied a poor model generalization. The supervised models based on sensor responses for 90°C headspace samples had higher correct identification rates (Figure 94) and better discrimination (Figure 96).

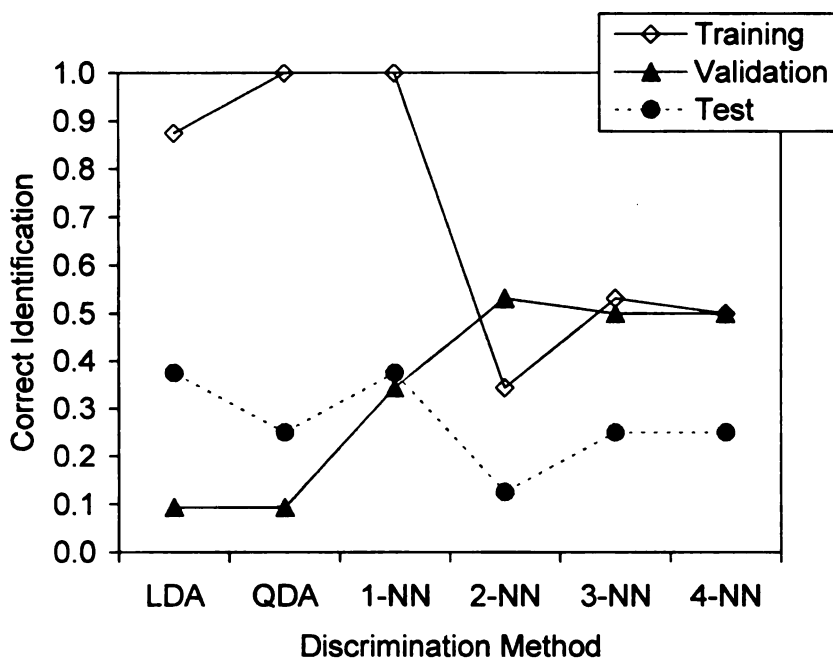


Figure 93 Correct classification rates of various discrimination methods (LDA, QDA, and k-NN for k = 1 to 4) applied to the sensor responses for 60°C headspace of interior and surface slabs of the Cheddar cheese samples exposed to fluorescent light for 0, 2, 4, or 6 weeks.

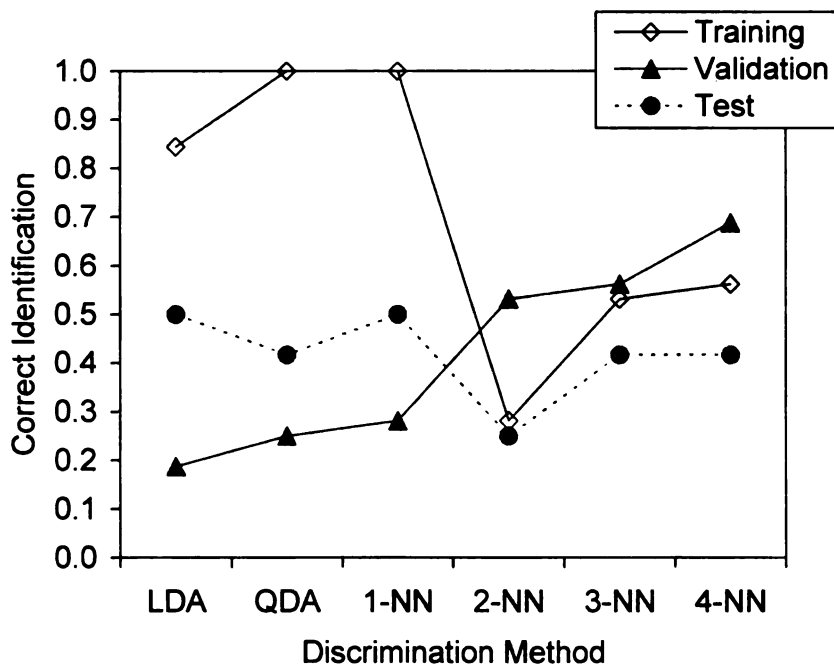


Figure 94 Correct classification rates of various discrimination methods (LDA, QDA, and k-NN for k = 1 to 4) applied to the sensor responses for 90°C headspace of interior and surface slabs of the Cheddar cheese samples exposed to fluorescent light for 0, 2, 4, or 6 weeks.

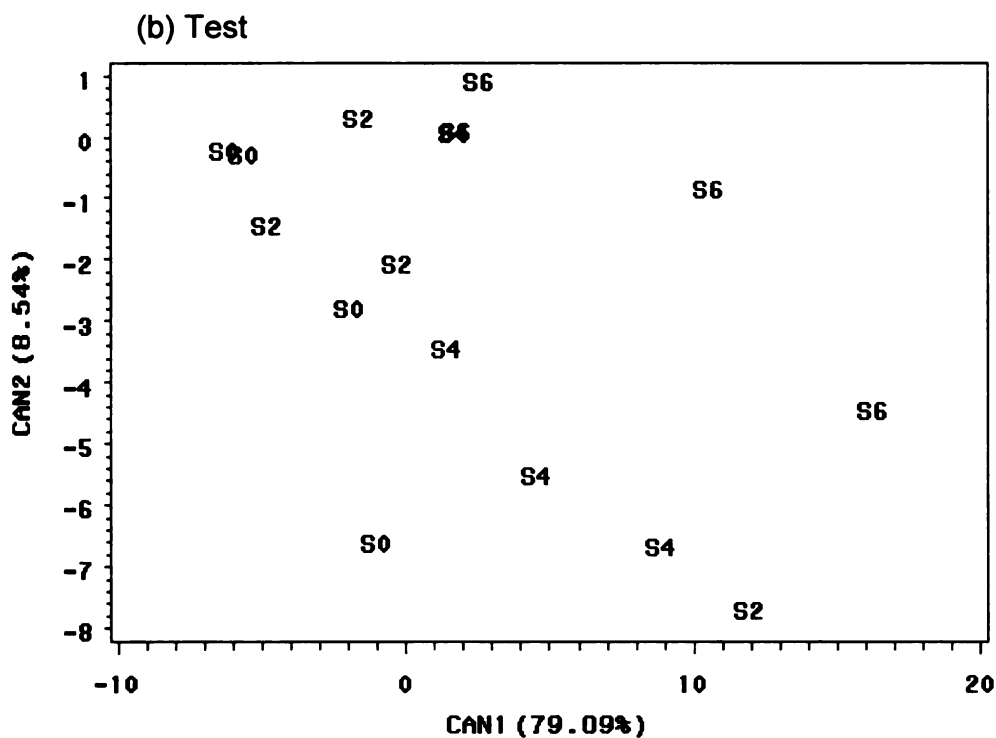
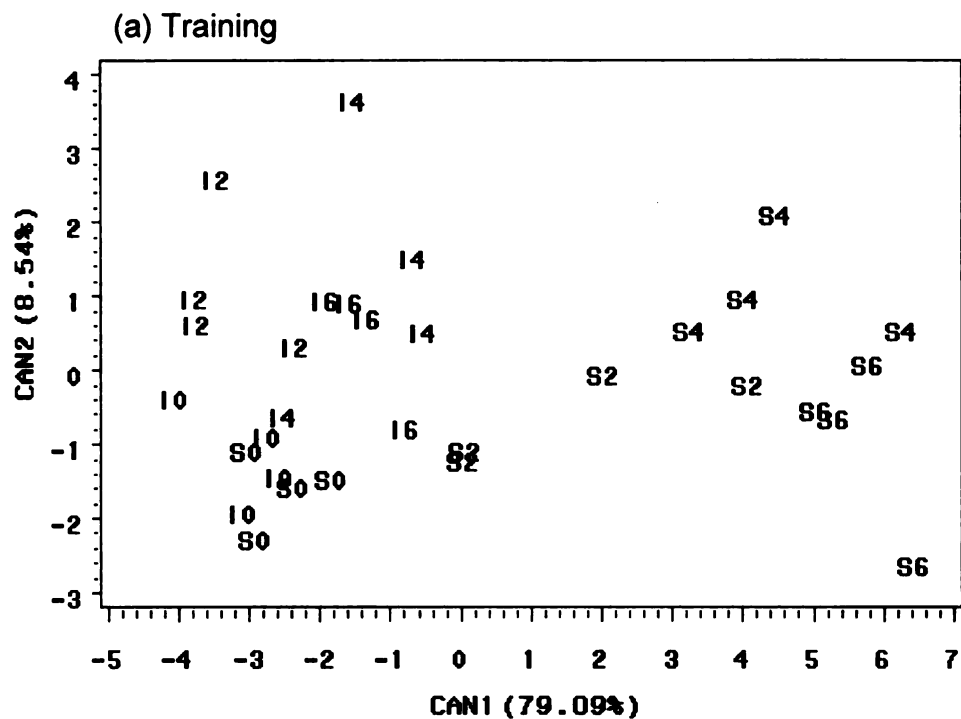


Figure 95 Canonical discriminant scatter plots of the (a) training (b) test data sets. Headspace samples of interior (I0, I2, I4, I6) and surface (S0, S2, S4, S6) slabs of the Cheddar cheese, generated at 60°C.

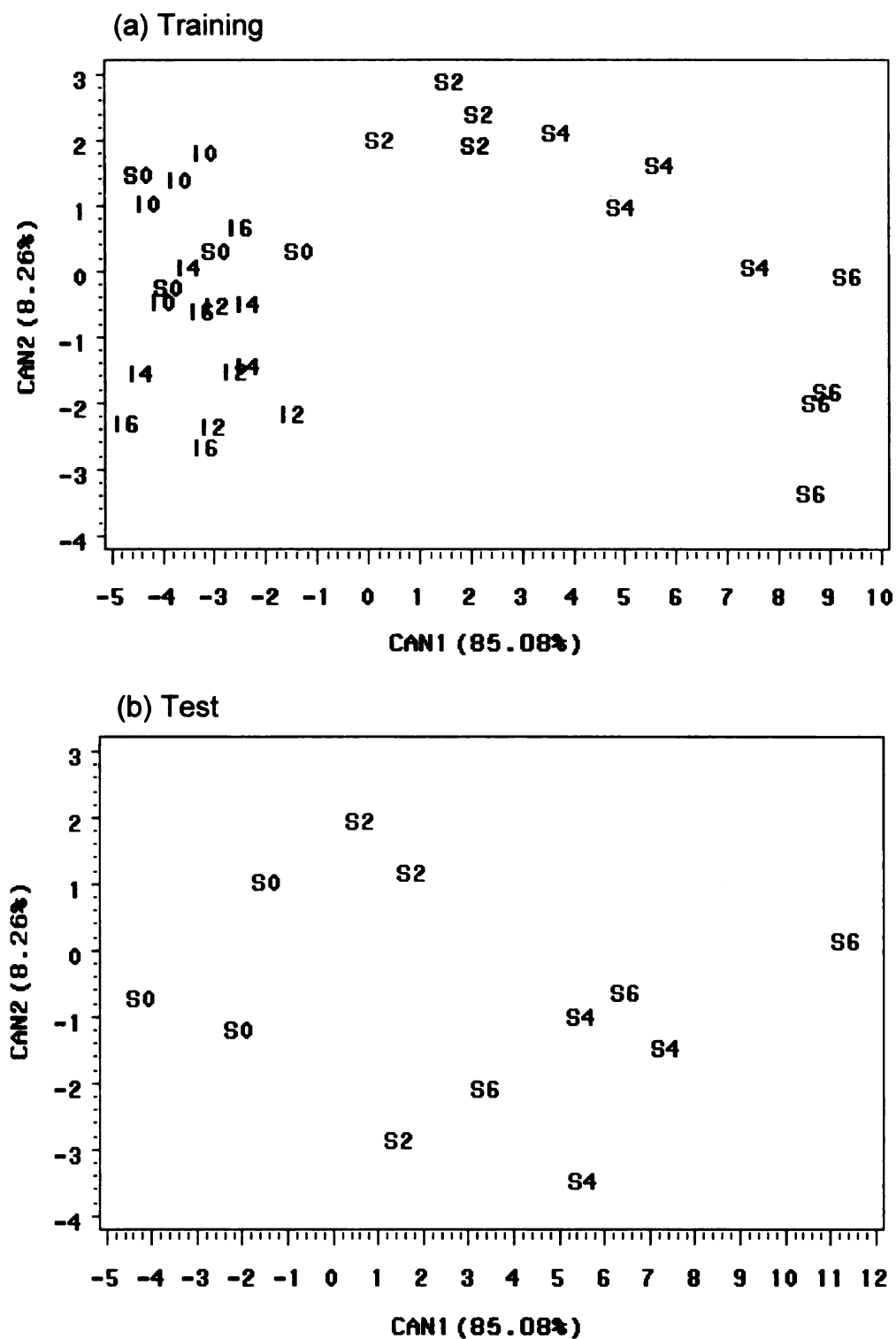


Figure 96 Canonical discriminant scatter plots of the (a) training (b) test data sets. Headspace samples of interior (I0, I2, I4, I6) and surface (S0, S2, S4, S6) slabs of the Cheddar cheese, generated at 90°C.

The electronic nose can analyze the sample headspace as a whole and is not concerned about “not covering all volatiles that are responsible for the light-induced flavor changes”, as the SPME-GC attempted to do. As expected, the sample S0 (top surface without light exposure) was close to all interior slab samples, which were not exposed to light. The grouping of light-oxidized cheese samples in both PCA and LDA (Figure 92b and Figure 96) was in agreement with the sensory score trend (Figure 83 and Figure 84).

Quantitative PLS and MLP models were used to investigate the correlations between the sensory scores and the sensor responses of the electronic nose to the 60°C and 90°C headspace samples of the light oxidized Cheddar cheese (Figure 97 to Figure 100). Considering the RMSE and predicted sensory score, 90°C headspace samples provided better fitted PLS and MLP models, and more precise prediction of sensory scores. The 90°C PLS model had a similar model RMSE but a better test set prediction, compared to the 90°C MLP model. The PLS approach was to find latent component(s) from the sensor responses that were also relevant for sensory scores, which can be well defined since higher volatile contents and sensor responses were expected from light-oxidized samples with lower sensory scores.

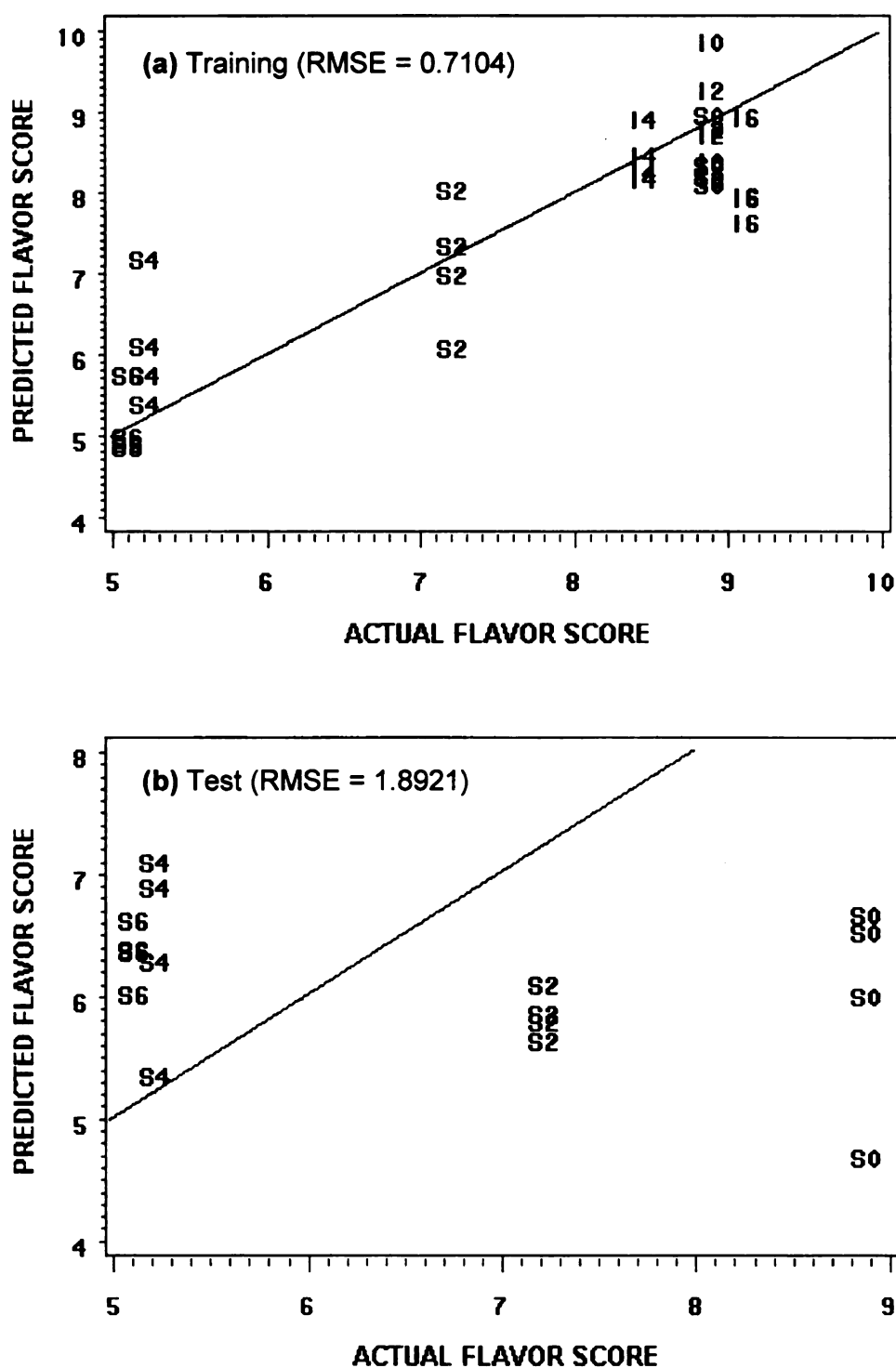


Figure 98 MLP predicted versus actual flavor scores of interior (I0, I2, I4, I6) and surface (S0, S2, S4, S6) slabs of the Cheddar cheese, based on electronic nose sensor responses for 60°C headspace. Models were applied to (a) training and (b) test data. The reference line indicates equal values of predicted and actual sensory scores.

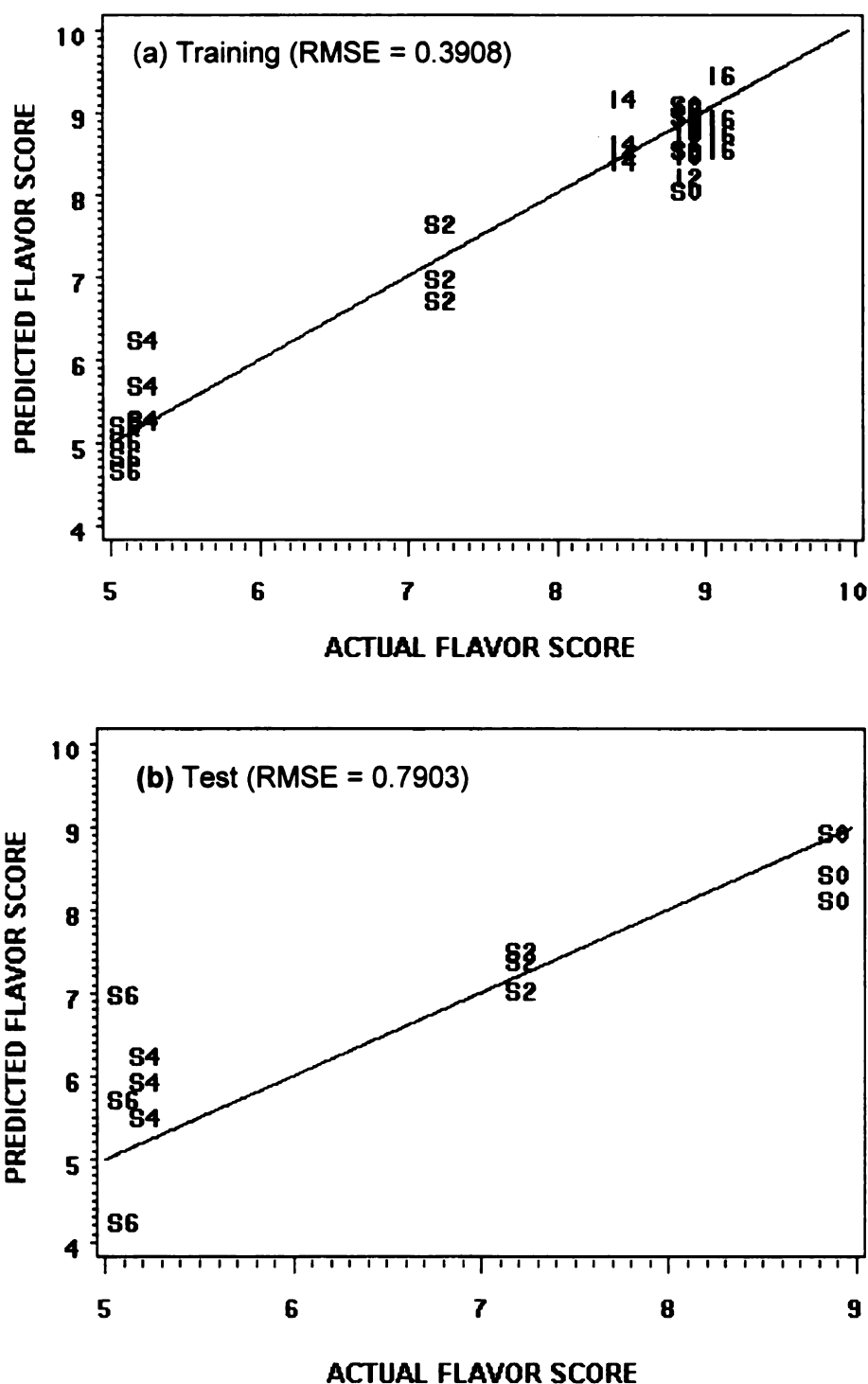


Figure 99 PLS predicted versus actual flavor scores of interior (I0, I2, I4, I6) and surface (S0, S2, S4, S6) slabs of the Cheddar cheese, based on electronic nose sensor responses for 90°C headspace. Models were applied to (a) training and (b) test data. The reference line indicates equal values of predicted and actual sensory scores.

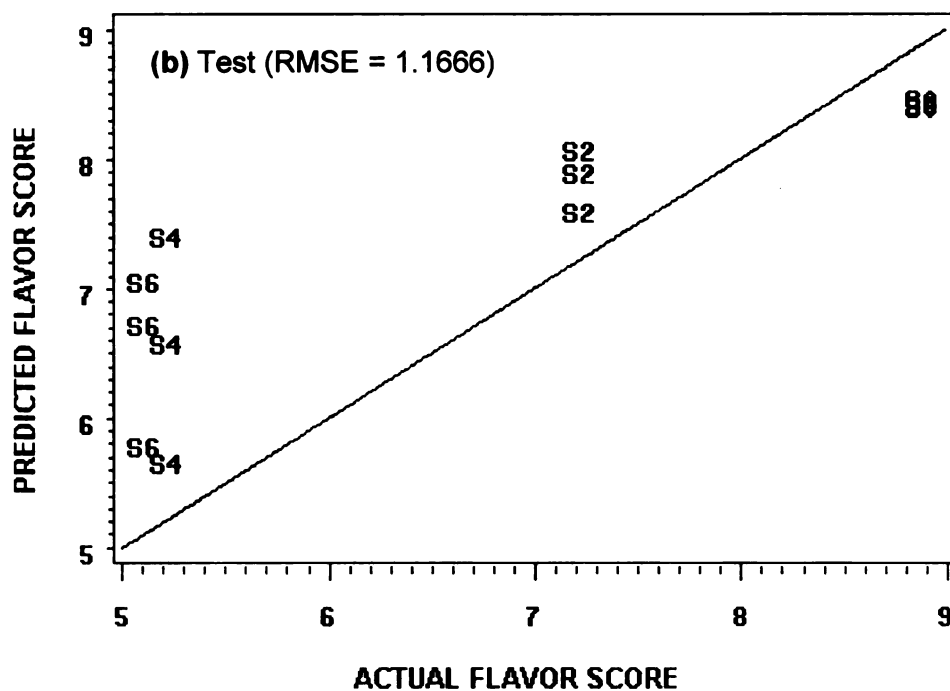
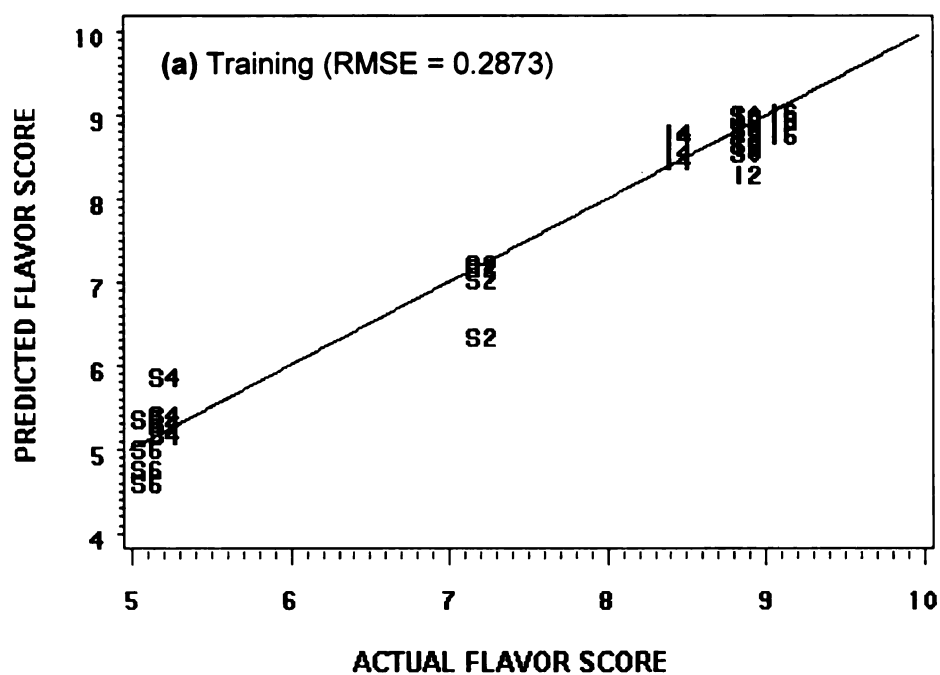


Figure 100 MLP predicted versus actual flavor scores of interior (I0, I2, I4, I6) and surface (S0, S2, S4, S6) slabs of the Cheddar cheese, based on electronic nose sensor responses for 90°C headspace. Models were applied to (a) training and (b) test data. The reference line indicates equal values of predicted and actual sensory scores.

Light-induced color and flavor quality changes were limited to the top surface of the vacuum-packaged Cheddar cheese, which was exposed to light (2000 lx). Discoloration and off-flavors were detected by an 8-member trained panel after exposure to light for 2 weeks, and the quality changes were more pronounced after 4 and 6 weeks. Color measurement indicated that a continuous decrease in yellowness contributed the most to the discoloration, along with a relatively small decrease in redness and an increase in lightness. No body and texture changes in light-oxidized Cheddar cheeses occurred. The electronic nose has the advantage of being able to analyze the sample headspace as a whole and is not concerned about “not covering all volatiles that are responsible for the light-induced flavor changes” which is what the SPME-GC technique tries to do. The discriminant models based on sensor responses for 90°C headspace samples had higher correct identification rates and better discrimination than at 60°C. The 90°C PLS model had a similar model RMSE but a better test set prediction, compared to the 90°C MLP model.

CHAPTER 5

CONCLUSIONS

Both consumer and trained panelists detected the light-oxidized off-flavor in reduced fat (2%) milk developed in glass bottles under 8 hours of light exposure (1000 lx) at 5°C. The CAR/PDMS fiber was selected to collect the headspace volatiles of light oxidized milk. Headspace pentanal and hexanal increased as the light exposure time increased. Using a 95°C headspace temperature for the electronic nose analysis provided better model discrimination than 45°C or 70°C, due to the higher volatile contents generated at the higher headspace temperatures. The first canonical discriminant was indicative of the extent of light-oxidation. Light-oxidized milk was poorly recognized as a function of light exposure time, but samples with a similar extent of light oxidation were close to each other in the discriminant models. By defining the harmful light exposure time as a milk deterioration threshold, the 95°C LDA model correctly recognized 97% of the milk samples exposed to light for 8 hours or longer. Quantitatively, the 95°C PLS model provided better prediction of the sensory scores than the 95°C MLP model.

The different packaging materials (237 ml glass, HDPE, HDPE-TiO₂, PET bottles, and PE-coated paper cartons) were clearly discriminated and identified using the electronic nose. However, no significant packaging off-flavors in water or 2% milk were perceived by consumer panels, except water stored in HDPE bottles had a very mild flavor difference ($p < 0.10$) from pure water. The water and

milk samples stored in the various packages were only partially differentiated in electronic nose analysis. HDPE was found to have less headspace volatiles than PET and PE-coated cartons when the packaging materials were analyzed directly, but the sensory tests indicated that the water and 2% milk in HDPE had more intense off-flavor than in PET and PE-coated cartons. The effect of packaging materials on light-induced oxidation in milk was closely related to their light barrier properties. PE-coated paper cartons reduced light-oxidation of 2% milk significantly (12 hours of light exposure, 1000 lx), while HDPE-TiO₂ gave only partial light protection. Compared to light-oxidized off-flavors, the packaging off-flavors were less intense and more difficult to detect. Packaging off-flavors in water and 2% milk were not clearly defined by either sensory evaluation or electronic nose analysis.

Light-induced quality changes (color and flavor) were limited to the top surface of the vacuum-packaged Cheddar cheese, which was the portion that was exposed to light (2000 lx). Discoloration and off-flavors were detected by the trained panel after exposure to light for 2 weeks. Color measurement showed a continuous decrease in yellowness contributed the most to the discoloration, along with a relatively small decrease in redness and increase in lightness. No body and texture changes in light-oxidized Cheddar cheeses were noticed. The electronic nose has the advantage of analyzing the sample headspace as a whole. The discriminant models of sensor responses using 90°C headspace samples had higher correct identification rates and better discrimination than at

60°C. The 90°C PLS model had a similar model RMSE, but was able to better predict the test set, compared to the 90°C MLP model.

The established discriminant and correlation models have shown the potential of the electronic nose to be used as a complementary approach to sensory evaluation to determine light-oxidized off-flavors in packaged milk and Cheddar cheese.

Recommendations for future work

1. A standardized method for evaluation of light-induced changes in different foods is needed.
2. Preconcentration techniques such as DH and SPME may be used for headspace sampling, to improve the differentiation of milk with different extent of light oxidation.
3. For low- or non- volatile off-flavored compounds in liquid or aqueous systems (e.g. certain packaging off-flavors), an electronic tongue consists of an array of liquid sensors can perform in a similar manner as an electronic nose to the volatiles. The technology has been commercialized and used in many applications such as analyzing beverages (e.g. wine [191], juices [192, 193], and milk [193]) and monitoring fermentation [194].
4. Numerous mathematical techniques have been proposed to compensate the sensor drifts and to reduce the instability of the discriminant models for quality control routine. Verification and improvement of these long term calibration techniques in food and packaging applications are needed.

APPENDICES

A.1. SAS and Matlab programs

A.1.1. Data import in SAS (SAS 8.0, SAS Institute, Cary, NC)

```
/*Input macro variables below:*/
%let dsn = mk9501;          /*training data set name*/
%let dsnv = mk9502;         /*test data set name*/
%let score = mkscore;       /*sensory scores of training set*/
%let scorev = mkscore;      /*sensory scores of test set*/

data &dsn;
infile "d:\enose\&dsn..txt" firstobs=2 expandtabs;
input obs id$ n samp$ LY_LG LY_G LY_AA LY_Gh LY_gCT1 LY_gCT T30_1 P10_1
P10_2 P40_1 T70_2 PA2;
if samp = 'CTR' then samp = '0'; if samp = '2LT' then samp = '2';
if samp = '4LT' then samp = '4'; if samp = '8LT' then samp = '8';
if samp = '12L' then samp = '12'; if samp = '24L' then samp = '24';
if samp = '36L' then samp = '36'; if samp = '48L' then samp = '48';
if samp = '48D' then samp = 'd';
run;

data &score;
infile "d:\enose\&score..txt" firstobs=2 expandtabs;
input smean smed logpen logdmds loghex; run;

data &dsn; merge &dsn &score; run;

data &dsnv;
infile "d:\enose\&dsnv..txt" firstobs=2 expandtabs;
input obs id$ n samp$ LY_LG LY_G LY_AA LY_Gh LY_gCT1 LY_gCT T30_1 P10_1
P10_2 P40_1 T70_2 PA2;
if samp = 'CTR' then samp = '0'; if samp = '2LT' then samp = '2';
if samp = '4LT' then samp = '4'; if samp = '8LT' then samp = '8';
if samp = '12L' then samp = '12'; if samp = '24L' then samp = '24';
if samp = '36L' then samp = '36'; if samp = '48L' then samp = '48';
if samp = '48D' then samp = 'd';
run;

data &scorev;
infile "d:\enose\&scorev..txt" firstobs=2 expandtabs;
input smean smed logpen logdmds loghex; run;

data &dsnv; merge &dsnv &scorev; run;
```

A.1.2. HCA and PCA using SAS

```
options ls=64 ps=45 nodate nonumber;
goptions reset=all;

/*Input macro variables below:*/
%let dsn = mk9501;          /*training data set name*/
%let sn   = 95oC;           /*sample name, in text*/

/*Hierarchical Clustering Analysis*/
/*Single linkage (nearest neighbor) as the algorithm for similarities.
*/

proc cluster data=&dsn noeigen method=single nonorm out=clout;
id id;
var LY_LG LY_G LY_AA LY_Gh LY_gCT1 LY_gCT T30_1 P10_1 P10_2 P40_1 T70_2
PA2;
run;

proc tree data=clout;
id id;
title2 "Hierarchical Clustering Analysis (&sn)";
run;

/*Principle component analysis: proc princomp*/
/*Compute principle components from covariance matrix.
  Proc factor was applied to generate scree plot.*/

proc princomp data=&dsn cov out=sout;
var LY_LG LY_G LY_AA LY_Gh LY_gCT1 LY_gCT T30_1 P10_1 P10_2 P40_1 T70_2
PA2;
run;

proc factor data=&dsn scree;
var LY_LG LY_G LY_AA LY_Gh LY_gCT1 LY_gCT T30_1 P10_1 P10_2 P40_1 T70_2
PA2;
run;

data labels;
set sout;
retain xsys '2' ysys '2';
y=prin2;
x=prin1;
text=samp;
keep xsys ysys x y text;

proc gplot data=sout;
plot prin2*prin1 /annotate=labels;
label prin1='PC1' prin2='PC2';
symbol v=none;
title2 "Principle Component Analysis (&sn)";
run;
```

```

data label2;
set sout;
retain xsys '2' ysys '2';
y=prin3;
x=prin2;
text=samp;
keep xsys ysys x y text;

proc gplot data=sout;
plot prin3*prin2 /annotate=label2;
label prin2='PC2' prin3='PC3';
symbol v=none;
title2 "Principle Component Analysis (&sn)";
run;

data label3;
set sout;
retain xsys '2' ysys '2' zsys '2';
z=prin3;
y=prin2;
x=prin1;
text=samp;
keep xsys ysys zsys x y z text;

proc g3d data = sout;
scatter prin2*prin1 = prin3 /grid shape = 'point' annotate=label3;
label prin1='PC1' prin2='PC2' prin3 = 'PC3';
title2 "Principle Component Analysis 3D_1 (&sn)";
run;

data label4;
set sout;
retain xsys '2' ysys '2' zsys '2';
z=prin3;
y=prin1;
x=prin2;
text=samp;
keep xsys ysys zsys x y z text;

proc g3d data = sout;
scatter prin1*prin2 = prin3 /grid shape = 'point' annotate=label4;
label prin1='PC1' prin2='PC2' prin3 = 'PC3';
title2 "Principle Component Analysis 3D_2 (&sn)";
run;

```

A.1.3. LDA/QDA and k-NN using SAS

```
goptions reset=all;

/*Input macro variables below*/
%let dsn = mk4501;           /*training data set name*/
%let dsnv = mk4502;          /*validation data set name*/
%let sn = 45oC;              /*sample name, in text*/

/*Testing the Equality of Normal Population Parameters*/
proc discrim data=&dsn method=normal pool=test wcov pcov bcov manova;
class samp;
var LY_LG LY_G LY_AA LY_Gh LY_gCT1 LY_gCT T30_1 P10_1 P10_2 P40_1 T70_2
PA2;
title2 "Testing the Equality of Normal Population Parameters (&sn)";
run;

/*LDA: normal populations with same cov*/

proc discrim data=&dsn out=lout outstat=lstat
              method=normal list pool=yes pcov manova
              crosslist outcross = lcross
              testdata=&dsn testlist testout = ltest;

class samp;
var LY_LG LY_G LY_AA LY_Gh LY_gCT1 LY_gCT T30_1 P10_1 P10_2 P40_1 T70_2
PA2;
title2 "Linear Discriminant Analysis (&sn)";
run;

/*QDA: normal populations with different cov*/

proc discrim data=&dsn out=qout outstat=qstat
              method=normal list pool=no wcov
              crosslist outcross = qcross
              testdata=&dsn testlist testout = qtest;

class samp;
var LY_LG LY_G LY_AA LY_Gh LY_gCT1 LY_gCT T30_1 P10_1 P10_2 P40_1 T70_2
PA2;
title2 "Quadratic Discriminant Analysis (&sn)";
run;

/*k-NN; k=1~4*/

/*k=1*/
proc discrim data=&dsn out=klout outstat=klstat
              k=1 crosslist outcross = klcross
              testdata=&dsn testlist testout = kltest;

class samp;
var LY_LG LY_G LY_AA LY_Gh LY_gCT1 LY_gCT T30_1 P10_1 P10_2 P40_1 T70_2
PA2;
title2 'Nonparametric Discriminant Analysis: kNN, k = 1';
run;

/*k=2*/
proc discrim data=&dsn out=k2out outstat=k2stat
              k=2 crosslist outcross = k2cross
```

```

                                testdata=&dsnv testlist testout = k2test;
class samp;
var LY_LG LY_G LY_AA LY_Gh LY_gCT1 LY_gCT T30_1 P10_1 P10_2 P40_1 T70_2
PA2;
title2 'Nonparametric Discriminant Analysis: kNN, k = 2';
run;

/*k=3*/
proc discrim data=&dsn out=k3out outstat=k3stat
                                k=3 crosslist outcross = k3cross
                                testdata=&dsnv testlist testout = k3test;

class samp;
var LY_LG LY_G LY_AA LY_Gh LY_gCT1 LY_gCT T30_1 P10_1 P10_2 P40_1 T70_2
PA2;
title2 'Nonparametric Discriminant Analysis: kNN, k = 3';
run;

/*k=4*/
proc discrim data=&dsn out=k4out outstat=k4stat
                                k=4 crosslist outcross = k4cross
                                testdata=&dsnv testlist testout = k4test;

class samp;
var LY_LG LY_G LY_AA LY_Gh LY_gCT1 LY_gCT T30_1 P10_1 P10_2 P40_1 T70_2
PA2;
title2 'Nonparametric Discriminant Analysis: kNN, k = 4';
run;

/*Canonical Discriminant Analysis*/

proc discrim data=&dsn out=canout outstat=canstat
                                canonical crosslist outcross = cancross
                                testdata=&dsnv testlist testout = cantest;

class samp;
var LY_LG LY_G LY_AA LY_Gh LY_gCT1 LY_gCT T30_1 P10_1 P10_2 P40_1 T70_2
PA2;
title2 "Canonical Discriminant Analysis (&sn)";
run;

/*Plot Canonical Discriminant Model: 2D and 3D*/
/*2D plot-model*/
data labels;
set cancross;
retain xsys '2' ysys '2';
y=can2;
x=can1;
text=samp;
keep xsys ysys x y text;

proc gplot data=cancross;
plot can2*can1 /annotate=labels;
label can1='CAN1' can2='CAN2';
symbol v=none;
title2 "Canonical Discriminant Analysis: Model (&sn)";
run;

/*3D plot-model*/
data label3; set cancross;

```



```

retain xsys '2' ysys '2' zsys '2';
z=can3; y=can2; x=can1;
text=samp;
keep xsys ysys zsys x y z text;

proc g3d data = cancross;
scatter can2*can1 = can3 /grid shape = 'point' annotate=label3;
label can1='CAN1' can2='CAN2' can3 = 'CAN3';
title2 "Canonical Discriminant Analysis: Model 3D (&sn)";
run;

/*Plot Canonical Discriminant Test Data; labeled with original
grouping*/
/*2D plot-test*/
data labels;
set cantest;
retain xsys '2' ysys '2';
y=can2;
x=can1;
text=samp;
keep xsys ysys x y text;

proc gplot data=cantest;
plot can2*can1 /annotate=labels;
label can1='CAN1' can2='CAN2';
symbol v=none;
title2 "Canonical Discriminant Analysis: Test (&sn)";
run;

/*3D plot test*/
data label3; set cantest;
retain xsys '2' ysys '2' zsys '2';
z=can3; y=can2; x=can1;
text=samp;
keep xsys ysys zsys x y z text;

proc g3d data = cantest;
scatter can2*can1 = can3 /grid shape = 'point' annotate=label3;
label can1='CAN1' can2='CAN2' can3 = 'CAN3';
title2 "Canonical Discriminant Analysis: Test 3D (&sn)";
run;

/*Plot Canonical Discriminant Test Data; labeled with identified
grouping*/
/*2D plot-testid*/
data labels;
set cantest;
retain xsys '2' ysys '2';
y=can2;
x=can1;
text=_into_;
keep xsys ysys x y text;

proc gplot data=cantest;
plot can2*can1 /annotate=labels;
label can1='CAN1' can2='CAN2';
symbol v=none;

```

```

title2 "Canonical Discriminant Analysis: Test_id (&sn)";
run;

/*3D plot testid*/
data label3; set cantest;
retain xsys '2' ysys '2' zsys '2';
z=can3; y=can2; x=can1;
text=_into_;
keep xsys ysys zsys x y z text;

proc g3d data = cantest;
scatter can2*can1 = can3 /grid shape = 'point' annotate=label3;
label can1='CAN1' can2='CAN2' can3 = 'CAN3';
title2 "Canonical Discriminant Analysis: Test_id 3D (&sn)";
run;

/*Export classification results of resubstitution, cross-validation and
test data*/
data classes;
set lout(rename=_into_=lout); set lcross(rename=_into_=lcross); set
ltest(rename=_into_=ltest);
set qout(rename=_into_=qout); set qcross(rename=_into_=qcross); set
qtest(rename=_into_=qtest);
set klout(rename=_into_=klout); set klcross(rename=_into_=klcross); set
kltest(rename=_into_=kltest);
set k2out(rename=_into_=k2out); set k2cross(rename=_into_=k2cross); set
k2test(rename=_into_=k2test);
set k3out(rename=_into_=k3out); set k3cross(rename=_into_=k3cross); set
k3test(rename=_into_=k3test);
set k4out(rename=_into_=k4out); set k4cross(rename=_into_=k4cross); set
k4test(rename=_into_=k4test);
set canout(rename=_into_=canout); set cancross(rename=_into_=cancross);
set cantest(rename=_into_=cantest);
keep samp lout lcross ltest qout qcross qtest klout klcross kltest
k2out k2cross k2test k3out k3cross k3test
      k4out k4cross k4test canout cancross cantest;
run;

```

A.1.4. PLS using SAS and MLP using Matlab

A.1.4.1. Partial Least Square Analysis (PLS)

```
options ls=64 ps=45 nodate nonumber;
options reset=all;
%INCLUDE 'd:\enose\plsplot.sas';

/* plsplot.sas is available at http://www.sas.com */

/*****
/*Partial Least Square (PLS) sensory scores vs.sensor response*/

/*Input macro variables below:*/
%let dsn = mk9501; /*training data set name*/
%let dsnv = mk9502; /*validation data set name*/
%let sn = 95oC; /*sample name, in text*/
%let y_name = smean; /*Y variable(s) */
%let x_name = enose; /*X variables (s) */

%global xvars yvars predname resname xscrname yscrname num_x num_y lv;
%let xvars=LY_LG LY_G LY_AA LY_Gh LY_gCT1 LY_gCT T30_1 P10_1 P10_2
P40_1 T70_2 PA2;
%let yvars=smean;
%let ypred=yhat1;
%let yres=yres1;
%let predname=yhat;
%let resname=res;
%let xscrname=xscr;
%let yscrname=yscr;
%let num_y=1;
%let num_x=12;

title2 "PLS (&sn) Y: &y_name; X's: &x_name";
proc pls data=&dsn method=pls(algorithm=svd) outmodel=est1
      cv=one censcale;
model &yvars = &xvars;
output out=outpls p=&ypred yresidual=&yres
xresidual=xres1-xres12 xscore=xscr yscore=yscr
stdy=stdy stdx=stdx h=h press=press t2=t2
xqres=xqres yqres=yqres;
run;

/*Stop here and check the output*/
/*****
/* According CVTEST result, decide lv = number of latent components */
%let lv=4; *** Number of PLS components in model ***;
/*****/

/*Plot predicted vs. actual scores*/
data labels; set outpls;
retain xsys '2' ysys '2'; y=&ypred; x=&yvars;
text=samp;
keep xsys ysys x y text;
proc gplot data=outpls;
```

```

plot &ypred*&yvars /annotate=labels;
label &ypred='Predicted' &yvars='Actual ADSA Flavoring Score';
symbol v=none;
run;

/*Plot predicted vs. actual scores with 45o ref line */
data anno;
function='move'; xsys='1'; ysys='1'; x=0; y=0; output;
function='draw'; xsys='1'; ysys='1'; color='red'; x=100; y=100; output;
run;

proc gplot data=outpls;
plot &ypred*&yvars / anno=anno haxis=axis1 vaxis=axis2;
label &ypred='Predicted' &yvars='Actual ADSA Flavoring Score';
symbol1 i=none v=dot c=blue;
run;

%plot_scr(outpls);
%plotxscr(outpls);

%res_plot(outpls);
%nor_plot(outpls);

%get_bpls(est1,dsout=bpls);
%get_vip(est1,dsvip=vip_data);
data eval;
merge bpls vip_data;
run;
proc print data=eval;
run;

/*****
/*PLS: Analyzing test data using the PLS model above*/
options reset=all;
title2 "PLS (&sn) Y: &y_name; X's: &x_name";

/*step 1: refit the model with missing values on validation set*/
data dsnj; set &dsn &dsnv(drop=&yvars); run;
proc pls data=dsnj method=pls(algorithm=svd) outmodel=est1 cv=one;
model &yvars = &xvars;
output out=outpls2 p=&ypred yresidual=&yres
xresidual=xres1-xresl2 xscore=xscr yscore=yscr
stdy=stdy stdx=stdx h=h press=press t2=t2
xqres=xqres yqres=yqres;
run;

/*step 2: put the predicted values and actual observations in the same
data set. */
data outplsv; set outpls2; if obs > 36; keep &ypred samp n; run;
data dsnv; set &dsnv(keep=&yvars samp n); run;
data predict; merge dsnv outplsv; run;

/*Plot predicted vs. actual scores*/
data labels; set predict;
retain xsys '2' ysys '2'; y=&ypred; x=&yvars;
text=samp;
keep xsys ysys x y text;

```

```

proc gplot data=predict;
plot &ypred*&yvars /annotate=labels;
label &ypred='Predicted' &yvars='Actual ADSA Flavoring Score';
symbol v=none;
run;

/*step 3: calculate the residuals at the points in the test set. */
data predictr; set predict;
yres1=&yvars-&ypred;
run;

%res_plot(predictr);

/*****
/*Export the predicted values and residuals, for calculating root-mean-
square (rme) of the models*/

data &dsn.rme;
set outpls (rename=yres1=res01); set predictr (rename=yres1=res02);
keep res01 res02;
run;

PROC EXPORT DATA= WORK.&dsn.rme
            OUTFILE= "D:\tmp\&dsn.rme.xls"
            DBMS=EXCEL2000 REPLACE;

RUN;

```

A.1.4.2. Multilayer Perceptrons (MLP)

The Neural Network Toolbox 4.0 of Matlab 6.1 (The MathWorks Inc., Natick, MA) was launched (Figure 101) by typing in

```
>> nntool
```

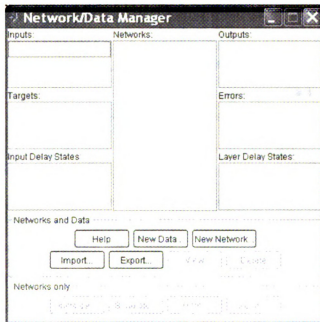


Figure 101 Start-up view of Neural Network Toolbox 4.0 embedded in Matlab 6.1.

A feed-forward backpropagation network was constructed, with a tan-sigmoid function in the hidden layer, and a linear function in output layer. An independent data set was applied for validation (early stopping to avoid over-fitting) as well as for test (estimating a network's ability to generalize).

A.2 Designs and Forms of Sensory Tests

A.2.1. Triangle tests

A.2.1.1. Triangle test form (an example)

Triangle Test			
Name _____ Date <u>9/26/2002</u>			
Sample: 2% milk # 1			
Instructions Four independent sets (D, A, B, C) of samples will be presented sequentially. Each set has 3 samples; 2 are identical; determine which one is the odd sample. If no difference is apparent, you must guess. Smell and taste samples from left to right. You may spit the sample out after judging (foam cup is provided). Rinse your mouth by water between samples if necessary. Which is the odd sample? (Check the box)			
Set A	<input type="checkbox"/> 425	<input type="checkbox"/> 565	<input type="checkbox"/> 716
Set B	<input type="checkbox"/> 513	<input type="checkbox"/> 422	<input type="checkbox"/> 641
Set C	<input type="checkbox"/> 356	<input type="checkbox"/> 562	<input type="checkbox"/> 814
Set D	<input type="checkbox"/> 610	<input type="checkbox"/> 701	<input type="checkbox"/> 375

COMMENTS:

A.2.1.2. Design of triangle tests on light-oxidized 2% milk

Set	Sample	Treatment	Coding
A	CONTROL 24 HR	without light exposure	102 763 685
		24 hours of light exposure	893 582 967
B	CONTROL 12 HR	without light exposure	204 665 048
		12 hours of light exposure	912 462 460
C	CONTROL 8 HR	without light exposure	506 615 951
		8 hours of light exposure	884 046 169
D	CONTROL 4 HR	without light exposure	473 133 371
		4 hours of light exposure	683 464 581

Panelist	Serve Order	A			B			C			D		
1	ABDC	893	763	967	912	665	048	884	615	951	473	464	581
2	ACDB	102	582	685	912	462	048	884	046	951	473	133	581
3	ADBC	893	582	685	204	462	048	884	615	169	473	464	371
4	ABCD	893	582	685	912	665	460	506	615	169	683	133	371
5	BDCA	893	582	685	912	462	048	506	615	169	473	133	581
6	DBCA	102	763	967	204	462	460	884	046	951	683	133	581
7	ADCB	893	763	685	204	665	460	506	046	169	683	133	371
8	DBAC	893	763	685	204	462	460	506	046	951	683	133	581
9	BDAC	102	582	685	912	462	048	884	615	169	683	464	371
10	CABD	893	763	685	912	665	460	506	046	951	683	133	371
11	BCDA	102	582	967	912	665	048	506	046	169	683	464	371
12	DCAB	893	763	967	204	665	460	506	046	169	683	464	371
13	CDAB	893	763	967	912	665	460	884	615	169	473	464	581
14	BCAD	893	763	967	204	462	048	506	046	951	473	464	371
15	BADC	102	582	685	204	462	048	884	046	951	473	464	581
16	DACB	102	763	967	912	665	048	884	615	951	473	133	581
17	CDBA	102	582	967	912	665	048	884	615	169	683	464	371
18	CADB	102	763	967	204	462	460	506	615	169	683	133	581
19	CBAD	893	763	685	204	665	460	506	046	951	473	464	371
20	DCBA	102	582	967	204	462	048	884	615	951	473	464	581
21	DABC	102	582	685	912	665	460	506	046	169	473	464	371
22	BACD	102	763	967	204	462	460	506	615	169	473	133	581
23	CBDA	893	582	685	912	462	048	884	615	951	683	133	371
24	ACBD	102	582	967	204	665	460	884	046	951	683	133	581

A.2.1.3. Design of triangle tests on water stored in various packaging materials

Set	Sample	Treatment	Coding
A	CONTROL GLASS	4L glass jugs	472 271 875
		237 ml glass bottles	979 252 737
B	CONTROL HDPE	4L glass jugs	681 831 709
		237 ml HDPE bottles	379 502 428
C	CONTROL PET	4L glass jugs	150 378 853
		237 ml PET bottles	697 860 593
D	CONTROL CARTON	4L glass jugs	838 370 546
		237 ml paper cartons	568 702 444

Panelist	Serve Order	A			B			C			D		
1	CBAD	979	271	875	681	502	709	150	860	593	568	370	546
2	DACB	472	271	737	681	831	428	697	378	853	838	702	444
3	DBAC	979	271	875	379	502	709	697	860	853	568	370	444
4	BADC	472	252	875	379	502	709	150	860	593	568	702	546
5	ADCB	472	271	737	379	831	428	150	860	593	838	702	444
6	CDAB	979	271	737	379	831	428	697	378	593	838	370	444
7	ACBD	472	252	737	681	502	428	150	378	593	568	370	546
8	ABDC	979	271	875	379	831	428	150	860	853	838	702	546
9	CDBA	472	252	737	379	831	709	150	378	593	568	370	444
10	BDCA	979	252	875	379	831	709	150	860	853	838	370	444
11	DCBA	472	252	737	681	502	709	150	860	853	838	702	546
12	BDAC	979	271	875	681	831	428	697	378	593	568	370	546
13	DCAB	979	271	737	681	502	428	697	378	853	838	370	444
14	DABC	472	252	875	681	502	428	150	860	853	838	702	444
15	BACD	472	271	737	681	831	428	150	378	593	568	702	546
16	ABCD	979	252	875	379	502	709	697	860	853	838	702	546
17	ADBC	472	252	875	681	502	709	150	378	593	568	370	444
18	CABD	472	252	875	379	831	709	697	378	593	568	702	546
19	BCAD	979	271	737	681	831	428	697	378	593	568	702	546
20	DBCA	979	252	875	379	831	709	697	860	853	838	702	546
21	CBDA	979	252	875	681	502	428	697	860	853	838	702	444
22	ACDB	979	271	737	379	502	709	150	860	593	838	370	444
23	CADB	472	271	737	681	502	709	697	378	853	568	370	546
24	BCDA	472	252	737	379	831	428	697	378	853	568	370	444

A.2.1.4. Design of triangle tests on 2% milk stored in various packaging materials

Set	Sample	Treatment	Coding
A	CONTROL GLASS	4L glass jugs 237 ml glass bottles	371 694 716 425 565 511
B	CONTROL HDPE	4L glass jugs 237 ml HDPE bottles	873 732 641 513 422 172
C	CONTROL PET	4L glass jugs 237 ml PET bottles	356 434 116 498 562 814
D	CONTROL CARTON	4L glass jugs 237 ml paper cartons	212 701 924 610 493 375

Panelist	Serve Order	A	B	C	D
1	DABC	425 565 716	513 422 641	356 562 814	610 701 375
2	DCAB	371 565 511	873 422 641	498 434 116	610 493 924
3	BDAC	425 694 716	873 422 172	356 562 814	212 701 375
4	BDCA	425 694 716	513 732 641	356 434 814	610 701 375
5	ADCB	425 694 511	513 732 172	498 434 116	610 701 375
6	CBAD	371 565 716	873 422 641	498 562 116	212 493 375
7	CDAB	371 565 511	513 732 641	498 562 116	212 701 375
8	DBAC	425 694 511	873 732 172	498 562 116	212 701 375
9	BCDA	371 694 511	513 732 641	356 562 116	610 493 924
10	BACD	371 694 511	873 732 172	498 434 814	212 701 375
11	CDBA	371 565 511	873 422 172	356 562 814	212 493 924
12	DCBA	425 694 716	513 422 641	498 434 814	212 493 375
13	CBDA	371 565 716	873 732 172	498 434 814	610 701 375
14	ACBD	425 565 716	513 732 172	356 562 116	212 493 924
15	ACDB	371 694 511	873 422 641	356 434 814	610 701 924
16	ADBC	371 565 716	513 422 641	356 562 116	212 493 375
17	ABCD	425 694 716	513 732 172	498 434 814	610 701 924
18	DACB	425 694 511	513 732 172	356 562 814	610 493 924
19	CADB	371 694 511	513 422 641	498 434 116	212 493 924
20	BADC	425 565 716	513 732 641	356 562 116	610 701 924
21	DBCA	425 565 716	873 732 172	498 562 116	212 493 924
22	ABDC	425 694 511	873 422 172	356 434 814	610 701 924
23	CABD	371 565 511	873 422 172	498 434 116	610 493 924
24	BCAD	371 565 716	873 422 641	356 434 814	212 493 375

A.2.1.5. Design of triangle tests on 2% milk stored in various packaging materials and exposed to 12 hours of fluorescent light

Set	Sample	Treatment	Coding
A	CONTROL	237 ml glass bottles, without light exposure	950 606 891
	HDPE	237 ml HDPE bottles, 12 hours of light exposure	231 485 762
B	CONTROL	237 ml glass bottles, without light exposure	921 176 635
	HDPE-TiO ₂	237 ml HDPE-TiO ₂ bottles, 12 hours of light exposure	738 405 916
C	CONTROL	237 ml glass bottles, without light exposure	681 831 709
	PET	237 ml PET bottles , 12 hours of light exposure	379 502 428
D	CONTROL	237 ml glass bottles, without light exposure	304 193 202
	CARTON	237 ml paper cartons, 12 hours of light exposure	189 682 541

Panelist	Serve Order	A			B			C			D		
1	CBDA	231	606	891	738	176	635	681	831	428	189	193	202
2	DBCA	950	606	762	738	176	635	681	831	428	189	193	202
3	CDBA	231	606	891	921	405	635	681	502	428	304	682	541
4	DCBA	950	485	891	921	405	916	379	831	709	304	682	202
5	ACDB	950	485	762	921	405	916	379	502	709	304	682	541
6	ADBC	231	606	762	738	176	916	681	502	709	189	193	202
7	BCDA	231	606	891	738	405	635	681	831	428	189	682	202
8	BADC	231	485	891	921	176	916	379	502	709	304	682	202
9	DCAB	950	485	891	921	176	916	379	502	709	189	682	202
10	ABDC	231	606	762	921	405	635	379	831	428	189	682	202
11	CADB	950	485	762	921	405	635	379	831	428	189	193	541
12	BDCA	231	606	762	738	176	635	681	502	428	189	193	541
13	DBAC	231	485	891	738	176	635	379	831	709	304	682	541
14	CABD	231	606	891	738	176	916	379	831	428	304	193	541
15	ADCB	950	606	762	738	176	916	681	502	709	304	682	202
16	DABC	950	485	762	921	176	916	379	502	709	189	193	541
17	BDAC	950	485	762	921	405	916	681	502	428	304	682	202
18	CDAB	231	485	891	738	405	635	379	831	709	304	682	541
19	CBDA	950	606	762	921	405	916	681	502	709	304	193	541
20	DBCA	950	485	891	738	176	916	681	502	709	189	193	541
21	CDBA	231	606	762	738	405	635	379	831	428	304	193	541
22	DCBA	950	485	891	921	176	916	681	502	428	189	193	202
23	ACDB	231	485	891	738	405	635	379	831	709	304	193	541
24	ADBC	950	606	762	921	405	635	681	831	428	189	682	202

A.2.2. Milk scoring card based on ADSA guidelines

SCORE SHEET FOR MILK (SET A)								
NAME: _____		GENDER: <input type="checkbox"/> F <input type="checkbox"/> M		AGE: _____		DATE: _____		
DIRECTIONS:		Rate milk samples (from left to right) for the criticisms.					# 1	
		Specify the intensity of the off-flavors (S: Slight, D: Definite, P: Pronounced)						
		For example, a sample with slight cooked flavor is rated at "cooked" column as ● <u>S</u>						
SAMPLE	821	444	615	791	921	738	176	405
FLAVOR (1-10)	_____	_____	_____	_____	_____	_____	_____	_____
ACID	<input type="radio"/> _____	<input type="radio"/> _____	<input type="radio"/> _____	<input type="radio"/> _____	<input type="radio"/> _____	<input type="radio"/> _____	<input type="radio"/> _____	<input type="radio"/> _____
BITTER	<input type="radio"/> _____	<input type="radio"/> _____	<input type="radio"/> _____	<input type="radio"/> _____	<input type="radio"/> _____	<input type="radio"/> _____	<input type="radio"/> _____	<input type="radio"/> _____
COOKED	<input type="radio"/> _____	<input type="radio"/> _____	<input type="radio"/> _____	<input type="radio"/> _____	<input type="radio"/> _____	<input type="radio"/> _____	<input type="radio"/> _____	<input type="radio"/> _____
FEED	<input type="radio"/> _____	<input type="radio"/> _____	<input type="radio"/> _____	<input type="radio"/> _____	<input type="radio"/> _____	<input type="radio"/> _____	<input type="radio"/> _____	<input type="radio"/> _____
FERMENTED/FRUITY	<input type="radio"/> _____	<input type="radio"/> _____	<input type="radio"/> _____	<input type="radio"/> _____	<input type="radio"/> _____	<input type="radio"/> _____	<input type="radio"/> _____	<input type="radio"/> _____
FLAT	<input type="radio"/> _____	<input type="radio"/> _____	<input type="radio"/> _____	<input type="radio"/> _____	<input type="radio"/> _____	<input type="radio"/> _____	<input type="radio"/> _____	<input type="radio"/> _____
FOREIGN	<input type="radio"/> _____	<input type="radio"/> _____	<input type="radio"/> _____	<input type="radio"/> _____	<input type="radio"/> _____	<input type="radio"/> _____	<input type="radio"/> _____	<input type="radio"/> _____
GARLIC/ONION	<input type="radio"/> _____	<input type="radio"/> _____	<input type="radio"/> _____	<input type="radio"/> _____	<input type="radio"/> _____	<input type="radio"/> _____	<input type="radio"/> _____	<input type="radio"/> _____
LACKS FRESHNESS	<input type="radio"/> _____	<input type="radio"/> _____	<input type="radio"/> _____	<input type="radio"/> _____	<input type="radio"/> _____	<input type="radio"/> _____	<input type="radio"/> _____	<input type="radio"/> _____
MALTY	<input type="radio"/> _____	<input type="radio"/> _____	<input type="radio"/> _____	<input type="radio"/> _____	<input type="radio"/> _____	<input type="radio"/> _____	<input type="radio"/> _____	<input type="radio"/> _____
OXIDIZED-LIGHT	<input type="radio"/> _____	<input type="radio"/> _____	<input type="radio"/> _____	<input type="radio"/> _____	<input type="radio"/> _____	<input type="radio"/> _____	<input type="radio"/> _____	<input type="radio"/> _____
OXIDIZED-METAL	<input type="radio"/> _____	<input type="radio"/> _____	<input type="radio"/> _____	<input type="radio"/> _____	<input type="radio"/> _____	<input type="radio"/> _____	<input type="radio"/> _____	<input type="radio"/> _____
RANCID	<input type="radio"/> _____	<input type="radio"/> _____	<input type="radio"/> _____	<input type="radio"/> _____	<input type="radio"/> _____	<input type="radio"/> _____	<input type="radio"/> _____	<input type="radio"/> _____
SALTY	<input type="radio"/> _____	<input type="radio"/> _____	<input type="radio"/> _____	<input type="radio"/> _____	<input type="radio"/> _____	<input type="radio"/> _____	<input type="radio"/> _____	<input type="radio"/> _____
UNCLEAN	<input type="radio"/> _____	<input type="radio"/> _____	<input type="radio"/> _____	<input type="radio"/> _____	<input type="radio"/> _____	<input type="radio"/> _____	<input type="radio"/> _____	<input type="radio"/> _____
COMMENT:								

A.2.3. Score cards for difference-from-control and ADSA rating of light-oxidized Cheddar cheese

SCORE SHEET FOR CHEDDAR CHEESE								
NAME: _____					DATE: _____			
GENDER: <input type="checkbox"/> F <input type="checkbox"/> M AGE: _____					(# 1)			
DIRECTIONS: Rate cheese samples (coded in 3-digit numbers) and compare with the control. Specify the intensity of the criticisms (S: Slight, D: Definite, P: Pronounced).								
1. COLOR DIFFERENCE FROM CONTROL								
SAMPLE	405	391	738	821	544	921	615	176
NO DIFFERENCE	<input type="radio"/>	<input type="radio"/>	<input type="radio"/>	<input type="radio"/>	<input type="radio"/>	<input type="radio"/>	<input type="radio"/>	<input type="radio"/>
VERY SLIGHT DIFFERENCE	<input type="radio"/>	<input type="radio"/>	<input type="radio"/>	<input type="radio"/>	<input type="radio"/>	<input type="radio"/>	<input type="radio"/>	<input type="radio"/>
SLIGHT DIFFERENCE	<input type="radio"/>	<input type="radio"/>	<input type="radio"/>	<input type="radio"/>	<input type="radio"/>	<input type="radio"/>	<input type="radio"/>	<input type="radio"/>
MODERATE DIFFERENCE	<input type="radio"/>	<input type="radio"/>	<input type="radio"/>	<input type="radio"/>	<input type="radio"/>	<input type="radio"/>	<input type="radio"/>	<input type="radio"/>
LARGE DIFFERENCE	<input type="radio"/>	<input type="radio"/>	<input type="radio"/>	<input type="radio"/>	<input type="radio"/>	<input type="radio"/>	<input type="radio"/>	<input type="radio"/>
EXTREME DIFFERENCE	<input type="radio"/>	<input type="radio"/>	<input type="radio"/>	<input type="radio"/>	<input type="radio"/>	<input type="radio"/>	<input type="radio"/>	<input type="radio"/>
2. BODY AND TEXTURE: (1-5)- please neglect "gassy" and "open" criticisms								
SAMPLE	405	391	738	821	544	921	615	176
BODY AND TEXTURE (1-5)	_____	_____	_____	_____	_____	_____	_____	_____
CORKY	<input type="radio"/> _____	<input type="radio"/> _____	<input type="radio"/> _____	<input type="radio"/> _____	<input type="radio"/> _____	<input type="radio"/> _____	<input type="radio"/> _____	<input type="radio"/> _____
CRUMBLY	<input type="radio"/> _____	<input type="radio"/> _____	<input type="radio"/> _____	<input type="radio"/> _____	<input type="radio"/> _____	<input type="radio"/> _____	<input type="radio"/> _____	<input type="radio"/> _____
GASSY	<input type="radio"/> _____	<input type="radio"/> _____	<input type="radio"/> _____	<input type="radio"/> _____	<input type="radio"/> _____	<input type="radio"/> _____	<input type="radio"/> _____	<input type="radio"/> _____
MEALY	<input type="radio"/> _____	<input type="radio"/> _____	<input type="radio"/> _____	<input type="radio"/> _____	<input type="radio"/> _____	<input type="radio"/> _____	<input type="radio"/> _____	<input type="radio"/> _____
OPEN	<input type="radio"/> _____	<input type="radio"/> _____	<input type="radio"/> _____	<input type="radio"/> _____	<input type="radio"/> _____	<input type="radio"/> _____	<input type="radio"/> _____	<input type="radio"/> _____
PASTY	<input type="radio"/> _____	<input type="radio"/> _____	<input type="radio"/> _____	<input type="radio"/> _____	<input type="radio"/> _____	<input type="radio"/> _____	<input type="radio"/> _____	<input type="radio"/> _____
SHORT	<input type="radio"/> _____	<input type="radio"/> _____	<input type="radio"/> _____	<input type="radio"/> _____	<input type="radio"/> _____	<input type="radio"/> _____	<input type="radio"/> _____	<input type="radio"/> _____
WEAK	<input type="radio"/> _____	<input type="radio"/> _____	<input type="radio"/> _____	<input type="radio"/> _____	<input type="radio"/> _____	<input type="radio"/> _____	<input type="radio"/> _____	<input type="radio"/> _____
COMMENT:	_____	_____	_____	_____	_____	_____	_____	_____
*BODY AND TEXTURE DIFFERENCE FROM CONTROL								
SAMPLE	405	391	738	821	544	921	615	176
NO DIFFERENCE	<input type="radio"/>	<input type="radio"/>	<input type="radio"/>	<input type="radio"/>	<input type="radio"/>	<input type="radio"/>	<input type="radio"/>	<input type="radio"/>
VERY SLIGHT DIFFERENCE	<input type="radio"/>	<input type="radio"/>	<input type="radio"/>	<input type="radio"/>	<input type="radio"/>	<input type="radio"/>	<input type="radio"/>	<input type="radio"/>
SLIGHT DIFFERENCE	<input type="radio"/>	<input type="radio"/>	<input type="radio"/>	<input type="radio"/>	<input type="radio"/>	<input type="radio"/>	<input type="radio"/>	<input type="radio"/>
MODERATE DIFFERENCE	<input type="radio"/>	<input type="radio"/>	<input type="radio"/>	<input type="radio"/>	<input type="radio"/>	<input type="radio"/>	<input type="radio"/>	<input type="radio"/>
LARGE DIFFERENCE	<input type="radio"/>	<input type="radio"/>	<input type="radio"/>	<input type="radio"/>	<input type="radio"/>	<input type="radio"/>	<input type="radio"/>	<input type="radio"/>
EXTREME DIFFERENCE	<input type="radio"/>	<input type="radio"/>	<input type="radio"/>	<input type="radio"/>	<input type="radio"/>	<input type="radio"/>	<input type="radio"/>	<input type="radio"/>

3. FLAVOR (1-10)

SAMPLE	405	391	738	821	544	921	615	176
FLAVOR (1-10)	_____	_____	_____	_____	_____	_____	_____	_____
BITTER	<input type="radio"/> _____	<input type="radio"/> _____	<input type="radio"/> _____	<input type="radio"/> _____	<input type="radio"/> _____	<input type="radio"/> _____	<input type="radio"/> _____	<input type="radio"/> _____
FEED	<input type="radio"/> _____	<input type="radio"/> _____	<input type="radio"/> _____	<input type="radio"/> _____	<input type="radio"/> _____	<input type="radio"/> _____	<input type="radio"/> _____	<input type="radio"/> _____
FERMENTED	<input type="radio"/> _____	<input type="radio"/> _____	<input type="radio"/> _____	<input type="radio"/> _____	<input type="radio"/> _____	<input type="radio"/> _____	<input type="radio"/> _____	<input type="radio"/> _____
FLAT/LOW FLAVOR	<input type="radio"/> _____	<input type="radio"/> _____	<input type="radio"/> _____	<input type="radio"/> _____	<input type="radio"/> _____	<input type="radio"/> _____	<input type="radio"/> _____	<input type="radio"/> _____
FRUITY	<input type="radio"/> _____	<input type="radio"/> _____	<input type="radio"/> _____	<input type="radio"/> _____	<input type="radio"/> _____	<input type="radio"/> _____	<input type="radio"/> _____	<input type="radio"/> _____
HEATED	<input type="radio"/> _____	<input type="radio"/> _____	<input type="radio"/> _____	<input type="radio"/> _____	<input type="radio"/> _____	<input type="radio"/> _____	<input type="radio"/> _____	<input type="radio"/> _____
HIGH ACID	<input type="radio"/> _____	<input type="radio"/> _____	<input type="radio"/> _____	<input type="radio"/> _____	<input type="radio"/> _____	<input type="radio"/> _____	<input type="radio"/> _____	<input type="radio"/> _____
OXIDIZED	<input type="radio"/> _____	<input type="radio"/> _____	<input type="radio"/> _____	<input type="radio"/> _____	<input type="radio"/> _____	<input type="radio"/> _____	<input type="radio"/> _____	<input type="radio"/> _____
RANCID	<input type="radio"/> _____	<input type="radio"/> _____	<input type="radio"/> _____	<input type="radio"/> _____	<input type="radio"/> _____	<input type="radio"/> _____	<input type="radio"/> _____	<input type="radio"/> _____
SULFIDE	<input type="radio"/> _____	<input type="radio"/> _____	<input type="radio"/> _____	<input type="radio"/> _____	<input type="radio"/> _____	<input type="radio"/> _____	<input type="radio"/> _____	<input type="radio"/> _____
UNCLEAN	<input type="radio"/> _____	<input type="radio"/> _____	<input type="radio"/> _____	<input type="radio"/> _____	<input type="radio"/> _____	<input type="radio"/> _____	<input type="radio"/> _____	<input type="radio"/> _____
WHEY TAIN	<input type="radio"/> _____	<input type="radio"/> _____	<input type="radio"/> _____	<input type="radio"/> _____	<input type="radio"/> _____	<input type="radio"/> _____	<input type="radio"/> _____	<input type="radio"/> _____
YEASTY	<input type="radio"/> _____	<input type="radio"/> _____	<input type="radio"/> _____	<input type="radio"/> _____	<input type="radio"/> _____	<input type="radio"/> _____	<input type="radio"/> _____	<input type="radio"/> _____
COMMENT:								

*FLAVOR DIFFERENCE FROM CONTROL (0-5)

SAMPLE	405	391	738	821	544	921	615	176
NO DIFFERENCE	<input type="radio"/>	<input type="radio"/>	<input type="radio"/>	<input type="radio"/>	<input type="radio"/>	<input type="radio"/>	<input type="radio"/>	<input type="radio"/>
VERY SLIGHT DIFFERENCE	<input type="radio"/>	<input type="radio"/>	<input type="radio"/>	<input type="radio"/>	<input type="radio"/>	<input type="radio"/>	<input type="radio"/>	<input type="radio"/>
SLIGHT DIFFERENCE	<input type="radio"/>	<input type="radio"/>	<input type="radio"/>	<input type="radio"/>	<input type="radio"/>	<input type="radio"/>	<input type="radio"/>	<input type="radio"/>
MODERATE DIFFERENCE	<input type="radio"/>	<input type="radio"/>	<input type="radio"/>	<input type="radio"/>	<input type="radio"/>	<input type="radio"/>	<input type="radio"/>	<input type="radio"/>
LARGE DIFFERENCE	<input type="radio"/>	<input type="radio"/>	<input type="radio"/>	<input type="radio"/>	<input type="radio"/>	<input type="radio"/>	<input type="radio"/>	<input type="radio"/>
EXTREME DIFFERENCE	<input type="radio"/>	<input type="radio"/>	<input type="radio"/>	<input type="radio"/>	<input type="radio"/>	<input type="radio"/>	<input type="radio"/>	<input type="radio"/>

(# 1)

A.2.4 Designs of difference-from-control and ADSA rating of light-oxidized Cheddar cheese

Specimen Position	Light Exposure (wk)	Coding
Interior	0	821
Interior	2	391
Interior	4	738
Interior	6	405
Surface	0	544
Surface	2	615
Surface	4	921
Surface	6	176

Panelist	Specimen							
	1	2	3	4	5	6	7	8
1	405	391	738	821	544	921	615	176
2	738	405	391	821	921	544	176	615
3	405	391	821	738	921	176	544	615
4	391	405	821	738	615	176	544	921
5	738	405	821	391	921	544	615	176
6	405	821	391	738	921	615	176	544
7	405	738	391	821	615	176	921	544
8	821	738	405	391	615	921	176	544
9	738	821	405	391	615	544	921	176

A.3 Boxplot Interpretation

A box plot (or box-and-whisker plot, [195]) displays a statistical summary of a variable: median, quartiles, range and, possibly and extreme values.

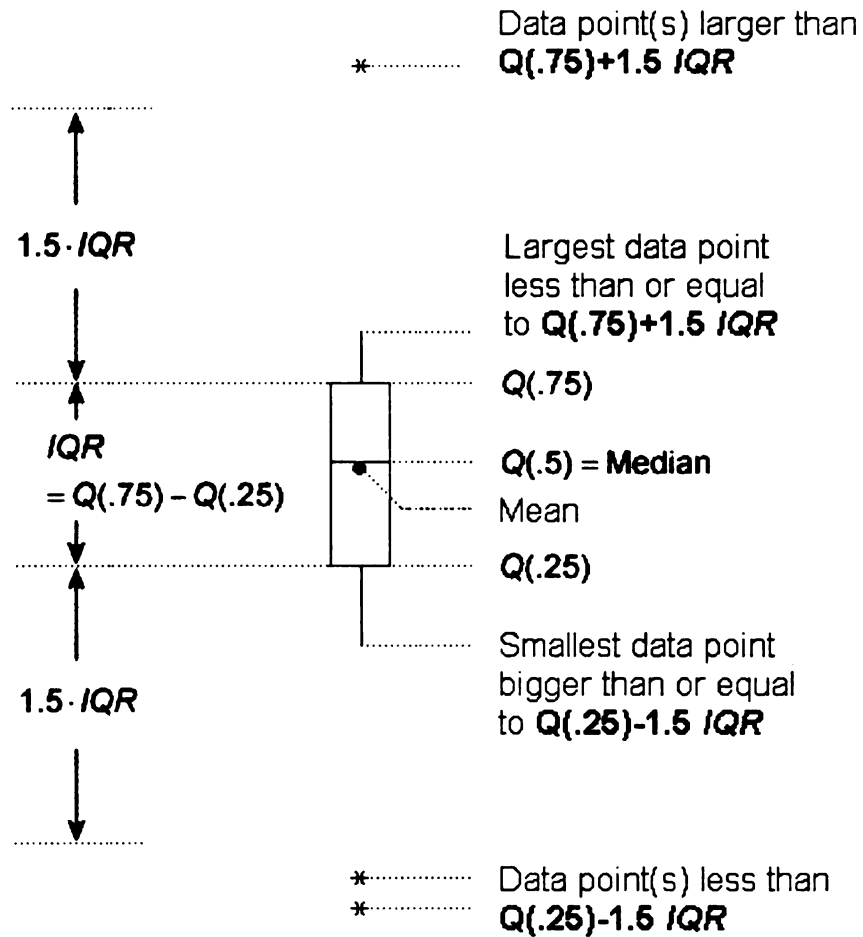


Figure 102 Boxplot Interpretation. IQR: interquartile range. $Q(.25)$: 25th percentile; $Q(.5)$: 50th percentile; $Q(.75)$: 75th percentile.

A.4. Preliminary results

Several sets of preliminary experiments were performed. To access the repeatability and reproducibility of the sample preparation, sensory evaluation and instrumental analysis, the results may be compared to those in Chapter 4.

A.4.1. Light-oxidized off-flavors in 2% milk

A.4.1.1. Sensory evaluation

Table 28 Sensory scores of light-oxidized 2% milk based on ADSA guidelines. Scores were given by an 8-member trained panel.

Duration of light exposure (hours)	Sensory score
4	7.38 \pm 1.60
8	7.00 \pm 2.07
12	5.75 \pm 2.55
24	5.63 \pm 2.92

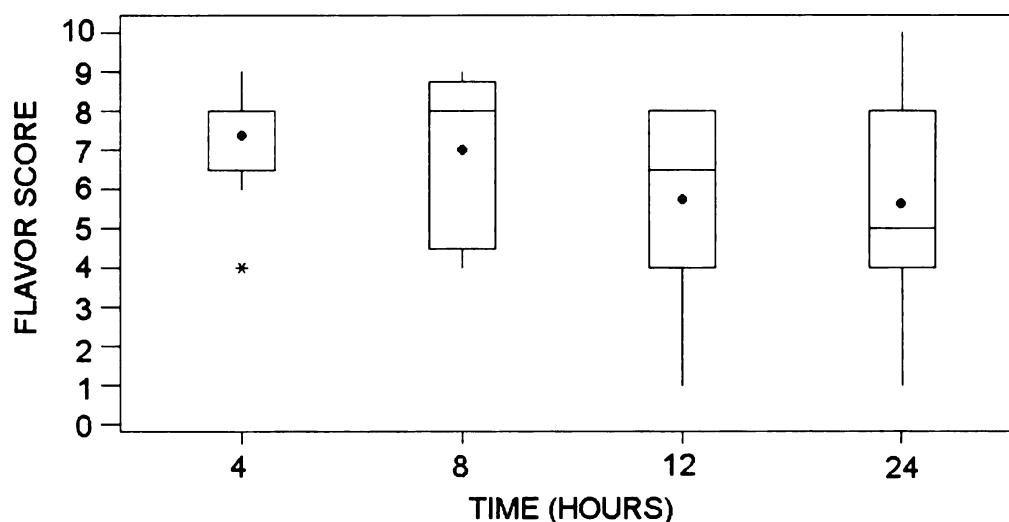


Figure 103 Flavor sensory scores based on ADSA guidelines of 2% milk in glass bottles exposed to 4, 8, 12 and 24 hours of fluorescent light (1000 lx, 5°C).
•: mean values of each treatment; *: possible outliers.

A.4.1.2. Headspace analysis using SPME-GC

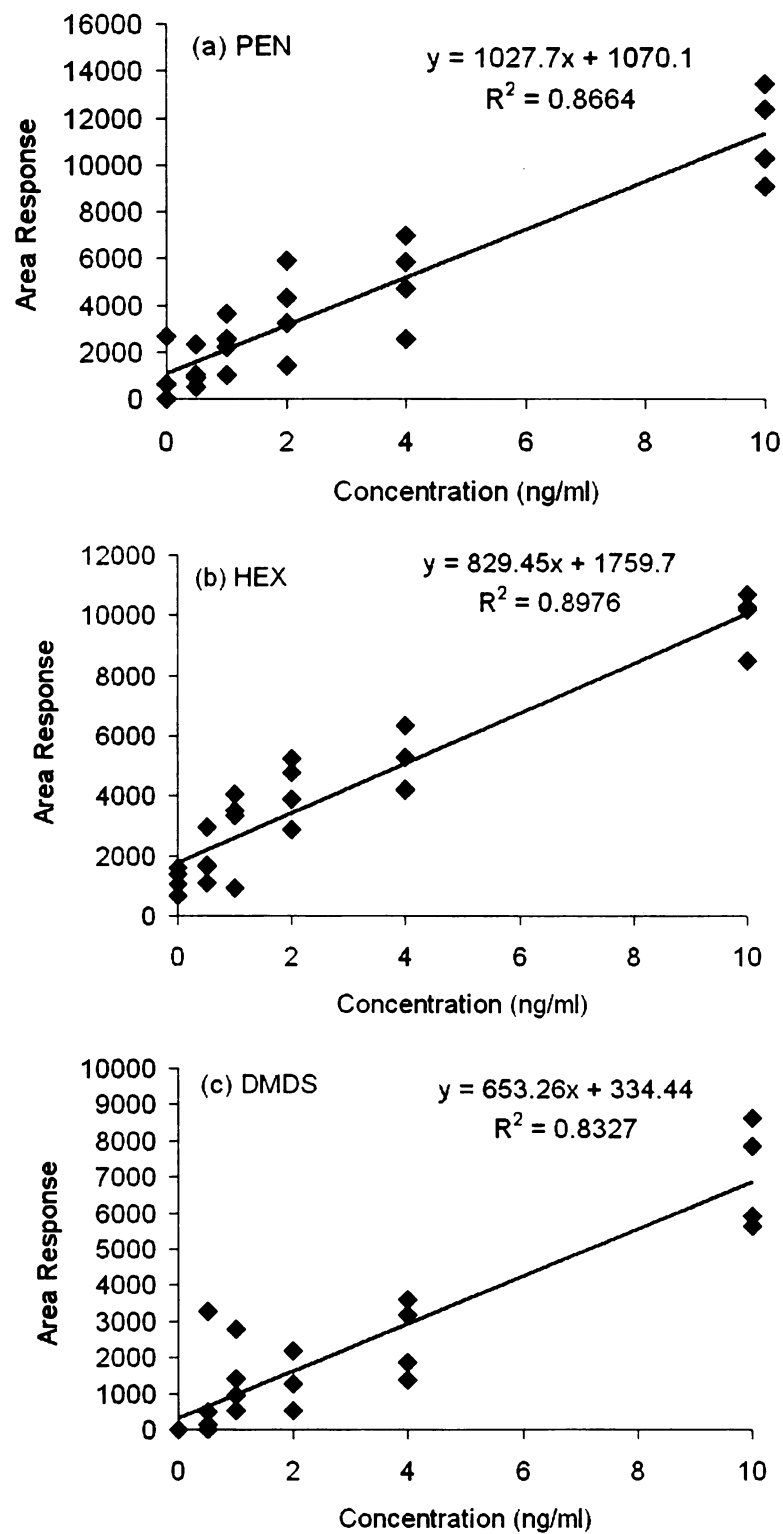


Figure 104 Calibration curves of (a) pentanal (b) hexanal and (c) dimethyl disulfide in 2% milk.

A.4.1.2. Headspace analysis using the electronic nose

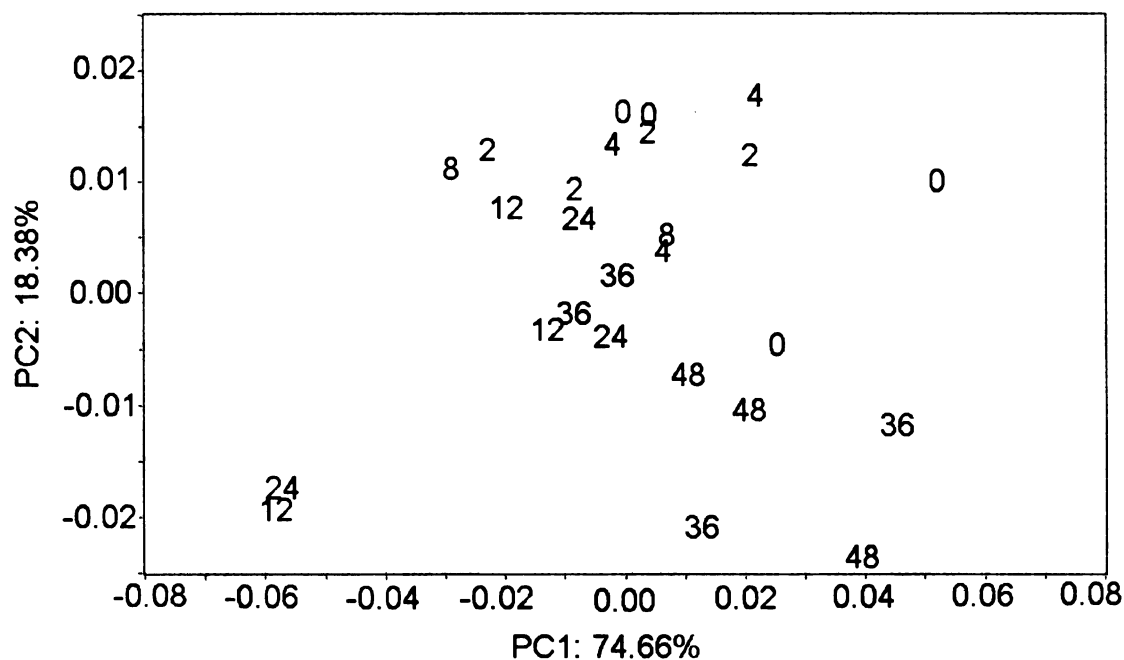


Figure 105 PCA based on 45°C electronic nose sensor responses of 2% milk samples exposed to light (1000 lx) for 0, 2, 4, 8, 12, 24, 36 and 48 hours.

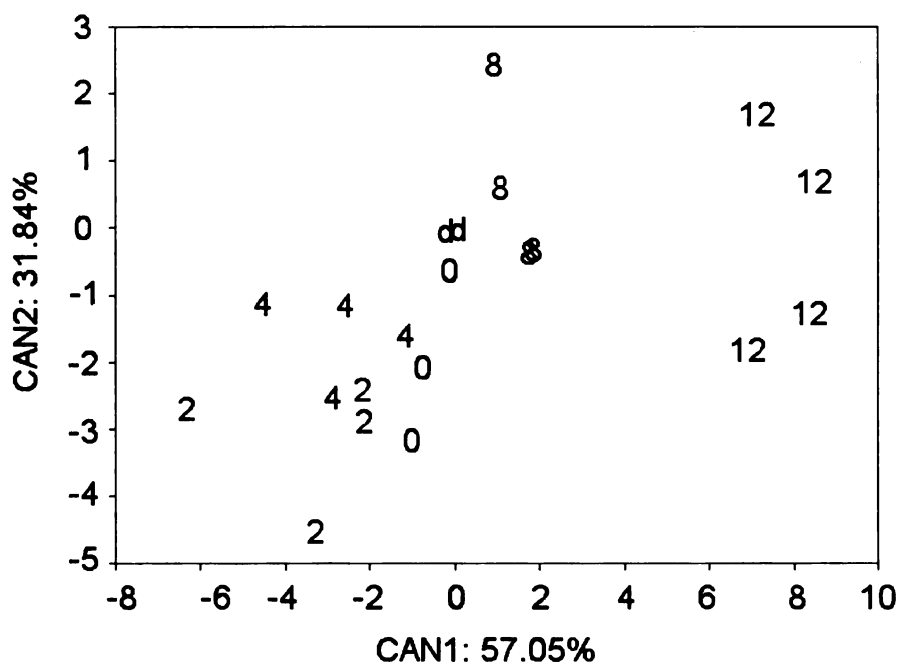


Figure 106 LDA based on 95°C electronic nose sensor responses of 2% milk samples exposed to light (1000 lx) for 0, 2, 4, 8 and 12 hours at 5°C.

A.4.2. Light oxidation of Cheddar cheese

A.4.2.1. Discoloration of Cheddar cheese

Table 29 CIE L* a* b* values of Cheddar cheese samples exposed to fluorescent light (2000 lx) for 0 and 2 weeks.

Duration of light exposure (wks)	L*	a*	b*
0	74.35±0.42 ¹	12.64±0.27	52.06±1.06
2	74.04±0.29	12.59±0.37	49.50±3.64

¹ Standard deviation of the sample

A.4.2.2. Light-induced flavor changes of cheese

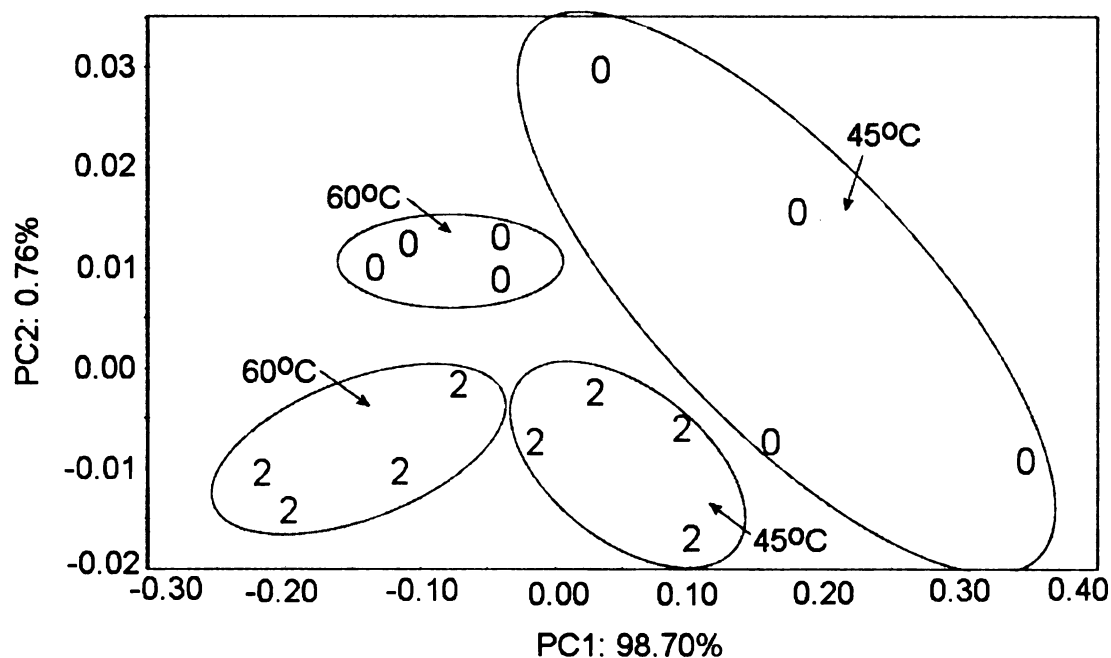


Figure 107 PCA based on 45°C and 60°C electronic nose sensor responses of Cheddar cheese samples exposed to fluorescent light (2000 lx) for 0 and 2 weeks.

BIBLIOGRAPHY

1. Dimick, P.S., 1982. Photochemical effects on flavor and nutrients of fluid milk. *Can. Inst. Food Sci. Technol. J.*, 15(4): p.247-256.
2. Bosset, J.O., Gallmann, P.U., and Sieber, R., 1993. Influence of light transmittance of packaging materials on the shelf-life of milk and dairy products - a review. *Lait*, 73(1): p.3-49.
3. Skibsted, L.H., 2000. Light-induced changes in dairy products. *Bulletin of the International Dairy Federation*, (346): Packaging of milk products: p.4-9.
4. Borle, F.S., Sieber, R., and Bosset, J.O., 2001. Photo-oxidation and photoprotection of foods, with particular reference to dairy products. An update of a review article (1993-2000). *Sciences des Aliments*, 21(6): p.571-590.
5. Mortensen, G., Bertelsen, G., Mortensen, B.K., and Stapelfeldt, H., 2004. Light-induced changes in packaged cheeses—a review. *International Dairy Journal*, 14: p.85-102.
6. Chapman, K.W., Whited, L.J., and Boor, K.J., 2002. Sensory threshold of light-oxidized flavor defects in milk. *J. Food Sci.*, 67(7): p.2770-2773.
7. Dimick, P.S., 1973. Effect of fluorescent light on the flavor and selected nutrients of homogenized milk held in conventional containers. *J. Milk Food Technol.*, 36(7): p.383-387.
8. Coleman, W.W., Watrous, G.H., Jr., and Dimick, P.S., 1976. Organoleptic evaluation of milk in various containers exposed to fluorescent light. *J. Milk Food Technol.*, 39(8): p.551-553.
9. Anonymous, 1997. Important facts about milk in plastic bottles. The Plastic Bottle Institute. The Society of the Plastics Industry, Inc, Washington, DC. p.2.
10. Haisman, D.R., Groenendijk, C.B.M., and O'Sullivan, G.J., 1992. The effect of light on the flavour and nutritional content of milk. Paperboard vs. plastic containers. *Food Technol. New Zealand*, 27(2): p.16-20.
11. Bravo, A., Hotchkiss, J.H., and Acree, T.E., 1992. Identification of odor-active compounds resulting from thermal oxidation of polyethylene. *J. Agric. Food Chem.*, 40(1881-1885).

12. Van Aardt, M., Duncan, S.E., Bourne, D., Marcy, J.E., Long, T.E., Hackney, C.R., and Heisey, C., 2001. Flavor threshold for acetaldehyde in milk, chocolate milk, and spring water using solid phase microextraction gas chromatography for quantification. *J. Agric. Food Chem.*, 49(3): p.1377-1381.
13. Leong, C.M.O., Harte, B.R., Partridge, J.A., Ott, D.B., and Downes, T.W., 1992. Off-flavor development in milk packaged in polyethylene-coated paperboard cartons. *J. Dairy Sci.*, 75(8): p.2105-2111.
14. Gardner, J.W. and Bartlett, P.N., 1994. A brief history of electronic noses. *Sens. Act. B*, 18(1-3): p.210-211.
15. Mielle, P., 1996. 'Electronic noses': towards and objective instrumental characterization of food aroma. *Trends Food Sci. Technol.*, 7: p.432-438.
16. Payne, J.S., 1998. Electronic nose technology - an overview of current technology and commercial availability. *Food Sci. Technol. Today*, 12(4): p.196-200.
17. Bradley, D.G. and Min, D.B., 1992. Singlet oxygen oxidation of foods. *Crit. Rev. Food Sci. Nutr.*, 31(3): p.211-236.
18. Bradley, D.G., Lee, H.O., and Min, D.B., 2003. Singlet oxygen detection in skim milk by electron spin resonance spectroscopy. *J. Food Sci.*, 68(2): p.491-494.
19. Allen, C. and Parks, O.W., 1975. Evidence for methional in skim milk exposed to sunlight. *J. Dairy Sci.*, 58(11): p.1609-1611.
20. Jung, M.Y., Yoon, S.H., Lee, H.O., and Min, D.B., 1998. Singlet oxygen and ascorbic acid effects on dimethyl disulfide and off-flavor in skim milk exposed to light. *J. Food Sci.*, 63(3): p.408-412.
21. Forss, D.A., 1979. Review of the progress of dairy science: mechanisms of formation of aroma compounds in milk and milk products. *J Dairy Res*, 46(4): p.691-706.
22. Gilmore, T.M. and Dimick, P.S., 1979. Photochemical changes in major whey proteins of cow's milk. *J. Dairy Sci.*, 62(2): p.189-194.
23. Finley, J.W. and Shipe, W.F., 1971. Isolation of a flavour producing fraction from light exposed milk. *J. Dairy Sci.*, 54(1): p.15-20.
24. Dimick, P.S., 1976. Effect of fluorescent light on amino acid composition of serum proteins from homogenized milk. *J. Dairy Sci.*, 59(2): p.305-308.

25. Jung, M.Y., Lee, K.H., and Kim, S.Y., 2000. Riboflavin-sensitized photochemical changes in beta-lactoglobulin in an aqueous buffer solution as affected by ascorbic acid. *J. Agric. Food Chem.*, 48(9): p.3847-3850.
26. Hedrick, T.I. and Glass, L., 1975. Chemical changes in milk during exposure to fluorescent light. *J. Milk Food Technol.*, 38(3): p.129-131.
27. Sattar, A. and DeMan, J.M., 1975. Photooxidation of milk and milk products: a review. *Crit. Rev. Food Sci. Nutr.*, 7(1): p.13-37.
28. Marsili, R.T., 1999. Comparison of solid-phase microextraction and dynamic headspace methods for the gas chromatographic–mass spectrometric analysis of light-induced lipid oxidation products in milk. *J. Chromatogr. Sci.*, 37(1): p.17-23.
29. McBean, L.D. and Speckman, E.W., 1988. Nutritive value of dairy foods, in *Fundamentals of dairy chemistry*, N.P. Wong, Editor. Van Nostrand Reinhold Company: New York. p.343-407.
30. Toyosaki, T., Yamamoto, A., and Mineshita, T., 1988. Kinetics of photolysis of milk riboflavin. *Milchwissenschaft*, 43: p.143-145.
31. Singh, R.P., Heldman, D.R., and Kirk, J.R., 1975. Kinetic analysis of light-induced riboflavin loss in whole milk. *J. Food Sci.*, 40(1): p.164-167.
32. Hoskin, J.C. and Dimick, P.S., 1979. Evaluation of fluorescent light on flavor and riboflavin content of milk held in gallon returnable containers. *J. Food Prot.*, 42(2): p.105-109.
33. Hoskin, J.C., 1988. Effect of fluorescent light on flavor and riboflavin content of milk held in modified half-gallon containers. *J. Food Prot.*, 51(1): p.19-23.
34. Deger, D. and Ashoor, S.H., 1987. Light-induced changes in taste, appearance, odor, and riboflavin content of cheese. *J. Dairy Sci.*, 70(7): p.1371-1376.
35. Kristensen, D., Hansen, E., Arndal, A., Trinderup, R.A., and Skibsted, L.H., 2001. Influence of light and temperature on the colour and oxidative stability of processed cheese. *Int. Dairy J.*, 11(10): p.837-843.
36. Mortensen, G., Sørensen, J., Danielsen, B., and Stapelfeldt, H., 2003. Effect of specific wavelengths on light-induced quality changes in Havarti cheese. *J. Dairy Res.*, 70.: p.413–421.
37. Fanelli, A.J., Burlew, J.V., and Gabriel, M.K., 1985. Protection of milk packaged in high density polyethylene against photodegradation by fluorescent light. *J. Food Prot.*, 48(2): p.112-117.

38. Vassila, E., Badeka, A., Kondyli, E., Savvaidis, I., and Kontominas, M.G., 2002. Chemical and microbiological changes in fluid milk as affected by packaging conditions. *Int. Dairy J.*, 12(9): p.715-722.
39. Kristensen, D., Orlie, V., Mortensen, G., Brockhoff, P., and Skibsted, L.H., 2000. Light-induced oxidation in sliced Havarti cheese packaged in modified atmosphere. *Int. Dairy J.*, 10(1/2): p.95-103.
40. Frederiksen, C.S., Haugaard, V.K., Poll, L., and Becker, E.M., 2003. Light-induced quality changes in plain yoghurt packed in polylactate and polystyrene. *Eur. Food Res. Technol.*, 217: p.61-69.
41. Whited, L.J., Hammond, B.H., Chapman, K.W., and Boor, K.J., 2002. Vitamin A degradation and light-oxidized flavor defects in milk. *J. Dairy Sci.*, 85(2): p.351-354.
42. Thompson, J.N. and Erdody, P., 1974. Destruction by light of vitamin A added to milk. *Can. Inst. Food. Sci. Technol. J.*, 7: p.157.
43. Zahar, M., Smith, M.Z., and Warthesen, J.J., 1987. Factors related to the light stability of vitamin A in various carriers. *J. Dairy Sci.*, 70: p.13-19.
44. Bartholomew, B.P. and Ogden, L.V., 1990. Effect of emulsifiers and fortification methods on light stability of vitamin A in milk. *J. Dairy Sci.*, 73: p.1485-1488.
45. Bonczar, G., Regula, A., and Grega, T., 2004. The vitamin C content in fermented milk beverages obtained from ewe's milk. *Electronic Journal of Polish Agricultural Universities*, 7(1):
[p.http://www.ejpau.media.pl/series/volume7/issue1/food/art-06.html](http://www.ejpau.media.pl/series/volume7/issue1/food/art-06.html).
46. Satter, A., deMan, J.M., and Alexander, J.C., 1977. Light-induced degradation of vitamins. I. Kinetic studies on riboflavin decomposition in solution. *Can. Inst. Food. Sci. Technol. J.*, 10: p.61-64.
47. Satter, A., deMan, J.M., and Alexander, J.C., 1977. Light induced degradation on vitamins. II. Kinetic studies on ascorbic acid decomposition in solution. *Can. Inst. Food. Sci. Technol. J.*, 10: p.65-68.
48. Yang, T.W. and Min, D.B., 1994. Dynamic headspace analyses of volatile compounds of Cheddar and Swiss cheese during ripening. *J. Food Sci.*, 59: p.1309-1312.
49. Jung, M.Y., Kim, S.K., and Kim, S.Y., 1995. Riboflavin sensitized photooxidation of ascorbic acid: kinetics and amino acid effects. *Food Chem.*, 55: p.397-403.

50. Lee, K.H., Jung, M.Y., and Kim, S.Y., 1998. Effects of ascorbic acid on the light-induced riboflavin degradation and color changes in milks. *J. Agric. Food Chem.*, 46: p.407-410.
51. King, J.M. and Min, D.B., 1998. Riboflavin photosensitized singlet oxygen oxidation of vitamin D. *J. Food Sci.*, 63(1): p.31-34.
52. Renken, S.A. and Warthesen, J.J., 1993. Vitamin D stability in milk. *J. Food Sci.*, 58: p.552-556.
53. Li, T.-L. and Min., D.B., 1998. Stability and photochemistry of vitamin D2 in model system. *J. Food Sci.*, 63(3): p.413-417.
54. Dunkley, W.L., Pangborn, R.M., and Franklin, J.D., 1963. Fluorescent light influences flavor and vitamins in milk. *The Milk Dealer*, 52(11): p.52, 53, 55, 92, 93.
55. Hansen, A.P., Turner, L.G., and Aurand, L.W., 1975. Fluorescent light-activated flavor in milk. *J. Milk Food Technol.*, 38(7): p.388-392.
56. Smith, T., 1998. Proper milk packaging strategies overcome effects of light. *Packaging Technology & Engineering*, 7(5): p.59-61, 65.
57. Mottar, J., 1982. Light transmission. Technical guide for the packaging of milk and milk products. Vol. Document 143: International Dairy Foundation, ISSN 0250-5118. pp.28.
58. Rysstad, G., Ebbesen, A., and Eggestad, J., 1998. Sensory and chemical quality of UHT-milk stored in paperboard cartons with different oxygen and light barriers. *Food Addit. Contam.*, 15(1): p.112-122.
59. Bradley, R.L., Jr., 1980. Effect of light on alteration of nutritional value and flavor of milk: A review. *J. Food Prot.*, 43(4): p.314-320.
60. Sattar, A. and deMan, J.M., 1973. Effect of packaging material on light induced quality deterioration of milk. *Can. Inst. Food Technol.*, 6(3): p.170-174.
61. Lundahl, D.S., Lukes, B.K., McDaniel, M.R., and Henderson, L.A., 1986. A semi- ascending paired difference method for determining sensory thresholds of added substances to background media. *J. Sensory Studies*, 1(3/4): p.291-306.
62. Chapman, K., 2002. New study validates light blocking efforts- teens taste light-oxidation in milk and don't like it. *Dairy Foods*, 103(9): p.40-42.
63. Peled, R. and Mannheim, C.H., 1977. Off-flavours from packaging materials. *Modern-Packaging*, 50(3): p.45-48, 65.

64. Anonymous, 2001. Packaging opportunities for fluid milk. Dairy Foods, 3: p.http://www.dairyfoods.com/FILES/HTML/dmi_03_toc/0,6870,,00.html.
65. Bravo, A. and Hotchkiss, J.H., 1993. Identification of volatile compounds resulting from the thermal oxidation of polyethylene. J. Appl. Polym. Sci., 47: p.1741-1748.
66. Das, R., 2003. Development of electronic nose method for evaluation of HDPE data, correlated with organoleptic testing, in School of Packaging. Michigan State University: East Lansing.
67. Berg, N., Sensoric and instrumental analysis of off-flavor giving compounds from polyethylene. in Third International symposium on migration. 1980. Hamburg, Germany.
68. Foldes, E. and Turcsanyi, B., 1992. Transport of small molecules in polyolefins. I. Diffusion of Irganox 1010 in polyethylene. J. Appl. Polym. Sci., 46(3): p.507-515.
69. Schwoppe, A.D., Till, D.E., Ehntholt, D.J., Sidman, K.R., and Whelan, R.H., 1987. Migration of Irganox 1010 from ethylene-vinyl acetate films to foods and foods simulating liquids. Food Chemistry and Toxicology, 25(4): p.327-330.
70. Al-Malaika, S., Ashley, H., and Issenhuth, S., 1994. The antioxidant role of α -tocopherol in polymers. I. The nature of transformation products of α -tocopherol formed during melt processing of LDPE. J. Polym. Sci., A, Polym. Chem., 32(16): p.3099-3113.
71. Ho, Y.C., Yam, K.L., Young, S.S., and Zambetti, P.F., 1995. Comparison of vitamin E, Irganox 1010 and BHT as antioxidants on release of off-flavor from HDPE bottles. J. Plast. Film Sheeting, 10(194-212).
72. Koszinowski, J. and Piringer, O., 1986. Evaluation of off-odors in food packaging: the role of conjugated unsaturated carbonyl compounds. J. Plast. Film Sheeting, 2(1): p.40-50.
73. Maneesin, P., 2001. GC-MS and electronic nose analysis on off-flavor components in HDPE containers and correlation with sensory evaluation, in School of Packaging. Michigan State University: East Lansing. p.20.
74. Hoff, A. and Jacobsson, S., 1981. Thermo-oxidative degradation of low-density polyethylene close to industrial processing conditions. J. Appl. Polym. Sci., 26(3409-3423).
75. Srivastava, D.N. and Rawat, R.S., 1978. Selection of flexible single-service container for in-pack processing of market milk. J. Food Sci. Technol. India, 15(3): p.127-129.

76. Judge, T., 1998. Portability improves profitability. Improved packaging is driving major sales upswings for many processors. *Dairy Field*, 181(7): p.20.
77. Van Aardt, M., Duncan, S.E., Marcy, J.E., Long, T.E., and Hackney, C.R., 2001. Effectiveness of poly(ethylene terephthalate) and high-density polyethylene in protection of milk flavor. *J. Dairy Sci.*, 84(6): p.1341-1347.
78. Mehta, R.S. and Bassette, R., 1978. Organoleptic, chemical and microbiological changes in ultra-high-temperature sterilized milk stored at room temperature. *J. Food Prot.*, 41(10): p.806-810.
79. Mehta, R.S. and Bassette, R., 1979. Volatile compounds in UHT-sterilized milk during fluorescent light exposure and storage in the dark. *J. Food Prot.*, 42(3): p.256-258.
80. ADSA, 2002. 82nd Collegiate Dairy Products Evaluation Contest.
81. Gandhi, H., 1996. Identification of off-flavor components found in milk packaged in gable-top paperboard containers, in Department of Food Science and Human Nutrition. Michigan State University: East Lansing.
82. Bray, S.L., Duthie, A.H., and Rogers, R.P., 1977. Consumers can detect light-induced flavor in milk. *J. Food Prot.*, 40(9): p.586-587.
83. Christy, G.E., Amantea, G.F., and Irwin, R.E.T., 1981. Evaluation of effectiveness of polyethylene overwraps in preventing light-induced oxidation of milk in pouches Packaging materials. *J. Can. Inst. Food Sci. Technol.*, 14(2): p.135-138.
84. Nelson, K.H. and Cathcart, W.M., 1984. Transmission of light through pigmented polyethylene milk bottles. *J. Food Prot.*, 47(5): p.346-348.
85. Cladman, W., Scheffer, S., Goodrich, N., and Griffiths, M.W., 1998. Shelf-life milk packaged in plastic containers with and without treatment to reduce light transmission. *Int. Dairy J.*, 8(7): p.629-636.
86. Zygoura, P., Moyssiadi, T., Badeka, A., Kondyli, E., Savvaidis, I., and Kontominas, M.G., 2004. Shelf life of whole pasteurized milk in Greece: effect of packaging material. *Food Chem.*, 87(1): p.1-9.
87. Erickson, M.C., 1997. Chemical and microbial stability of fluid milk in response to packaging and dispensing. *Int. J. Dairy Technol.*, 50(3): p.107-111.
88. Petersen, M., Wiking, L., and Stapelfeldt, H., 1999. Light sensitivity of two colorants for Cheddar cheese. Quantum yields for photodegradation in an

- aqueous model system in relation to light stability of cheese in illuminated display. *J. Dairy Res.*, 66: p.599-607.
89. Najar, S.V., Bobbio, F.O., and Bobbio, P.A., 1988. Effects of light, air, anti-oxidants and pro-oxidants on annatto extracts (*Bixa orellana*). *Food Chem.*, 29(4): p.283-289.
 90. Hong, C.M., Wendorff, W.L., and Bradley, R.L., Jr., 1995. Factors affecting light-induced pink discoloration of annatto-colored cheese. *J. Food Sci.*, 60(1): p.94-97.
 91. Hong, C.M., Wendorff, W.L., and Bradley, R.L., Jr., 1995. Effects of packaging and lighting on pink discoloration and lipid oxidation of annatto-colored cheeses. *J. Dairy Sci.*, 78(9): p.1896-1902.
 92. Shumaker, E.K. and Wendorff, W.L., 1998. Factors affecting pink discoloration in annatto-colored pasteurized process cheese. *J. Food Sci.*, 63(5): p.828-831.
 93. Morgan, G.F.V., 1933. Discoloration in New Zealand Cheddar cheese. Muddy, pink and bleached defects. I. Bacteriological investigations. *J. Dairy Res.*, 4: p.238-245.
 94. Moir, G.M., 1933. Discoloration in New Zealand Cheddar cheese. Muddy, pink and bleached defects. II. Bacteriological investigations. *J. Dairy Res.*, 4: p.238-245.
 95. Barniceat, C.R., 1937. The reactions and properties of annatto as a cheese colour. *J. Dairy Res.*, 8: p.61-73.
 96. Barniceat, C.R., 1950. Cheese discoloration: oxidation of bixin in annatto-coloured cheeses promoted by sulphhydryl compounds. *J. Dairy Res.*, 21: p.209-213.
 97. Govindarajan, S. and Morris, H.A., 1973. Pink discoloration in cheddar cheese. *J. Food Sci.*, 38(4): p.675-678.
 98. Kristoffersen, T., Stussi, D.B., and Gould, I.A., 1964. Consumer packed cheese. I. Flavor stability. *J. Dairy Sci.*, 47: p.496-501.
 99. Soxholt, E., 1996. Table of foods. 4th ed: Søborg: Danish Veterinary and Food Administration.
 100. Mortensen, G., Sørensen, J., and Stapelfeldt, H., 2002. Light-induced oxidation in semihard cheeses. Evaluation of methods used to determine levels of oxidation. *J. Agric. Food Chem.*, 50(15): p.4364-4370.

101. Mortensen, G., Sørensen, J., and Stapelfeldt, H., 2002. Comparison of peroxide value methods used for semihard cheeses. *J. Agric. Food Chem.*, 50(18): p.5007-5011.
102. Mortensen, G., Sørensen, J., and Stapelfeldt, H., 2003. Effect of modified atmosphere packaging and storage conditions on photooxidation of sliced Havarti cheese. *Eur. Food Res. Technol.*, 216(1): p.57-62.
103. Mortensen, G., Sørensen, J., and Stapelfeldt, H., 2003. Response surface models used for prediction of photooxidative quality changes in havarti cheese. *Eur. Food Res. Technol.*, 216(2): p.93-98.
104. Kristensen, D. and Skibsted, L.H., 1999. Comparison of three methods based on electron spin resonance spectrometry for evaluation of oxidative stability of processed cheese. *J. Agric. Food Chem.*, 47(8): p.3099-3104.
105. Colchin, L.M., Owens, S.L., Lyubachevskaya, G., Boyle-Roden, E., Russek-Cohen, E., and Rankin, S.A., 2001. Modified atmosphere packaged cheddar cheese shreds: influence of fluorescent Light exposure and gas type on color and production of volatile compounds. *J. Agric. Food Chem.*, 49(5): p.2277-2282.
106. Wold, J.P., Jørgensen, K., and Lundby, F., 2002. Nondestructive measurement of light-induced oxidation in dairy products by fluorescence spectroscopy and imaging. *J. Dairy Sci.*, 85(7): p.1693-1704.
107. Kim, G.Y., Lee, J.H., and Min, D.B., 2003. Study of light-induced volatile compounds in goat's milk cheese. *J. Agric. Food Chem.*, 51(5): p.1405-1409.
108. Leland, J.V., Reineccius, G.A., and Lahiff, M., 1987. Evaluation of copper-induced oxidized flavor in milk by discriminant analysis of capillary gas chromatographic profiles. *J. Dairy Sci.*, 70(3): p.524-533.
109. Zhang, D. and Mahoney, A.W., 1990. Effect of iron fortification on quality of cheddar cheese. 2. Effect of aging and fluorescent light on pilot scale cheeses. *J. Dairy Sci.*, 73(9): p.2252-2258.
110. Min, D.B. and Boff, J.M., 2002. Chemistry and reaction of singlet oxygen in foods. *COMPREHENSIVE REVIEWS IN FOOD SCIENCE AND FOOD SAFETY*, 1: p.58-61.
111. Psomiadou, E. and Tsimidou, M., 2002. Stability of virgin olive oil. 2. photo-oxidation studies. *J Agric Food Chem.*, 50(4): p.722-727.
112. Haila, K. and Heinonen, M., 1994. Action of beta-carotene on purified rapeseed oil during light storage. *Lebensm Wiss Technol.*, 27(6): p.573-577.

113. Gardner, J.W. and Bartlett, P.N., 1999. Electronic noses: principles and applications. New York: Oxford University Press Inc.
114. Hines, E.L., Boilot, P., Gardner, J.W., and Gongora, M.A., 2003. Pattern analysis for electronic noses, in Handbook of Machine Olfaction: electronic nose technology, T.C. Pearce, Schiffman, S.S., Nagle, H.T., and Gardner, J.W., Editors. Wiley-VCH: Weinheim, Germany. p.133-160.
115. Hartman, J.D., 1954. A possible objective method for the rapid estimation of flavors in vegetables. Proc. Am. Soc. Hort. Sci., 64(335).
116. Persaud, K. and Dodd, G.H., 1982. Analysis of discrimination mechanisms of the mammalian olfactory system using a model nose. Nature, 299: p.352-355.
117. Ikegami, A. and Kaneyasu, M., 1985. Olfactory detection using integrated sensors., in Proceedings of the 3rd International Conference on Solid-State Sensors and Actuators (Transducers 85). IEEE Press: New York. p.136-139.
118. Anonymous, 2004. Review electronic noses: R&D efforts and commercial availability. NOSE Network of Excellence, <http://www.nose-network.org/review/>.
119. Nanto, H. and Stetter, J.R., 2003. Introduction to Chemosensors, in Handbook of Machine Olfaction: electronic nose technology, T.C. Pearce, Schiffman, S.S., Nagle, H.T., and Gardner, J.W., Editors. Wiley-VCH: Weinheim, Germany. p.79-104.
120. Vanneste, E. and Geise, H.J., 2003. Commercial electronic nose instruments, in Handbook of Machine Olfaction: electronic nose technology, T.C. Pearce, Schiffman, S.S., Nagle, H.T., and Gardner, J.W., Editors. Wiley-VCH: Weinheim, Germany. p.161-179.
121. Schaller, E., Bosset, J.O., and Escher, F., 1998. 'Electronic noses' and their application to food. Lebensm. Wiss. Technol., 31(4): p.305-316.
122. Haugen, J.E. and Kvaal, K., 1998. Electronic nose and artificial neural network. Meat Sci., 49(Suppl. 1): p.S273-S286.
123. Schaller, E. and Bosset, J.O., 1998. 'Electronic noses' and their applications in the food industry: A review. Semin. Food Anal., 3: p.119-124.
124. Beebe, K.R., Pell, R.J., and Seasholtz, M.B., 1998. Chemometrics: a practical guide. New York: John Wiley & Sons.

125. Amine, H., Bazzo, S., and Labreche, S., 1998. Intensity and quality discrimination using the Fox 4000 gas sensor array system. *Electronic noses & sensor array based systems: design & applications*, ed. W.J. Hurst. Lancaster, PA: Technomic Publishing. 235-248.
126. Marsili, R.T., 1999. SPME-MS-MVA as an electronic nose for the study of off-flavors in milk. *J. Agric. Food Chem.*, 47(2): p.648-654.
127. Pearce, T.C., Schiffman, S.S., Nagle, H.T., and Gardner, J.W., 2003. *Handbook of Machine Olfaction: electronic nose technology*. Wiley-VCH: Weinheim, Germany.
128. Bassette, R., Fung, D.Y.C., and Mantha, V.R., 1986. Off-flavors in milk. *Crit. Rev. Food Sci. Nutr.*, 24(1): p.1-52.
129. Sberveglieri, G., Comini, E., Faglia, G., Niederjaufner, G., Benussi, G., Contarini, G., and Povo, M., 1998. A novel electronic nose based on semiconductor thin films gas sensor to distinguish different heat treatments of milk. *Semin. Food Anal.*, 3(1): p.67-76.
130. Deffenderfer, O., Feast, S., and Garneau, F.-X., 2003. Recognition of Natural Products, in *Handbook of Machine Olfaction: electronic nose technology*, T.C. Pearce, Schiffman, S.S., Nagle, H.T., and Gardner, J.W., Editors. Wiley-VCH: Weinheim, Germany. p.461-480.
131. Visser, F.R. and Taylor, M., 1998. Improved performance of the Aromascan A32S electronic nose and its potential for detecting aroma differences in dairy products. *Journal of Sensory Studies*, 13(1): p.95-120.
132. Mulville, T., 2000. UHT - the nose knows. *Food Manufacture*, 75(3): p.27-28.
133. Zondervan, C., Muresan, S., de Jonge, H.G., van Velzen, E.U.T., Wilkinson, C., Nijhuis, H.H., and Leguijt, T., 1999. Controlling maillard reactions in the heating process of blockmilk using an electronic nose. *J. Agric. Food Chem.*, 47(11): p.4746-4749.
134. Vallejo-Cordoba, B. and Nakai, S., 1993. Using a simultaneous factor optimization approach for the detection of volatiles in milk dynamic headspace gas chromatographic analysis. *J. Agric. Food Chem.*, 41(12): p.2381-2384.
135. Vallejo-Cordoba, B. and Nakai, S., 1994. Keeping-quality assessment of pasteurized milk by multivariate analysis of dynamic headspace gas chromatographic data. 1. Shelf-life prediction by principal component regression. *J. Agric. Food Chem.*, 42(4): p.989-993.

136. Vallejo-Cordoba, B. and Nakai, S., 1994. Keeping-quality assessment of pasteurized milk by multivariate analysis of dynamic headspace gas chromatographic data. 2. Flavor classification by linear discriminant analysis. *J. Agric. Food Chem.*, 42(4): p.994-999.
137. Vallejo-Cordoba, B., Arteaga, G.E., and Nakai, S., 1995. Predicting milk shelf-life based on artificial neural networks and headspace gas chromatographic data. *J. Food Sci.*, 60(5): p.885-888.
138. Marsili, R.T., 2000. Shelf-life prediction of processed milk by solid-phase microextraction, mass spectrometry, and multivariate analysis. *J. Agric. Food Chem.*, 48(8): p.3470-3475.
139. Kosikowski, F.V. and Moccuto, G., 1958. Advances in cheese technology. *FAO Agricultural studies*. No 38.
140. Jou, K.D. and Harper, W.J., 1998. Pattern recognition of Swiss cheese aroma compounds by SPME/GC and an electronic nose. *Milchwissenschaft*, 53(5): p.259-263.
141. Wijesundera, C. and Walsh, T., 1998. Evaluation of an electronic nose equipped with metal oxide sensors for cheese grading. *The Australian Journal of Dairy Technology*, 53(2): p.141.
142. Drake, M.A., Gerard, P.D., Kleinhenz, J.P., and Harper, W.J., 2003. Application of an electronic nose to correlate with descriptive sensory analysis of aged Cheddar cheese. *Lebensm Wiss Technol.*, 36(1): p.13-20.
143. Pillonel, L., Ampuero, S., Tabacchi, R., and Bosset, J.O., 2003. Analytical methods for the determination of the geographic origin of Emmental cheese: volatile compounds by GC/MS-FID and electronic nose. *European Food Research and Technology*, 216(2): p.179-183.
144. Schaller, E., Bosset, J.O., and Escher, F., 1999. Practical experience with 'electronic nose' systems for monitoring the quality of dairy products. *Chimia*, 53: p.98-102.
145. Schaller, E., Bosset, J.O., and Escher, F., 2000. Feasibility study: detection of 'rind taste' off-flavour in Swiss Emmental cheese using an 'electronic nose' and a GC-MS. *Mitteilungen aus Lebensmitteluntersuchung und Hygiene*, 91(5): p.610-615.
146. Schaller, E., Zenhäusern, S., Zesiger, T., Bosset, J.O., and Escher, F., 2000. Use of preconcentration techniques applied to a MS-based electronic nose. *Analisis*, 28(8): p.743-749.
147. Squibb, A., 2001. Don't sniff at electronic noses. *Food Processing UK*, 70(10): p.22.

148. Trihaas, J., van den Tempel, T., and Nielsen, P.V., 2002. Quality control of danish blue cheese with an electronic nose. ISOEN symposium, Rom, Italien.
149. Trihaas, J., van den Tempel, T., and Nielsen, P.V., 2002. Electronic nose: Smelling the microbiological quality of cheese. ISOEN symposium, Rom, Italien.
150. Trihaas, J., van den Tempel, T. and Nielsen, P.V., 2002. Ripening monitoring of Danish blue cheese by means of electronic nose system, trained sensory panel and GC-MS. The 10th WEURMAN symposium, Dijon, France, June 24-28.
151. O'Riordan, P.J. and Delahunty, C.M., 2003. Characterisation of commercial Cheddar cheese flavour. 1. Traditional and electronic nose approach to quality assessment and market classification. *Int. J. Dairy Technol.*, 13(5): p.355-370.
152. O'Riordan, P.J. and Delahunty, C.M., 2003. Characterisation of commercial Cheddar cheese flavour. 2. Study of Cheddar cheese discrimination by composition, volatile compounds and descriptive flavour assessment. *Int. J. Dairy Technol.*, 13(5): p.371-389.
153. Van Deventer, D. and Mallikarjunan, P., 2002. Comparative performance analysis of three electronic nose systems using different sensor technologies in odor analysis of retained solvents on printed packaging. *J. Food Sci.*, 67(8): p.3170-3183.
154. Van Deventer, D. and Mallikarjunan, P., 2002. Optimizing an electronic nose for analysis of volatiles from printing inks on assorted plastic films. *Innovative Food Science and Emerging Technologies*, 3(1): p.93-99.
155. Poling, J., Lucas, Q., and Weber, K., 1997. Quality control of packaging with the electronic nose Fox 4000. *Journal of Automatic Chemistry*, 19(4): p.115-116.
156. Heiniö, R.L. and Ahvenainen, R., 2002. Monitoring of taints related to printed solid boards with an electronic nose. *Food addit contam.*, 19(suppl.): p.209-220.
157. Arthur, C.L. and Pawliszyn, J., 1990. Solid phase microextraction with thermal desorption using fused silica optical fibers. *Anal. Chem.*, 62(19): p.2145 - 2148.
158. Supelco, 1997. SPME/HPLC interface combines fast sample extraction with efficient analysis for explosives, in Bulletin 098. Sigma-Aldrich Co.

159. Supelco, 1998. Solid Phase Microextraction: theory and optimization of conditions, in Bulletin 923. Sigma-Aldrich Co.
160. Pawliszyn, J., 2001. Solid phase microextraction, in Headspace analysis of foods and flavors, R.L. Rouseff and Cadwallader, K.R., Editors. Kluwer Academic / Plenum Publishers: New York. p.73-87.
161. Supelco, 2001. A practical guide to quantitation with Solid Phase Microextraction, in Bulletin 928. Sigma-Aldrich Co.
162. Supelco, 2001. SPME Applications Guide, in Bulletin 925B. Sigma-Aldrich Co.
163. Contarini, G. and Povolò, M., 2002. Volatile fraction of milk: comparison between purge and trap and solid phase microextraction techniques. *J. Agric. Food Chem.*, 50(25): p.7350 -7355.
164. González-Córdova, A.F. and Vallejo-Córdova, B., 2003. Detection and prediction of hydrolytic rancidity in milk by multiple regression analysis of short-chain free fatty acids determined by solid phase microextraction gas chromatography and quantitative flavor intensity assessment. *J. Agric. Food Chem.*, 51(24): p.7127-7131.
165. Chin, H.W., Bernhard, R.A., and Rosenberg, M., 1996. Solid phase microextraction for cheese volatile compound analysis. *J. Food Sci.*, 61(6): p.1118-1122, 1128.
166. Pérès, C., Viallon, C., and Berdague, J.L., 2001. Solid-phase microextraction-mass spectrometry: a new approach to the rapid characterization of cheeses. *Anal. Chem.*, 73(5): p.1030-1036.
167. Lecanu, L., Ducruet, V., Jouquand, C., Gratadoux, J.J., and Feigenbaum, A., 2002. Optimization of headspace solid-phase microextraction (SPME) for the odor analysis of surface-ripened cheese. *J Agric Food Chem*, 50(13): p.3810-3817.
168. Pinho, O., Ferreira, I.M.P.L.V.O., and Ferreira, M.A., 2002. Solid-phase microextraction in combination with GC/MS for quantification of the major volatile free fatty acids in ewe cheese. *Anal. Chem.*, 74(20): p.5199-5204.
169. Lee, J.H., Diono, R., Kim, G.Y., and Min, D.B., 2003. Optimization of solid phase microextraction analysis for the headspace volatile compounds of Parmesan cheese. *J Agric Food Chem*, 51(5): p.1136-1140.
170. Pinho, O., Pérès, C., and Ferreira, I.M.P.L.V.O., 2003. Solid-phase microextraction of volatile compounds in Terrincho ewe cheese. Comparison of different fibers. *J. Chromatogr. A*, 1011(1-2): p.1-9.

171. Pinho, O., Ferreira, I.M.P.L.V.O., and Ferreira, M.A., 2003. Quantification of short-chain free fatty acids in 'Terrincho' ewe cheese: intravarietal comparison. *J. Dairy Sci.*, 86(10): p.3102-3109.
172. Frank, D.C., Owen, C.M., and Patterson, J., 2004. Solid phase microextraction (SPME) combined with gas-chromatography and olfactometry-mass spectrometry for characterization of cheese aroma compounds. *Lebensm Wiss Technol.*, 37(2): p.139-154.
173. Pionnier, E., Chabanet, C., Mioche, L., Quere, J.L.L., and Salles, C., 2004. 1. In vivo aroma release during eating of a model cheese: relationships with oral parameters. *J. Agric. Food Chem.*, 52(3): p.557-564.
174. Zambonin, C.G., Monaci, L., and Aresta, A., 2001. Determination of cyclopiazonic acid in cheese samples using solid-phase microextraction and high performance liquid chromatography. *Food Chem.*, 75(2): p.249-254.
175. Zambonin, C.G., Monaci, L., and Aresta, A., 2002. Solid-phase microextraction-high performance liquid chromatography and diode array detection for the determination of mycophenolic acid in cheese. *Food Chem.*, 78(2): p.249-254.
176. Johnson, R.A. and Wichern, D.W., 1998. Applied multivariate statistical analysis. Upper Saddle River, New Jersey: Prentice-Hill.
177. Hastie, T., Tibshirani, R., and Friedman, J., 2001. The elements of statistical learning: data mining, inference, and prediction. New York: Springer.
178. Fisher, R.A., 1938. The statistical utilization of multiple measurements. *Annals of Eugenics*, 8: p.376-386.
179. Duda, R.O., Hart, P.E., and Stork, D.G., 2000. Pattern classification. New York: John Wiley & Sons.
180. Morrison, D.F., 1976. Multivariate statistical methods. 2nd ed. New York: McGraw-Hill. 252.
181. Abdi, H., 2003. Partial least squares regression (PLS-regression). *Encyclopedia for research methods for the social sciences*, ed. M. Lewis-Beck, Bryman, A., and Futing, T. Thousand Oaks, CA: Sage.
182. Tobias, R.D., 1997. An Introduction to Partial Least Squares Regression. TS-509. SAS Institute Inc: Cary, NC.

183. Abdi, H., 2003. Neural networks. Encyclopedia for research methods for the social sciences, ed. M. Lewis-Beck, Bryman, A., and Futing, T. Thousand Oaks, CA: Sage.
184. Haykin, S., 1999. Neural networks: a comprehensive foundation. 2nd ed. Upper Saddle River, NJ: Prentice Hall.
185. Demuth, H. and Beale, M., 2001. Neural network toolbox for use with Matlab. ver.4 ed. Natick, MA: The MathWorks Inc.
186. Bodyfelt, W., Tobias, J., and Trout, G.M., 1988. The sensory evaluation of dairy products. New York: Van Nostrand Reinhold.
187. HunterLab, 1996. CIE L* a* b* color scale. HunterLab Applications Note, 8(7): p.1-4.
188. Gordon, S., 2001. Color management and RIP software for digital textile printing: managing color for optimal results. Kimberly-Clark Corporation: p.http://www.techexchange.com/thelibrary/DTPColorMgmt_RIPS.html.
189. HunterLab, 1995. Instrument geometries and color measurements. Part 1: 45°/0° and 0°/45°. HunterLab Applications Note, 6(7): p.1-2.
190. Lee, J.H., 2002. Photooxidation and Photosensitized Oxidation of Linoleic Acid, Milk, and Lard, in Food Science and Nutrition. Ohio State University: Columbus, OH.
191. Legin, A., Rudnitskaya, A., Lvova, L., Vlasov, Y., Natale, C.-d., and D'Amico, A., 2003. Evaluation of Italian wine by the electronic tongue: recognition, quantitative analysis and correlation with human sensory perception. *Analytica Chimica Acta.*, 484(1): p.33-44.
192. Clanchin, B., Lucas, Q., and Jina, O.S., 2003. Quality analysis using E-nose and E-tongue technology. *Soft Drinks International*: p.34-35.
193. Ciosek, P., Augustyniak, E., and Wroblewski, W., 2004. Polymeric membrane ion-selective and cross-sensitive electrode-based electronic tongue for qualitative analysis of beverages. *Analyst.*, 129(7): p.639-644.
194. Esbensen, K., Kirsanov, D., Legin, A., Rudnitskaya, A., Mortensen, J., Pedersen, J., Vognsen, L., Makarychev-Mikhailov, S., and Vlasov, Y., 2004. Fermentation monitoring using multisensor systems: feasibility study of the electronic tongue. *Anal. Bioanal. Chem.*, 378(2): p.391-395.
195. Tukey, J.W., 1977. Box-and-Whisker Plots., in *Explanatory Data Analysis*. Addison-Wesley: Reading, MA. p.39-43.

MICHIGAN STATE UNIVERSITY LIBRARIES



3 1293 02736 2775